

**PHOTOOXIDATION OF NEONICOTINOIDS
(IMIDACLOPRID) IN AQUEOUS SOLUTION BY
VACUUM UV INDUCED ADVANCED OXIDATION
PROCESS**

**SU ORTAMINDA BULUNAN NEONİKOTİNOİDLERİN
(İMİDAKLOPRİD) VAKUM UV İŞİK İLE TETİKLENEN
İLERİ OKSİDASYON PROSESLERİ İLE GİDERİMİ**

HALİL DERİN

ASSOC. PROF. DR. SELİM LATİF SANİN

Supervisor

Submitted To

Graduate School Of Science And Engineering Of Hacettepe University As A partial
Fulfillment To The Requirements For The Award Of The Degree Of Doctor Of
Philosophy In Environmental Engineering

2021

Dedicated to my parents, Fatma Derin and Mustafa Derin, and to my wife, Dr. Smevra
Derin and my son, Ali İhsan Derin.

ABSTRACT

PHOTOOXIDATION OF NEONICOTINOIDS (IMIDACLOPRID) IN AQUEOUS SOLUTION BY VACUUM UV INDUCED ADVANCED OXIDATION PROCESS

Halil DERİN

Doctor of Philosophy, Department of Environmental Engineer

Supervisor: Assoc. Prof. Dr. Selim Latif SANİN

February 2021, 158 pages

Anthropogenic activities have caused pollutions of water sources with organic micro pollutants most of which are recalcitrant and not easily degradable in nature. In recent years, such pollutants have been frequently detected in various water sources and are considered to be one of the major threats to water quality. Among organic micro pollutants, imidacloprid which is the first introduced neonicotinoid insecticide and the most commonly used one, receives a high attention since its widespread presence in water bodies and persistence to conventional biological and chemical water/wastewater treatment methods. Imidacloprid pollution of aquatic systems has been found in several countries. Advanced oxidation processes (AOPs) has been successfully applied to oxidize recalcitrant organic pollutants in water and wastewater treatments. Vacuum ultraviolet (VUV) based AOP has gained attention in recent years to treat organic contaminants in

water. Unlike to other AOPs, VUV irradiation is capable of generating hydroxyl radicals in water without addition of oxidants and catalysts.

Primary goal of this doctoral study was to investigate effectiveness of VUV process on the degradation of imidacloprid in water. Additionally, effects of various experimental parameters, flow rate, initial pH of solution, initial imidacloprid concentration, presence of inorganic ions (HCO_3^- , CO_3^{2-} , NO_3^-), water matrix, presence and absence of dissolved oxygen on the VUV induced photooxidation of imidacloprid was investigated. Independent performance verification of the VUV process was executed by discoloration of commercially available reactive textile dyes (Synozol Red KH-L and Synozol Yellow KH-L) in water. Effects of sleeve materials (clear fused quartz and high purity synthetic quartz) were also investigated during the discoloration study.

The results showed that imidacloprid and reactive textile dyes were rapidly degraded by the VUV process. pH of the experimental solution played an important role in the degradation of imidacloprid by the VUV process. Significant decrease (15.33%) in the rate of degradation of imidacloprid was observed at basic pH=11 condition. Presence of inorganic ions (HCO_3^- , CO_3^{2-} , and NO_3^-) also noticeably impacted the decomposition of imidacloprid via VUV photons. Among the experimental parameters water matrix affected the VUV photooxidation of imidacloprid the most due to presence of natural organic matters (NOM). Nevertheless, complete imidacloprid reduction was attained in less than 5 minutes of reaction time even in the presence of inorganic ions and natural organic matters. It was found that presence of dissolved oxygen did not have a significant impact on the degradation and mineralization processes. Kinetic analyses showed that degradation of imidacloprid by the VUV process under the all tested experimental conditions followed a pseudo first order reaction kinetic. Observed reduction rate constants of imidacloprid ($C_o = 5 \text{ mg/L}$) depending on the experimental conditions varied between 1.3877 min^{-1} and 1.9213 min^{-1} . Almost 80% of 10 mg/L imidacloprid was mineralized by the VUV process within 2 hours of irradiation. LC/MS Q-TOF analyses revealed the generation of several byproducts during the VUV induced photooxidation of imidacloprid.

Separate hydrolysis experiments revealed that imidacloprid was very stable under acidic (pH=3) and natural (original, pH=6.469) conditions during 104 days of hydrolysis time. Hydrolytic degradation of imidacloprid significantly increased under tested basic (pH=11) condition. First order kinetic pattern with the hydrolytic rate constant of 0.0083 day⁻¹ and half-life of 83.51 days was observed at the tested alkaline solution.

Additionally, it was found that Synozol Red KH-L and Synozol Yellow KH-L were also effectively removed by the VUV process. Textile dye experimental results showed that purity of the quartz sleeve used in the VUV photooxidation system had significant impact on the discoloration efficiency.

Keywords: Organic micro pollutants, Imidacloprid, Neonicotinoids, VUV irradiation, Advanced Oxidation Process, Photooxidation, Hydroxyl radicals, Hydrolytic degradation, Synozol Red KH-L, and Synozol Yellow KH-L

ÖZET

SU ORTAMINDA BULUNAN NEONİKOTİNOİDLERİN (İMİDAKLOPRİD) VAKUM UV IŞIK İLE TETİKLENEN İLERİ OKSİDASYON PROSESLERİ İLE GİDERİMİ

Halil DERİN

Doktora, Çevre Mühendisliği Bölümü

Tezdanışmanı: Doç. Dr. Selim Latif SANİN

Şubat 2021, 158 sayfa

Antropojenik faaliyetler, çoğu inatçı olan ve doğada kolayca parçalanamayan organik mikro kirleticilerle su kaynaklarının kirlenmesine çeşitli yollarla neden olmuştur. Son yıllarda, organik mikro kirleticiler çeşitli su kaynaklarında sıklıkla tespit edilmekte ve su kalitesine yönelik en büyük tehditlerden biri olarak kabul edilmektedir. Organik mikro kirleticiler arasında, ilk piyasaya sürülen ve en yaygın kullanılan neonikotinoid insektisit olan imidakloprid, su kaynaklarında yaygın bir şekilde bulunmasından, geleneksel biyolojik ve kimyasal su ve atıksu arıtma yöntemlerine karşı dirençli olmasından dolayı su kaynaklarının korunması açısından büyük ilgi görmektedir. Yüzey ve yeraltı sularının imidakloprid kaynaklı kirliliği birçok ülkede tespit edilmiştir. İnatçı organik kirleticilerin su ve atıksudan gideriminde ileri oksidasyon prosesleri (İOP) başarıyla uygulanmaktadır. Vakum ultraviyole (VUV) bazlı ileri oksidasyon süreci, bu tür kirleticilerin sudan

gideriminde etkinliğinden dolayı, son yıllarda dikkatleri üzerine çekmiştir. Diğer İOP'den farklı olarak, VUV ışına herhangi bir oksitleyici ya da katalizör ilavesine gerek duymaksızın çok kuvvetli bir oksitleyici olan hidroksil radikallerini su ortamında oluşturabilmektedir.

Bu doktora çalışmasının birincil amacı, VUV ışımının imidaklopridin sudan giderimi üzerindeki etkinliğini tespit etmektir. Ayrıca, akış hızı, çözeltinin başlangıç pH'ı, imidakloprid başlangıç konsantrasyonu, inorganik iyonların varlığı, su matrisi, ve çözünmüş oksijenin varlığı gibi çeşitli deneysel parametrelerin imidaklopridin VUV ile fotooksidasyonu üzerindeki etkileri araştırılmıştır. VUV ışımının bağımsız performans doğrulaması ticari olarak temin edilebilen reaktif tekstil boyalarının (Sinozol Kırmızı ve Sinozol Sarı) sudan arıtılmasıyla gerçekleştirilmiştir. VUV ışımada kullanılan kılıf malzemelerinin (berrak erimiş kuvars ve yüksek saflıkta sentetik kuvars) kirleticilerin sudan giderimine olan etkileri de bu doktora çalışması kapsamında araştırılmıştır.

Sonuçlar, imidakloprid ve reaktif tekstil boyalarının incelenen tüm deneysel parametreler altında VUV ışına ile sudan hızlı bir şekilde giderildiğini göstermiştir. Çözelti pH'ı imidaklopridin VUV ışına ile bozunumunda önemli bir rol oynamıştır. Bazik (pH=11) koşullar altında imidaklopridin bozunma oranında önemli düşüş (15.33%) gözlenmiştir. İnorganik iyonların (HCO_3^- , CO_3^{2-} ve NO_3^-) varlığının da imidaklopridin VUV fotonlar ile sudan giderim sürecini etkilediği tespit edilmiştir. Deneysel sonuçlar imidaklopridin VUV ışına ile arıtımını en çok etkileyen deneysel parametrenin doğal organik maddelerin yüzey sularındaki varlığından dolayı su matrisi olduğunu göstermiştir. Fakat imidaklopridin VUV ışına ile sudan tamamen giderimi, inorganik iyonlar ve doğal organik maddelerin varlığında bile 5 dakikadan daha kısa bir sürede gerçekleşmiştir. Çözünmüş oksijenin imidaklopridin VUV foton ile bozunma ve mineralizasyon süreçleri üzerinde önemli bir etkiye sahip olmadığı tespit edilmiştir. Kinetik analizler, test edilen tüm deneysel koşullar altın imidaklopridin VUV ışına ile gideriminin birinci derece bir reaksiyon kinetiğini izlediğini göstermiştir. Deneysel koşullara bağlı olarak imidaklopridin ($C_0 = 5 \text{ mg/L}$) belirlenen bozunma hız sabitleri 1.3877 gün^{-1} ile 1.9213 gün^{-1} arasında değişiklik göstermiştir. 10 mg/L başlangıç konsantrasyonuna sahip imidaklopridin yaklaşık 80% lik mineralizasyonu 2 saat VUV ışına sonucunda elde

edilmiştir. İmidaklopridin VUV ışımaya ile bozunumu sırasında bazı yan (ara) ürünlerin oluştuğu sıvı kromatografi kütle spektrometresi ile tespit edilmiştir.

Bağımsız hidroliz deneyleri imidaklopridin 104 günlük hidroliz süresi boyunca asidik (pH = 3) ve doğal (orijinal, pH = 6.469) koşullar altında oldukça kararlı olup bozunmadığını göstermiştir. İmidaklopridin hidrolitik bozunması, test edilen bazik (pH = 11) koşul altında önemli ölçüde artmıştır. 0.0083 gün^{-1} birinci derece hidrolitik hız sabiti ve 83.51 gün yarılanma ömrü alkali çözeltide tespit edilmiştir.

Ayrıca, deney bulguları VUV ışımaya tekstil boyalarının sudan arıtımında da oldukça etkili bir yöntem olduğunu göstermiştir. Kullanılan kuvars kılıfın saflığının VUV fotooksidasyon ile kirleticilerin sudan gideriminde çok önemli bir etkiye sahip olduğu da tekstil boyası deneyleriyle ortaya konulmuştur.

Anahtar kelimeler: Organik mikro kirleticiler, İmidakloprid, Neonikotinoid, Vakum UV ışımaya, İleri Oksidasyon Prosesi (İOP), Fotooksidasyon, Hidroksil radikali, Hidrolitik Bozunma, Sinozol Kırmızı ve Sinozol Sarı

ACKNOWLEDGEMENTS

I would like to express my gratitude and sincere thanks to my university supervisor Assoc. Prof. Dr. Selim Latif Sanin for his guidance, feedback and support throughout this research. He gave me the possibility to start and complete this doctoral degree in Environmental Engineering.

I would also like to express my deepest appreciation to Prof. Dr. Gülen Güllü and Prof. Dr. İpek İmamođlu who are the members of thesis monitoring committee for their continual advices and helpful discussions.

I also wish to express my sincere thanks to Assoc. Prof. Dr. İlknur Durukan Temuge and Asst. Prof. Dr. Soner akmak for their support and encouragement especially during difficult times.

Special thanks go to Dr. Eszter Arany from University of Szeged for her valuable supports especially in the determination of photon flux of the VUV lamp by Methanol Actinometry Method.

I wish to offer my heartfelt thanks to my parents, Fatma Derin and Mustafa Derin. You have brought me to life, raised me, taught me and loved me, continuously and unconditionally. I cannot and will never forget that.

From the bottom of my heart I thank to my wife, Dr. Sümeyra Derin and my son, Ali Ihsan Derin who was born near the end of this doctoral study and had to come with me to the laboratory even when he was couple of months old. My wife has endlessly loved and supported me in whatever I pursue. She has always believed in me and been by my side throughout this doctoral degree and endured me during the ups and downs of this journey. This thesis would certainly not have existed without you and your enormous motivation and patience.

I greatly appreciate the 2211-A General Domestic Doctoral Scholarship that I received from The Scientific and Technological Research Council of Turkey (TÜBİTAK) during 4 years of my doctoral study.

I also sincerely appreciate the financial support received from The Scientific and Technological Research Council of Turkey (TÜBİTAK) for the project with a title of “Photooxidation of Neonicotinoids (Imidacloprid) in Aqueous Solution by Vacuum UV Induced Advanced Oxidation Process”.

This work was partially supported by TÜBİTAK with Grant No: 119Y011 under 1002 Fast Support Program.

TABLE OF CONTENTS

ABSTRACT.....	i
ÖZET.....	iv
ACKNOWLEDGEMENTS.....	vii
TABLE OF CONTENTS	ix
LIST OF FIGURES.....	xiv
LIST OF TABLES	xxiii
SYMBOLS AND ABBREVIATIONS	xxv
1. INTRODUCTION.....	1
1.1. Background	1
1.2. Advanced Oxidation Processes	3
1.3. Research Summary and Scope	4
1.4. Thesis Structure.....	5
2. LITERATURE REVIEW	6
2.1. Neonicotinoids.....	6
2.2. Imidacloprid	6
2.2.1. Environmental Fate of Imidacloprid	8
2.2.2. Concern of Imidacloprid	8
2.2.3. Imidacloprid removal from aqueous solution.....	10
2.3. Vacuum UV based Advanced Oxidation Process (AOP)	19
2.3.1. VUV based photooxidation (removal) of organic pollutants	21

3. RESEARCH OBJECTIVES	24
4. MATERIALS AND METHODS	26
4.1. Chemicals	26
4.2. Aqueous Solvents	27
4.2.1. Ultrapure Water	28
4.2.2. Tap Water	28
4.2.3. Pond Water	28
4.3. Experimental Solutions	28
4.3.1. Preperation of Imidacloprid Stock and Working Solutions	28
4.3.2. Preperation of Confidor Imidacloprid Stock and Working Solutions.....	29
4.3.3. Preperation of Reactive Textile Dyes Stock and Working Solutions	29
4.4. Experimental Setup.....	29
4.4.1. VUV Photooxidation System	29
4.4.2. Photoreactor	31
4.4.3. VUV Lamp	32
4.4.4. High Purity Synthetic Quartz Sleeve	33
4.4.5. Clear Fused Quartz Sleeve	33
4.4.6. Peristaltic Pump	34
4.4.7. Circulating Tube	34
4.4.8. pH and conductivity meter	34
4.5. Experimental Method.....	34
4.5.1. Adsorption Experiment	34
4.5.2. Hydrolysis Experiment.....	35
4.5.3. Degradation Experiment.....	35
4.5.4. Mineralization Experiment	40

4.6. Actinometric Measurement of Photon Flux of the VUV Lamp	40
4.6.1. Methanol Actinometry	40
4.7. Analytical Methods.....	42
4.7.1. UV-Vis Spectrophotometer	42
4.7.2. Liquid Chromatography and Quadrupole Time of Flight Mass Analyzer (LC/MS Q-TOF).....	43
4.7.3. Gas Chromatography Mass Spectrometry (GC/MS)	44
4.7.4. Total Organic Carbon Analyzer (TOC)	46
5. RESULTS AND DISCUSSION	47
5.1. Photon Flux of the VUV Lamp	47
5.2. Adsorption of Imidacloprid	47
5.3. Hydrolysis of Imidacloprid	49
5.4. Degradation of Imidacloprid by VUV photooxidation.....	50
5.4.1. Effects of Flowrate of the experimental solution	50
5.4.2. Effects of initial pH of the experimental solution.....	56
5.4.3. Effects of initial concentration of Imidacloprid.....	63
5.4.4. Effects of Inorganic ions	69
5.4.5. Effects of Water Matrix.....	76
5.4.6. Effects of Oxygenated and Deoxygenated conditions on the degradation of Imidacloprid	80
5.5. Mineralization of Imidacloprid by VUV photooxidation	84
5.5.1. Effects of Oxygenated and Deoxygenated conditions on the mineralization of Imidacloprid	84
5.6. VUV photooxidation Byproducts of Imidacloprid	87
5.7. Degradation of Reactive Textile Dyes by VUV photooxidation	89
5.7.1. Effects of Flowrate of the experimental solution	89

5.7.2. Effects of initial concentration of the reactive textile dyes	94
5.7.3. Effects of material of quartz sleeve on the discoloration of the reactive textile dye	107
6. CONCLUSION	115
7. RECOMMENDATION	120
8. REFERENCES	121
Appendices	129
APPENDIX 1	129
APPENDIX 1.1. Supplementary Data for Screening of pH Adjusters for Acidic and Alkaline Conditions.....	129
APPENDIX 1.2. Supplementary Data for UV-Vis Analysis.....	130
APPENDIX 1.3. Supplementary Data for LC/MS Q-TOF Analysis	131
APPENDIX 1.4. Supplementary Data for GC/MS Analysis	134
APPENDIX 2	136
APPENDIX 2.1. Supplementary Data for Effects of Flowrate of the experimental solution on the degradation of Imidacloprid	136
APPENDIX 2.2. Supplementary Data for Effects of initial pH of the experimental solution on the degradation of Imidacloprid	138
APPENDIX 2.3. Supplementary Data for Effects of initial concentration of imidacloprid on the degradation of Imidacloprid	140
APPENDIX 2.4. Supplementary Data for Effects of inorganic ions on the degradation of Imidacloprid	142
APPENDIX 2.5. Supplementary Data for Effects of Water Matrix on the degradation of Imidacloprid	144
APPENDIX 2.6. Supplementary Data for Effects of Oxygen saturated condition on the degradation of Imidacloprid.....	145

APPENDIX 2.7. Supplementary Data for Effects of Oxygenated and Deoxygenated conditions on the mineralization of Imidacloprid	146
APPENDIX 2.8. Supplementary Data for VUV photooxidation Byproducts of Imidacloprid	146
APPENDIX 3	149
APPENDIX 3.1. Supplementary Data for Effects of Flowrate of the experimental solution on the discoloration of Red Dye.....	149
APPENDIX 3.2. Supplementary Data for Effects of initial concentration of imidacloprid on the discoloration of Reactive Textile Dyes.....	151
APPENDIX 3.3. Supplementary Data for Effects of material of quartz sleeve on the discoloration of the reactive textile dyes	156

LIST OF FIGURES

Figure 4.1 Scheme of VUV Photooxidation System.....	30
Figure 4.2 The VUV Photooxidation System.	31
Figure 5.1 MeOH reduction via VUV irradiation.	47
Figure 5.2 Adsorptional loss of Imidacloprid ($C_o=10$ mg/L) without turning the VUV lamp on as a function of irradiation time.	48
Figure 5.3 Adsorptional loss of Red dye ($C_o=10$ mg/L) without turning the VUV lamp on as a function of irradiation time.....	49
Figure 5.4 Hydrolytic degradation of Imidacloprid ($C_o=10$ mg/L) under basic (pH=11) condition.....	50
Figure 5.5 VUV induced photodegradation of Imidacloprid ($C_o = 5$ mg/L) under $Q = 500$ mL/min flow rate condition.....	51
Figure 5.6 VUV induced photodegradation of Imidacloprid ($C_o = 5$ mg/L) under $Q = 750$ mL/min flow rate condition.....	51
Figure 5.7 VUV induced photodegradation of Imidacloprid ($C_o = 5$ mg/L) under $Q = 1000$ mL/min flow rate condition.....	52
Figure 5.8 VUV initiated degradation of Imidacloprid ($C_o = 5$ mg/L) under various flow rate conditions..	52
Figure 5.9 Pseudo first-order degradation of Imidacloprid ($C_o = 5$ mg/L) under various flow rate conditions..	55
Figure 5.10 Imidacloprid ($C_o = 5$ mg/L) removal efficiency by VUV induced photodegradation under various flow rates.....	56
Figure 5.11 VUV induced photodegradation of Imidacloprid ($C_o = 5$ mg/L) under natural (original, pH \approx 6.5) condition.....	57
Figure 5.12 VUV induced photodegradation of Imidacloprid ($C_o = 5$ mg/L) under acidic (pH=3) condition..	57

Figure 5.13 VUV induced photodegradation of Imidacloprid ($C_o = 5$ mg/L) under basic (pH=11) condition..	58
Figure 5.14 VUV initiated photodegradation of Imidacloprid ($C_o = 5$ mg/L) under different pH conditions..	58
Figure 5.15 Pseudo first-order degradation of Imidacloprid ($C_o = 5$ mg/L) under different pH conditions..	61
Figure 5.16 Imidacloprid ($C_o = 5$ mg/L) removal efficiency by VUV induced photodegradation under various pH conditions.....	62
Figure 5.17 VUV induced photodegradation of Imidacloprid ($C_o = 2.5$ mg/L).....	63
Figure 5.18 VUV induced photodegradation of Imidacloprid ($C_o = 5$ mg/L).....	64
Figure 5.19 VUV induced photodegradation of Imidacloprid ($C_o = 10$ mg/L).....	64
Figure 5.20 VUV initiated photodegradation of Imidacloprid under various initial concentrations.....	65
Figure 5.21 Pseudo first-order degradation of Imidacloprid under various initial concentrations.....	67
Figure 5.22 Imidacloprid removal efficiency by VUV induced photodegradation under various initial concentrations..	68
Figure 5.23 VUV induced photodegradation of Imidacloprid ($C_o = 5$ mg/L) in absence of inorganic ions..	70
Figure 5.24 VUV induced photodegradation of Imidacloprid ($C_o = 5$ mg/L) in presence of carbonate ion ($CO_3^{2-}=5$ mg/L).....	70
Figure 5.25 VUV induced photodegradation of Imidacloprid ($C_o = 5$ mg/L) in presence of bicarbonate ion ($HCO_3^-=5$ mg/L).....	71
Figure 5.26 VUV induced photodegradation of Imidacloprid ($C_o = 5$ mg/L) in presence of nitrate ion ($NO_3^-=5$ mg/L).....	71
Figure 5.27 VUV induced photodegradation of Imidacloprid ($C_o = 5$ mg/L) in presence of various inorganic ions.....	72

Figure 5.28 Pseudo first-order degradation of Imidacloprid ($C_0 = 5$ mg/L) in presence of various inorganic ions.....	74
Figure 5.29 Imidacloprid ($C_0 = 5$ mg/L) removal efficiency by VUV induced photodegradation in presence of inorganic ions.....	75
Figure 5.30 VUV induced photodegradation of Imidacloprid ($C_0 = 5$ mg/L) in tap water..	76
Figure 5.31 VUV induced photodegradation of Imidacloprid ($C_0 = 5$ mg/L) in pond water.	77
Figure 5.32 VUV induced photodegradation of Imidacloprid ($C_0 = 5$ mg/L) in various water matrices.....	77
Figure 5.33 Pseudo first-order degradation of Imidacloprid ($C_0 = 5$ mg/L) in various water matrices..	79
Figure 5.34 Imidacloprid ($C_0 = 5$ mg/L) removal efficiency by VUV induced photodegradation in various water matrices.....	80
Figure 5.35 VUV induced photodegradation of Imidacloprid ($C_0 = 5$ mg/L) in oxygenated and deoxygenated solutions.....	81
Figure 5.36 Pseudo first-order degradation of Imidacloprid ($C_0 = 5$ mg/L) in oxygenated and deoxygenated solutions.....	81
Figure 5.37 Imidacloprid ($C_0 = 5$ mg/L) removal efficiency by VUV induced photodegradation constants in oxygenated and deoxygenated solutions.....	83
Figure 5.38 Zero-order mineralization (TOC reduction) of Imidacloprid ($C_0 = 10$ mg/L) in oxygenated and deoxygenated solutions.....	84
Figure 5.39 First-order mineralization (TOC reduction) of Imidacloprid ($C_0 = 10$ mg/L) in oxygenated and deoxygenated solutions.....	85
Figure 5.40 Imidacloprid Mineralization (TOC reduction) efficiency of VUV irradiation in oxygenated and deoxygenated solutions.....	87
Figure 5.41 VUV induced discoloration of Red dye ($C_0 = 10$ mg/L) under $Q = 350$ mL/min flow rate condition.....	90

Figure 5.42 VUV induced discoloration of Red dye ($C_o = 10$ mg/L) under $Q = 500$ mL/min flow rate condition..	90
Figure 5.43 VUV induced discoloration of Red ($C_o = 10$ mg/L) under $Q = 750$ mL/min flow rate condition.....	91
Figure 5.44 VUV induced discoloration of Red dye ($C_o = 10$ mg/L) under various flow rate condition.....	91
Figure 5.45 Pseudo first-order discoloration of Red dye under various flow rate conditions.....	93
Figure 5.46 Red dye disappearance efficiency of VUV irradiation under various flow rates.....	94
Figure 5.47 VUV induced discoloration of Red dye ($C_o = 10$ mg/L).....	95
Figure 5.48 VUV induced discoloration of Red dye ($C_o = 25$ mg/L).....	95
Figure 5.49 VUV induced discoloration of Red dye ($C_o = 50$ mg/L).....	96
Figure 5.50 VUV initiated discoloration of Red dye under various initial concentrations.	96
Figure 5.51 Pseudo first-order discoloration of Red dye under various initial concentrations.....	98
Figure 5.52 Red dye disappearance efficiency of VUV irradiation under various initial concentrations.....	99
Figure 5.53 VUV induced discoloration of Yellow dye ($C_o = 10$ mg/L).....	99
Figure 5.54 VUV induced discoloration of Yellow dye ($C_o = 25$ mg/L).....	100
Figure 5.55 VUV induced discoloration of Red dye ($C_o = 50$ mg/L).....	100
Figure 5.56 VUV initiated discoloration of Yellow dye under various concentrations..	101
Figure 5.57 Pseudo first-order discoloration of Yellow dye under various initial concentrations.....	101
Figure 5.58 Yellow dye disappearance efficiency of VUV irradiation under various initial concentrations.....	102

Figure 5.59 VUV induced discoloration of Red and Yellow dyes at $C_o = 10$ mg/L.....	103
Figure 5.60 VUV initiated discoloration kinetic of Red and Yellow dyes at $C_o = 10$ mg/L.	103
Figure 5.61 VUV induced discoloration of Red and Yellow dyes at $C_o = 25$ mg/L.....	104
Figure 5.62 VUV initiated discoloration kinetics of Red and Yellow dyes at $C_o = 25$ mg/L.	105
Figure 5.63 VUV induced discoloration of Red and Yellow dyes at $C_o = 50$ mg/L.....	106
Figure 5.64 VUV initiated discoloration kinetics of Red and Yellow dyes at $C_o = 50$ mg/L.	106
Figure 5.65 Effects of materials of quartz sleeve on discoloration of Red dye ($C_o = 10$ mg/L).....	108
Figure 5.66 Effects of materials of quartz sleeve on discoloration kinetics of Red dye (C_o $= 10$ mg/L).....	108
Figure 5.67 Effects of materials of quartz sleeve on discoloration efficiency of Red dye ($C_o = 10$ mg/L).....	110
Figure 5.68 Effects of materials of quartz sleeve on discoloration of Red dye ($C_o = 25$ mg/L).....	110
Figure 5.69 Effects of materials of quartz sleeve on discoloration kinetics of Red dye (C_o $= 25$ mg/L).....	111
Figure 5.70 Effects of materials of quartz sleeve on discoloration efficiency of Red dye ($C_o = 25$ mg/L).....	112
Figure 5. 71 Effects of materials of quartz sleeve on discoloration of Red dye ($C_o = 50$ mg/L).....	113
Figure 5.72 Effects of materials of quartz sleeve on discoloration kinetics of Red dye (C_o $= 50$ mg/L).....	113
Figure 5.73 Effects of materials of quartz sleeve on discoloration efficiency of Red dye ($C_o = 50$ mg/L).....	114

Figure A.1.1 UV-Vis Absorbance Spectrum of H ₂ SO ₄ , HCl, HNO ₃ , NaOH and Confidor Imidacloprid (C ₀ = 5.25 mg/L).....	129
Figure A.1.2 UV-Vis Absorbance Spectrum of various Confidor Imidacloprid concentration along with H ₂ SO ₄ , HCl, HNO ₃ and NaOH.....	129
Figure A.1.3 UV-Vis Absorbance Spectrum of various Confidor Imidacloprid concentration along with H ₂ SO ₄ , HCl, and NaOH.....	130
Figure A.1.4 Absorbance Spectrum of Standard Imidacloprid.....	130
Figure A.1.5 UV-Vis Calibration Curve and Correlation Coefficient (R ²) of Standard Imidacloprid at 270 nm wavelength.....	131
Figure A.1.6 LC/MS Q-TOF Calibration Chromatogram of Standard Imidacloprid using DAD at 270 nm wavelength.....	132
Figure A.1.7 LC/MS Q-TOF Calibration Curve and Correlation Coefficient (R ²) of Standard Imidacloprid.....	133
Figure A.1.8 LC/MS Q-TOF Chromatogram of 5 mg/L Imidacloprid Standard at 0 (zero) minute of irradiation time.....	133
Figure A.1.9 LC/MS Q-TOF mass spectrum of Imidacloprid Standard.....	134
Figure A.1.10 GC/MS Calibration Chromatogram of Methanol.....	134
Figure A.1.11 GC/MS Calibration Curve and Correlation Coefficient (R ²) of Methanol.....	135
Figure A.1.12 GC/MS mass spectrum of Methanol.....	135
Figure A.2.1 VUV induced photodegradation of Imidacloprid (C ₀ = 5 mg/L) under Q = 500 mL/min flow rate condition.	136
Figure A.2.2 VUV induced photodegradation of Imidacloprid (C ₀ = 5 mg/L) under Q = 750 mL/min flow rate condition.....	136
Figure A.2.3 VUV induced photodegradation of Imidacloprid (C ₀ = 5 mg/L) under Q = 1000 mL/min flow rate condition.....	137

Figure A.2.4 VUV induced photodegradation of Imidacloprid ($C_o = 5$ mg/L) under various flow rate conditions..	137
Figure A.2.5 VUV induced photodegradation of Imidacloprid ($C_o = 5$ mg/L) under natural (original, $pH \approx 6.5$) condition.	138
Figure A.2.6 VUV induced photodegradation of Imidacloprid ($C_o = 5$ mg/L) under acidic ($pH=3$) condition..	138
Figure A.2.7 VUV induced photodegradation of Imidacloprid ($C_o = 5$ mg/L) under basic ($pH=11$) condition..	139
Figure A.2.8 VUV induced photodegradation of Imidacloprid ($C_o = 5$ mg/L) under different pH conditions..	139
Figure A.2.9 VUV induced photodegradation of Imidacloprid ($C_o = 2.5$ mg/L).....	140
Figure A.2.10 VUV induced photodegradation of Imidacloprid ($C_o = 5$ mg/L).....	140
Figure A.2.11 VUV induced photodegradation of Imidacloprid ($C_o = 10$ mg/L).....	141
Figure A.2.12 VUV induced photodegradation of Imidacloprid under various initial concentrations.....	141
Figure A.2.13 VUV induced photodegradation of Imidacloprid ($C_o = 5$ mg/L) in presence of carbonate ion ($CO_3^{2-}=5$ mg/L).....	142
Figure A.2.14 VUV induced photodegradation of Imidacloprid ($C_o = 5$ mg/L) in presence of bicarbonate ion ($HCO_3^-=5$ mg/L).....	142
Figure A.2.15 VUV induced photodegradation of Imidacloprid ($C_o = 5$ mg/L) in presence of nitrate ion ($NO_3^-=5$ mg/L).....	143
Figure A.2.16 VUV induced photodegradation of Imidacloprid ($C_o = 5$ mg/L) in presence of various inorganic ions.....	143
Figure A.2.17 VUV induced photodegradation of Imidacloprid ($C_o = 5$ mg/L) in tap water.	144
Figure A.2.18 VUV induced photodegradation of Imidacloprid ($C_o = 5$ mg/L) in pond water.....	144

Figure A.2.19 VUV induced photodegradation of Imidacloprid ($C_o = 5$ mg/L) in various water matrix.....	145
Figure A.2.20 VUV induced photodegradation of Imidacloprid ($C_o = 5$ mg/L) in presence and absence of oxygen.	145
Figure A.2.21 VUV induced mineralization (TOC reduction) of Imidacloprid ($C_o = 10$ mg/L) in presence and absence of oxygen.	146
Figure A.2.22 Overlapped LC/MS Q-TOF chromatograms of 5 mg/L imidacloprid at 0 and 1 min of VUV irradiation time	146
Figure A.2.23 LC/MS Q-TOF mass spectrum of byproduct set 1 at 1 min of irradiation time (at retention time of 2.623 min).....	147
Figure A.2.24 LC/MS Q-TOF mass spectrum of byproduct set 2 at 1 min of irradiation time (at retention time of 2.938 min).....	147
Figure A.2.25 LC/MS Q-TOF mass spectrum of byproduct set 3 at 1 min of irradiation time (at retention time of 3.203 min).....	148
Figure A.2.26 LC/MS Q-TOF mass spectrum of byproduct set 4 at 1 min of irradiation time (at retention time of 3.402 min).....	148
Figure A.3.1 VUV initiated discoloration of Red dye ($C_o = 10$ mg/L) under $Q = 350$ mL/min flow rate condition.	149
Figure A.3.2 VUV initiated discoloration of Red dye ($C_o = 10$ mg/L) under $Q = 500$ mL/min flow rate condition.	149
Figure A.3.3 VUV initiated discoloration of Red dye ($C_o = 10$ mg/L) under $Q = 750$ mL/min flow rate condition.	150
Figure A.3.4 VUV initiated discoloration of Red dye ($C_o = 10$ mg/L) under various flow rate condition.	150
Figure A.3.5 VUV initiated discoloration of Red dye ($C_o = 10$ mg/L).....	151
Figure A.3.6 VUV initiated discoloration of Red dye ($C_o = 25$ mg/L).	151
Figure A.3.7 VUV initiated discoloration of Red dye ($C_o = 50$ mg/L).....	152

Figure A.3.8 VUV induced discoloration of Red dye under various initial concentrations..	152
.....	
Figure A.3.9 VUV initiated discoloration of Yellow dye ($C_o = 10$ mg/L).....	153
Figure A.3.10 VUV initiated discoloration of Yellow dye ($C_o = 25$ mg/L).....	153
Figure A.3.11 VUV initiated discoloration of Yellow dye ($C_o = 50$ mg/L).....	154
Figure A.3.12 VUV induced discoloration of Yellow dye under various initial concentrations.....	154
Figure A.3.13 Disappearance of Red and Yellow dyes at $C_o = 10$ mg/L.....	155
Figure A.3.14 Disappearance of Red and Yellow dyes at $C_o = 25$ mg/L.....	155
Figure A.3.15 Disappearance of Red and Yellow dyes at $C_o = 50$ mg/..	156
Figure A.3.16 Effects of quartz sleeve on discoloration of Red dye ($C_o = 10$ mg/L...)	156
Figure A.3.17 Effects of quartz sleeve on discoloration of Red dye ($C_o = 25$ mg/L)...	157
Figure A.3.18 Effects of quartz sleeve on discoloration of Red dye ($C_o = 50$ mg/L)...	157

LIST OF TABLES

Table 2.1 Physical and Chemical Properties of Imidacloprid.	7
Table 2.2 Oxidation potential of some oxidants.	21
Table 4.1 List of chemicals.	26
Table 4.2 Specifications and Dimensions of Photoreactor.	32
Table 4.3 Specifications and Dimensions of the VUV lamp.	32
Table 4.4 Dimensions of the High Purity Synthetic Quartz Sleeve.	33
Table 4.5 Temperature gradient profile of GC column.	46
Table 5.1 VUV induced degradation rate constants of Imidacloprid ($C_o = 5$ mg/L) under various flow rate conditions.	55
Table 5.2 VUV induced degradation rate constants of Imidacloprid ($C_o = 5$ mg/L) under various pH conditions.	62
Table 5.3 VUV induced degradation rate constants of Imidacloprid with various initial imidacloprid concentrations.	68
Table 5.4 Reported reduction rates of Imidacloprid by VUV and other AOPs.	69
Table 5.5 VUV induced degradation rate constants of Imidacloprid ($C_o = 5$ mg/L) in presence of inorganic ions.	75
Table 5.6 VUV induced pseudo first order degradation rate constants of Imidacloprid ($C_o = 5$ mg/L) in various water matrices (ultrapure water, tap water, and pond water).	79
Table 5.7 VUV induced Imidacloprid ($C_o = 5$ mg/L) degradation rate constants in oxygenated and deoxygenated solutions.	83
Table 5.8 VUV induced mineralization (TOC reduction) rate constants of Imidacloprid ($C_o = 10$ mg/L) in oxygenated and deoxygenated solutions.	86

Table 5.9 Detected byproducts/fragment ions of imidacloprid in the VUV process by LC/MS Q-TOF analysis.	88
Table 5.10 VUV induced discoloration rate constants of Red dye ($C_o = 10$ mg/L) under various flow rate conditions.	93
Table 5.11 VUV induced discoloration rate constants of Red dye at various concentrations.	98
Table 5.12 VUV induced discoloration rate constants of Yellow dye at various concentrations.	102
Table 5.13 VUV induced discoloration rate constants of Red and Yellow dyes at $C_o = 10$ mg/L initial concentration.	104
Table 5.14 VUV induced discoloration rate constants of Red and Yellow dyes at $C_o = 25$ mg/L initial concentration.	105
Table 5.15 VUV induced discoloration rate constants of Red and Yellow dyes at $C_o = 50$ mg/L initial concentration.	107
Table 5.16 VUV induced discoloration rate constants of Red dye ($C_o = 10$ mg/L) obtained using different materials of quartz sleeve.	109
Table 5.17 VUV induced discoloration rate constants of Red dye ($C_o = 25$ mg/L) obtained using different materials of quartz sleeve.	112
Table 5.18 VUV induced discoloration rate constants of Red dye ($C_o = 50$ mg/L) obtained using different materials of quartz sleeve.	114
Table A.1.1 Separation Condition of Analytical Column.	131
Table A.1.2 Operational Condition of Q-TOF MS.	132

SYMBOLS AND ABBREVIATIONS

Symbols

C_{water}	Concentration of water molecules
C_{methanol}	Initial methanol concentration
Cl^-	Chloride ion
e^-_{aq}	Solvated Electron
$\text{H}\cdot$	Hydrogen Atom
$\text{HO}\cdot$	Hydroxyl Radical
H_2O	Water
H_2O_2	Hydrogen Peroxide
H_2SO_4	Sulphuric Acid
HCl	Hydrochloric Acid
HNO_3	Nitric Acid
k	Rate Constant
k^0_{obs}	Observed 0 th order degradation rate constant
K_{oc}	Soil Sorption Coefficient
K_{ow}	Octanol-Water Partition Coefficient
$\text{KC}_8\text{H}_5\text{O}_4$	Potassium Hydrogen Phthalate
NaOH	Sodium Hydroxide
NO_3^-	Nitrate ion

$\bullet\text{O}^-$	Hydroxyl Radical's conjugate base
O_3	Ozone
P_{VUV}	Photon Flux of VUV Lamp
R^2	Correlation Coefficient
SO_4^{2-}	Sulfate ion
TiO_2	Titanium Dioxide
V	Total irradiated volume
λ	Wavelength
ϕ	Quantum yield
$\phi_{\text{H}_2\text{O}}$	Quantum yield of water photolysis
$\phi_{\text{CH}_3\text{OH}}$	Quantum yield of methanol photolysis
$\xi_{\text{H}_2\text{O}}$	Fraction of photons absorbed by water
$\xi_{\text{CH}_3\text{OH}}$	Fraction of photons absorbed by methanol
$\epsilon_{\text{H}_2\text{O}}$	Molar absorption coefficient of water
$\epsilon_{\text{CH}_3\text{OH}}$	Molar absorption coefficient of methanol

Abbreviations

AA	Acetic Acid
ACN	Acetonitrile
AOP	Advanced Oxidation Process
FA	Formic Acid

GC/MS	Gas Chromatography Mass Spectrometry
HC	Hydrodynamic Cavitation
HC+H ₂ O ₂	Hydrodynamic Cavitation and Hydrogen Peroxide
LC-DAD	Liquid Chromatography equipped with Diode Array Detector
LC/MS	Liquid Chromatography Mass Spectrometry
Q-TOF	Quadrupole Time of Flight Detector
MeOH	Methanol
Red	Synozol Red K-HL
SIM	Selected Ion Monitoring
TOC	Total Organic Carbon
UV	Ultraviolet Light
UV-Vis	Ultraviolet Visible Spectrophotometer
UV/H ₂ O ₂	Ultraviolet Light and Hydrogen Peroxide
UV/O ₃	Ultraviolet Light and Ozone
UV/TiO ₂	Ultraviolet Light and Titanium Dioxide
VUV	Vacuum Ultraviolet Light
Yellow	Synozol Yellow K-HL

1. INTRODUCTION

1.1. Background

Technological improvements have led to production of various chemicals in our daily life. In order to treat various diseases of human and animals as well as to increase production of agriculture and also for other reasons, consumption of these chemicals is necessary. Such chemicals (i.e. pesticides) are called as organic micro pollutants or alternatively as emerging pollutants. The reason why they are called as organic micro pollutants is due to their presence at low concentrations ranging from ppt to ppb in water systems. However, most of anthropogenic chemicals are not easily degradable as they are not designed for and yet such chemicals are persistent to conventional biotic and abiotic treatments. Pharmaceuticals, pesticides, herbicides are examples of the persistent pollutants and are considered to be one of the major threats to water quality [1][2]. In recent years, such pollutants have been detected in various water sources and recognized as serious problem of water sources not generally because of their concentration level but because of their persistent nature. Apparently, consumption of these chemicals have caused environmental pollution specifically water pollution. There is an increasing concern about the presence of such pollutants in aquatic systems since they can impair the quality of water bodies and adversely affect the aquatic organisms.

Fresh water is utmost important for human, flora and fauna lives and yet it is very limited. Only 3 % of water on earth is fresh water and only 0.3 % of fresh water is in rivers [3]. Majority of fresh water resides in glaciers. This very limited amount of fresh water is too valuable and required to be protected from further pollution. Contamination of fresh water by these compounds can be directly or indirectly. Industrial and residential wastewaters cause direct pollution whereas run-off from agricultural lands and leakage from waste lands result in indirect pollution. Among these contaminants, new group of insecticides named neonicotinoids (i.e. imidacloprid) receive a high attention since they are widely used and not easily removed with conventional biological and chemical treatment methods and yet frequently encountered in water sources. Neonicotinoids are synthetic derivatives of nicotine. They have unique physicochemical properties which allow them to be useful for wide range of application. They are mostly used for foliar and seed treatments as well as soil drench and stem application within agriculture and floriculture [4][5][6][7]. They are also present in several household products which are used against

insects, cockroaches, termites as well as parasite treatment of animals [6][8]. Only 1.6 to 20% of applied neonicotinoid insecticides used for soil and seed treatments is uptaken by the plants [9] while majority, 80 to 98.4 %, of them is left in the environment, soil, aquatic system, in which they have raised concerns [10].

They have high solubility value in water matrix. They are able to travel far from discharge points and cause impairments in surface water quality as well as underground water. Moreover, their impact to environment and living beings which are dwell in is not entirely very well understood. Representative of the first generation neonicotinoid insecticides, namely Imidacloprid was placed on the market in 1991 and since its launch, products containing imidacloprid are registered in more than 120 countries for use over 140 agricultural crops, and is one of the fastest growing insecticides in terms of sales [11][7] [12].

So as to minimize adverse effects of insects on agricultural crops and accordingly to be able to increase agricultural production and to meet increasing population's agricultural demand, neonicotinoid insecticides have been widely used in all around the world as well as in Turkey. Neonicotinoid insecticides are applied directly to soil or sprayed over crop fields and hence, released directly to the environment. As a result of these applications, they are entered into soil and consequently into ground water due to their low to medium soil adsorption coefficients or especially into surface water by runoff. Their widespread presence in surface water of several countries including United States, particularly across the agriculturally intensive states, was reported [13]. Biotic environment including human have been exposed to neonicotinoids subsequently.

Imidacloprid is the first introduced neonicotinoid insecticide and the most commonly used one. But, there has been growing concern over the usage of imidacloprid due to its potential adverse effects on bee populations [14][15] [16] and aquatic living organisms [11][17]. Imidacloprid finds its way to water body due to its physico-chemical properties. It is, in deed, frequently found in water sources including rivers and ground water [18][19][20][21]. However, its presence in water resources causes various environmental problems due to its high water solubility and low biological and chemical degradations [22]. Unfortunately, imidacloprid was even found in finished drinking water and tap water in United States [13]. Levels of neonicotinoids (i.e. imidacloprid) residues in drinking water are of public concern with human health risk.

Imidacloprid was included in the priority list of contaminants in United States EPA and watch list substances for European Union-Wide Monitoring. According to the European Union Directive on water quality (COUNCIL DIRECTIVE 98/83/EC), the maximum admissible concentration for each individual pesticide is 0.1 µg/L whereas it is 0.5 µg/L for the sum of pesticides including their metabolites. Since imidacloprid adversely affects various species (bees, nontarget aquatic organisms), shows resistance to conventional chemical and biological oxidations and thus even was found in potable water and poses a potential threat to human, it is very important to effectively remove imidacloprid from water matrices. Therefore, feasible, safer, greener and effective removal of imidacloprid from water is primarily aimed in this doctoral study.

Similar to imidacloprid, reactive textile dyes are commonly exploited in textile industry with the exception of being micro pollutants. Instead reactive dyes can be named among the macro pollutants. Textile industry generates large amount of highly colored wastewater that is generally toxic aquatic lively beings and resistant to be destructed by conventional treatment methods [23]. Synthetic dyes are the major textile industry contaminants to receiving water bodies [24]. Among the synthetic dyes, reactive dyes are widely used in textile industry due to their various properties. The reactive dyes containing highly colored industrial wastewater exerts environmental impacts and hence cause environmental concerns due to the less amount of sunlight penetration and increased oxygen depletion in the water body as well as the persistence to biological decomposition and high hydrolytic stability in nature, and subsequently a longer staying periods in aquatic ecosystems [23][25]. Therefore, such wastewaters produced in textile industry must be treated properly before they are discharged into receiving water body. Effective removal of two reactive dyes (Synozol Red KH-L and Synozol Yellow KH-L) from water is secondarily aimed in this doctoral study.

1.2. Advanced Oxidation Processes

Advanced oxidation processes (AOPs) which basically rely on generation of very reactive and unselective hydroxyl radical (HO•) have been used to treat and oxidize such pollutants effectively. Various combination of oxidants, catalysts, and radiations have been developed (O₃, fenton, photo-fenton, electro photo-fenton, hydrodynamic cavitation (HC), UV/H₂O₂, O₃/H₂O₂, UV/O₃, UV/TiO₂, Vis/TiO₂, UV/O₃/TiO₂, etc.) as AOPs to remove recalcitrant pollutants including imidacloprid from aqueous solutions. All these mentioned AOPs require addition of chemicals, catalysts or combination of them to

generate highly reactive radicals, particularly hydroxyl radical ($\text{HO}\cdot$) which is a very strong oxidant (2.8 V) and capable of oxidizing and mineralizing organic pollutants [26]. However, added chemicals may cause additional challenges for the treatment of water sources and burden on the available budget. pH adjustment and accordingly close monitoring of system's pH, increase in sludge production, additional treatment steps to remove the added chemicals from sludge and/or water/wastewater, management of the chemicals, requirement of skilled personnels, and ect. can be given as examples of the challenges. Nonetheless, these challenges can be and sometimes must be accepted to meet legislative requirements of water and wastewater treatments. Unlike to above mentioned AOPs, vacuum ultraviolet (VUV) irradiation of water generates high concentration of highly reactive $\cdot\text{OH}$ which initiates several simultaneous and sequential advanced oxidation processes with no need of addition of chemicals or catalysts [27].

Conventional treatment methods are not capable to sufficiently remove reactive dyes from aqueous media either [28]. Advanced Oxidation Processes (AOPs) are, on the other hand, the promising technology for effective removal of the reactive dyes from aqueous media. Alternative AOPs, $\text{H}_2\text{O}_2/\text{UV}$, UV/TiO_2 , electron beam irradiation, O_3 , $\text{H}_2\text{O}_2/\text{O}_3$, fenton processes have been utilized for the treatment of such contaminants [23][24][25][28]. Addition of H_2O_2 and O_3 however increases operational expenses like transporting and storing chemicals and risks that may be resulted from handling of chemicals and generating ozone at the site. In contract, Vacuum UV irradiation of water is an alternative and greener AOP.

1.3. Research Summary and Scope

In this PhD thesis study, it is aimed to sustainably and effectively oxidize and remove aqueous imidacloprid from water without addition of oxidants and/or catalysts by using a laboratory scale VUV photooxidation system which consists of a photoreactor, a low pressure mercury lamp, a solution reservoir, a magnetic stirrer, and a peristaltic pump. For this purpose, a low pressure mercury lamp (a VUV lamp) emitting both at 254 nm and 185 nm photons was utilized as an Advanced Oxidation Process (AOP) to produce $\cdot\text{OH}$ in situ and to remove imidacloprid from aqueous solution. Effects of experimental parameters like initial imidacloprid concentration, flow rate and initial pH of the solution, water matrix, presence of inorganic ions (HCO_3^- , CO_3^{2-} , NO_3^-), presence and absence of dissolved oxygen on the VUV induced degradation of aqueous imidacloprid were investigated and determined for the merit of scientific research as well.

Effectiveness of the constructed VUV photooxidation system on discoloration of two reactive textile dyes, Synozol Red KH-L and Synozol Yellow KH-L, was also investigated within the scope of the research.

Detailed information about the objectives of this research is presented in Chapter 3.

1.4. Thesis Structure

This chapter (Chapter 1) describes background information of the thesis subject, application of AOPs for removal of aquatic pollutants, summary and scope of the research.

The following chapter (Chapter 2) presents literature review about imidacloprid, its environmental fate and concerns, its removal from aqueous solutions as well as VUV based AOP.

In Chapter 3, objectives of the thesis are presented

Chapter 4 provides information on the materials and methods used to execute experiments in this doctoral study.

In Chapter 5, results of investigation of the VUV induced photooxidation of aqueous imidacloprid and reactive textile dyes, effects of applied method as well as experimental conditions such as various flow rates, initial pH, initial compound concentration, presence of inorganic ions and natural organic matters, oxygen saturated and oxygen free conditions on the degradation of the tested compounds, imidacloprid and reactive textile dyes, were discussed.

Chapter 6 describes the conclusions of the conducted doctoral study presented in earlier chapters.

Finally, Chapter 7 provides recommendations for the future work.

2. LITERATURE REVIEW

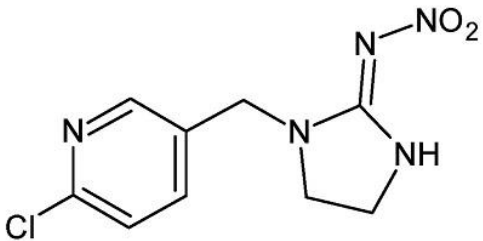
2.1. Neonicotinoids

Neonicotinoids are new group of insecticides, derived from nicotine. Due to their physicochemical properties, they have a wide range of application including seed treatment, foliar treatment, and stem application [5][7]. During the last decade they are the fastest growing insecticides for agricultural application in terms of sales [29]. They in fact contained 24% of insecticide overall and 80% of insecticidal seed treatments of Europe in 2008 [6][30]. They are highly soluble in water and capable of traveling far from where they are discharged and cause contamination in surface water as well as underground water. Supposedly, they are generally low in toxicity to mammals, birds, and fish [31]. They show resistance to conventional biological and chemical treatment methods. Moreover, their impact to environment and water living beings is not entirely very well understood and under the investigation by researchers. The use of Imidacloprid in USA as a first marketed neonicotinoid was approved in 1994 and an almost decade (2004) later four neonicotinoids: imidacloprid, thiacloprid, acetamiprid, and thiamethoxam were approved in the European Union for agricultural use [11][7].

2.2. Imidacloprid

Imidacloprid [1-[(6-Chloro-3-Pyridinyl) methyl]- N-nitro -2- Imidazolidinimine] is an insecticide that was developed to mimic nicotine. Nicotine is naturally found in many plants, including tobacco, and is toxic to insects. Imidacloprid, a new chloronicotinyl compound is used to control and proven to be effective against sucking insects, termites, some soil insects, some species of chewing insects and fleas on pets and utilized for soil treatments, seed dressing, and foliar treatment [32]. Representative of the first generation neonicotinoid insecticides, Imidacloprid was placed on the market in 1991 and since its launch, products containing imidacloprid have gained registrations in about 120 countries for use over 140 agricultural crops, and is one of the fastest growing insecticides in terms of sales [11][12][7]. Physical and chemical properties of Imidacloprid are presented in Table 2.1.

Table 2.1 Physical and Chemical Properties of Imidacloprid[33].

Chemical structure of Imidacloprid	
Molecular weight	255.662 g/mol
Solubility (in water)	610 mg/L at 20 °C
Octanol-Water Partition Coefficient (K _{ow})	0.57 at 21 °C
Vapor pressure	3 x 10 ⁻¹² mmHg at 20 °C
Henry's constant	1.7 x 10 ⁻¹⁰ Pa·m ³ /mol
Soil Sorption Coefficient (K _{oc})	156-960, mean values 249-336
Melting Point	144 °C

Products containing imidacloprid come in many forms, including liquids, granules, dusts, and packages that dissolve in water. Imidacloprid products may be used on agricultural crops and soils, houses, or used in flea products for.

Imidacloprid is a systemic insecticide, which means that plants take it up from the soil or through the leaves and it spreads throughout the plant's stems, leaves, fruit, and flowers. Insects that chew or suck on the treated plants end up eating the imidacloprid as well. Once the insects eat the imidacloprid, it damages their nervous system and they eventually die [34].

Chloronicotinic insecticide Imidacloprid is a relatively stable and has a moderate to high leaching potential. Imidacloprid also has a relatively high water solubility. Therefore, it can pose a risk for pollution to ground and surface water matrices, especially right after

flush flood due to runoff and may eventually cause negative environmental and health effects [35][36]. People could be exposed to imidacloprid if they are applying a product to their gardens, agricultural crops or on a pet. Besides, because imidacloprid is a systemic insecticide, people could be exposed to imidacloprid if they ate the fruit, leaves, or roots of plants that were grown in soil treated with imidacloprid. Reportedly Imidacloprid may cause apathy, spasms and thyroid lesion due to acute exposure [37][38][39].

Imidacloprid is classified as moderately hazardous (Class II) by World Health Organization (WHO). US Environmental Protection Agency (EPA) classified Imidacloprid as moderately toxic by ingestion (oral II), very low toxicity by dermal contact (dermal IV), and variable toxicity by inhalation (inhalation I (aerosol), IV (dust)).

2.2.1. Environmental Fate of Imidacloprid

Imidacloprid can stay variably in soil depending on characteristics of the soil. Sorption of imidacloprid to soil generally increases with soil organic matter content [40]. Sorption tendency also depends on imidacloprid concentration in the soil. Sorption is decreased at high imidacloprid concentrations of soil. As imidacloprid moves away from the area of high concentration, sorption again increases, limiting further movement [41].

Imidacloprid's sorption to soil also decreases in the presence of dissolved organic carbon in soil. The mechanism may be through either competition between the dissolved organic carbon and the imidacloprid for sorption sites in the soil or from interactions between imidacloprid and the organic carbon in solution. Owing medium to high mobility in soil, Imidacloprid may leach from soil into groundwater under some conditions and leaching into ground water would increase in the presence of dissolved organic carbon [42]. Imidacloprid was reported to be found in groundwater in Netherlands and USA.

Imidacloprid is broken down in water by photolysis [40]. Imidacloprid is stable to hydrolysis in acidic or neutral conditions, but hydrolysis increases with increasing alkaline pH and temperature [43].

Volatilization potential of imidacloprid is low due to its low vapor pressure (Table 2.1). Therefore, imidacloprid is not expected to volatilize from water.

2.2.2. Concern of Imidacloprid

Imidacloprid is much more toxic to insects and other invertebrates than it is to mammals and birds because it binds better to the receptors of insect nerve cells [31]. On the other

hands, there has been serious concern because of its impact on bee populations and other beneficial insects [14][15][16][17][44]. Usage of Imidacloprid's commercial product Gaucho following to its widespread use was banned in 1999 for application on sunflower seeds in France after death of 1/3rd of bees. For same reason it was also banned for application onto sweetcorn seeds in 2004. Evidently, bee population has risen again following the ban. Furthermore, in 2008 its usage for some seed treatments was suspended in Germany because of mass bee deaths. Seed drilling application in agricultural land and the dust which was resulted from the drilling application moved over and descended the neighbor crops where the bees reportedly had been feeding. Due to state government of California's pressure in USA Imidacloprid in 2011 voluntarily withdrawn from application on almonds which are major crop for bees. The mobility of lady beetles was also affected and limited by Imidacloprid [38]. Scientists are actively studying the effects of imidacloprid on bees and other invertebrates rigorously.

It has also raised concern due to potential harmful effects on aquatic environment [11][17]. Presence of imidacloprid in water streams causes potential environmental problems due to its high solubility, non biodegradability and persistence in nature [39].

Moreover, it was reported that birds feed on insects have also been exposed to neonicotinoids via food chain [45]. A recent study conducted in Netherland revealed that decrease in population of birds was observed due to application and usage of imidacloprid [46].

Since the first neonicotinoid's launch, contamination of surface waters with neonicatinoids have been observed and increased [47]. Wide application and chemical properties of neonicatinoids have caused their increase in surface waters. Recent nation wide studies conducted in U.S. have revealed that neonicatinoids were detected in 63% of 48 rivers [19][20][21]. Another recent study in U.S. also revealed presence of residual Imidacloprid in surface water. A similar study conducted in Canada has also reported that neonicotinoids were detected in 91% of samples which were collected from various wetlands [18]. Neonicotinoids, especially imidacloprid were also detected in several rivers of Sidney City in Australia [30]. Similar findings were too reported in Netherlands [48], Sweden [49] and Vietnam [50]. 89 to 100% of cases in surface water confirmed the presence of Imidacloprid. And residual concentration of Imidacloprid mostly above the benchmarks for aquatic beings' protection.

Imidacloprid was detected in river that is received effluent of waste water treatment plant of a city located in Spain [51]. This Study has also revealed that conventional waste water treatment plants are not capable of treating imidacloprid effectively and they are also potential direct source of neonicotinoid contamination. Sadaria [22] reported in their study that 6 different neonicotinoids including imidacloprid were poorly removed in conventional wastewater treatment plant and wetland in U.S. Therefore, ineffective removal of neonicotinoids in conventional waste water treatment plants has increased concern of neonicotinoids in water matrices.

A recent study conducted in Iowa U.S. reported very interesting and worrying results that neonicotinoids were not removed properly even in drinking water treatment plants [13]. Ineffective removal of imidacloprid was reported from drinking water samples which were taken from drinking water treatment plants of Iowa University and Iowa City.

Due to widespread application and poor removal with treatment methods human was exposed to neonicotinoids at different concentrations. 1142 neonicotinoids exposure cases were reported between 2000 and 2012 at 6 different poison centers located in Texas, U.S. 77% of these cases were imidacloprid exposures [52].

2.2.3. Imidacloprid removal from aqueous solution

Imidacloprid either in standard form or in commercial product form (i.e. Confidor) is susceptible to photolytic irradiation as well as photocatalytic and other advanced oxidation processes. Moza [53]; Wamhoff and Schneider [54], Schippers and Schwack [55], Wei [56], Lavine [57] used different light sources for photolytic irradiation of aqueous imidacloprid and reported first order degradation pattern with several photoproducts.

Early study of photolysis of aqueous imidacloprid solution was executed by Moza [53] with utilization of high pressure mercury lamp ($\lambda \geq 290\text{nm}$). 2 mg/L initial imidacloprid concentration in deionized water with total volume of 200 mL was irradiated during 4 hours of reaction time. First order disappearance rate constant of imidacloprid was reported as $1.6 \times 10^{-4} \text{ s}^{-1}$. 4 hours of irradiation resulted in 90% removal of initial imidacloprid along with several photoproducts.

Another photolysis study of standard imidacloprid ($C_0 = 1.5 \times 10^{-3} \text{ M}$) and Confidor imidacloprid ($C_0 = 1.5 \times 10^{-3} \text{ M}$) by Wamhoff and Schneider [53] was exercised utilizing the sunlight with duration of 650 min reaction time. They used HPLC grade water and

tap water for photolysis experiments. They also tried to enhance Confidor imidacloprid degradation in tap water by applying TiO_2 . Rate constant of standard Imidacloprid photolysis in HPLC grade water was recorded as $105.8 \times 10^{-3} \text{ s}^{-1}$ with first order degradation kinetic. Commercial product imidacloprid experiment in tap water resulted much slower rate constant of $5.5 \times 10^{-3} \text{ s}^{-1}$. When TiO_2 added to Confidor imidacloprid solution, rate constant was unexpectedly decreased further down to $4.8 \times 10^{-3} \text{ s}^{-1}$. First order disappearance was also observed for Confidor imidacloprid degradation.

Wei [56] investigated direct photolysis and sensitized photooxidation of aqueous imidacloprid solution via middle pressure lamp, UV lamp and black light fluorescent lamp respectively. Different intensity of lamps (24 W and 125 W), wavelengths (254 nm and 365 nm) as well as sensitizers (TiO_2 , acetone, and H_2O_2) were studied to observe their effects on disappearance of dissolved imidacloprid. Higher light intensity at the same wavelength (254 nm) shortened half life of aqueous imidacloprid from 9 to 5.4 min. On the other hand, half life of imidacloprid was increased notably to ≈ 1090 min by higher wavelength of 365 nm at the same light intensity (24 W). 6.4×10^{-4} , 0.077, and 0.128 min^{-1} first order photolysis rate constants were observed for black light fluorescent lamp (24 W, 365 nm), UV lamp (24 W, 254 nm), and middle pressure lamp (125 W, 254 nm) respectively. Studied initial imidacloprid concentration of 20 mg/L in 200 mL doubly distilled water was fully removed in quartz reactor by direct UV photolysis after 40 min of irradiation. TiO_2 and black light fluorescent lamp induced photocatalysis of imidacloprid achieved the highest degradation comparing to other sensitizers (acetone and H_2O_2).

Dell'Arciprete [59] studied photolysis of aqueous imidacloprid along with two other neonicotinoids in the presence and absence of H_2O_2 . In order to produce hydroxyl radical ($\text{HO}\cdot$) in the photooxidation system, H_2O_2 was added into the solution and subjected to irradiation of low pressure mercury lamp (UV lamp, $\lambda_{\text{max}} = 254 \text{ nm}$). 80 mg/L imidacloprid solution with volume of 250 mL was irradiated by the UV lamp during the photolysis experiments of 3 hours. On the other hand, photooxidation experiments which rely on $\text{HO}\cdot$ initiated reaction of the target compound were carried out using 5 mM initial concentration of H_2O_2 by keeping all the other experimental conditions of the photolysis unchanged. Experiments were executed at original pH (close to neutrality) values of the tested solutions. Pseudo first order kinetic pattern was reported for depletion of

imidacloprid with observed rate constants of $9.2 \times 10^{-4} \text{ s}^{-1}$ and $1.2 \times 10^{-3} \text{ s}^{-1}$ for the photolysis and the photooxidation of aqueous imidacloprid respectively.

Another set of experiment, namely flash photolysis was executed to determine rate constants of the reaction between $\text{HO}\cdot$ and imidacloprid. Thiocyanate ion (SCN^-) was used as $\text{HO}\cdot$ scavenger in the competition method so as to determine rate constant of imidacloprid with $\text{HO}\cdot$. Diffusion controlled rate constant of $6 \times 10^{10} \text{ M}^{-1} \text{ s}^{-1}$ was reported for the reaction of $\text{HO}\cdot$ and imidacloprid.

Several byproducts of imidacloprid were reported by Dell'Arciprete [59] as in line with what was reported by other researchers. TOC reduction analysis of aqueous imidacloprid confirmed the production of the byproducts since extent of mineralization was very low (< 3%).

More recent photolysis study of aqueous imidacloprid along with its reduction products in doubly distilled water was exercised by Lavine [57]. $2 \times 10^{-4} \text{ M}$ initial concentration of imidacloprid with 300 mL volume was subjected to irradiation of UV lamp with a quartz filter (wavelength $\geq 210 \text{ nm}$) to simulate sunlight. Similar to other photolysis studies first order reaction kinetic was observed along with several photoproducts. It took 2 hours to degrade imidacloprid from aqueous solution with disappearance half life of 0.314 h.

Literature review shows that mostly TiO_2 in various state and form as well as ZnO and other catalysts were used for photocatalytic degradation experiments [7] [60][61][12][62] [63][64]. As in the case of photolytic irradiation, first order degradation pattern was observed along with organic byproducts for photocatalytic application as well.

Aguera [60] studied photocatalytic potential of TiO_2 and natural sunlight on aqueous imidacloprid and commercial product Confidor Imidacloprid degradation in a pilot plant. Experimental aqueous solutions with 50 mg/L initial imidacloprid concentration were prepared with water received from Desalination Plant. They used Confidor Imidacloprid directly to prepare experimental solution without extracting Imidacloprid from commercial formulation that also contains other ingredients. They exposed the imidacloprid solution to sunlight from 9 am to 6 pm. Entire degradation of Confidor Imidacloprid ($C_0 = 50 \text{ mg/L}$) was experienced after 270 min photocatalytic natural sunlight irradiation with initial TiO_2 concentration of 210 mg/L. In contrast, complete removal of standard imidacloprid solution with same initial concentration was achieved

after 140 min. The observed difference in reduction rate was attributed to presence of coexisting compounds in formulated Confidor solution since they competed with imidacloprid for hydroxyl radicals (HO•).

Mineralization study by monitoring TOC reduction was also investigated. It took more than 700 min to decrease 90% of initial TOC for Confidor Imidacloprid solution ($C_0 = 50$ mg/L) under natural light induced photocatalytic degradation whereas 200 min was enough for same level of removal in case of standard Imidacloprid.

Typically mineralization rate is lower than degradation rate as also was in the case of this study. This result showed the existence of byproducts which were stable to applied photocatalytic TiO₂ and natural sunlight irradiation. Performed analytical measurements also confirmed several degradation products. Photocatalytic irradiation required 450 min to completely degrade the byproducts of Confidor Imidacloprid solution ($C_0 = 50$ mg/L).

Degradation and mineralization of aqueous imidacloprid with 20 mg/L initial concentration in doubly distilled water was investigated using photoelectrocatalytic (TiO₂/Ti electrodes and +1.5 V applied potential) process under irradiation of UVA lamp with max at 365 nm in a batch type photoelectrochemical reactor by Phillippidis [62]. Application of photoelectrocatalytic process resulted significant enhancement (249% increment) in observed rate constant of aqueous imidacloprid disappearance compared to those observed with photolytic and photocatalytic processes. Spectrophotometrically followed photoelectrocatalytic degradation of imidacloprid fitted to first order kinetic regime with rate constant of 0.00936 min⁻¹ at initial pH 5.6. Higher rate constant was reported for photoelectrocatalytic degradation in acidic condition. Shifting initial pH of test solution from 3 to 9 resulted significant decrease in photoelectrocatalytically induced degradation rate constant of Imidacloprid from 0.01362 min⁻¹ to 0.00252 min⁻¹. 82% of initial imidacloprid ($C_0 = 20$ mg/L) was removed from the tested solution after 3 hours of photoelectrocatalytic oxidation. Even though application of photoelectrocatalytic process improved dissolved organic carbon (DOC) reduction compared to photolytic and photocatalytic treatments, it was also still low in terms of mineralization efficiency. It achieved only 66% decrease after 18 h of photoelectrocatalytic oxidation while photocatalytic treatment resulted only 36%.

Another research [7] investigated photocatalytic removal of imidacloprid along with two other neonicotinoids (thiamethoxam and clothianidin) by utilizing 6 low-pressure

mercury fluorescent lamps with UVA (max. at 355 nm) radiation and immobilized titanium dioxide (TiO₂). Double deionized water was used for preparation of aqueous solution of neonicotinoids with initial concentration of 100 mg/L for degradation experiments. Photocatalytic irradiation was executed up to 120 minutes. All tested neonicotinoids, imidacloprid being the highest removed insecticide were effectively disappeared after 120 minutes of irradiation. Photocatalytic degradation with immobilized TiO₂ successfully performed 98.8% imidacloprid disappearance within 2 hours of treatment. Observed rate constant of Imidacloprid decay which followed the first order kinetic regime was recorded as 0.035 min⁻¹.

Efficiency of mineralization was monitored by measurements of total organic carbon (TOC). However, the rate of mineralization was low for all tested neonicotinoids. Even though the highest mineralization was experienced for Imidacloprid, achieved TOC reduction of imidacloprid was only 19.1% after 2 hours of photocatalytic degradation with immobilized TiO₂. This finding points out that other organic byproducts were formed from Imidacloprid as in the case of other reported studies. Existence of organic byproducts were also determined via chromatographic measurements.

Fenoll [63] investigated zinc oxide (ZnO, 200 mg/L) and titanium dioxide (TiO₂, 200 mg/L) induced photocatalytic degradation of aqueous imidacloprid (C₀ = 0.1 mg/L) along with 2 other neonicotinoids by applying natural light and UV artificial light (8W low pressure mercury lamp with major emission output at 366 nm) irradiation of 2 hours. ZnO achieved better reduction result than TiO₂ in terms of effect of catalysts. Application of Sodium Persulfate (Na₂S₂O₈, 250 mg/L) as electron acceptor along with the catalysts considerably increased removal rate of imidacloprid compared to individual ZnO and TiO₂ based photocatalysis. ZnO/Na₂S₂O₈ and TiO₂/Na₂S₂O₈ application under UV light irradiation succeeded total degradation of all neonicotinoids in 10 and 30 min respectively. Imidacloprid had the highest disappearance rate constant among the tested neonicotinoids via applied systems. In terms of neonicotinoids removal efficiency, solar irradiation gave better result than artificial light since greater percentage of solar light was absorbed by catalysts compared to UV light. Observed degradation kinetic fitted pseudo first order with rate constants of Imidacloprid varied from 0.0171 min⁻¹ (TiO₂ under UV light) to 2.4110 min⁻¹ (ZnO/Na₂S₂O₈ under solar light) under different light sources and various catalysts. The highest apparent reduction rate constant (2.4110 min⁻¹) of imidacloprid was experienced during ZnO/Na₂S₂O₈ treatment under solar light with half life of 0.3 min.

DOC analysis revealed low mineralization efficiency of the tested systems along with production of several byproducts which were also detected by analytical measurements.

Amir Akbari Shorgoli and Mohammad Shokri [64] more recently studied photocatalytic degradation as well as mineralization of aqueous imidacloprid (30% purity) with immobilized TiO₂ nanoparticles (C_o = 200 mg/L) in presence of UVC light (max at 254 nm). 400 mL volume of various initial imidacloprid concentrations (20, 40, and 60 mg/L) were illuminated via 15 W UVC lamp during 180 min of treatment time to assess efficiency of immobilized TiO₂ nanoparticles on photocatalytic oxidation of imidacloprid. Disappearance of aqueous imidacloprid was followed spectrophotometrically at its absorbance peak (270 nm). Observed degradation kinetic of imidacloprid followed pseudo first order for all studied initial concentrations and associated rate constants of 0.0704, 0.0594, and 0.0445 min⁻¹ were respectively reported for 20, 40, and 60 mg/L of initial imidacloprid concentrations during 30 min of reaction. As expected, the highest reduction was observed at the lowest initial concentration tested. Decrement of initial pH of the tested solution from 8 to 5 resulted marginal increment in the oxidation efficiency. 68% mineralization (TOC reduction) after 180 min reaction was achieved by the tested photocatalytic method whereas observed degradation of aqueous imidacloprid (C_o = 20 mg/L) was 90.24% at the same time period. This result revealed the generation of organic byproducts from imidacloprid by the studied photocatalytic method.

Research [65] was conducted on ozonation of imidacloprid in ultrapure water - acetonitrile mixture (99:1, v/v). 25, 50, and 100 g/m³ ozone concentrations in the inlet gas were applied to 39 mg/L initial imidacloprid concentration during 90 minutes of treatment time. Pseudo-first order reaction with reaction rates of 0.147 and 0.129 min⁻¹ for standard imidacloprid solution and seed loading solution were calculated respectively when concentration of ozone was 100 g/m³. Applied 100 g/m³ ozone concentration resulted more than 99% imidacloprid removal in both tested solutions at 45 minutes of reaction with ozone.

Applied 50 and 25 g/m³ inlet ozone concentration resulted 99.9 and 96.5% degradation of seed loading solution respectively at 90 minutes of ozonation. However, to reach 99.8% degradation, it took 45 minutes for 100 g/m³ ozone concentration. Determined degradation rate constants of seed loading solution were 0.036, 0.071 and 0.129 min⁻¹ for 25, 50 and 100 g/m³ ozone concentrations respectively. It was reported that thirteen degradation products were observed during the ozonation.

A recent study [66] focused on degradation of aqueous imidacloprid solution via hydrodynamic cavitation (HC) and combination of HC along with several AOPs (HC+fenton, HC+photofenton, HC+photolytic, and HC+photocatalytic). Influence of inlet pressure (5–20 bar) and operating pH (2–7.5) were initially investigated and optimized during 2 hours of HC alone experiments. Reported experiments were executed with 5 L imidacloprid solution having initial concentration of 25 mg/L. Optimum inlet pressure and solution pH of HC were found experimentally as 15 bar and 2.7. Further decrement in solution pH from 2.7 to 2 achieved an only slight increase in removal. Unlike to pH, increase of inlet pressure beyond 15 bar resulted a decrease in degradation. Experimentally determined these optimal conditions were applied to subsequent combined HC and AOP processes. Same amount of solution volume and initial concentration of Imidacloprid were exercised during the followingly performed experiments as well. First order degradation of imidacloprid was observed during the HC alone application. 26.24% imidacloprid removal was obtained with reaction rate constant of $2.565 \times 10^{-3} \text{ min}^{-1}$ after 120 minute of HC treatment.

Substantial enhancement in the disappearance rate of imidacloprid was observed via HC + Fenton process which resulted an almost 98% removal of imidacloprid in 15 min recorded with reaction rate constant of $250.749 \times 10^{-3} \text{ min}^{-1}$ using applied molar ratio of imidacloprid:H₂O₂ as 1:40. First order degradation pattern was also observed for HC + Fenton treatment method. Removal rate of imidacloprid increases with an increment in the molar ratio of imidacloprid:H₂O₂ till 1:40 and decreases at the 1:50. Optimal molar ratio was reported as 1:40. On the other hand, fenton process itself without HC was able to remove only 64.43% percent of initial imidacloprid with rate constant of $66.711 \times 10^{-3} \text{ min}^{-1}$ during the same period of time.

Expected increment in degradation rate of imidacloprid was experienced for HC + photofenton process as well. Photo-fenton treatment of aqueous imidacloprid degraded 81.60% of initial concentration recorded with $99.372 \times 10^{-3} \text{ min}^{-1}$ rate constant in 15 min of reaction time. Combination of photo-fenton with HC however, concluded 99.23% removal along with $297.012 \times 10^{-3} \text{ min}^{-1}$ rate constant at the same experiment time. First order degradation was reported for HC + photo-fenton process as well.

Increased removal rate constants and percentages were also experienced by applying combined HC + photolytic and HC + photocatalytic processes compared to individual

photolytic and photocatalytic processes. 200 mg/L niobium pentoxide (Nb_2O_5) was used as catalyst both in photocatalytic and HC + photocatalytic processes. 45.46% and 55.18% imidacloprid degradation was recorded after 120 min of treatment for photolytic and photocatalytic methods respectively. Likewise to aforementioned processes, first order degradation regimes were also observed with $5.034 \times 10^{-3} \text{ min}^{-1}$ and with $6.837 \times 10^{-3} \text{ min}^{-1}$ rate constants for photolytic and photocatalytic processes respectively.

Effectiveness of the tested processes were also investigated and compared in regards of mineralization potential during the disappearance of imidacloprid. Treatment of imidacloprid by HC resulted very small reduction (9.89%) in TOC even after 3 hours of operation. Low mineralization capacity of HC indicated presence of organic byproducts that showed resistance to further degradation by HC. Higher extents of mineralization of 48.25% and 48.96% were observed for combined HC + Fenton, HC + Photofenton respectively. The results showed that combined AOPs substantially increased TOC elimination as compared to HC alone process. Although HC + photolytic, and HC + photocatalytic processes were capable of reducing TOC at higher degree than individual HC, they were still not effective in terms of mineralization. Only small portion of imidacloprid, 13.34% and 19.78% were mineralized by HC + photolytic, and HC + photocatalytic processes respectively. Hybrid HC + Fenton, HC + Photofenton processes were the most effective ones among the tested processes. Overall results showed that generated intermediate or endproducts were stable to further degradation by the all tested processes.

Iglesias [67] investigated disappearance of aqueous imidacloprid in distilled water under electro-Fenton system with ironalginate gel beads (EF-FeAB). 100 mg/L initial concentration of standard imidacloprid was degraded in a batch electro-Fenton reactor with 150 mL effective volume. Various initial FeAB concentration as well as initial pH of solution were executed to report their effects on degradation of imidacloprid. Higher removal of imidacloprid was observed by lowering the initial FeAB load within the exercised range (4.27 – 16.84 g). 95 % imidacloprid reduction was experienced for all tested FeAB load under electro-Fenton oxidation. Acidic condition was more favorable for reduction of imidacloprid under the tested pH range (2 – 7). Increment in degradation efficiency was observed with decrement in initial pH of solution. First order degradation pattern was observed for imidacloprid under the electro-Fenton process with immobilized Fe ions (EF-FeAB) oxidation as well as for electro-Fenton with free Fe ions and

electrochemical processes. Increase of reduction rate constant in the order of EF-FeAB > EF with free ions > electrochemical processes was reported with 0.0405 min^{-1} , 0.0264 min^{-1} , 0.0112 min^{-1} respectively in 120 min of treatment.

Disappearance and mineralization of aqueous imidacloprid with initial concentration of 20 mg/L were investigated by Patil [68] using ultrasound (US) based oxidation processes individually or combination with several AOPs (US+H₂O₂, US+CuO, US+Advanced Fenton Process (AFP), US+ H₂O₂+UV (max. at 365 nm). Laboratory scale ultrasonic horn and larger scale ultrasonic bath were utilized as source of sonication to treat 100 mL and 7 L aqueous imidacloprid solution respectively. Various initial pH of solution, copper oxide (CuO) loading, H₂O₂ loading experiments were carried out to determine their effects on the degradation of aqueous imidacloprid as well as to optimize the experimental conditions. US driven reduction of aqueous imidacloprid increased by decreasing initial pH of solution under the tested pH range (3 – 11). Switching solution pH value from 11 to 3 resulted substantial increment in removal from 38% to 68.7% during 2 hours of US treatment. Since there was only slight increase in removal of imidacloprid at pH 3 as compared to pH 5 (66.8% reduction), further experiments were carried out at pH 5 as chosen optimized value. Increasing H₂O₂ concentration from 15 to 35 mg/L resulted higher reduction of imidacloprid. However, 80 mg/L H₂O₂ did not improve the removal, actually slight decrement was observed compared to 35 mg/L. Therefore, 35 mg/L was determined as optimal H₂O₂ loading. Similarly, increasing CuO concentration from 250 mg/L to 2000 mg/L resulted higher degradation from 68.8% to 77.7%. Defined optimal conditions were used in subsequent experiments. Higher degradation yield of aqueous imidacloprid was observed for combined processes especially for US+H₂O₂, US+AFP, and US+UV+ H₂O₂. The highest degradation efficiency (98.5%) and extent of mineralization (79% TOC reduction) were recorded for US+UV+ H₂O₂ oxidation process during 2 hours of treatment. 66.8%, 77.7%, 92.7%, 96.5%, and 98.5% degradation of aqueous imidacloprid was reported for US, US+CuO, US+H₂O₂, US+AFP, and US+H₂O₂+UV respectively. First order degradation kinetic of imidacloprid was reported under the all tested methods with exception of second order kinetic under US+AFP. Observed first order rate constants were $0.008861 \text{ min}^{-1}$, 0.0127 min^{-1} , 0.02695 min^{-1} , 0.039 min^{-1} for US, US+CuO, US+H₂O₂, and US+ H₂O₂+UV respectively. Observed second order rate constant of US+AFP was reported as $0.01282 \text{ min}^{-1} \text{ L/g}$. As in the case of degradation efficiency, extent of mineralization (TOC reduction) was reported to

increase in the same order for the all tested processes. Substantial increment was observed in TOC reduction (71%) of imidacloprid solution via US+AFP process after 2 hours of treatment as compared to 15% reduction obtained by individual US. Lastly, higher degradation yield of aqueous imidacloprid was experienced via ultrasonic horn in comparison to ultrasonic bath due to higher cavitation capacity of ultrasonic horn.

Even though same order of reaction was experienced by all these authors, rate constants were different owing to application of different reactor designs, amount of catalyasts, lamp powers and intensities, radiation sources and wavelengths. Furthermore, mineralization degree of aqueous imidacloprid with sunlight or UV light induced direct photolysis was quite low. On the other hand, effectiveness of photocatalytic oxidation on imidacloprid mineralization showed differences from low to medium level.

So, not only full degradation but also high mineralization of aqueous imidacloprid via any treatment method would make big difference in environmental fate of imidacloprid and associated concerns as well as protection of water resources and lively beings and in turn human helth.

Our goal was to investigate photodegradation of imidacloprid in aqueous solution by VUV induced photooxidation and to determine removal efficiency and rate constant of the process. Furthermore, effects of initial imidacloprid concentration, flow rate, initial pH and dissolved oxygen, presence of commonly found inorganic ions, water matrix, presence and absence of dissolved oxygen were investigated. Lastly, we tried to determine degradation products of imidacloprid with VUV photolysis.

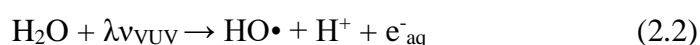
2.3. Vacuum UV based Advanced Oxidation Process (AOP)

Vacuum UV based Advanced Oxidation Process (AOP) has gained importance to treat contaminants in water since it does not require addition of catalyst or other chemicals for the generation of highly reactive hydroxyl radicals ($\text{HO}\cdot$) in contrast to other AOPs. VUV photolysis is in fact, a photochemical process just like UV photolysis. But, photons of the VUV lamp, namely, 185 nm photons are primarily absorbed by water molecules in water based system and degradation of contaminats are initiated by $\text{HO}\cdot$ whereas in UV photolysis, photons (254 nm photons) are mainly absorbed by the target contaminats which are then excited and degraded accordingly. The reason behind absorption of VUV photons mainly by water molecules is that water has high absorptivity at vacuum-uv range ($100 \text{ nm} < \lambda < 200 \text{ nm}$) and typically has a higher molar concentration (55.5 M) compared

to the contaminants in aqueous solution. Due to high absorption coefficient of water at this wavelength, 90% of 185 nm radiation is absorbed at approximately 5.5 mm thick water layer close to the VUV lamp surface [69]. Low penetration depth of the VUV irradiation into water solution is main drawback of the VUV induced AOP. As a result, any reactor either flow through annular photoreactor or else which has diameter > 5.5 mm in radiation direction will have two separate reaction zones. The first zone which is closer to the lamp surface, is where VUV photolysis of water takes place and accordingly is where highly reactive and non-selective oxidant HO• and other radicals (H•, e⁻_{aq}) which are responsible of oxidation and mineralization of compounds in water are produced.

Low pressure mercury lamps with special high purity quartz envelope, in other words Vacuum UV lamps, generate high energy photons (i.e. 185 nm photon). Spectral irradiance output of low pressure mercury lamps at 185 nm wavelength is reportedly around 8 to 10% of the irradiance at 254 nm. Nevertheless, photonic energy at 185 nm is greater than that of 254 nm. Produced high photonic energy (6.7 eV) is transferred to the water molecule since it exhibits high absorption at these short wavelengths. As a result, water molecule is excited and high concentration of highly reactive •OH radical is produced due to deactivation of the excited water molecule without adding any other chemical reagent or catalysts [70].

VUV light induced water photolysis occurs via water homolysis (2.1) and water ionization (2.2).



The Quantum yield in other words, quantum efficiency of 185 nm reported for the formation of •OH radical is 0.33 [71][27] and 0.045 [27] for water homolysis (equation 2.1) and water ionization (equation 2.2), respectively.

The hydroxyl radical (HO•) is one of the most powerful non-selective oxidants. It has the second largest oxidation potential, with a value of 2.80 V [72][73], after fluorine (Table 2.2). HO• reacts rapidly and unselectively with other organic substances with reaction rate constants in the order of 10⁸ to 10¹⁰ M⁻¹ s⁻¹ [74]. HO• basically reacts with organic compounds by three different ways; 1. addition of HO• to double bonds, 2. H-atoms

abstraction, which yields carbon centered radical 3. reaction mechanisms where HO• acquires an electron from an organic substance.

Table 2.2 Oxidation potential of some oxidants [75].

Oxidant	Oxidation potential [V]
Fluorine	3.06
Hydroxyl radical	2.8
Ozone	2.07
Hydrogen Peroxide	1.8
Chlorine Dioxide	1.5
Chlorine	1.4

Generation of highly reactive HO• by VUV lamp with no addition of chemicals or catalysts is very appealing for feasible, greener, and safer treatment of water with AOP since it eliminates transportation, storage, handling of chemicals and associated costs as in the case of other AOPs.

2.3.1. VUV based photooxidation (removal) of organic pollutants

VUV photolysis was found to be a promising method in the decomposition of contaminants from aqueous water and wastewater solutions.

Al-Momani [76] investigated VUV photolysis of three textile commercial dye families, namely Intracron reactive dyes, Direct dyes, and Nylanthrene acid dyes along with actual textile industry wastewater that contains mixture of the same dyes. Initial BOD₅/COD values of the all studied textile dye solutions and the industrial wastewater were either zero or almost zero which means that they are not practically biodegradable. 100 mg/L initial concentration of 420 mL textile dye solution was irradiated by a low pressure mercury lamp (VUV lamp, 120 W) which emits both 254 nm and 185 nm photons, in batch operating circular photoreactor. Experimentation was executed at room temperature without buffering pH of the dye solution. Color disappearance of the tested dye solutions and the textile industry wastewater was followed by a UV Vis spectrophotometer. ≥90 % discoloration of all the tested textile dyes was achieved by the VUV lamp induced photooxidation after 7.5 minutes of treatment time while it took 13 minutes to reach same

level of color removal for the actual textile wastewater. Intracron reactive dye family was the most susceptible one for the VUV illumination whereas Nylanthrene acid dyes were the least. Apparently, biodegradability of the dye solutions and the textile wastewater were increased by the VUV irradiation. Meanwhile, more or less 30 % COD elimination of the dye solutions was achieved for the time (7.5 min) required for ≥ 90 % discoloration. On the other hand, 18 % COD reduction of the real textile wastewater was observed after 13 minutes of VUV irradiation. They also compared UV and VUV photolysis in terms of COD reduction of the experimental solutions. In order to block 185 nm photon of the same VUV lamp they used Infrasil quartz. Therefore, only irradiation of 254 nm light reached the solutions to study UV photolysis of the solutions. The VUV photolysis (185 nm + 254 nm) was superior to UV one (only 254 nm) in reduction of the textile dyes. 25 % decrement was observed via UV photolysis compared to the VUV one.

Azrague and Osterhus [2] examined UV, VUV photolysis, and semiconductor TiO_2 based photocatalytic oxidation of two organic micro pollutants, sulfamethoxazole and atrazine, from natural water. In addition, effectiveness of the tested processes on the degradation of para-chlorobenzoic acid (pCBA) which is usually used as probe compound for OH in AOPs were investigated in both natural and distilled water. Effects of solution pH which is an important parameter in AOPs and dissolved organic carbon (DOC) were examined as well. Experimentation was carried out using a circular type photoreactor which had 340 mL effective solution volume, working in batch mode. Photolytic and photocatalytic experiments were exercised in presence and absence of immobilized TiO_2 . Two 15 W low pressure mercury lamps emitting only at 254 nm and both at 185/254nm were utilized as source of photons and located at the center of the photoreactor. Experimental solutions were circulated through the photoreactor under turbulent flow regime during the degradation of the tested compounds.

In terms of degradation efficiency of sulfamethoxazole, atrazine, and pCBA, the VUV photolysis was reported to be the most effective one for all three tested compounds. Pseudo first order kinetic pattern was observed for the investigated pollutants via applied treatment processes. Higher degradation rate of pCBA via VUV irradiation was observed at lower pH of buffered experimental solution. Presence of DOC originating from natural organic matter (NOM) resulted decrement in removal rate since NOM consumed some of the available radicals (i.e. OH) produced upon irradiation. They also studied effects of total inorganic carbon (TIC) by adding appropriate amount of NaHCO_3 on reduction

efficiency. Apparently, degradation rate constants of the all tested pollutants showed decrement because of reactions took place between OH and carbonic species (carbonate (CO_3^{2-}) and bicarbonate (HCO_3^-)). However, influence of DOC onto degradation of the pollutants was reported to be greater than TIC.

Photolysis of two taste and odour compounds, geosmin and 2-methylisoborneol (2-MIB), by 11 W low pressure mercury UV (254 nm) and VUV (185 + 254 nm) lamps in ultrapure and natural water was studied by Kutschera [77]. Effects of various solution pH (3 to 11) modified using HCl and/or NaOH, were also investigated. 100 ng/L initial concentration of geosmin and 2-MIB solutions with total volume of 100 mL were circulated in laboratory scale flow through photoreactor during experimentation. UV photolysis was reported to be inadequate to degrade the tested compounds while VUV induced photooxidation was very effective in contrast. The VUV process was able to fully degrade the both tested pollutants in reaction time of 30 second. Pseudo first order kinetic pattern was reported for degradation of the both pollutants via VUV photolysis. Observed reduction rate constant of geosmin was greater than that of 2-MIB, which was attributed to the higher reaction rate constant of geosmin with OH compared to reaction rate constant of 2-MIB. Rate constants of the both pollutants were lower in natural water due to presence of natural organic matter (NOM) which showed scavenging effects of OH produced by VUV photolysis of water molecule. This finding was also confirmed by increasing dissolved organic carbon content of experimental solutions in ultrapure water which accompanied decreased rate constants of the pollutants. Moreover, presence of bicarbonate, also a well known OH scavenger, using potassium hydrogen carbonate in ultrapure water lowered the apparent rate constants. Evidently, water matrix played an important role in the degradation of the pollutants in VUV initiated AOP.

3. RESEARCH OBJECTIVES

Primary goal of this doctoral study was to effectively degrade imidacloprid from water (ultrapure water, tap water, and pond water) safely and environmentally without addition of catalysts or chemicals by a VUV lamp that emits both at 254 nm and 185 nm wavelengths as an AOP. Additionally, effects of various experimental parameters, flow rate, initial pH of solution, initial concentration, presence of inorganic ions (HCO_3^- , CO_3^{2-} and NO_3^-), water matrix, presence and absence of dissolved oxygen on the VUV induced photooxidation of imidacloprid were investigated. Degradation kinetic, rate constant and removal percentage of dissolved imidacloprid were examined in flow through photooxidation system and reported accordingly.

Independent performance verification of the VUV based AOP was executed by discoloration of commercially available reactive textile dyes (Synozol Red KH-L and Synozol Yellow KH-L) in water. As in the case of imidacloprid degradation, kinetic regime, rate constant, and removal percentage were examined and presented as a part of this doctoral thesis.

Lastly, Effects of sleeve materials (clear fused quartz and high purity synthetic quartz) were also investigated during the discoloration studies and comparison of observed rates and disappearance percentages were reported as well.

In this perspective, overall objectives were:

- To investigate effectiveness of VUV lamps to degrade and remove imidacloprid from water
- To compare observed VUV induced reaction kinetic and rate constant of imidacloprid with previously reported ones that were obtained via other AOPs and treatment methods
- To investigate effects of different initial imidacloprid concentration on VUV induced degradation of imidacloprid
- To investigate effects of different flow rates and initial pH values of experimental solution on VUV induced degradation of imidacloprid
- To investigate effects of presence and absence of dissolved oxygen on VUV induced degradation and mineralization of imidacloprid

- To investigate effects of water matrices on removal of imidacloprid by VUV lamp
- To investigate effects of inorganic ions (HCO_3^- , CO_3^{2-} , and NO_3^-) on imidacloprid disappearance rate
- To investigate effectiveness of VUV lamps to discolor reactive textile dyes from water
- To compare effects of quartz and high purity synthetic quartz on discoloration of the textile dyes

4. MATERIALS AND METHODS

4.1. Chemicals

The chemicals used in this doctoral study and their purity along with supplier information are listed in Table 4.1. The chemicals were used as received from the suppliers.

Table 4.1 List of chemicals.

Chemical	Purity	Supplier
Imidacloprid (C ₉ H ₁₀ ClN ₅ O ₂)	Analytical Standard (99.8%, w/w)	Dr. Ehrenstorfer
Imidacloprid (C ₉ H ₁₀ ClN ₅ O ₂)	Analytical Standard (99.8%, w/w)	Bayer Corp Science (Turkey)
Confidor SC 350 (Imidacloprid)	Not reported	Commercially available insecticide
Methanol (CH ₃ OH)	≥%99.9, gradient grade for LC-MS	Merck
Acetonitrile (C ₂ H ₃ N)	≥%99.9, hypergrade for LC-MS	Merck
Sulfuric Acid (H ₂ SO ₄)	95-97%	Merck
Hydrochloric Acid (HCl)	37-38%	Sigma Aldrich
Nitric Acid (HNO ₃)	65%	Merck
Formic Acid (CH ₂ O ₂)	Reagent	Agilent Technologies
Acetic Acid (C ₂ H ₄ O ₂)	99.88-100.5%, puriss	Sigma Aldrich

Chemical	Purity	Supplier
Sodium Hydroxide (NaOH)	98-100.5%, puriss	Sigma Aldrich
Sodium Bicarbonate (NaHCO ₃)	≥%99.7, ACS reagent	Sigma Aldrich
Sodium Carbonate (Na ₂ CO ₃)	99.5-100.5%, puriss	Sigma Aldrich
Sodium Nitrate (NaNO ₃)	99-100.5%, extra pure	Merck
Potassium Hydrogen Phthalate (C ₈ H ₅ KO ₄)	Reagent	Merck
Oxygen gas	99.999%	Ankara Gaz
Nitrogen gas	99.999%	Ankara Gaz
Synozol Red K-HL	Not reported	Kisco Corp. (Turkey)
Synozol Yellow K-HL	Not reported	Kisco Corp. (Turkey)

4.2. Aqueous Solvents

During the VUV induced photooxidation of imidacloprid degradation experiments, three types of water samples, ultrapure water, tap water, and pond water, were used as solvents. Most of the photooxidation experiments were executed with ultrapure water so as to eliminate matrix effects of water samples that may directly or indirectly impact the decomposition of imidacloprid. Experimentation with ultrapure water in which there is no impurities or at the least level would allow to determine actual degradation kinetics of imidacloprid induced solely by the VUV photooxidation. On the other hand, experiments carried out with tap and pond water showed effects of water constituents on the observed rate constant and removal efficiency of imidacloprid.

4.2.1. Ultrapure Water

Ultrapure water with resistivity of 18.2 MΩ.cm was obtained from Elga PureLab ultrapure water system and used for preparation of stock and experimental solutions as well as calibration studies of UV-Vis Spectrophotometer, LC/MS, and GC/MS. Optimization of the VUV photooxidation system under various flow rates and pH values were also executed with ultrapure water. pH and conductivity values of ultrapure water were measured as 6.937 and 0.0552 μS/cm, respectively.

4.2.2. Tap Water

Tap water from the Unit Operation Lab of Environmental Engineering Department of Hacettepe University was used for comparison experiments to observe effects of water constituents on the degradation of imidacloprid. Tap water was used immediately after it was collected without filtration or any other application. pH and conductivity values of tap water used were measured as 7.325 and 405.582 μS/cm respectively.

4.2.3. Pond Water

In October pond water sample was collected from a pond (nameless) located in Hacettepe University to investigate effects of natural organic matter (i.e. humic substances) on the disappearance of imidacloprid. Pond water, shortly after sampling was filtrated with cellulose acetate membrane filter (0.45 μm) by means of vacuum filtration unit for its use in the degradation experiments. Right after its collection and following to filtration, pH and conductivity values of the pond water used were measured as 8.011 and 1268.98 μS/cm respectively.

4.3. Experimental Solutions

4.3.1. Preperation of Imidacloprid Stock and Working Solutions

Stock solution was prepared from standard imidacloprid (99.8% purity) which is in solid form. Appropriate amount of the standard imidacloprid was weighed and dissolved in ultrapure water. Teflon covered magnetic stirrer bar was used to have imidacloprid fully dissolved within the solution. High quality glasswares which had previously and thoroughly cleaned with ultrapure water were used for preparation of the stock solution. By dilution with ultrapure water, stock solution containing 200 mg/L imidacloprid in total volume of 1000 mL was obtained and refrigerated at 4 °C in the dark. Periodic UV-Vis measurements of samples of the stock solution showed that obtained stock solution was

stable and steady against degradation for several months at 4 °C in the dark. Working solution, on the other hand, at desired concentration of imidacloprid were obtained daily by diluting the stock solution with ultrapure water.

4.3.2. Preperation of Confidor Imidacloprid Stock and Working Solutions

Unlike to standard imidacloprid, commercially available confidor imidacloprid was in concentrated suspension form. In other words, commercial product was in liquid form with very high concentration of imidacloprid. According to manufacturer (Bayer Corp Science) its imidacloprid concentration is 350 g/L (350,000 mg/L). In this case, appropriate volume of formulated solution was obtained with volumetric micro pipets and diluted with ultrapure water to prepare stock solution of imidacloprid at 350 mg/L concentration. Prepared stock solution likewise to standard one was stored in a fridge (4 °C) and kept in the dark. Even though confidor imidacloprid stock solution also contains additional formulation ingredients, the stock solution was stable for several months as well under the beforementioned storage condition. Finally, experimental working solutions were prepared daily by diluting the stock solution with ultrapure water.

4.3.3. Preperation of Reactive Textile Dyes Stock and Working Solutions

As in the case of preperation of imidacloprid stock solution, ultrapure water was used to prepare stock solutions of the reactive textile dyes. Commercially available two reactive dyes, namely Synozol Red KH-L (hereafter Red) and Synozol Yellow KH-L (hereafter Yellow) were used to prepare stock solutions of their own. Reactive dyes were also in solid state. Two seperate reactive dye stock solutions with 5000 mg/L concentration were prepared by weighing appropriate amount of Red and Yellow and then dissolving in ultrapure water seperately. Obtained stock solutions were kept in dark at 4 °C and also stable against discoloration for several months under this storage conditions. Working solutions of desired concentration were obtained daily by diluting the stock solution with ultrapure water.

4.4. Experimental Setup

4.4.1. VUV Photooxidation System

A VUV lamp was mounted into stainless steel annular reactor in which experimental solution was continuously circulated by a peristaltic pump at a pre-defined flow rate. The VUV lamp emitting both at 254 nm and 185 nm was surrounded by clear fused quartz

glass wall to allow transmission of both 254 and 185 nm wavelengths radiations as oppose to soft glass or Ti-doped quartz that both allow only passage of 254 nm wavelength radiation while blocking 185 nm radiation. The VUV lamp was enclosed into high purity synthetic quartz sleeve to not only allow passage of 185 nm photons into experimental solution but also to protect the VUV lamp against air flow, water flow and leakage, temperature fluctuations and breakage. Teflon tube was used to minimize additional negative effects (i.e. adsorption) in the VUV photooxidation system. A schematic diagram and picture of the photooxidation system used during this doctoral study are presented in Figure 4.1 and 4.2 respectively.

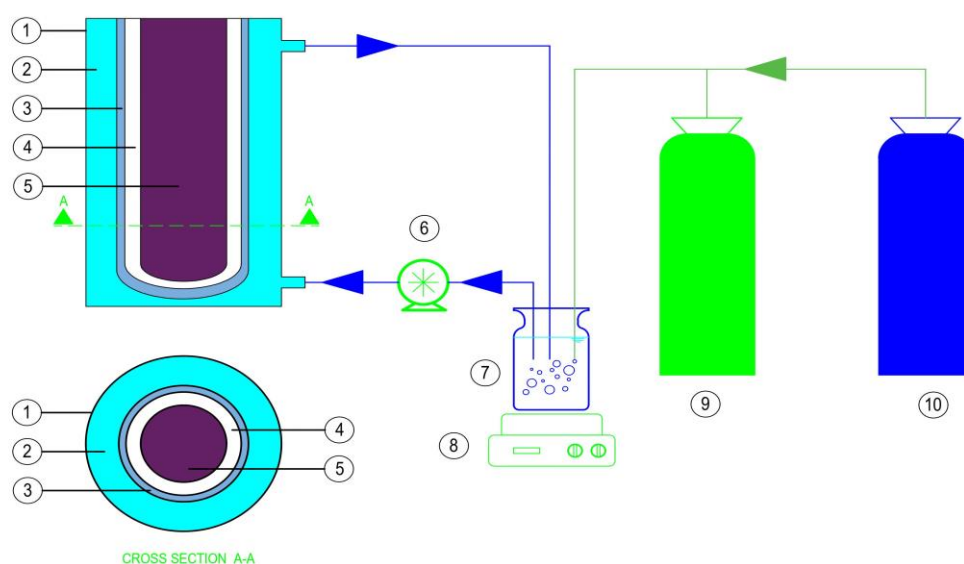


Figure 4.1 Scheme of VUV Photooxidation System.

- | | |
|---------------------------------------|------------------------------|
| 1: Annular photoreactor; | 6: Peristaltic pump; |
| 2: Experimental solution; | 7: Reservoir; |
| 3: Quartz sleeve; | 8: Magnetic stirrer; |
| 4: Space between sleeve and VUV lamp; | 9: N ₂ cylinder; |
| 5: VUV lamp; | 10: O ₂ cylinder; |



Figure 4.2 The VUV Photooxidation System.

4.4.2. Photoreactor

Circular stainless steel flow through reactor with working pressure of 800000 Pa (8 bar) and volumetric flow capacity of 7571 mL/min (2 gpm) was used as photoreactor during the VUV induced photooxidation of aqueous imidacloprid. Total length and inside (inner) diameter of the photoreactor were 265 mm and 50 mm respectively. However, there are two attached joints jutting out at the both sides of the photoreactor which eventually reached total length of 298 mm with 2 lids on. Empty volume of the photoreactor was 485 mL whereas effective water volume was 360 mL after the VUV lamp and the synthetic quartz sleeve enclosed in. The reactor gap, in other words radial distance between inside wall of the annular reactor and outside wall of the synthetic quartz sleeve, in which solution flows, was 13.5 mm. Experimental solution was fed into the flow through photoreactor from the bottom of the reactor. Specifications and dimensions of the photoreactor is given in Table 4.2.

Table 4.2 Specifications and Dimensions of Photoreactor.

Working Pressure	800000 Pa
Volumetric flow rate capacity	7571 mL/min
Length	265 mm
Length with joints and lids	298 mm
Inner Diameter	50 mm
Empty Volume	485 mL
Effective Volume	360 mL

4.4.3. VUV Lamp

A low pressure mercury lamp (LightTech, GPH287T5/VH/4) was used as a source of 254 nm and 185 nm irradiations. Clear fused quartz was used to make the body of the VUV lamp to allow transmission of energy at both 185nm and 254nm wavelengths. The VUV lamp had coaxial radiation field and positive energy direction (outward). Power of the lamp was 14 W. The VUV lamp had 207 mm arc length (effective illumination length) out of 287 mm total length. Diameter of the body wall of the VUV lamp was 15 mm. UV output of the VUV lamp at 254 nm was 4 W while UV output at 185 nm was 0.4 W (8-10% of 4 W) according to manufacturer. It was also reported [78][79] that 185 nm irradiation comprises 5 to 16% of 254 nm fluence depending on the specification of VUV lamps. Specifications and dimensions of the VUV lamp is presented in Table 4.3.

Table 4.3 Specifications and Dimensions of the VUV lamp.

Radiation Geometry	Positive (outward)
Lamp Power	14 watt
Tube Diameter	15 mm
Arc Length	207 mm
Total Length	287 mm
UV output @ 254 nm	4 watt
UV output @ 185 nm	0.4 watt

4.4.4. High Purity Synthetic Quartz Sleeve

Special high purity synthetic quartz sleeve domed shaped with open at one side was used to allow passage of 185 nm light into the experimental solution along with 254 nm light for degradation of aqueous imidacloprid. The VUV lamp was inserted into the synthetic sleeve. The Synthetic quartz sleeve not only allowed higher transmission at the desired wavelengths (185 nm) of the VUV lamp for oxidation of the target compound but also protected the VUV lamp against air flow, water flow and leakage, temperature fluctuations and breakage. Inside and outside diameters of the synthetic sleeve were 20 and 23 mm respectively which resulted 1.5 mm wall thickness. Length of the high purity synthetic sleeve was 295 mm. Physical dimensions of the sleeve is summarized in Table 4.4.

Table 4.4 Dimensions of the High Purity Synthetic Quartz Sleeve.

Inside Diameter	20 mm
Outside Diameter	23 mm
Length	295 mm
Wall thickness	1.5 mm

4.4.5. Clear Fused Quartz Sleeve

A clear fused quartz sleeve with the identical physical dimensions of the high purity synthetic quartz sleeve described above was used in comparison experiments of discoloration of two model compounds, Red and Yellow dyes, to investigate efficiency of 185 nm light passage into the experimental solution. The clear fused quartz sleeve apparently contains higher concentration of impurities compared to the high purity synthetic quartz sleeve. As a result, higher absorption of 185 nm irradiation by the clear fused quartz sleeve was expected. In the light of this information, importance of materials which were used to make the VUV lamp and the sleeve, in other words, purity of materials and their relevant effects on decomposition of the target compounds was evaluated by comparing the observed rate constants and removal percentage.

4.4.6. Peristaltic Pump

Cole-Parmer Masterflex L/S variable speed analog console peristaltic pump with led display was used during the VUV induced degradation and discoloration experiments. The peristaltic pump can fluid in either direction with reversible motor. Magnitude and direction of flows are controlled on the variable speed analog console of the peristaltic pump. Maximum pump speed is up to 600 rpm which is equivalent to 1000 mL/min volumetric flow rate with L/S 25 tube used during the experimentations. The pump was assembled (mounted) with Easy Load 3 Pump Head 77800-50 for connection of circulating tube.

4.4.7. Circulating Tube

Teflon tube was used during the disappearance experiments in order to minimize adsorption of the target compound and possible contamination that might be resulted from the tube itself.

4.4.8. pH and conductivity meter

Seven excellence laboratory pH and conductivity meter (Mettler Toledo) was used to measure pH and conductivity values of the tested solutions. Calibration of the pH and conductivity meter was periodically exercised by means of buffer solutions at pH 4.0, 7.0 and 10.0.

4.5. Experimental Method

4.5.1. Adsorption Experiment

Adsorption experiment of aqueous imidacloprid and reactive textile dye (i.e. Red) solutions were carried out in the photooxidation system without turning the VUV lamp on in order to investigate if there is any potential loss of the target compounds due to adsorption onto materials used in the photooxidation system other than the photooxidation induced. Tested solutions with 10 mg/L initial concentration were prepared with ultrapure water. Therefore, effects of water matrix which may positively increase adsorption potential of the compounds were avoided. Adsorption experiments were carried out at room temperature (22 ± 2). Quantitative degradation of aqueous imidacloprid and discoloration of Red dye in the adsorption experiment was followed spectrophotometrically.

4.5.2. Hydrolysis Experiment

Hydrolysis experiments of aqueous imidacloprid were studied under various initial pH, namely acidic, natural, and alkaline conditions. Studied solutions were prepared in ultrapure water to eliminate effects of impurities that may exist in water sample. Experimental solutions with initial concentration of 10 mg/L were prepared at predefined initial pH values of 3, 6.469 (natural=original), and 11 by using H₂SO₄ and NaOH since these pH modifiers do not generate additional 269/270 nm absorbance behavior at which Imidacloprid displays the highest absorbance peak. Tested solutions were refrigerated at 4 °C and kept in dark during the hydrolysis experimentation. 1 mL aliquots of hydrolyzed solutions were periodically taken from the tested solutions and hydrolytic degradation of imidacloprid was followed by UV Vis measurements at 269/270 nm wavelength.

4.5.3. Degradation Experiment

4.5.3.1. VUV induced Imidacloprid Degradation

VUV induced photodegradation of aqueous imidacloprid experiments were executed with flow through photooxidation system previously described in section 4.4.1 (Figures 4.1 and 4.2). Ultrapure water with resistivity of 18.2 MΩ.cm was used for preparation of experimental solutions. Stock solution was prepared from standard imidacloprid (99.8% purity) at the concentration of 200 mg/L with ultrapure water and stored at 4 °C in the dark as mentioned in section 4.3.1. Working solution of desired concentration of imidacloprid (10 mg/L, 5 mg/L and 2.5 mg/L) were obtained daily by diluting the stock solution with ultrapure water. Comparison experiments were executed with tap and pond water to study effects of water matrix (i.e. natural organic matter, inorganic ions) on the VUV induced photooxidation of aqueous imidacloprid.

500 mL working solution was recirculated between a flow through photoreactor and a reservoir at desired flow rate by a peristaltic pump during the VUV irradiation process for photooxidation process. The VUV lamp which has positive radiation geometry was placed at the center of the annular photoreactor. First of all, various flow rates (500 mL/min, 750 mL/min and 1000 mL/min) were investigated to determine optimum flow rate condition of the laboratory scale VUV photooxidation system used during the experimentation. Therefore, effects of hydrodynamics within the photoreactor were defined and recorded. Second of all, different initial pH values (acidic at pH 3, natural=original at pH ≈6.5, and alkaline at pH 11) of the experimental solution were

studied to determine effects of initial pH of the solution on decomposition of aqueous imidacloprid. As an outcome of the tested experimental conditions, flow rate (500 mL/min) and initial pH (natural=original at pH \approx 6.5) of the solution were chosen and used in the all following experiments. After that, effects of initial concentration (2.5 mg/L, 5 mg/L, and 10 mg/L) on the degradation kinetic and rate constant of imidacloprid were studied under the predefined optimal conditions of flow rate and solution pH. Ultrapure water was spiked with appropriate amount of imidacloprid stock solution to prepare desired concentration right before the irradiation experiments. Another set of experiments, oxygenated and deoxygenated experiments, in order to investigate their effects on the degradation as well as mineralization of aqueous imidacloprid were carried out by sparging O₂ (> 99.999% purity) and N₂ (> 99.999% purity) with flow rate of 600 mL/min into the solution in the reservoir. Introduction of O₂ and N₂ were respectively started 20 and 30 min before the start of the experiments and continued during the experimentation. Further experimental analysis of imidacloprid degradation were executed in presence of inorganic ions (HCO₃⁻, CO₃²⁻, NO₃⁻) since they are commonly found in natural water bodies to study their scavenging effects of HO• produced in situ and impacts on removal rate constant as well as kinetic pattern of aqueous imidacloprid under the tested photooxidation process.

The VUV lamp was turned on 30 minutes before the photooxidation to warm up the lamp and to reach stable output. 1 mL aliquots of irradiated solutions were collected at predefined treatment times for analysis. Collected samples subjected to analysis of LC/MS QTOF were immediately injected into chromatographic amber glass vials so as to avoid interaction with sunlight. In the case of UV-Vis measurement, the quartz cuvettes were used instead. Initial and final pH and conductivity values of the tested aqueous solutions were measured in situ. Quantitative measurements were carried out by UV-Vis spectrophotometer and LC/MS QTOF.

Degradation experiments were carried out at room temperature (22 ± 2). All the presented results are the averages of 3 separate experiments and the error bars show the standard deviation of the measured values.

4.5.3.1.A. Screening of pH Adjusters (Modifiers) for Acidic and Alkaline Conditions

Same photooxidation system was used for the irradiation experiments under both acidic and basic conditions. Irradiation volume, warm up period, and aliquot volume were same

as well. Furthermore, experimentally defined and chosen flow rate (500 mL/min) was used in these set of experiments. Samples were measured by the same UV-Vis spectrophotometer and LC/MS QTOF.

Sulfuric Acid (H_2SO_4), Hydrochloric Acid (HCl), Nitric Acid (HNO_3), and Sodium Hydroxide (NaOH) were evaluated to be used for adjustment of acidic and alkaline conditions. Firstly, these compounds were investigated individually by scanning between 200 and 800 nm wavelengths in UV-Vis spectrophotometer to determine their absorbance characteristics (Figure A.1.1). Therefore, it was determined that if any individual tested compound presents additional 269/270 nm absorbance behavior at which Imidacloprid displays the highest absorbance peak. Other than HNO_3 , none of the tested compounds showed 269/270 nm absorbance behavior (Figures A.1.2 and A.1.3) and therefore they are suitable for further screening and pH adjustment applications. On the other hand, HNO_3 displayed considerable 269/270 nm absorbance behavior (Figures A.1.1 and A.1.2). Secondly, molar absorption coefficients of these compounds at 185 nm photon were compared to choose the one that has the least molar absorption coefficient at this wavelength. This was also necessary to minimize inner filter effects (absorption of 185 nm photon) of the compounds that simultaneously exist in the experimental solution. By choosing the least keen compound to 185 nm photon for pH adjustment, majority of 185 nm photon will exclusively be absorbed by water molecule within the experimental solution and hence production of Hydroxyl Radical ($\bullet\text{OH}$) will not be jeopardized. Among the tested compounds and their dissociated ions, it was previously reported that Nitrate (NO_3^-) ion has the highest molar absorption coefficient at 185 nm photon followed by Chloride (Cl^-) and Sulfate (SO_4^{2-}) ions respectively [80][81]. NO_3^- and Cl^- ions have high molar absorption coefficients of 185 nm whereas SO_4^{2-} ion has negligible. Findings in this doctoral study (Figure A.1.1) were consistent with previously reported ones. Besides, Figure A.1.2 clearly displays that NO_3^- can also absorb photon at 254 nm as oppose to Cl^- and Sulfate SO_4^{2-} . This observation is also in agreement with what was reported on PhD Thesis of Clara Duca [82]. According to previous and this study, NO_3^- and Cl^- can act as inner filters and thus less photons will be available for the photolysis of water via 185 nm photon. Moreover, it is known that SO_4^{2-} react slowly with $\bullet\text{OH}$ radicals [83] so that it cannot act as $\bullet\text{OH}$ scavenger or as inner filter due to its negligible absorption at 185 nm. Lastly, it was also experimentally determined in this study that H_2SO_4 does not generate additional 269/270 nm absorbance either (Figures A.1.1 and

A.1.2). Therefore, SO_4^{2-} based H_2SO_4 would be more suitable for acidic pH adjustment and accordingly were used as acidic pH modifier in the irradiation experiments of this doctoral study.

For adjustment of alkaline pH condition, NaOH was used not only since Na^+ does not absorb at 185 nm but also does not scavenge $\bullet\text{OH}$ [82]. Furthermore, it was also experimentally determined in this study that NaOH does not generate additional 269/270 nm absorbance either (Figures A.1.1 and A.1.2).

In brief, for pH adjustment it is important to choose a compound that not only has negligible molar adsorption coefficients at 185 nm but also does not generate additional 269/270 nm absorbance at which Imidacloprid shows the highest absorbance peak. Furthermore, this compound should not tend to willingly react with Hydroxyl Radical ($\bullet\text{OH}$), in other words should not behave as $\bullet\text{OH}$ scavenger so that $\bullet\text{OH}$ would then be completely available for degradation of Imidacloprid and organic byproducts generated during the photooxidation process. When all these considered, H_2SO_4 and NaOH were used for pH adjustments of the experimental solution since they both do not generate additional 269/270 nm absorbance and have negligible molar absorption coefficients at 185 nm photon in the form of SO_4^{2-} and Na^+ . On top of that they do not act as $\bullet\text{OH}$ scavenger either.

Absorbance spectrum of Sulfuric Acid (H_2SO_4), Hydrochloric Acid (HCl), Nitric Acid (HNO_3), and Sodium Hydroxide (NaOH) along with Confidor Imidacloprid were reported in Appendix 1.1.

4.5.3.1.B. VUV induced Imidacloprid Degradation in presence of Inorganic ions

NaHCO_3 , Na_2CO_3 , NaNO_3 were used to investigate effects of inorganic ions (HCO_3^- , CO_3^{2-} , and NO_3^-) on the degradation of aqueous imidacloprid since these ions are ubiquitously found in natural water bodies. HCO_3^- , CO_3^{2-} , and NO_3^- might affect the degradation process either by absorbing 185 nm light and acting as inner filter or by scavenging $\text{HO}\bullet$ produced via water homolysis and ionization of 185 nm irradiation. 688.42 mg NaHCO_3 , 883.12 mg Na_2CO_3 , and 685.35 mg NaNO_3 were individually weighed and dissolved in ultrapure water to prepare three separate 1000 mg/L HCO_3^- , CO_3^{2-} , and NO_3^- stock solutions in total volume of 500 mL. Working solutions of the desired inorganic ions concentration (i.e. 5 mg/L) were prepared by diluting the stock solution with ultrapure water. Imidacloprid was then added into the experimental

solutions to achieve intended working concentration. Ionic experiments were executed with 5 mg/L initial imidacloprid concentration. Potential effects of the tested inorganic ions on the VUV induced photooxidation of imidacloprid degradation were investigated using the concentration ratio of imidacloprid:inorganic ion as 1:1. Generally, natural water contains more than 5 mg/L HCO_3^- and CO_3^{2-} , typically between 50 and 200 mg/L and even more depending on the water source. However, the reason behind the 1:1 ratio was to observe how fastly and effectively imidacloprid react with $\bullet\text{OH}$ in presence with the same initial concentration of HCO_3^- and CO_3^{2-} which are well known $\bullet\text{OH}$ scavengers and react with $\bullet\text{OH}$ at the rate constants of $8.5 \times 10^6 \text{ M}^{-1} \text{ s}^{-1}$ and $4 \times 10^8 \text{ M}^{-1} \text{ s}^{-1}$ respectively [74]. Experiments in the presence of the single ion were carried out separately to determine individual effects of the ions on the tested process and degradation of imidacloprid.

Initial pH values of experimental solutions that contain 5 mg/L HCO_3^- , CO_3^{2-} , and NO_3^- were measured to be 7.738, 9.911, and 6.292 respectively.

4.5.3.2. VUV induced Reactive Textile Dyes Degradation

Commercially available two reactive textile dyes, Synozol Red K-HL (hereafter Red) and Synozol Yellow K-HL (hereafter Yellow) were used for discoloration experiments under the VUV light. Appropriate amount of Red and Yellow textile dyes was weighed and dissolved in ultrapure water to prepare 5000 mg/L stock solution separately. Working solutions of desired concentration (10 mg/L, 25 mg/L, and 50 mg/L) were obtained by diluting the stock solution.

Same photooxidation system of Imidacloprid experiments described above was used for the irradiation experiments of the textile dyes. Flow rate, irradiation volume, warm up period, and aliquot volume were same as well. Initial and final pH and conductivity values were measured by the same pH and conductivity meter. Samples were measured by the same UV-Vis spectrophotometer to observe decoloritazion of the reactive dye solutions and to obtain disappereance kinetics along with rate constants.

All the presented results are the averages of 3 experiments and the error bars show the standard deviation of the measured values.

4.5.4. Mineralization Experiment

Mineralization rate is usually much slower than the disappearance rate of compounds (i.e. pesticides). As a result, several byproducts are generated within the time required for complete degradation of the compounds. It is important to study effectiveness of VUV induced photooxidation onto mineralization of imidacloprid to understand decomposition of imidacloprid better. Therefore, investigation of mineralization degree of imidacloprid by the VUV photooxidation was separately performed with TOC measurements.

Mineralization experiments of aqueous imidacloprid were carried out under oxygenated, natural, and deoxygenated conditions so as to understand effects of oxidants and radicals produced in situ on the extent of mineralization of aqueous imidacloprid. Experimental solutions with initial concentration of 10 mg/L were prepared in ultrapure water to eliminate effects of impurities that may exist in water sample and subjected to the VUV irradiation with duration time of 2 hours. The tested solutions were sparged by O₂ (> 99.999% purity) and N₂ (> 99.999% purity) gases for oxygen saturated and oxygen free conditions respectively with flow rate of 600 mL/min in the reservoir. Introduction of O₂ and N₂ were respectively started 20 and 30 min before the start of the experiments and continued during the experimentation. Mineralization experiments were carried out at room temperature (22 ± 2). Finally, TOC reduction of aqueous imidacloprid solutions were followed by TOC analyzer to determine extent of mineralization.

4.6. Actinometric Measurement of Photon Flux of the VUV Lamp

4.6.1. Methanol Actinometry

Photon Flux (P_{VUV}) of the VUV lamp at 185 nm was determined using methanol actinometry method [84][85]. Methodology behind the methanol actinometry, because it does not react with O₃ and nor does it absorb 254 nm light and being at low concentration (100 mM) compared to molar concentration of water (55.5 M), is disappearance of methanol during the VUV irradiation is principally due to reaction with HO•. It can be assumed that almost all the photons are absorbed by water under this circumstances and accordingly, HO• is produced due to 185 nm light induced water photolysis. Therefore, P_{VUV} value is proportional to VUV induced degradation rate of methanol (k_{obs}^0) in aqueous solution as presented in equation 4.1. Zero order rate constant k_{obs}^0 value was experimentally determined at 0.1 M (100 mM) initial methanol concentration since all methanols would react exclusively with hydroxyl radical (•OH) at low initial methanol

concentration [85][86]. VUV (185 nm) light induced degradation of methanol was measured via Gas Chromatography Mass Spectrometry (GC/MS) which is described in detail in section 4.7.3. Defined degradation rate (k_{obs}^0) was utilized to calculate absorbed photon flow (UV intensity at 185 nm) of the VUV lamp using equation 4.1.

The factor of 0.946 refers to the production of methanol (5.4 %) by the disproportionation reaction of hydroxymethyl radicals which slows down the $\bullet\text{OH}$ induced degradation of methanol [84][85].

$$P_{\text{VUV}} = \frac{1}{0.946} \times k_{\text{obs}}^0 \times \frac{V}{\phi_{\text{H}_2\text{O}} \times \xi_{\text{H}_2\text{O}} + \phi_{\text{CH}_3\text{OH}} \times \xi_{\text{CH}_3\text{OH}}} \quad (4.1)$$

P_{VUV} : Photon Flux of the VUV lamp at 185 nm ($\text{mol}_{\text{photon}} \text{s}^{-1}$)

k_{obs}^0 : VUV light induced zero order degradation rate of methanol ($\text{mol L}^{-1} \text{s}^{-1}$)

V: total irradiated volume of methanol solution (500 mL = 0.5 L)

$\phi_{\text{H}_2\text{O}}$: total quantum yield of water photolysis (0.33 + 0.045 = 0.375)

$\xi_{\text{H}_2\text{O}}$: fraction of photons absorbed by water

$\phi_{\text{CH}_3\text{OH}}$: total quantum yield of methanol photolysis (0.88)

$\xi_{\text{CH}_3\text{OH}}$: fraction of photons absorbed by methanol

Two unknowns, $\xi_{\text{H}_2\text{O}}$ and $\xi_{\text{CH}_3\text{OH}}$ in equation 4.1 were calculated from the molar absorption coefficients of water ($\epsilon_{\text{H}_2\text{O}}$) and methanol ($\epsilon_{\text{CH}_3\text{OH}}$) at 185 nm using equation 4.2. The molar absorption coefficients of methanol ($\epsilon_{\text{CH}_3\text{OH}}$) at 185 nm was previously reported as $6.3 \text{ M}^{-1} \text{ cm}^{-1}$ [80]. On the other hand, by using equation 4.3, the molar absorption coefficients of water ($\epsilon_{\text{H}_2\text{O}}$) can be calculated from linear absorption coefficients of water ($k_{\text{H}_2\text{O}}$) which was also found by Weeks [80] as 1.8 cm^{-1} .

$$\xi_{\text{CH}_3\text{OH}} = \frac{\epsilon_{\text{CH}_3\text{OH}} \times C_{\text{methanol}}}{\epsilon_{\text{CH}_3\text{OH}} \times C_{\text{methanol}} + \epsilon_{\text{H}_2\text{O}} \times C_{\text{water}}} \quad (4.2)$$

$$k_{\text{H}_2\text{O}} = \epsilon_{\text{H}_2\text{O}} \times C_{\text{H}_2\text{O}} \quad (4.3)$$

$$\xi_{\text{H}_2\text{O}} = 1 - \xi_{\text{CH}_3\text{OH}} \quad (4.4)$$

C_{water} : concentration of water molecules (55.5 M)

C_{methanol} : initial methanol concentration (0.1 M)

Firstly, by substituting k_{H_2O} and C_{H_2O} into equation 4.3, the molar absorption coefficients of water (ϵ_{H_2O}) was calculated as $0.0324 \text{ M}^{-1} \text{ cm}^{-1}$ which is in agreement with literature [87]. Secondly, fraction of photons absorbed by methanol (ξ_{CH_3OH}) was calculated as 0.2594 through equation 4.2. After that, fraction of photons absorbed by water (ξ_{H_2O}) was calculated to be 0.7406 by using equation 4.4.

In order to check if the calculated values above are correct or not, another calculating equation (equation 4.5) was used to determine ξ_{H_2O} and ξ_{CH_3OH} .

$$\xi_{H_2O} = \frac{k_{H_2O}}{k_{H_2O} + (\epsilon_{CH_3OH} \times C_{\text{methanol}})} \quad (4.5)$$

All the values in equation 4.5 are known and hence, ξ_{H_2O} was calculated to be 0.7407. As a result, ξ_{CH_3OH} was found as 0.2593 using equation 4.4. Calculated values were very similar to each other. 0.7407 and 0.2593 were selected as ultimate values of ξ_{H_2O} and ξ_{CH_3OH} respectively to calculate P_{VUV} .

Experimentally determined degradation rate of methanol (k°_{obs}) and accordingly calculated photon flux of the VUV lamp at 185 nm were presented in results and discussion chapter.

4.7. Analytical Methods

4.7.1. UV-Vis Spectrophotometer

Thermo Fisher Scientific Genesys 10S UV-Vis spectrophotometer was used for quantitative analysis of irradiated imidacloprid and textile dyes solution. Quartz glass cuvettes were used for absorbance measurements of imidacloprid samples since characteristic absorbance peak of imidacloprid was previously recorded as 269/270 nm. Typical polystyrene cuvettes block wavelengths below 300 nm whereas the quartz cuvettes allow passage of light down to 190 nm. And hence, degradation of imidacloprid could be followed spectrophotometrically. Optical path length of the quartz glass cuvettes used was 10 mm. Dimensions of the quartz glass cuvettes were 12,5 mm x 12,5 mm x 45 mm (w x d x h).

Standard Imidacloprid was scanned between 200 and 900 nm wavelengths in UV-Vis spectrophotometer to determine absorbance peak of imidacloprid (Figures A.1.4). As a result, the highest peak was observed at 269/270 nm as in line with previously reported findings for imidacloprid samples.

Similar methodology was followed for reactive textile dyes between 300 and 900 nm to determine their absorbance peaks by using polystyrene cuvettes with same dimensions (12,5 mm x 12,5 mm x 45 mm) instead. Absorbance peaks at 518 nm and 417 nm were recorded for Red and Yellow dyes respectively.

UV-Vis calibration study of imidacloprid solutions was executed with standard Imidacloprid. Appropriate amount of standard Imidacloprid (%99.8 purity) was dissolved in ultrapure water to prepare 100 mg/L imidacloprid stock solution. From this stock solution, 20, 10, 5, 2.5, 1.25, 0.625, 0.3125, and 0.15625 mg/L imidacloprid concentrations were prepared and used for calibration study of UV-Vis spectrophotometer (Figures A.1.5). Average of three separate measurements was used to construct calibration curve and correlation coefficient (R^2). Error bars represent the standard deviation of three replicates.

Constructed calibration curve and absorbance peaks of aqueous imidacloprid measured using UV-Vis were presented in Appendix 1.2.

4.7.2. Liquid Chromatography and Quadrupole Time of Flight Mass Analyzer (LC/MS Q-TOF)

Quantitative and qualitative analysis of irradiated imidacloprid solutions were analyzed by an Agilent 1200 series Liquid Chromatography and Quadrupole Time of Flight Mass Spectrometry (LC/MS Q-TOF) system comprised of a solvent holder, a binary pump, a vacuum degasser, an autosampler, a diode array detector, a thermostated column compartment, a 6530 Accurate-Mass Q-TOF detector and MassHunter data managing software (Agilent Technologies). The analytical column used for separation of aqueous imidacloprid and its degradation products was a Zorbax 300 SB-C18 (100 mm x 4.6 mm i.d., 3.5 μ m particle size), protected by a security guard cartridge Zorbax 300 SB-C18 (12.5 mm x 4.6 mm i.d.), both from Agilent Technologies. Imidacloprid samples were quantified at 270 nm wavelength using the diode array detector (DAD) while qualitative analysis (detection of byproducts) were executed with the Q-TOF mass spectrometry (MS). Peak areas were used for quantitative analysis of imidacloprid.

So as to define optimal eluent composition that would provide the best separation and detection response of aqueous imidacloprid by LC/MS Q-TOF, firstly, methanol (MeOH) and acetonitrile (ACN) were tested. Secondly, formic acid (FA) and acetic acid (AA) were evaluated with both solvents along with ultrapure water (H_2O). As a result of eluent

screening process, optimum composition was defined as mixture of acetonitrile and water acidified with 0.1% formic acid for mobile phase although both solvents resulted good responses. After that, various injection volumes, column flow rates, and column temperatures with previously defined mobile phase were studied to obtain the best chromatographic results. 20 μ L, 0.5 mL/min, and 40 $^{\circ}$ C were selected as optimal values for injection volume, column flow rate, and column temperature respectively. Finally, gradient and isocratic elutions were exercised under aforementioned conditions. Although both tried elution methods achieved good absorbance peak, isocratic elution (30% ACN + 70% H₂O with 0.1% FA) resulted slightly narrower peak and hence, was selected for separation and detection of aqueous imidacloprid samples. Retention time of imidacloprid was 3.698 min under applied optimal conditions.

Furthermore, different operating conditions of the MS detector equipped with electrospray jet stream ionization source (ESI), were also exercised to obtain the best detection results. Various gas temperature, drying gas flow, nebulizer pressure, and capillary voltage (V_{Cap}) of the ESI were studied and compared to optimize conditions of MS. After rigorous study and comparison, nebulizer pressure and V_{Cap} were defined as the most influencing parameters. MS detection of samples was carried out in positive ionization mode. Full scan was obtained by scanning from m/z 60 to 400.

External standard calibration method was carried out for analysis of aqueous imidacloprid. Eight standard imidacloprid solutions, 0.15625, 0.3125, 0.625, 1.25, 2.5, 5, 10, and 20 mg/L were analyzed by LC/MS Q-TOF to construct calibration curve which was obtained by plotting peak areas against concentrations of the target compound. Average of three separate measurements was used in calibration study. Error bars represent the standard deviation of three replicates.

Optimal separation and detection conditions along with calibration curve and chromatogram of aqueous imidacloprid were presented in Appendix 1.3. In addition, mass spectrum of parent compound (imidacloprid) and byproducts were also reported in Appendix 1.3.

4.7.3. Gas Chromatography Mass Spectrometry (GC/MS)

Quantitative degradation of methanol samples was followed by means of an Agilent Technologies Gas Chromatography Mass Spectrometry consists of 7890A Gas Chromatography (GC) System, a 5975C Inert Mass Selective Detector (MSD) with

Triple-Axis, and CTC PAL autosampler. MassHunter data managing software (Agilent Technologies) was used for quantitative analysis of the samples. Helium was used as carrier gas with flow rate of 1 mL/min and pressure of 8.2317 psi (0.568 bar). Electro Impact ionization source was 70 eV. An Agilent J&W DB FFAP (0.32 mm, i.d. x 30 m, length x 0.50 μ m, film thickness) capillary column was used to separate methanol samples by using temperature gradient presented in Table 4.5. The DB FFAP column was purposely selected since it is a polar column and suitable for analysis of alcohols. Sample Injection volume was 0.1 μ L using the split mode with a split ratio 20:1. Injector temperature was set at 150 °C. Selected Ion Monitoring (SIM) mode was used to detect methanol using characteristic ions of methanol (m/z 29, 31, and 32). Molar concentration of methanol was determined by external standard method using 0.25 M, 0.50 M, 1 M, 2 M, and 4 M HPLC grade methanol for GC/MS calibration.

GC/MS analysis of methanol in ultrapure water was carefully executed since water molecules can seriously damage the MS detector in GC injection method. First of all, methanol sample which had not been subjected to the VUV irradiation was analyzed via GC/MS by applying the scan mode in order to define detection time of methanol and water. Therefore, the time at which water molecules reach the detector was recorded. Residence times of methanol was recorded as 1.476 min whereas water molecule was detected around 2.5-2.7 min. Second of all, GC analysis was carried out to detect any other compound which might have been resulted from ionization of methanol or from washing solvents during the total run time of 9 min. No compound was detected especially after detection time of water molecules. Third of all, MS detector was programmed to be off at 2.4 min which was earlier than the residence time of water molecule and more importantly safely later than the residence time of methanol. Therefore, mass detector was protected from probable damage of the water molecules. Finally, determined detector off time was set in the SIM mode which was used for GC/MS analysis of methanol.

Various washing solvents which may also have ions at m/z 29, 31, and 32 within their ten largest peaks were investigated in order not to get confused with methanol in SIM mode. Acetone, n-heptane, and ethanol were eliminated since they have one or more ions at m/z 29, 31, and 32 within their ten largest peaks. On the other hand, acetonitrile did not have and hence chosen as washing solvent for GC/MS analysis of methanol.

Calibration curve, GC mass spectrum and chromatogram of methanol were presented in Appendix 1.4.

Table 4.5 Temperature gradient profile of GC column.

	Temperature Rate (°C/min)	Temperature Value (°C)	Hold Time (min)	Run Time (min)
Initial		60	3	3
Ramp 1	40	100	1	5
Ramp 2	40	220	1	9

4.7.4. Total Organic Carbon Analyzer (TOC)

A Shimadzu TOC-NL analyzer was used to determine TOC content of the aqueous imidacloprid samples. The combustion of the samples was carried at 680 °C. Potassium Hydrogen Phthalate ($\text{KC}_8\text{H}_5\text{O}_4$) was used to calibrate TOC analyzer.

5. RESULTS AND DISCUSSION

5.1. Photon Flux of the VUV Lamp

Methanol actinometry method was used to determine photon flux (P_{VUV}) of the VUV lamp at 185 nm [84][85]. Methodology of the methanol actinometry was previously explained in Section 4.6.1. In order to calculate P_{VUV} of the VUV lamp used in photooxidation experiments carried out throughout the doctoral study, reduction rate of methanol (k°_{obs}) in ultrapure water solution was experimentally determined to be $4 \times 10^{-7} \text{ mol L}^{-1} \text{ s}^{-1}$ (Figure 5.1). Subsequently, P_{VUV} was calculated as $4.18 \times 10^{-7} \text{ mol}_{\text{photon}} \text{ s}^{-1}$ by substituting defined k°_{obs} into equation 4.1 presented in chapter 4.

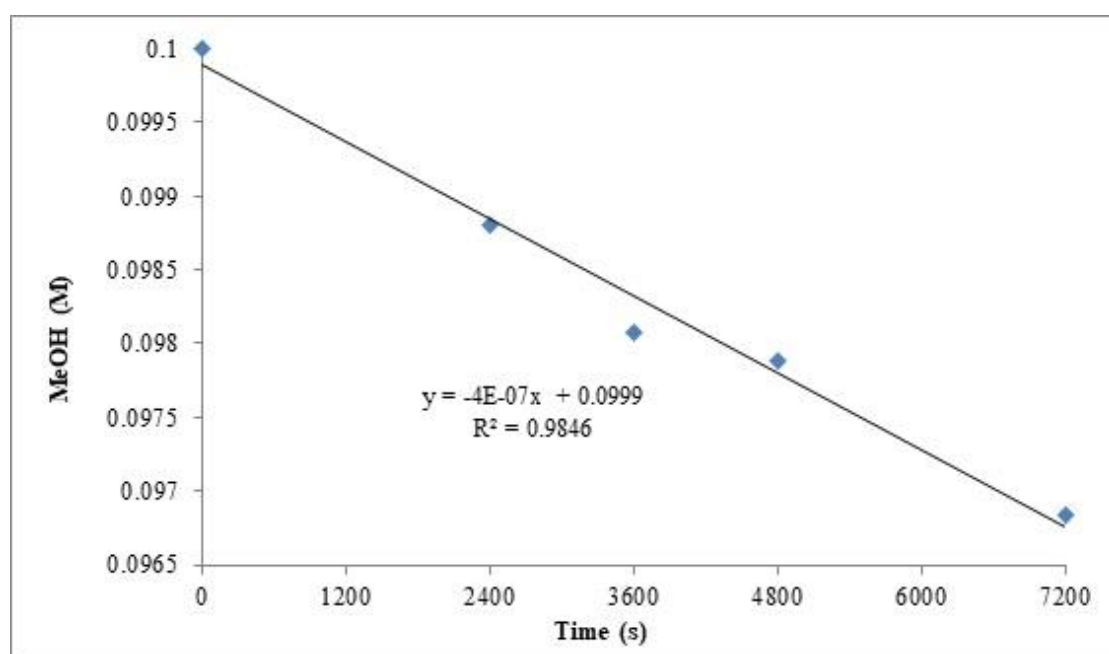


Figure 5.1 MeOH reduction via VUV irradiation.

5.2. Adsorption of Imidacloprid

Adsorption experiments of aqueous imidacloprid and reactive textile dye (i.e. Red) solutions were carried out in the photooxidation system without turning the VUV lamp on in order to investigate if there is any potential loss of the target compounds due to adsorption onto materials used in the photooxidation system other than the photooxidation induced one. Adsorption experiments were deliberately extended to 60

minutes which was safely longer than the time required to degrade both imidacloprid and red dye within the photooxidation system during the VUV irradiation in order not to fail to notice the potential adsorptional reduction of the target pollutants which may exhibit after repetitive circulation and contact with the used materials. Results obtained from the adsorption experiments were presented in Figure 5.2. and Figure 5.3. for imidacloprid and red textile dye solutions respectively. As seen in Figures 5.2. and 5.3., no loss due to adsorption was observed for both imidacloprid and red dye solutions within the VUV photooxidation system used in this doctoral work. As a result, degradation of the tested pollutants within the VUV system was solely attributed to photooxidation mechanism with no influence of adsorption mechanism.

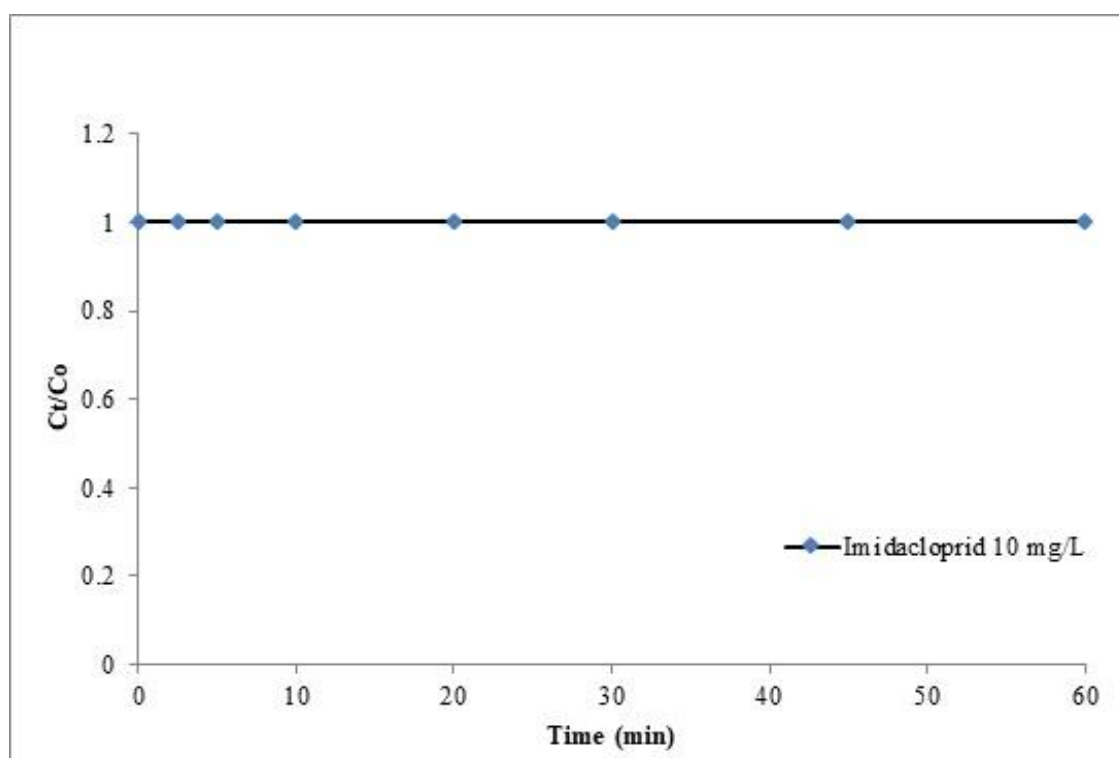


Figure 5.2 Adsorptional loss of Imidacloprid ($C_o=10$ mg/L) without turning the VUV lamp on as a function of irradiation time.

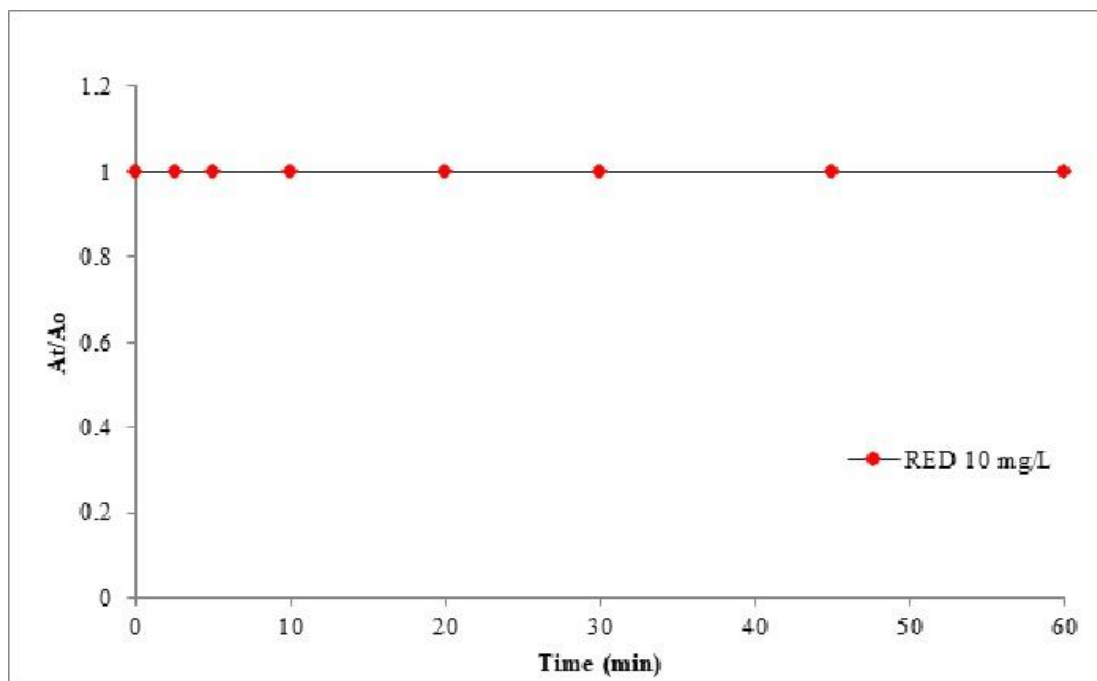


Figure 5.3 Adsorptional loss of Red dye ($C_0=10$ mg/L) without turning the VUV lamp on as a function of irradiation time.

5.3. Hydrolysis of Imidacloprid

Hydrolysis experiments of aqueous imidacloprid with 10 mg/L initial concentration were studied under acidic (pH=3), natural (original, pH=6.469), and alkaline (pH=11) conditions. In agreement with literature imidacloprid was stable under acidic and original pH conditions during 104 days of hydrolysis time [43][88]. As presented in Figure 5.4, on the other hand, hydrolytic degradation of imidacloprid significantly increased under tested basic condition. Similar findings were also reported in literature[43][89][90]. It was found that hydrolytic degradation of imidacloprid in basic solution followed first order kinetic pattern ($R^2 \geq 99$) with the hydrolytic rate constant of 0.0083 day^{-1} (Figure 5.4). The half-life of imidacloprid obeying first-order hydrolytic kinetic, then was calculated to be 83.51 days in this doctoral research.

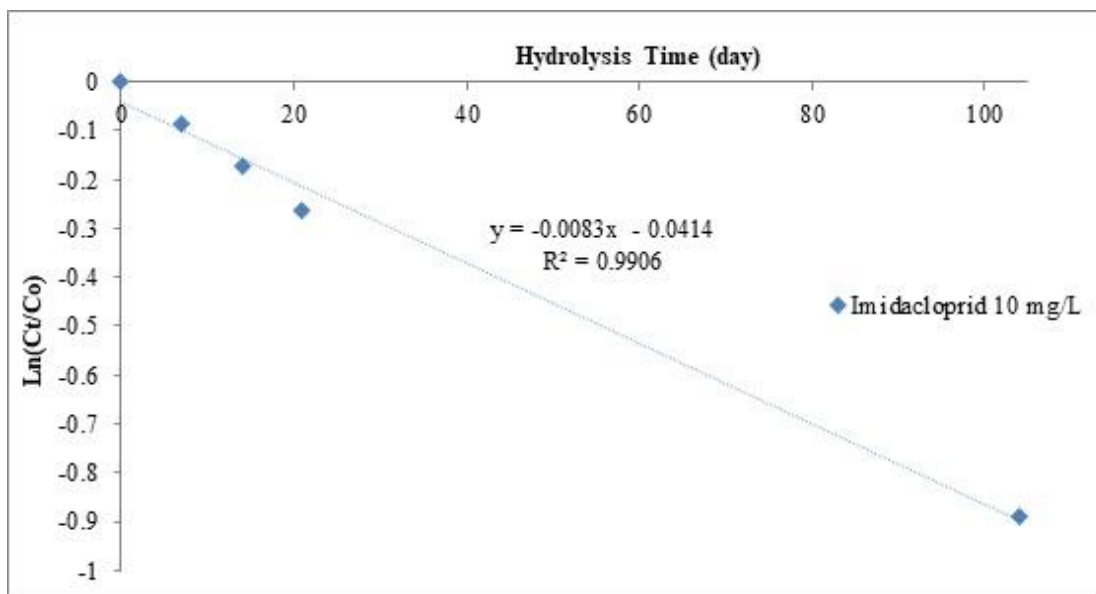


Figure 5.4 Hydrolytic degradation of Imidacloprid ($C_0=10$ mg/L) under basic (pH=11) condition.

5.4. Degradation of Imidacloprid by VUV photooxidation

Results of the VUV initiated photooxidation of aqueous imidacloprid experiments were presented and discussed herein. Supplementary data of the all following subsections and related experiments were reported in Appendix 2.

5.4.1. Effects of Flowrate of the experimental solution

As previously reported, low penetration depth of the VUV irradiation (185 nm) into water solution is main drawback of the VUV induced AOP. As a result, any reactor either flow through annular photoreactor or else which has diameter > 5.5 mm in radiation direction will have two separate reaction zones. The first zone which is closer to the lamp surface, is where VUV photolysis of water takes place and accordingly is where highly reactive and non-selective oxidant $\text{HO}\cdot$ and other radicals ($\text{H}\cdot$, e_{aq}^-) which are responsible of oxidation and mineralization of pollutants in water are produced. Second zone, on the other hand, lacks the produced reactive species ($\text{HO}\cdot$, $\text{H}\cdot$, e_{aq}^-). As a result, mass transfer limitation plays an important role on the photooxidation of the target pollutant. This limitation can be overcome to some extent by manipulating hydrodynamic conditions of the system. Therefore, in order to understand effects of hydrodynamic conditions on the VUV initiated degradation of aqueous imidacloprid, various solution flowrates (500 mL/min, 750 mL/min and 1000 mL/min) were investigated in this research.

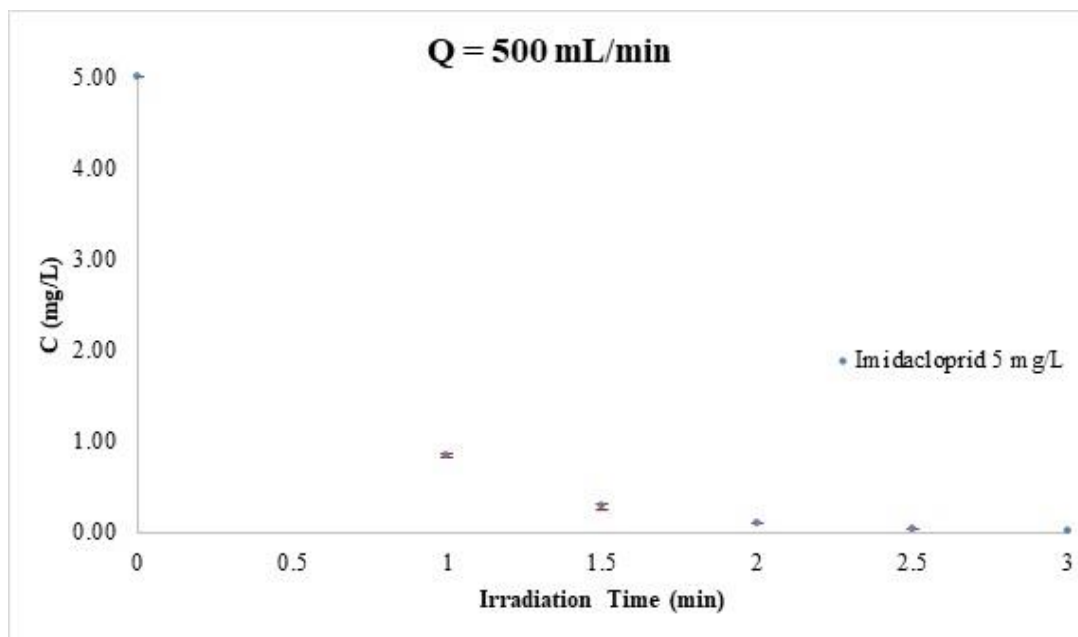


Figure 5.5 VUV induced photodegradation of Imidacloprid ($C_0 = 5 \text{ mg/L}$) under $Q = 500 \text{ mL/min}$ flow rate condition. The results are average of three replicates.

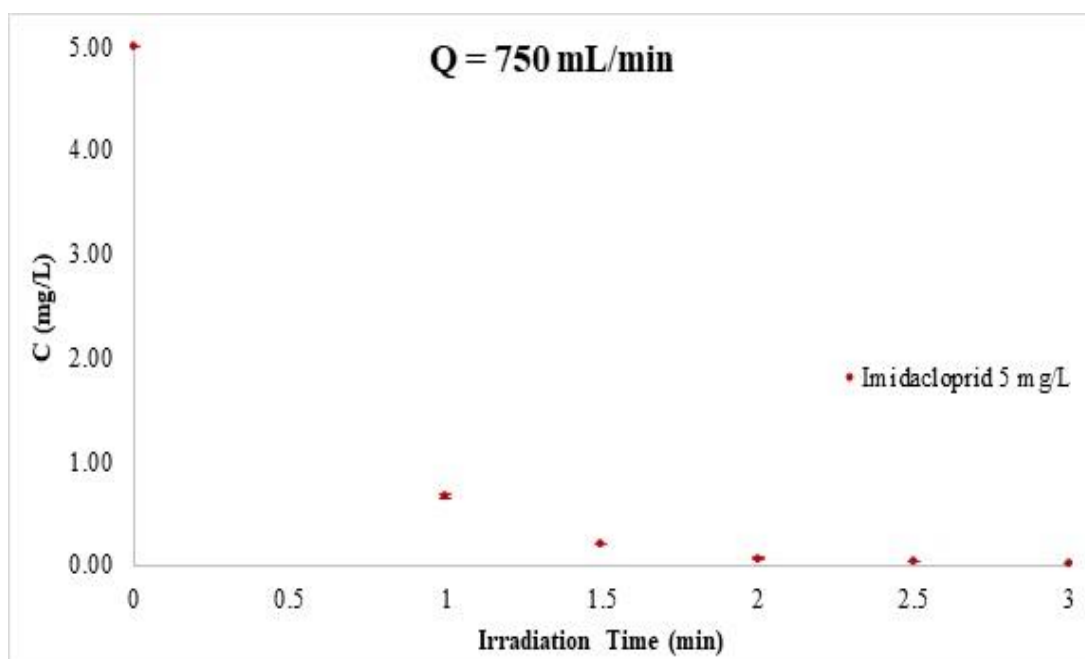


Figure 5.6 VUV induced photodegradation of Imidacloprid ($C_0 = 5 \text{ mg/L}$) under $Q = 750 \text{ mL/min}$ flow rate condition. The results are average of three replicates.

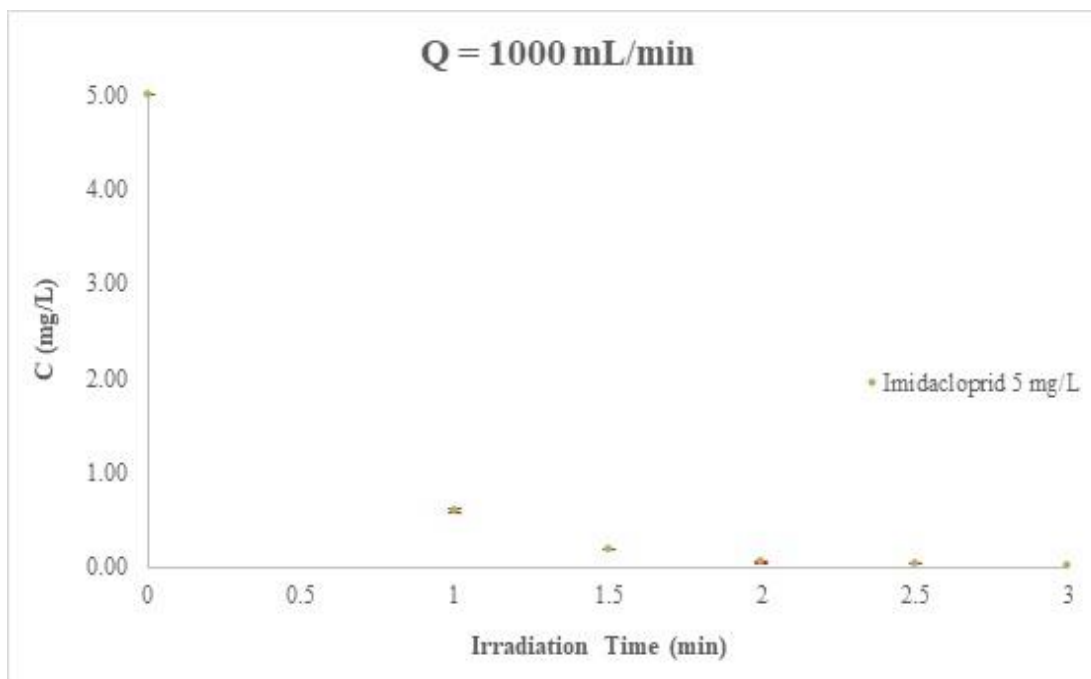


Figure 5.7 VUV induced photodegradation of Imidacloprid ($C_0 = 5 \text{ mg/L}$) under $Q = 1000 \text{ mL/min}$ flow rate condition. The results are average of three replicates.

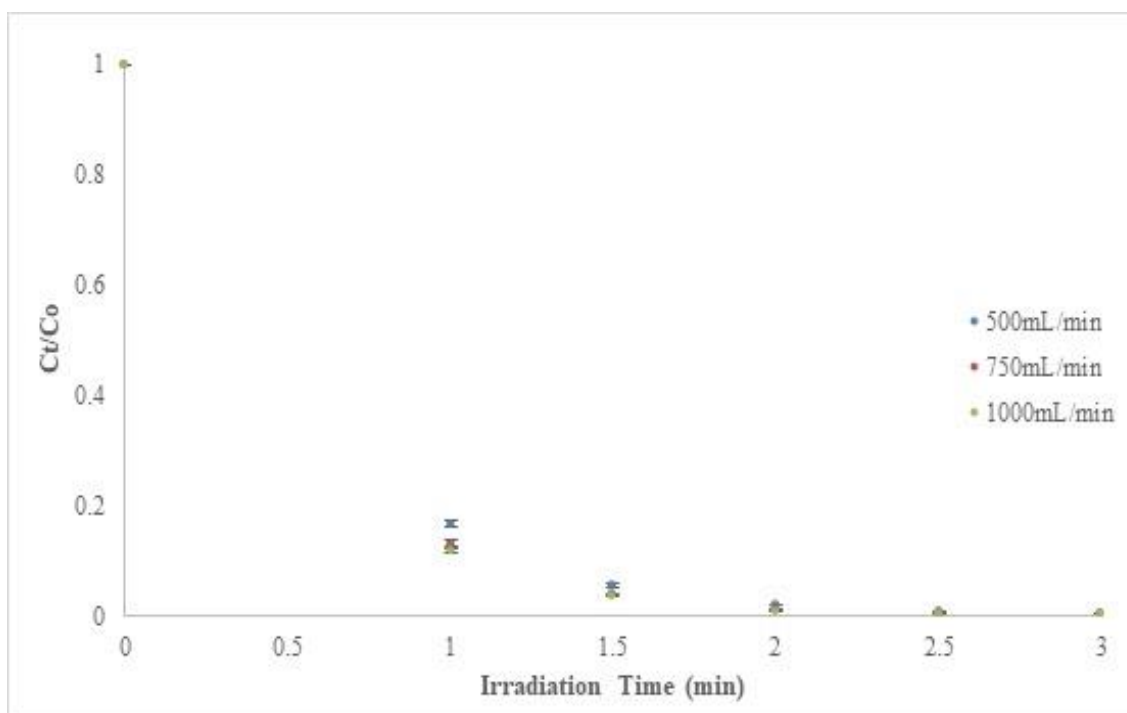


Figure 5.8 VUV initiated degradation of Imidacloprid ($C_0 = 5 \text{ mg/L}$) under various flow rate conditions. The results are average of three replicates.

Effects of solution flow rate onto photodegradation of imidacloprid with laboratory scale VUV photooxidation system were presented herein. Figures 5.5, 5.6, and 5.7 present VUV initiated degradation of aqueous imidacloprid under different flow rates conditions. Figure 5.9 shows that pseudo-first order degradation kinetic was observed for all the tested flowrates. Pseudo-first order degradation kinetic of aqueous imidacloprid by other AOPs was also reported previously [91][7][63][64]. Even though $\bullet\text{OH}$, which is the responsible reactive in degradation of pollutants in AOPs based treatment, reacts with organic compounds in second order rate, pseudo first order degradation kinetic was observed with imidacloprid since generation rate of $\bullet\text{OH}$ was equal to consumption rate and reached very quickly to steady state condition, so $\bullet\text{OH}$ concentration was considered as constant. Therefore, reduction of imidacloprid by VUV based AOP took place as a function of only its own concentration, rather than concentration of both imidacloprid and $\bullet\text{OH}$, which explains the observed degradation kinetic well.

Degradation kinetic of aqueous imidacloprid by VUV based AOP was shown in Eq. 5.1

$$-dC/dt = k_{\bullet\text{OH,IMD}} \times [\bullet\text{OH}] \times [C] \quad (5.1)$$

[C]: imidacloprid concentration

[$\bullet\text{OH}$]: steady state hydroxyl radical concentration

$k_{\bullet\text{OH,IMD}}$: 2nd order reaction rate constant of $\bullet\text{OH}$ and imidacloprid

As explained before, since generation and consumption rates of $\bullet\text{OH}$ were equal to each other and $\bullet\text{OH}$ steady state condition was established very rapidly, concentration of $\bullet\text{OH}$ considered to be constant. Degradation of imidacloprid was then expressed by Eq. 5.2 as;

$$-dC/dt = k' \times [C] \quad (5.2)$$

$k' = k_{\bullet\text{OH,IMD}} \times [\bullet\text{OH}]$, which is pseudo-first order degradation rate constant.

Rate of degradation of aqueous imidacloprid increased with an increment in flow rate as expected (Figure 5.9; Table 5.1). This was probably due to better mixing of solution within the reactor at higher flow rate and hence increasing contact of imidacloprid with $\bullet\text{OH}$ that is primarily responsible for oxidation of imidacloprid. As mentioned before, highly strong oxidant $\bullet\text{OH}$ with a very short half life ($10^{-14} - 10^{-17}$ s) in aqueous solution was produced and consumed within a narrow layer where oxidation takes place. It is very crucial for degradation of the target compound to be present within the oxidant active zone in order to have reaction with hydroxyl radical ($\bullet\text{OH}$). Even though there was no

substantial difference on observed degradation rate constants of aqueous imidacloprid with tested flow rates, slightly higher degradation rate constant was observed at 1000 mL/min flow rate value, the highest flow rate provided by the peristaltic pump used in this study, due to slightly higher turbulent hydrodynamic condition and accordingly better mixing that 1000 mL/min flow rate generated in the photoreactor. This result shows that in terms of degradation of pollutants in water, drawback of low penetration depth of VUV (185 nm) irradiation into water can be lessened to some extent by providing high turbulent hydrodynamic regime in the experimental reactors either with manipulating flow rates or else to increase mixing and allowing contact between the coexisting species ($\bullet\text{OH}$ and imidacloprid) in water. Nonetheless, increments in observed rate constant in this particular study were only 1.29% and 1.57 % for 750 mL/min and 1000 mL/min respectively. The reason behind this marginal increase in the rate constant is mass transfer limitation of imidacloprid within the photoreactor at studied flow rates. First of all, tested higher flow rates were not able to generate high enough turbulent within the reactor to sufficiently overcome the mass transfer limitation. Second of all and more importantly, water displays high absorptivity towards VUV light and hence 185 nm light could only be able to penetrate in narrow zone of experimental solution even in presence of higher flow rate. The flow rate has influence neither on the absorption of water at 185 nm wavelength nor on the penetration depth. Therefore, the target compound that resides in the bulk solution, in other words out of the narrow oxidant active zone, cannot react with $\bullet\text{OH}$ and other radicals ($\text{H}\bullet$, e^-_{aq}) unless the target compound is efficiently transported into the first zone. Lastly, $\bullet\text{OH}$ was produced and consumed very quickly within the oxidant active zone. So, $\bullet\text{OH}$ exist only in this narrow zone and was consumed instantly before reaching outside of this zone at tested flow rates. As a matter of fact, there is no flow regime that can carry $\bullet\text{OH}$ out of the narrow zone before it is consumed. So, all the effort of testing higher flow rates was to transport higher amount of imidacloprid of the bulk solution into this narrow zone which was provided only small addition of imidacloprid infiltration into reactive zone by the tested flow rates. As a result, small increment of rate constant was observed at 1000 mL/min flow rate which can be attributed to slight increase of turbulent flow and mixing in the photoreactor.

However, VUV initiated photodegradation of aqueous imidacloprid was very rapid indeed. 100 % removal efficiency of 5 mg/L initial concentration of imidacloprid was observed by the VUV photooxidation under the all tested flow rates in less than 3.5

minutes of irradiation (Figure 5.10). The results showed that VUV based AOP was, in fact, very effective for degradation of aqueous imidacloprid irrespective of flow rates. Observed high degradation rate constants under various flow rates revealed that even at low flow rate, VUV photooxidation of aqueous imidacloprid was significant and VUV based AOP was proven to be very effective method to degrade imidacloprid from water. Since there is no much difference of observed rate constants between the tested flow rates, 500 mL/min flow rate value was chosen and used for the all following experiments.

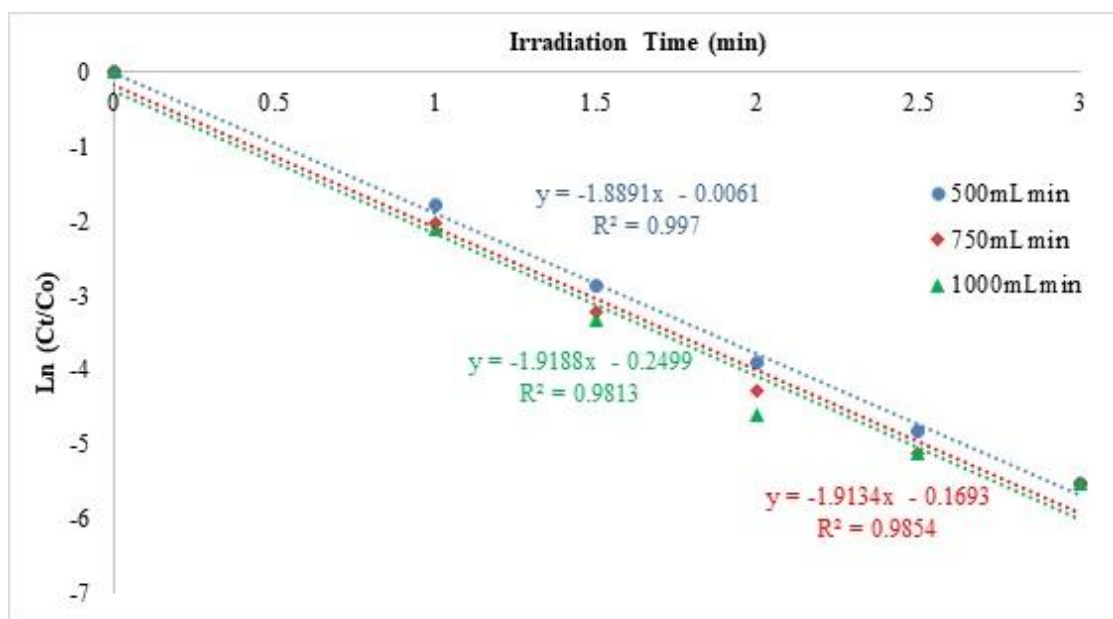


Figure 5.9 Pseudo first-order degradation of Imidacloprid ($C_o = 5$ mg/L) under various flow rate conditions. The results are average of three replicates.

Table 5.1 VUV induced degradation rate constants of Imidacloprid ($C_o = 5$ mg/L) under various flow rate conditions.

Flow Rate	Pseudo First Order Degradation Equation
500 mL/min	$y = -1.8891x - 0.0061$ $R^2 = 0.997$
750 mL/min	$y = -1.9134x - 0.1693$ $R^2 = 0.9854$
1000 mL/min	$y = -1.9188x - 0.2499$ $R^2 = 0.9813$

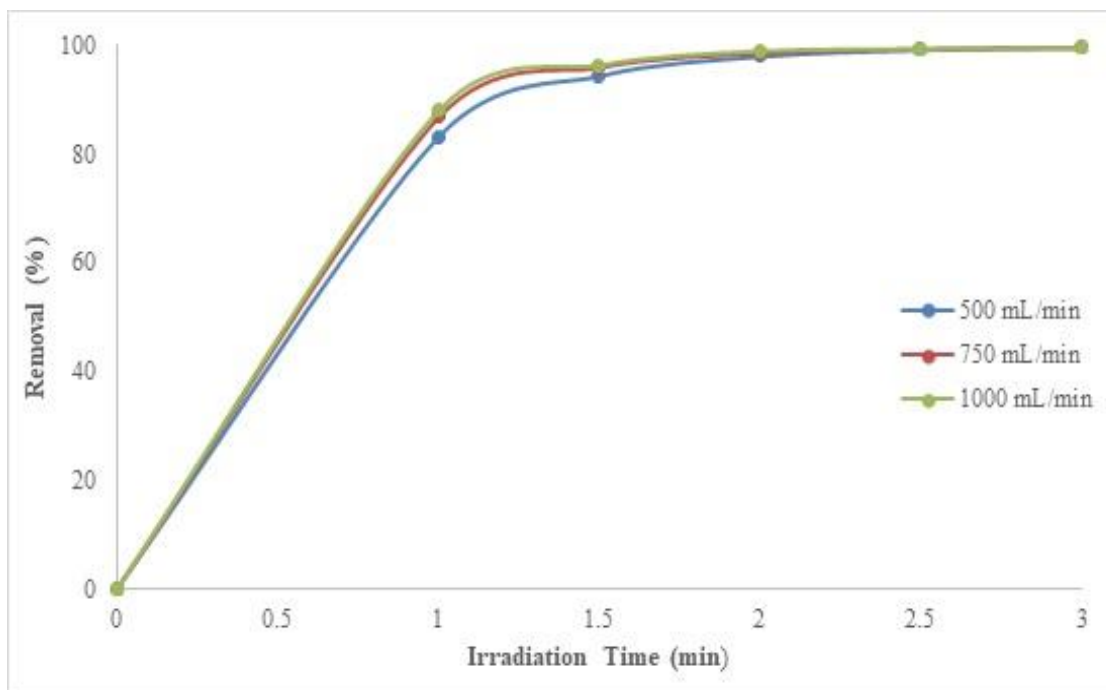


Figure 5.10 Imidacloprid ($C_0 = 5$ mg/L) removal efficiency by VUV induced photodegradation under various flow rates. The results are average of three replicates.

5.4.2. Effects of initial pH of the experimental solution

Solution pH plays an important role in most of AOPs. For example, basic condition is desired for O_3 based AOP since it increases decomposition of O_3 and more OH^- is available under this circumstances to react with O_3 to generate $\bullet OH$. On the other hand, strong acidic condition is required for fenton based AOP to generate high enough $\bullet OH$ which is the responsible reactive species for oxidation of pollutants by AOPs. Therefore, effects of initial pH of experimental solution on the VUV induced photodegradation of aqueous imidacloprid were studied under natural (original, $pH \approx 6.5$), acidic ($pH = 3$), and basic ($pH = 11$) conditions and presented in this doctoral research.

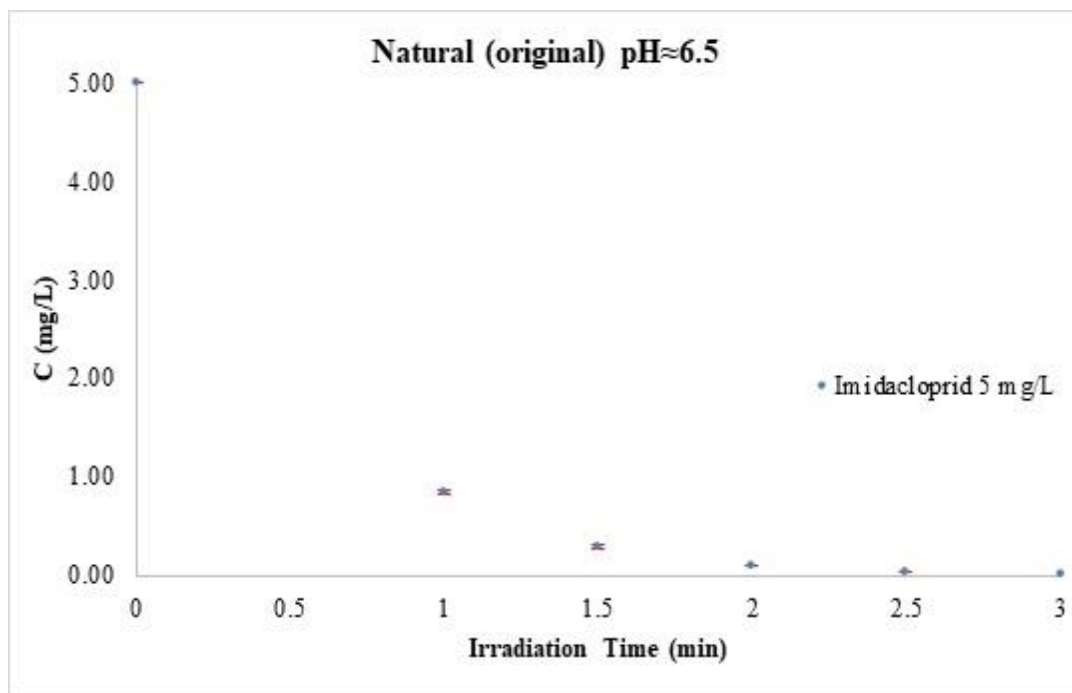


Figure 5.11 VUV induced photodegradation of Imidacloprid ($C_0 = 5 \text{ mg/L}$) under natural (original, $\text{pH} \approx 6.5$) condition. Error bars represent the standard deviations of three replicates.

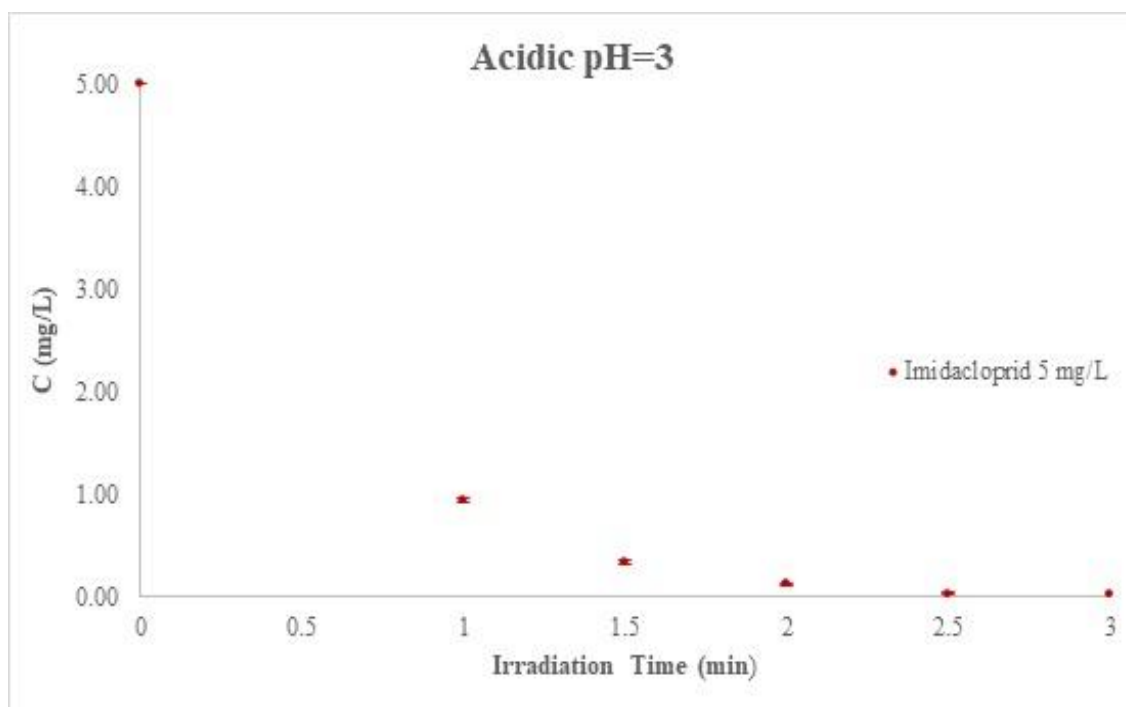


Figure 5.12 VUV induced photodegradation of Imidacloprid ($C_0 = 5 \text{ mg/L}$) under acidic ($\text{pH}=3$) condition. Error bars represent the standard deviations of three replicates.

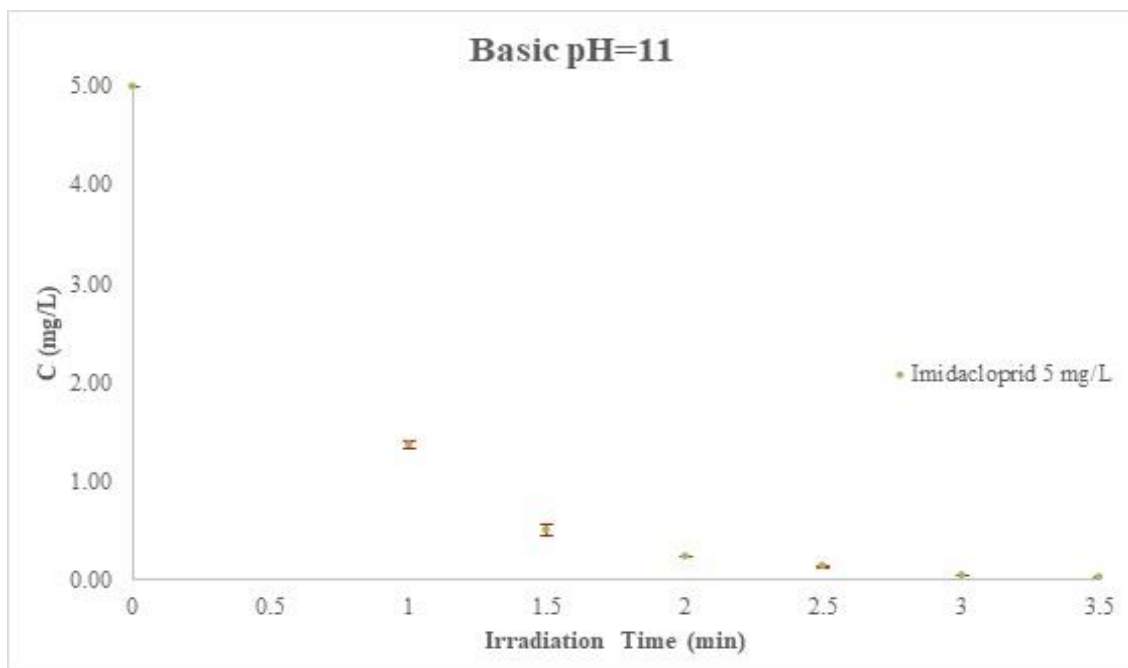


Figure 5.13 VUV induced photodegradation of Imidacloprid ($C_0 = 5 \text{ mg/L}$) under basic (pH=11) condition. Error bars represent the standard deviations of three replicates.

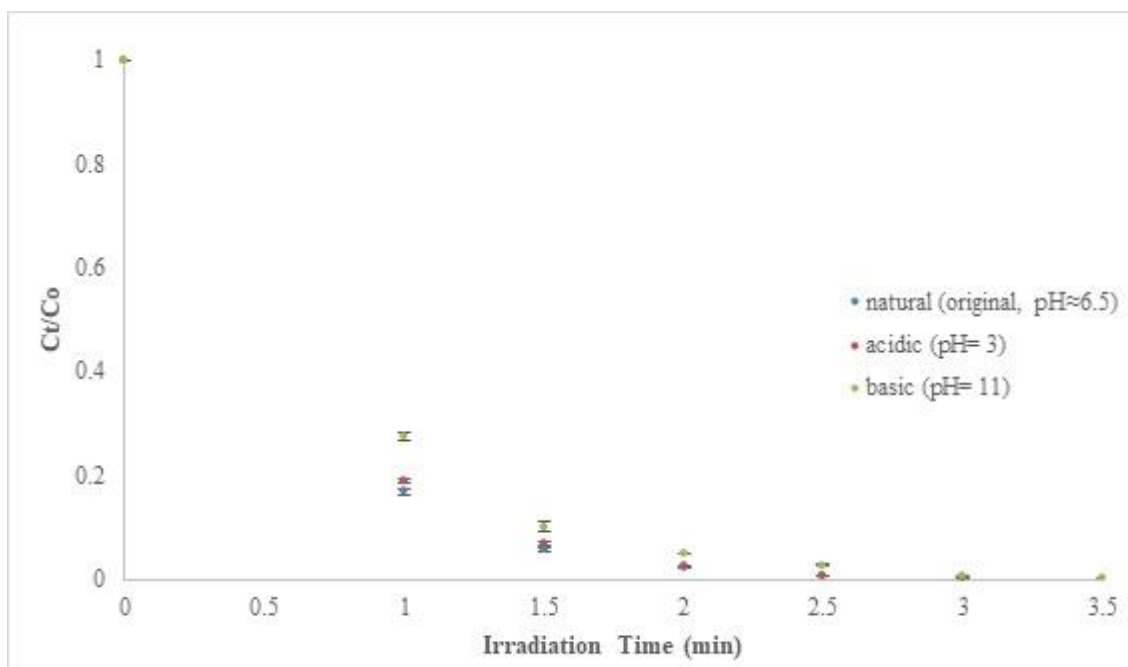


Figure 5.14 VUV initiated photodegradation of Imidacloprid ($C_0 = 5 \text{ mg/L}$) under different pH conditions. Error bars represent the standard deviations of three replicates.

Effects of solution pH onto photodegradation of imidacloprid with laboratory scale VUV photooxidation system were presented herein. Figures 5.11, 5.12, and 5.13 display VUV initiated degradation of aqueous imidacloprid under various pH conditions. Figures 5.14 and 5.15 reveal that pseudo first order degradation kinetic with $R^2 \geq 0.99$ was observed for all tested pH conditions as in the case of flow rates. Higher degradation rate constant was observed in the following order of acidic > natural (original) > basic conditions (Figures 5.14 and 5.15, Table 5.2). Considerable decrease (15.33 %) in the rate of degradation of imidacloprid was observed at basic condition at pH=11. Inhibition of degradation of target compounds under basic condition was also reported by other researchers [92][83][93][94]. This result might be attributed to reduction of oxidation potential of $\bullet\text{OH}$ and/or conversion of $\bullet\text{OH}$ to $\bullet\text{O}^-$ radical in strong alkaline solution (Equation 5.3). First explanation and maybe the driving force of decrement in rate constant with the increase of solution pH might be reduction of oxidation potential of $\bullet\text{OH}$ in alkaline media. Yang [83] reported that solution pH not only affected the redox potential of $\bullet\text{OH}$ but also its production rate. They observed significant decrease in pseudo first order degradation rate constants of alachlor, chloroneb, and atrazine by VUV irradiation when solution pH was increased from 5 to 9. Decline of oxidation power of $\bullet\text{OH}$ from 2.59 V at strong acidic condition to 1.65 V at alkaline condition was also reported by Koppenol and Liebman [92]. Moreover, similar finding was published by Chen [94] is that oxidation potential of $\bullet\text{OH}$ was declined from 2.62 V to 2.15 V with increment of solution pH from 3 to 11. Gholamreza Moussavi [93] experienced decline in cloxacillin degradation percentage by VUV photooxidation from 83.6% to 65.5% when the solution pH was increased from 3 to 10 as well. The observed removal decrement was attributed to the reduction of the oxidation potential of $\bullet\text{OH}$ at high solution pH. To support above findings, in addition, oxidation potential of $\bullet\text{OH}$ was reported to be $E_0 = 2.8$ V and $E_{14} = 1.96$ V for strong acidic and basic conditions by Kim and Vogelpohl [95]. It is known that reaction between OH^- and $\bullet\text{OH}$ is enhanced at alkaline condition and $\bullet\text{OH}$ is rapidly converted to its conjugate base $\bullet\text{O}^-$ with $k = 1.2 \times 10^{10} \text{ L mol}^{-1} \text{ s}^{-1}$ [74] under high pH condition.



$\bullet\text{O}^-$ radical with redox potential of 1.78 V [94] is less reactive than $\bullet\text{OH}$ and has a lower reaction rate constant with organic compounds compared to $\bullet\text{OH}$. At pH=11, produced $\bullet\text{OH}$ was converted to $\bullet\text{O}^-$ according to Equation 5.3. Therefore, not only less amount of

$\bullet\text{OH}$ but also less reactive $\bullet\text{O}^-$ were coexisting and available for oxidation of imidacloprid at $\text{pH} = 11$ and might be the another reason behind this experimental findings as second explanation. Another explanation is that when the pH was raised to 11, $\bullet\text{O}^-$ might be the primary reactant rather than $\bullet\text{OH}$ and since $\bullet\text{O}^-$ reacted more slowly than $\bullet\text{OH}$ with aqueous imidacloprid, lower degradation rate was accordingly recorded for $\text{pH}=11$.

These above mentioned facts might explain the decrease in observed rate constant of aqueous imidacloprid by VUV process in elevated pH condition and explicitly show the primary role of $\bullet\text{OH}$ in the disappearance of imidacloprid under normal circumstances.

The highest degradation rate was observed for acidic ($\text{pH}= 3$) initial pH condition of imidacloprid solution (Table 5.2). This finding can again be attributed to the highest oxidation potential of $\bullet\text{OH}$ which is experienced under strong acidic condition. Similar finding was also published by Iglesias [67] who investigated effects of pH on the reduction of imidacloprid by electro fenton system with ironalginate gel beads. They also reported higher degradation efficiency of imidacloprid at lower pH condition which was related to the higher oxidation power of $\bullet\text{OH}$ at low solution pH . As mentioned before, solution pH not only affects the redox potential of $\bullet\text{OH}$ but also its production rate [83]. Therefore, improved degradation efficiency can also be attributed to higher generation rate of $\bullet\text{OH}$ which was experienced by Patil [68] as well. Moreover, because recombination reaction of $\bullet\text{OH}$ radicals is disrupted in acidic condition, higher reduction rate of imidacloprid might have been observed in tested low pH as another explanation. Enhanced reduction of aqueous imidacloprid might also be due to the fact that, imidacloprid transforms from ionic to molecular state in acidic pH [66] and hence might have been located at nearby the oxidant active first zone experienced in VUV photooxidation and accordingly might have been more effectively reacted with $\bullet\text{OH}$. Increased degradation efficiency of pesticides by VUV based or other AOPs which are characterized by generation of $\bullet\text{OH}$, at low solution pH was also reported in literature as in agreement with our observation.

Observed degradation rate in acidic solution was slightly (only 1.7 %) higher than that of natural (original, $\text{pH}\approx 6.5$) condition since the difference of oxidation power of $\bullet\text{OH}$ in tested acidic and original pH conditions was not significant as reported by Koppenol and Liebman [92].

Figure 5.16 shows that it took only 3.5 minutes of irradiation to observe complete removal of 5 mg/L initial concentration of imidacloprid by the VUV photooxidation under acidic (pH= 3) and natural (original, pH≈6.5) conditions whereas it was recorded to be 4 minutes for basic (pH=11) condition. The results clearly showed that VUV photooxidation was unlike to other AOPs most of which require certain pH range, very effective for degradation of aqueous imidacloprid under the all tested pH conditions. Observed high degradation rate constants under various initial pH of solution also showed that the VUV photooxidation does not require specific pH arrangement nor does pH monitoring to degrade imidacloprid from water.

Since there is no much difference of observed rate constants between the tested natural (original) and acidic pH conditions, natural (original) pH condition was chosen and used for the all following experiments.

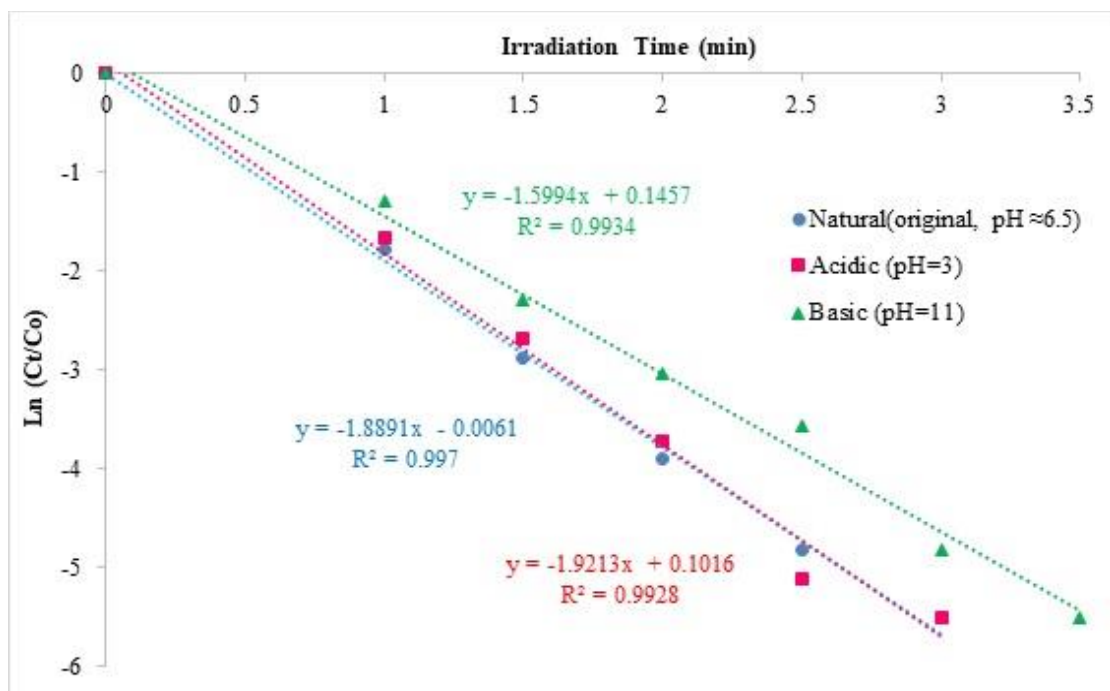


Figure 5.15 Pseudo first-order degradation of Imidacloprid ($C_o = 5$ mg/L) under different pH conditions. The results are average of three replicates.

Table 5.2 VUV induced degradation rate constants of Imidacloprid ($C_o = 5 \text{ mg/L}$) under various pH conditions.

Solution pH	Pseudo First Order Degradation Equation
Natural (original, pH≈6.5)	$y = -1.8891x - 0.0061$ $R^2 = 0.997$
Acidic (pH=3)	$y = -1.9213x + 0.1016$ $R^2 = 0.9928$
Basic (pH=11)	$y = -1.5994x + 0.1457$ $R^2 = 0.9934$

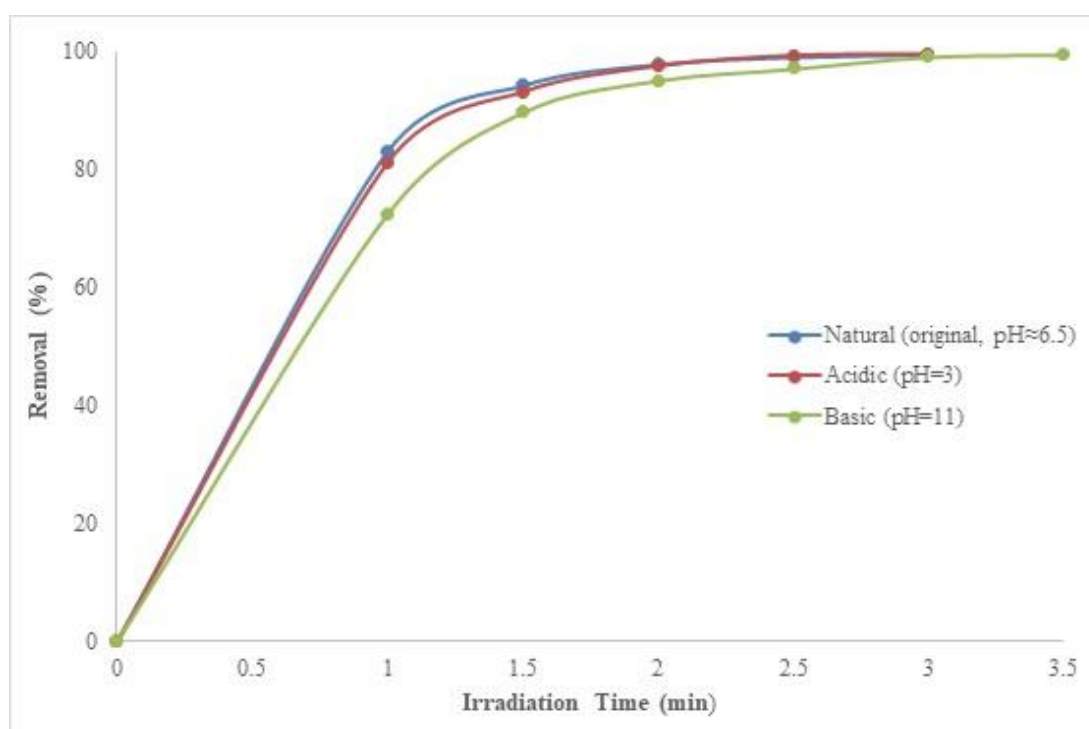


Figure 5.16 Imidacloprid ($C_o = 5 \text{ mg/L}$) removal efficiency by VUV induced photodegradation under various pH conditions. The results are average of three replicates.

5.4.3. Effects of initial concentration of Imidacloprid

Concentration of pollutants in real raw water and water treatment plants is not always constant and may fluctuate in the influent. Therefore, effectiveness of applied process to treat various concentrations of the target pollutants should be evaluated before its application. Besides, pollutants may show different pattern in degradation kinetic at various concentration level under the same treatment process. Investigation of this possibility is important before desinging the configuration of the treatment units. For these reasons, various initial concentrations of aqueous imidacloprid, 2.5, 5, 10 mg/L were investigated to observe degradation efficiency of VUV induced AOP and degradation kinetics of imidacloprid at tested initial concentrations in this doctoral study and results were presented in this subsection.

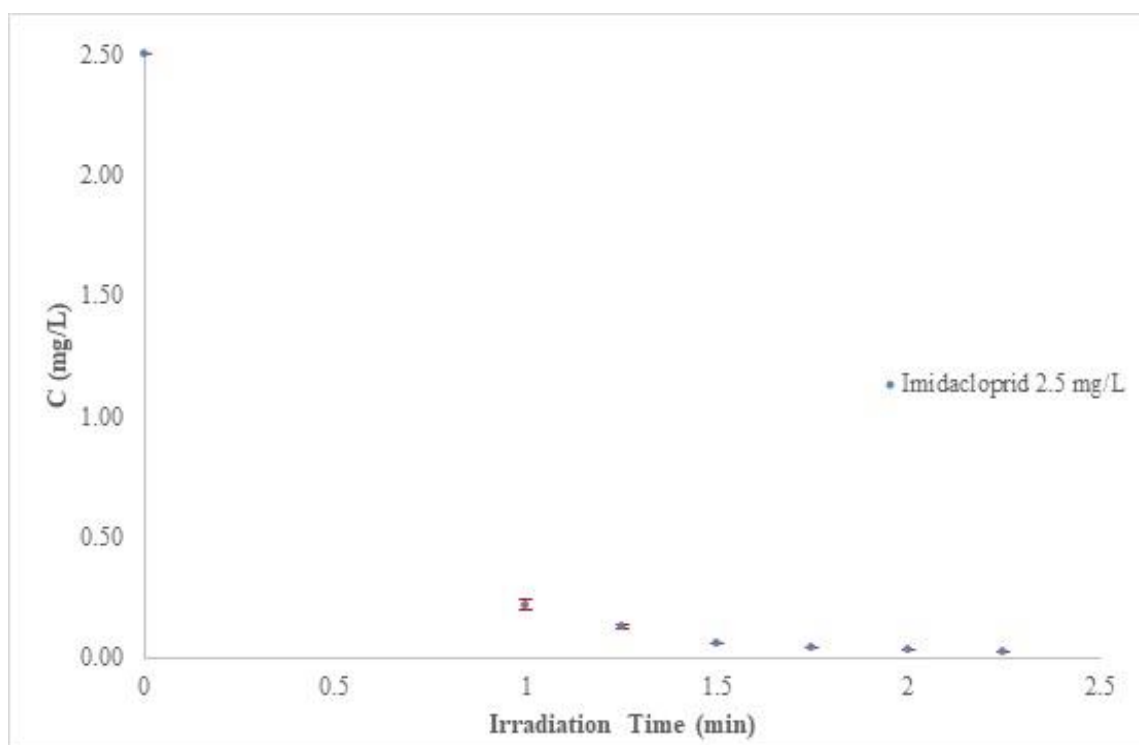


Figure 5.17 VUV induced photodegradation of Imidacloprid ($C_0 = 2.5$ mg/L). Error bars represent the standard deviations of three replicates.

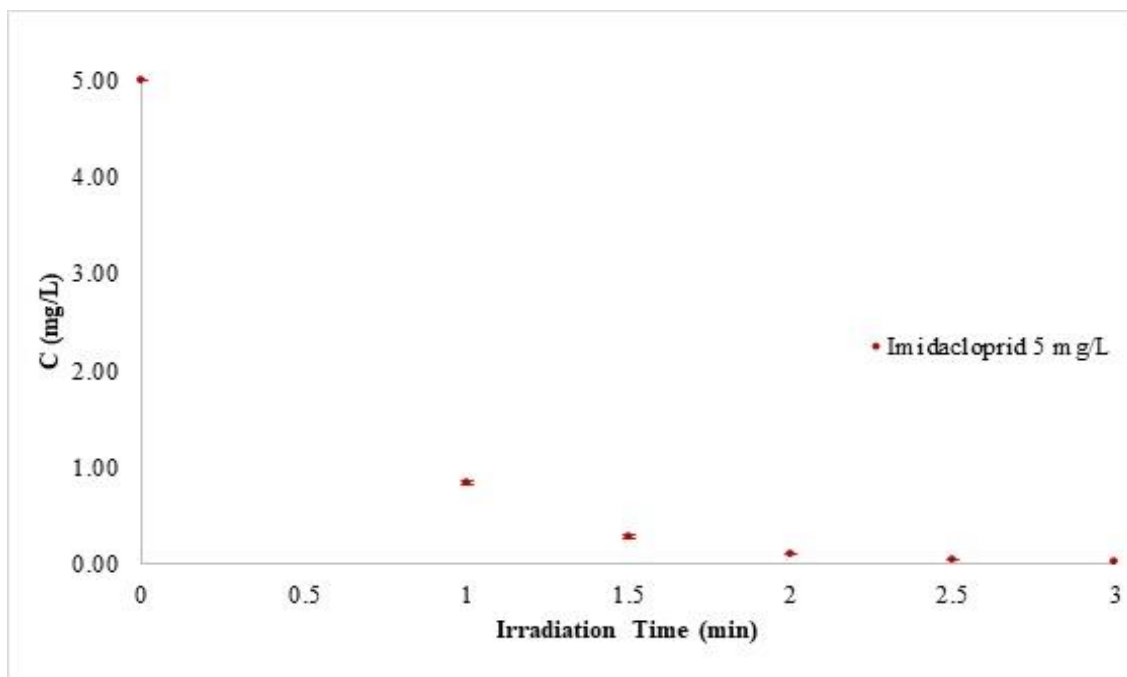


Figure 5.18 VUV induced photodegradation of Imidacloprid ($C_0 = 5 \text{ mg/L}$). Error bars represent the standard deviations of three replicates.

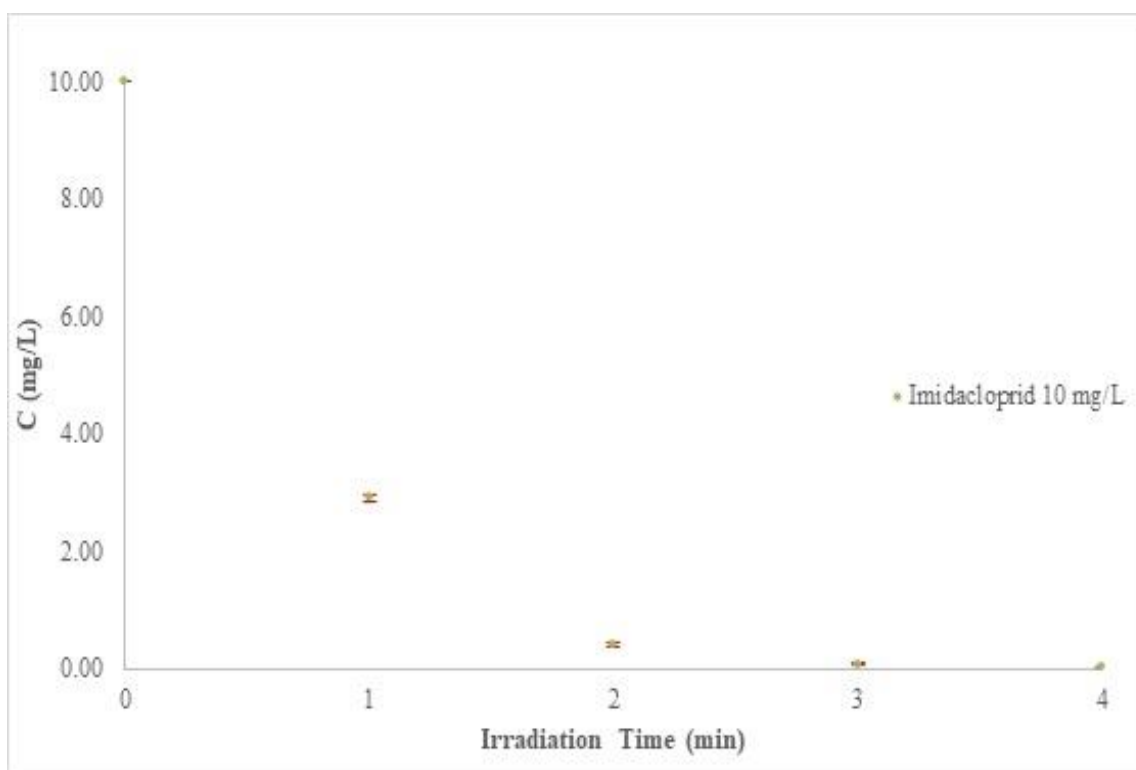


Figure 5.19 VUV induced photodegradation of Imidacloprid ($C_0 = 10 \text{ mg/L}$). Error bars represent the standard deviations of three replicates.

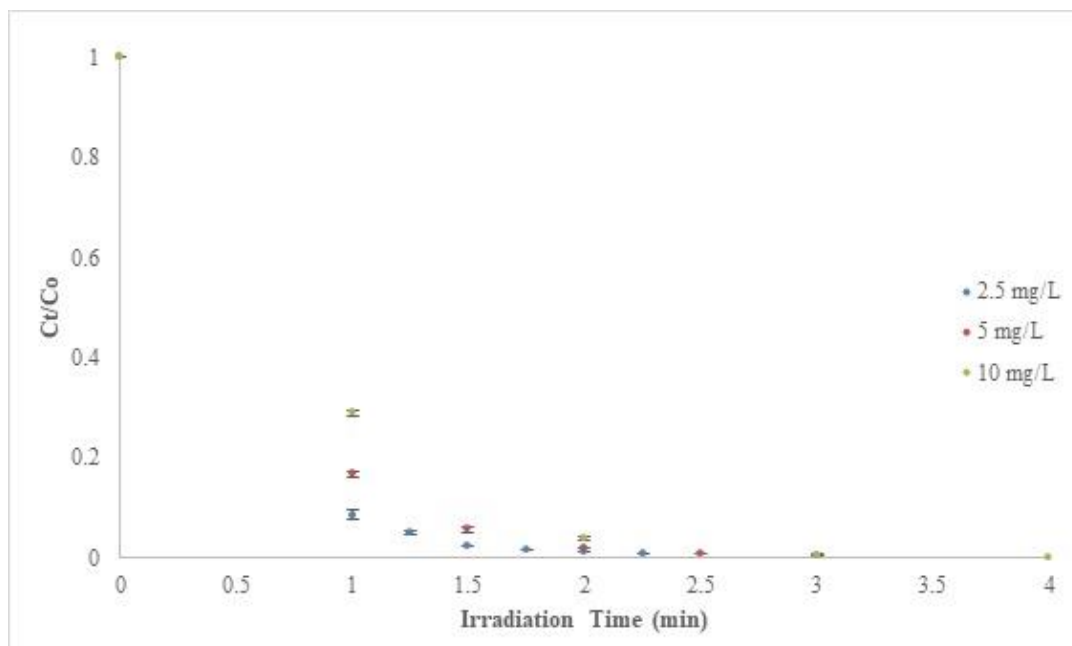


Figure 5.20 VUV initiated photodegradation of Imidacloprid under various initial concentrations. Error bars represent the standard deviations of three replicates.

Effects of initial concentration of aqueous imidacloprid on the photodegradation of itself by VUV process were presented herein. Figures 5.17, 5.18, and 5.19 present VUV induced degradation of aqueous imidacloprid with various initial concentrations. Figures 5.20 and 5.21 show that pseudo first order degradation kinetic with $R^2 \geq 0.99$ was observed for all the tested initial imidacloprid concentrations as in the case of flow rates and solution pH. Observed degradation rate and removal efficiency were decreased with the increment of initial imidacloprid concentration (Figures 5.21 and 5.22; Table 5.3). The reason behind this finding might be reduction of ratio of hydroxyl radical ($\bullet\text{OH}$) to imidacloprid since the amount of produced $\bullet\text{OH}$ by the VUV process was constant even though concentration of imidacloprid was increased. This result might also be attributed to the fact that higher amount of $\bullet\text{OH}$ reacted with imidacloprid at higher concentration and hence available steady state concentration of $[\bullet\text{OH}]$ became less. In other words, depletion of $\bullet\text{OH}$ went up with increased concentration of imidacloprid. As a result, since pseudo first order degradation rate constant, $k' = k_{\bullet\text{OH},\text{C}} \times [\bullet\text{OH}]$, is proportional to the steady state concentration of $[\bullet\text{OH}]$, decrement in $[\bullet\text{OH}]$ might have caused the decrease in the observed rate constant. Several researchers also reported decrement in the pseudo first order degradation constant of target compounds with higher initial concentration in agreement with our results [96][97][93][98][99].

Other researchers also investigated the degradation of aqueous imidacloprid by various AOPs. Bourgin [65] conducted ozonation of imidacloprid ($C_o = 39 \text{ mg/L}$) in ultrapure water with 25, 50, and 100 g/m^3 ozone concentrations in the inlet gas during 90 minutes of treatment time. Pseudo-first order degradation rates of 0.147 and 0.129 min^{-1} were reported for standard imidacloprid solution and seed loading solution respectively when concentration of ozone was 100 g/m^3 . Zabar [7] investigated photocatalytic removal of imidacloprid along with immobilized titanium dioxide (TiO_2). They observed 98.8% imidacloprid ($C_o = 100 \text{ mg/L}$) disappearance within 2 hours of treatment with rate constant of 0.035 min^{-1} . Study by Raut-Jadhav [66] focused on degradation of aqueous imidacloprid ($C_o = 25 \text{ mg/L}$) via hydrodynamic cavitation (HC) and combination of HC along with several AOPs (HC+fenton, HC+photofenton, HC+photolytic, and HC+photocatalytic). Substantial enhancement in the disappearance rate of imidacloprid was observed via HC + Fenton process which resulted a rate constant of $250.749 \times 10^{-3} \text{ min}^{-1}$ using molar ratio of imidacloprid: H_2O_2 as 1:40. Combination of photo-fenton with HC concluded even higher removal rate constant of $297.012 \times 10^{-3} \text{ min}^{-1}$. Iglesias [67] investigated disappearance of aqueous imidacloprid ($C_o = 100 \text{ mg/L}$) in distilled water under electro-Fenton system with ironalginate gel beads (EF-FeAB). Increase of reduction rate constant in the order of EF-FeAB > EF with free ions > electrochemical processes was reported with 0.0405 min^{-1} , 0.0264 min^{-1} , 0.0112 min^{-1} respectively in 120 min of treatment. In another study, Fenoll [63] examined zinc oxide (ZnO , 200 mg/L) and titanium dioxide (TiO_2 , 200 mg/L) induced photocatalytic degradation of aqueous imidacloprid ($C_o = 0.1 \text{ mg/L}$) in presence and absence of Sodium Persulfate ($\text{Na}_2\text{S}_2\text{O}_8$, 250 mg/L) as an electron acceptor by applying natural light and UV artificial light. $\text{ZnO}/\text{Na}_2\text{S}_2\text{O}_8$ and $\text{TiO}_2/\text{Na}_2\text{S}_2\text{O}_8$ application under UV light irradiation succeeded total degradation of imidacloprid in 10 and 30 min respectively. Observed degradation rate constants of imidacloprid varied from 0.0171 min^{-1} (TiO_2 under UV light) to 2.4110 min^{-1} ($\text{ZnO}/\text{Na}_2\text{S}_2\text{O}_8$ under solar light) under different light sources and various catalysts. The highest apparent reduction rate constant (2.4110 min^{-1}) of imidacloprid was experienced during $\text{ZnO}/\text{Na}_2\text{S}_2\text{O}_8$ treatment under solar light with half life of 0.3 min. Amir Akbari Shorgoli and Mohammad Shokri [64] more recently studied photocatalytic degradation of aqueous imidacloprid with immobilized TiO_2 nanoparticles ($C_o = 200 \text{ mg/L}$) in presence of UVC light. Observed reduction rate constants of 0.0704 , 0.0594 , and 0.0445 min^{-1} were respectively reported for 20, 40, and 60 mg/L of initial imidacloprid concentrations during 30 min of reaction.

Experienced performance and rate constants by all these authors were different due to application of different experimental conditions, reactor designs, amount of catalysts and target compound, lamp powers and intensities, radiation sources and wavelengths.

Performance of VUV initiated photodegradation of aqueous imidacloprid at various initial concentrations was found to be significant in this study. Figure 5.22 shows that it took only 2.5 min, 3.5 min, and 4.5 min of VUV irradiation to observe complete removal of 2.5 mg/L, 5 mg/L, 10 mg/L initial concentration of imidacloprid respectively. Rozsa[100] also reported complete degradation of aqueous imidacloprid (1×10^{-4} M) by VUV process within 10 minutes as in accordance with result of this study. VUV induced degradation rate constants of 2.1814 min^{-1} , 1.8891 min^{-1} , 1.6307 min^{-1} were determined in the same order of concentration (Figure 5.22; Table 5.3). Table 5.4 presents the comparison of reduction rates of aqueous imidacloprid obtained by the VUV process of this research and those of previously reported AOPs. VUV based AOP actually presented better performance than others in regards of decomposition of imidacloprid. Similar findings of improved degradation efficiency of organic pollutants by VUV process over the other AOPs were also previously reported [93][98] as in agreement with ours. Observed increment in degradation efficiency can be attributed to generation of higher amount of $\bullet\text{OH}$ by the VUV process.

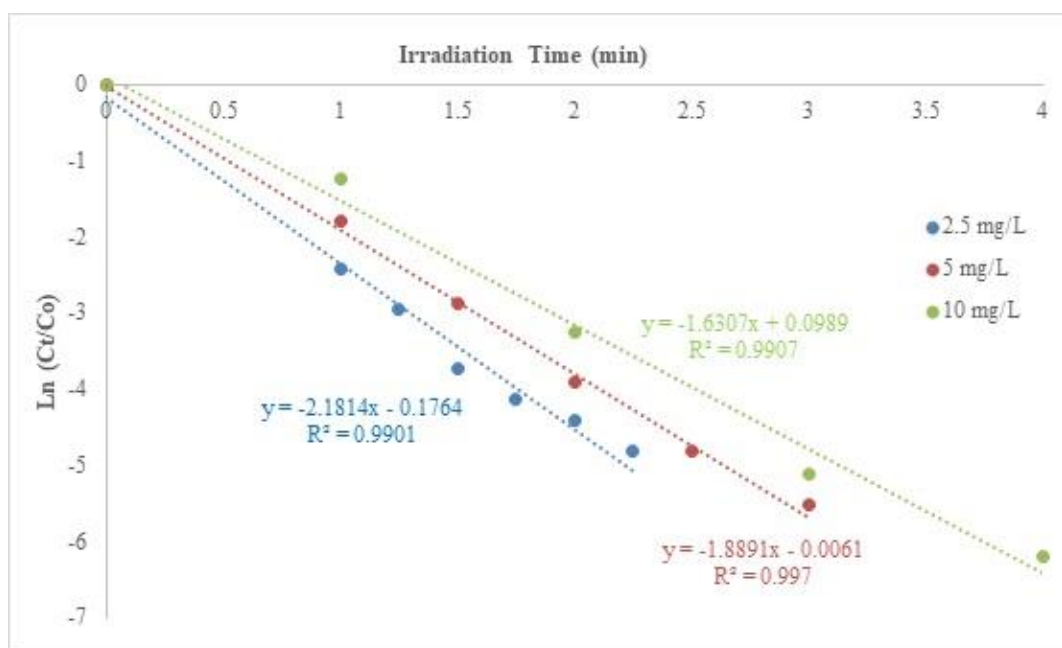


Figure 5.21 Pseudo first-order degradation of Imidacloprid under various initial concentrations. The results are average of three replicates.

Table 5.3 VUV induced degradation rate constants of Imidacloprid with various initial imidacloprid concentrations.

Initial Concentration (mg/L)	Pseudo First Order Degradation Equation
2.5	$y = -2.1814x - 0.1764$ $R^2 = 0.9901$
5	$y = -1.8891x - 0.0061$ $R^2 = 0.997$
10	$y = -1.6307x + 0.0061$ $R^2 = 0.9907$

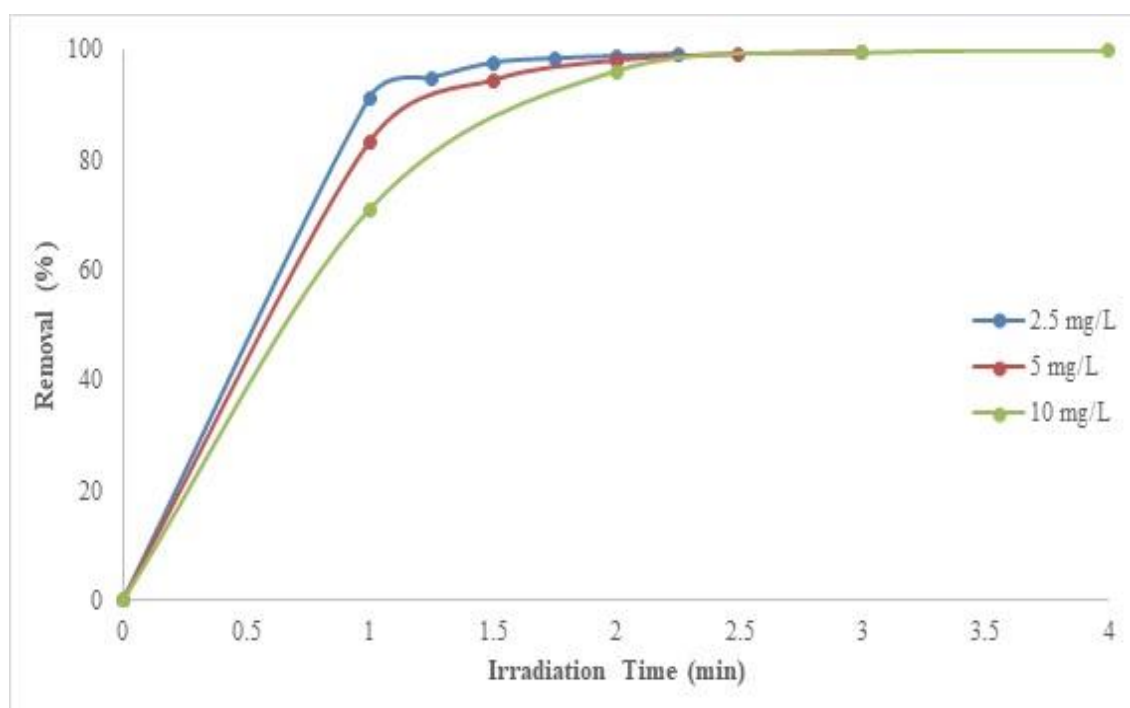


Figure 5.22 Imidacloprid removal efficiency by VUV induced photodegradation under various initial concentrations. The results are average of three replicates.

Table 5.4 Reported reduction rates of Imidacloprid by VUV and other AOPs.

Process	Imidacloprid concentration (mg/L)	Rate constant (min ⁻¹)	Reference
VUV	2.5 5 10	2.1814 1.8891 1.6307	Present study
O ₃	39	0.147	[65]
UVA/TiO ₂	100	0.035	[7]
HDC/fenton	25	0.2507	[66]
HDC/photofenton	25	0.2970	
EF-FeAB	100	0.0405	[67]
Solarlight/ZnO/Na ₂ S ₂ O ₈	0.1	2.4110	[63]
UVC/TiO ₂ nanoparticles	20	0.0704	[64]

5.4.4. Effects of Inorganic ions

Inorganic ions, HCO₃⁻, CO₃²⁻, and NO₃⁻, are commonly found in natural water bodies. Presence of these ions may affect the degradation process either by absorbing 185 nm photon and acting as inner filter or by scavenging HO• produced via water homolysis and ionization of 185 nm irradiation. Therefore, effects of such inorganic ions on the removal rate constant as well as kinetic pattern of aqueous imidacloprid by VUV process were evaluated separately in this doctoral study and presented herein.

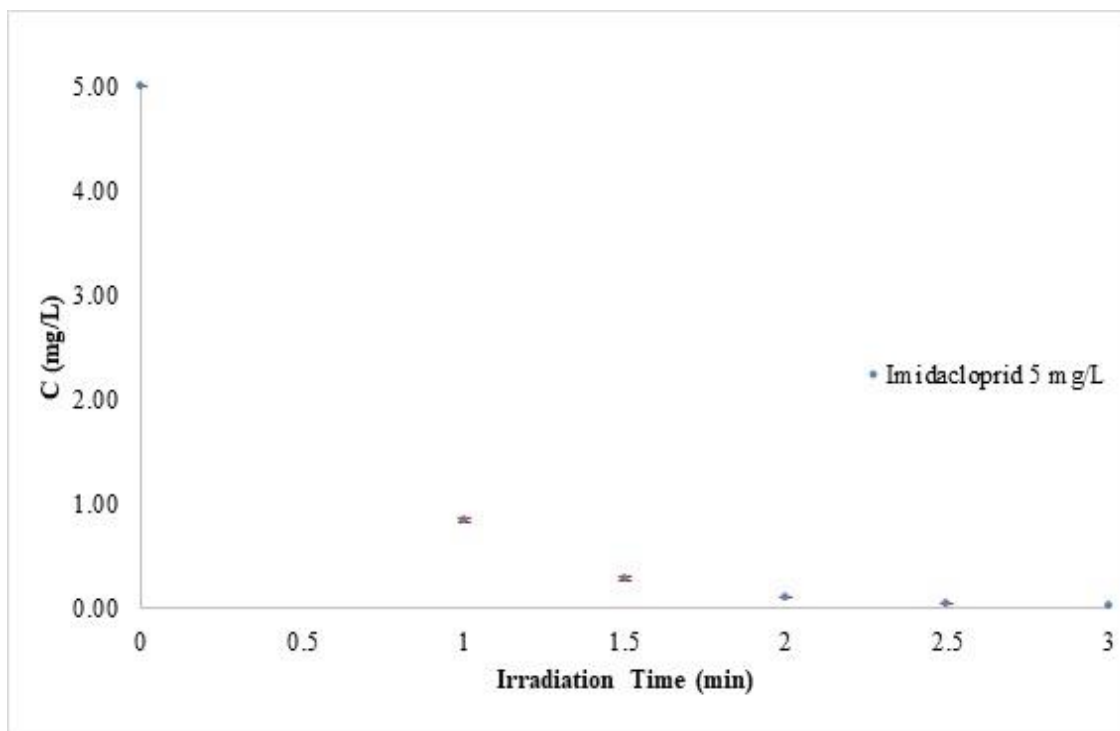


Figure 5.23 VUV induced photodegradation of Imidacloprid ($C_0 = 5 \text{ mg/L}$) in absence of inorganic ions. Error bars represent the standard deviations of three replicates.

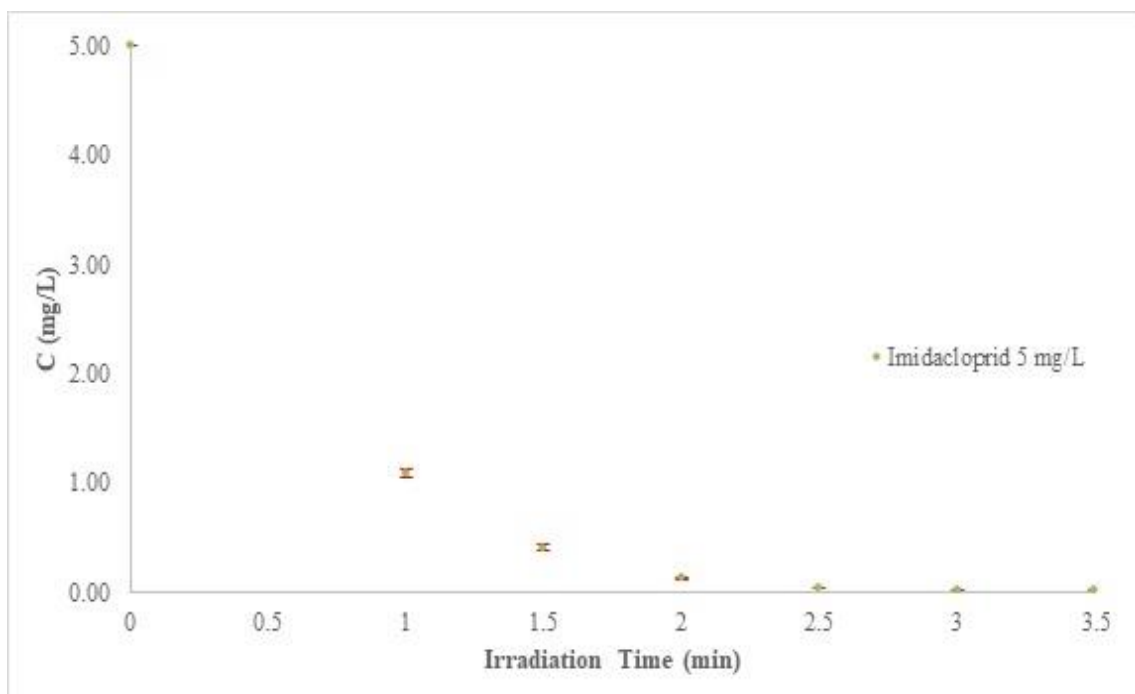


Figure 5.24 VUV induced photodegradation of Imidacloprid ($C_0 = 5 \text{ mg/L}$) in presence of carbonate ion ($\text{CO}_3^{2-} = 5 \text{ mg/L}$). Error bars represent the standard deviations of three replicates.

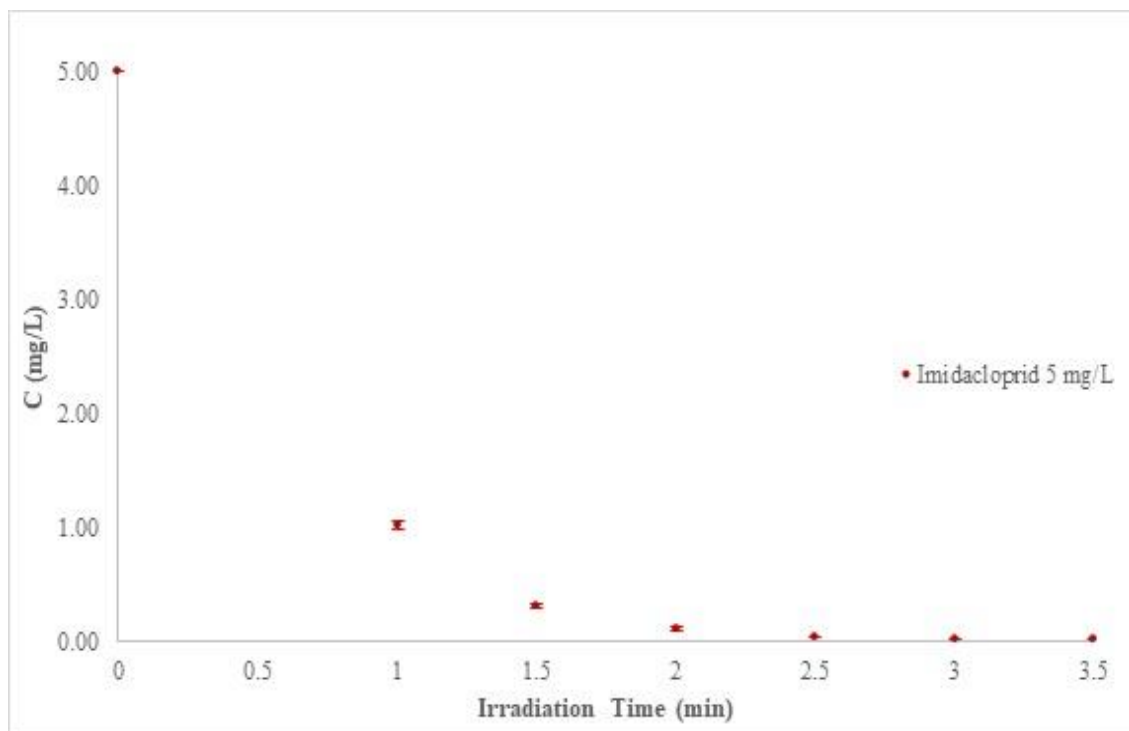


Figure 5.25 VUV induced photodegradation of Imidacloprid ($C_0 = 5 \text{ mg/L}$) in presence of bicarbonate ion ($\text{HCO}_3^- = 5 \text{ mg/L}$). Error bars represent the standard deviations of three replicates.

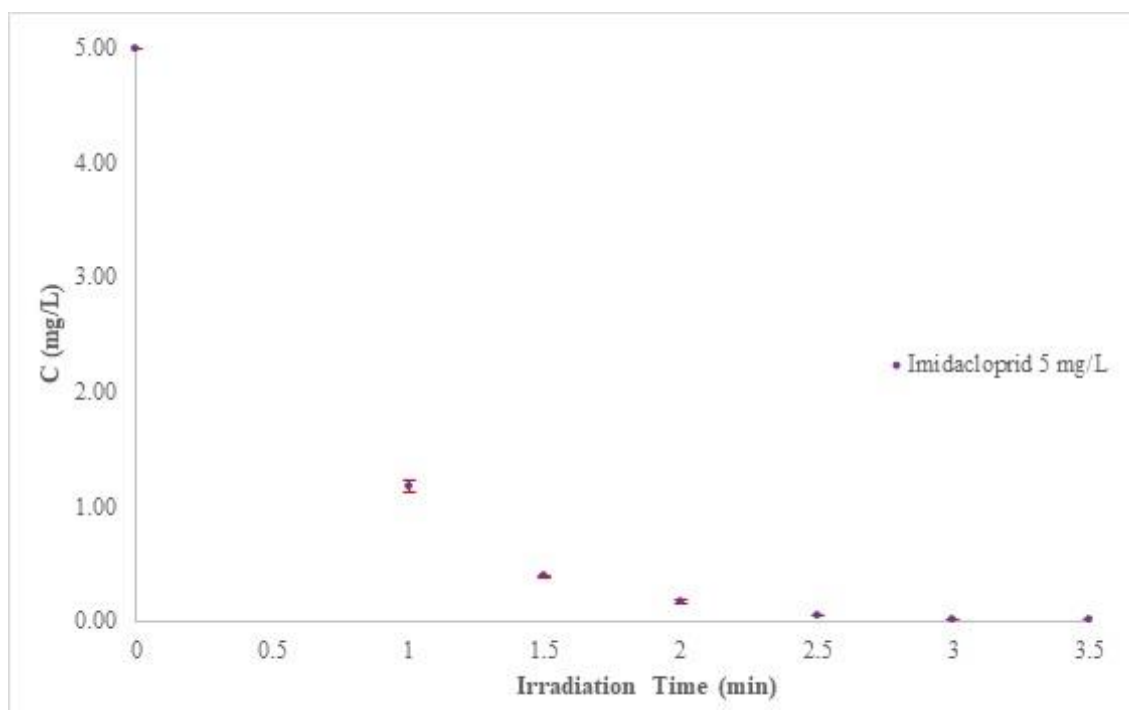


Figure 5.26 VUV induced photodegradation of Imidacloprid ($C_0 = 5 \text{ mg/L}$) in presence of nitrate ion ($\text{NO}_3^- = 5 \text{ mg/L}$). Error bars represent the standard deviations of three replicates.

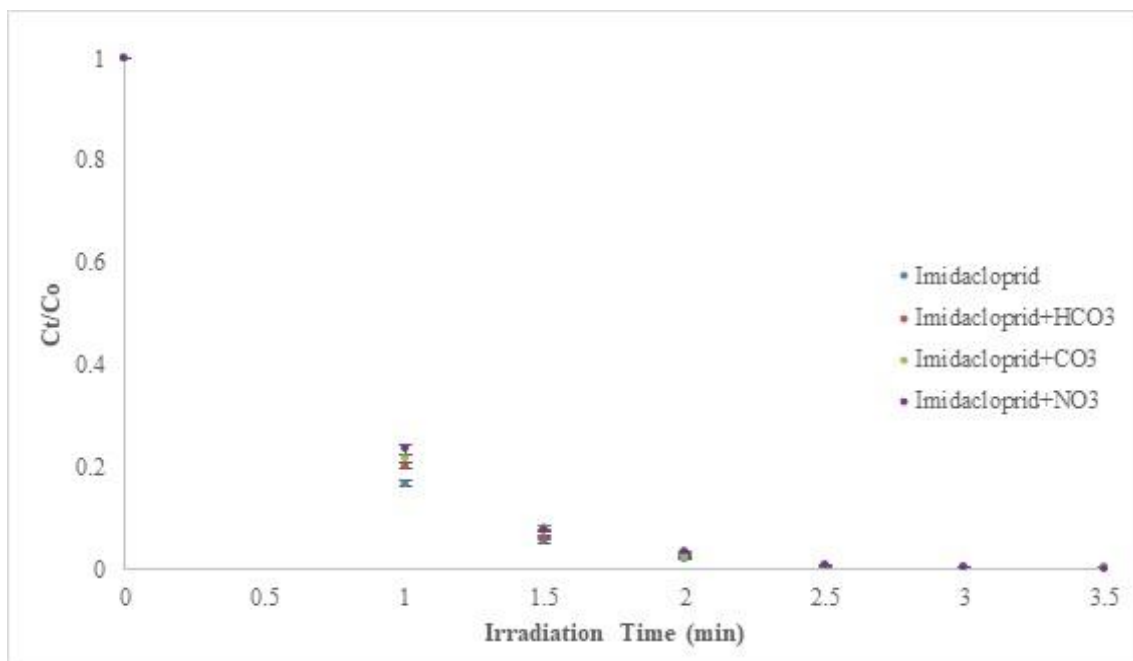
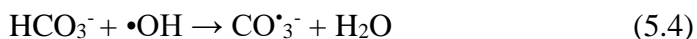


Figure 5.27 VUV induced photodegradation of Imidacloprid ($C_0 = 5 \text{ mg/L}$) in presence of various inorganic ions. Error bars represent the standard deviations of three replicates.

Effects of presence of inorganic ions on the photodegradation of aqueous imidacloprid by VUV process were reported in this subsection. Figures 5.23 through 5.26 present VUV induced degradation of aqueous imidacloprid in the absence and presence of inorganic ions (HCO_3^- , CO_3^{2-} , and NO_3^-). Figures 5.27 and 5.28 show that pseudo first order degradation kinetic with was observed for all the tested conditions. Observed degradation rate and removal efficiency were decreased in the presence of inorganic ions as expected (Figures 5.28 and 5.29; Table 5.5). Higher inhibition of imidacloprid degradation was observed in the order of $\text{CO}_3^{2-} > \text{HCO}_3^- > \text{NO}_3^-$ presence. Decrement of 10.68%, 9.88%, and 8.87% in the degradation rate constant of imidacloprid were recorded for CO_3^{2-} , HCO_3^- , and NO_3^- respectively. These results can be attributed to scavenging of $\text{HO}\cdot$ by HCO_3^- and CO_3^{2-} which are well known $\cdot\text{OH}$ scavengers, according to equations 5.4 and 5.5 [74] and absorption of 185 nm photon as well as $\cdot\text{OH}$ scavenging by NO_3^- which has high molar absorption coefficient of 185 nm photon [81]. HCO_3^- and CO_3^{2-} competed with imidacloprid to react with $\cdot\text{OH}$ and as a result, less amount of $\cdot\text{OH}$ were available for imidacloprid as first explanation of decrease in degradation of imidacloprid. Second explanation is that even though carbonate radical ($\text{CO}_3^{\cdot-}$) generated in the presence of

HCO_3^- and CO_3^{2-} , with oxidation potential of 1.78 V at pH 7 [72][2] is capable of oxidizing pollutants including imidacloprid, it is less reactive than $\bullet\text{OH}$, which accordingly resulted lower removal rate of imidacloprid. So, not only less amount of $\bullet\text{OH}$ and but also presence of less reactive of CO_3^{2-} might have caused the observed reduction.



Reaction rate constants of HCO_3^- and CO_3^{2-} with $\bullet\text{OH}$ in equations 5.4 and 5.5 are $8.5 \times 10^6 \text{ M}^{-1} \text{ s}^{-1}$ and $4 \times 10^8 \text{ M}^{-1} \text{ s}^{-1}$ respectively [74]. CO_3^{2-} react with $\bullet\text{OH}$ more or less 47 times faster than that of HCO_3^- . Adrian Serrano Mora [81] also reported that CO_3^{2-} has 28 to 45 times faster reaction rate than HCO_3^- with $\bullet\text{OH}$ [74][101][102]. Therefore, these rate constants can explain observing the highest degradation inhibition in presence of CO_3^{2-} . There was no significant difference in observed rate constants in presence of HCO_3^- and CO_3^{2-} . This can be attributed to the pH values of carbonated (CO_3^{2-}) and bicarbonate (HCO_3^-) experimental solutions. As presented in chapter 3 of this doctoral thesis, pH values of experimental solutions that contain 5 mg/L HCO_3^- and CO_3^{2-} were 7.738 and 9.911 respectively. Equilibria between carbonic species (HCO_3^- and CO_3^{2-} , H_2CO_3) in water is pH dependent. At pH 7.738 carbonic species are only in the form of HCO_3^- which makes up around 90% of total carbonic species at this measured pH and H_2CO_3 . On the other hand, at pH 9.911 carbonic species are only in the form of CO_3^{2-} and HCO_3^- which is again around 60%. So, at observed higher pH value, concentration of CO_3^{2-} was not enough high that might have resulted further degradation of imidacloprid compared to one experienced in the presence of HCO_3^- . It can be concluded that scavenging effects of HCO_3^- and CO_3^{2-} might exhibit differences in accordance with solution pH.

Presence of NO_3^- has resulted slightly less inhibition than carbonic species since NO_3^- has less reactivity with $\bullet\text{OH}$. Despite this fact (less reactivity with $\bullet\text{OH}$), decrease in rate constant in the presence of NO_3^- was almost as high as presence of other ions (Figure 5.28; Table 5.5) and could be attributed to high absorption coefficient of NO_3^- at 185 nm photon. NO_3^- might have acted as inner filter and absorbed some of the VUV photon. As a result, less amount of 185 nm might have excited the water molecules and subsequently less amount of $\bullet\text{OH}$ might have produced which could explain the observation of almost same level inhibition of imidacloprid degradation rate. Our observation is in agreement

with previously reported literatures. Moussavi [98] reported decrease of cyanide degradation in presence of HCO_3^- , CO_3^{2-} , and NO_3^- in the same order of inhibition that is experienced in this doctoral study. Decrement in imidacloprid degradation rate in the presence of HCO_3^- , CO_3^{2-} which are well known $\bullet\text{OH}$ scavengers, shows once again that $\bullet\text{OH}$ is the primary reactive species in the VUV induced degradation of imidacloprid.

Despite of decrease in observed degradation rates, which were 10.68%, 9.88%, and 8.87% in the presence of CO_3^{2-} , HCO_3^- , and NO_3^- respectively, VUV process was very effective in the degradation of imidacloprid (Figure 5.28). 100 % removal efficiency of 5 mg/L initial concentration of imidacloprid was observed in the presence of all studied ions in less than 4 minutes of VUV irradiation (Figure 5.29). These results also manifest that reaction rate of imidacloprid with $\bullet\text{OH}$ is higher than HCO_3^- , CO_3^{2-} , which is in accordance with literatures.

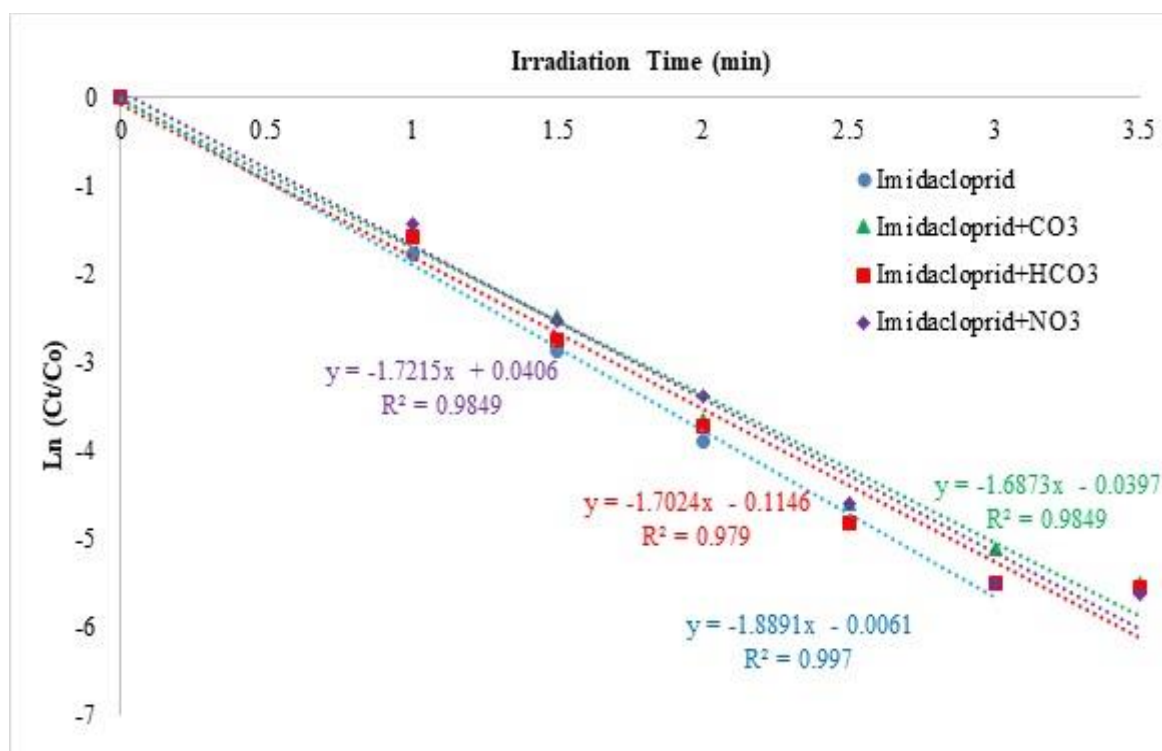


Figure 5.28 Pseudo first-order degradation of Imidacloprid ($C_0 = 5$ mg/L) in presence of various inorganic ions. The results are average of three replicates.

Table 5.5 VUV induced degradation rate constants of Imidacloprid ($C_o = 5$ mg/L) in presence of inorganic ions.

Inorganic Ion	Pseudo First Order Degradation Equation
Imidacloprid (alone)	$y = -1.8891x - 0.0061$ $R^2 = 0.997$
Carbonate Ion (CO_3^{2-})	$y = -1.6873x - 0.0397$ $R^2 = 0.9849$
Bicarbonate Ion (HCO_3^-)	$y = -1.7024x + 0.1146$ $R^2 = 0.979$
Nitrate Ion (NO_3^-)	$y = -1.7215x + 0.0406$ $R^2 = 0.9849$

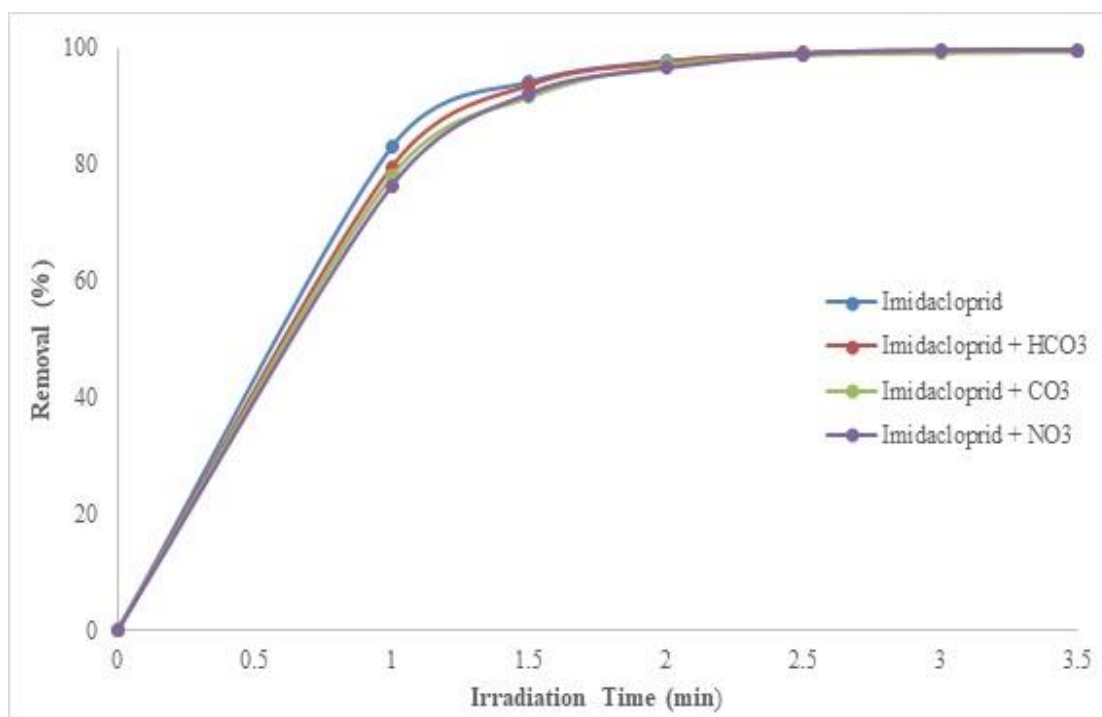


Figure 5.29 Imidacloprid ($C_o = 5$ mg/L) removal efficiency by VUV irradiation in presence of inorganic ions. The results are average of three replicates.

5.4.5. Effects of Water Matrix

Water matrix can affect VUV induced photodegradation of target pollutants either by absorbing 185 nm photon and acting as inner filter or scavenging produced radicals, especially $\bullet\text{OH}$. Tap water may contain mixture of common inorganic ions such as bicarbonate, carbonate, nitrate, chloride whereas pond water additionally accomodates natural organic matter (NOM) and other impurities. Effects of individual presence of inorganic ions, bicarbonate, carbonate, and nitrate on the imidacloprid degradation were investigated and reported in previous section. Synergistic effects of mixture of these ions along with natural organic matter and other impurities may result further inhibition on the degradation efficiency and rate constant. It was mostly reported in the literature that AOPs were affected at varying degrees by inorganic ions and NOM in the degradation of target pollutants. For these reasons, performance of VUV based AOP on the degradation of aqueous imidacloprid and degrees of inhibition exerted by such impurities of water were investigated in the presence of tap and pond water.

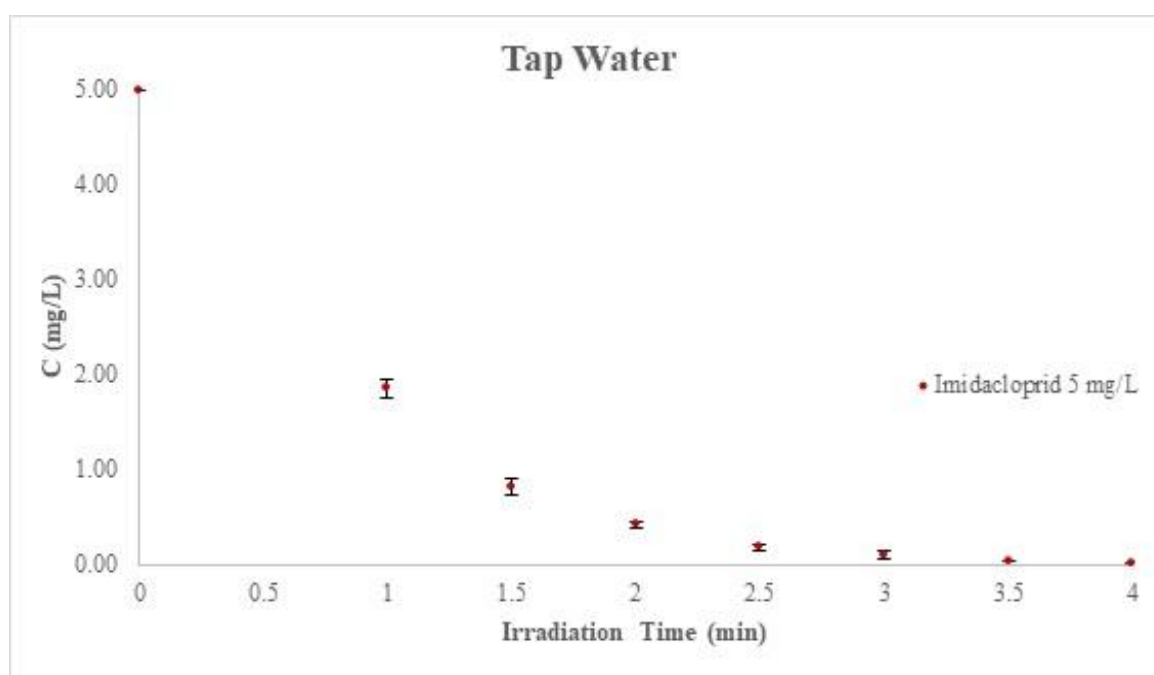


Figure 5.30 VUV induced photodegradation of Imidacloprid ($C_0 = 5$ mg/L) in tap water. Error bars represent the standard deviations of three replicates.

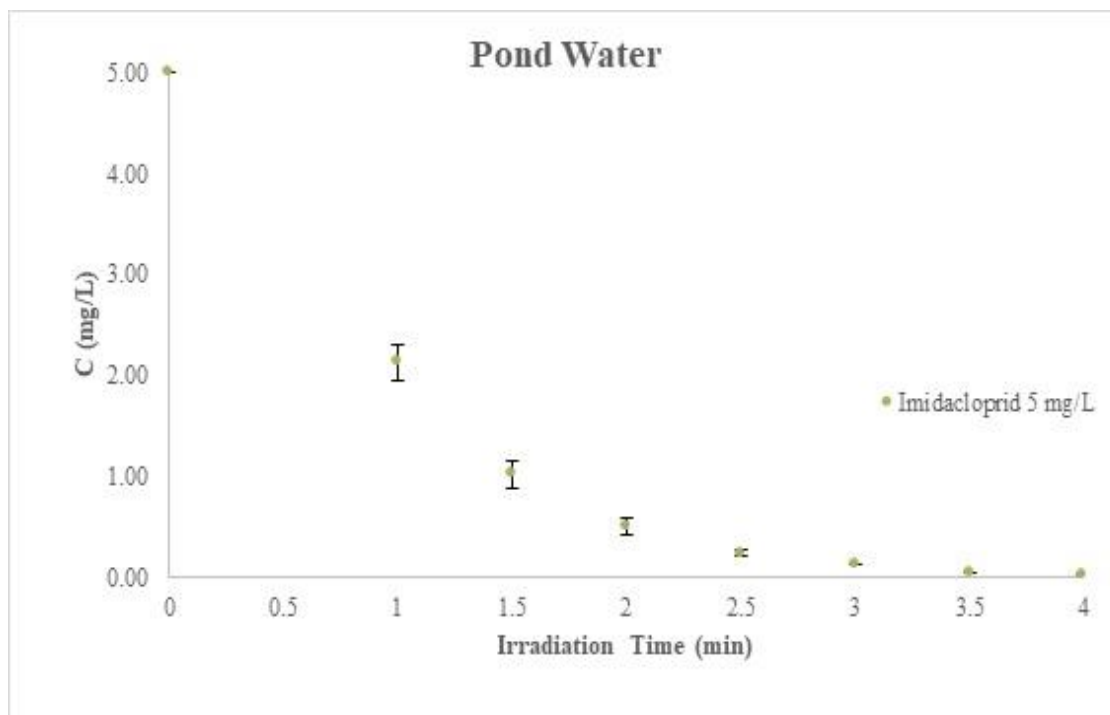


Figure 5.31 VUV induced photodegradation of Imidacloprid ($C_0 = 5 \text{ mg/L}$) in pond water. Error bars represent the standard deviations of three replicates.

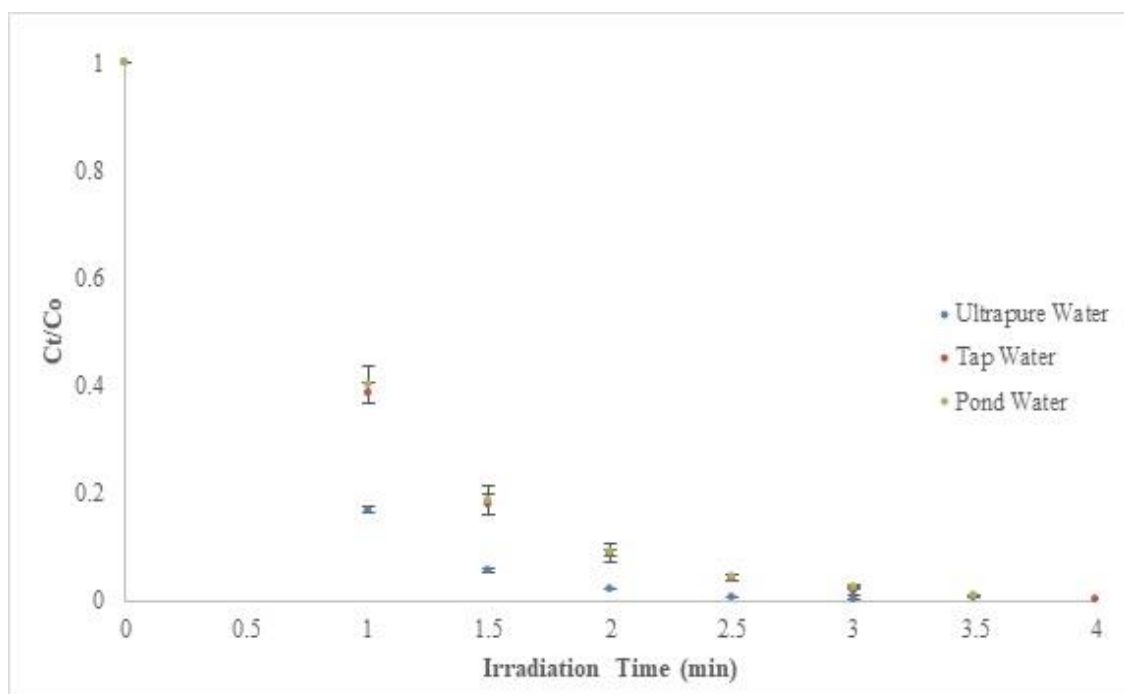


Figure 5.32 VUV induced photodegradation of Imidacloprid ($C_0 = 5 \text{ mg/L}$) in various water matrices. Error bars represent the standard deviations of three replicates.

Effects of water matrix on the VUV induced photodegradation of imidacloprid with 5 mg/L initial concentration were presented in Figures 5.30, 5.31, and 5.32 . It was found that degradation of imidacloprid in tap and pond water followed pseudo first order kinetic pattern as in the case of ultrapure water (Figures 5.32 and 5.33). As shown in Figures 5.33 and 5.34, removal of imidacloprid was decreased both in tap and pond water. Inhibition of degradation was the highest in the pond water due to presence of natural organic matters (NOM) which usually reported to have higher scavenging effects on $\bullet\text{OH}$ compared to inorganic ions. Similar findings were also reported by other researchers for the degradation of organic pollutants with AOPs [2][99]. This can then be attributed to high rate constant of $3 \times 10^8 \text{ M}_{\text{carbon}}^{-1} \text{ s}^{-1}$ between NOM and $\bullet\text{OH}$ [99][103]. NOM may influence the degradation of target pollutants in various ways. NOM can compete with the target pollutant to react with radicals. In the case of VUV irradiation, concentration of generated primary radicals was constant. Presence of oxidizable compound which was NOM in the pond water, would lower the amount of oxidants available for degradation of imidacloprid and subsequently efficiency of the VUV process, which might have been the primary reason for the decrement in rate constant of imidacloprid. Moreover, NOM might have absorbed some of the 185 nm photons in the VUV photooxidation system that hence, reduced photolysis of water by VUV photons and accordingly concentration of primary radicals, particularly $\bullet\text{OH}$. Therefore, lower removal efficiency of imidacloprid can also be attributed to inner filter effect of NOM. Clara Duca [82] found in her doctoral research that NOM exhibited high absorption coefficient at 185 nm photon which supports the later explanation. Decrements in the observed rate constant of imidacloprid degradation were 22% and 26.54% for tap and pond water respectively as shown in Figure 5.33 and Table 5.6. So, it can be expressed that water matrix, in other words, water quality considerably affected the performance of VUV process in the removal of imidacloprid. It was found that observed degradation rates were also less than what was attained in the individual presence of inorganic ions. This result can be attributed to synergistic effects of inorganic ions along with existence of natural organic matter and other impurities. Reduction of rate constant of imidacloprid in tap water can be attributed to presence of inorganic ions which not only can scavenge VUV produced $\bullet\text{OH}$, $\text{H}\bullet$, e_{aq}^- but also can produce less reactive species by reacting with them. For example, it was reported that Cl^- can form less reactive species of $\text{ClOH}\bullet^-$, $\text{Cl}\bullet$, $\text{Cl}_2\text{O}\bullet^-$ by reacting with $\bullet\text{OH}$ [99] which might have caused decrease in rate constant of imidacloprid.

Nonetheless, VUV initiated oxidation of aqueous imidacloprid was still very rapid in different water matrices. Complete removal efficiency of 5 mg/L initial concentration of imidacloprid was observed in less than 4.5 minutes of VUV irradiation under the investigated conditions (Figure 5.34). Observed degradation rate constants of imidacloprid in tap and pond water by the VUV process were greater than what were reported with other AOPs which was previously presented in Table 5.4.

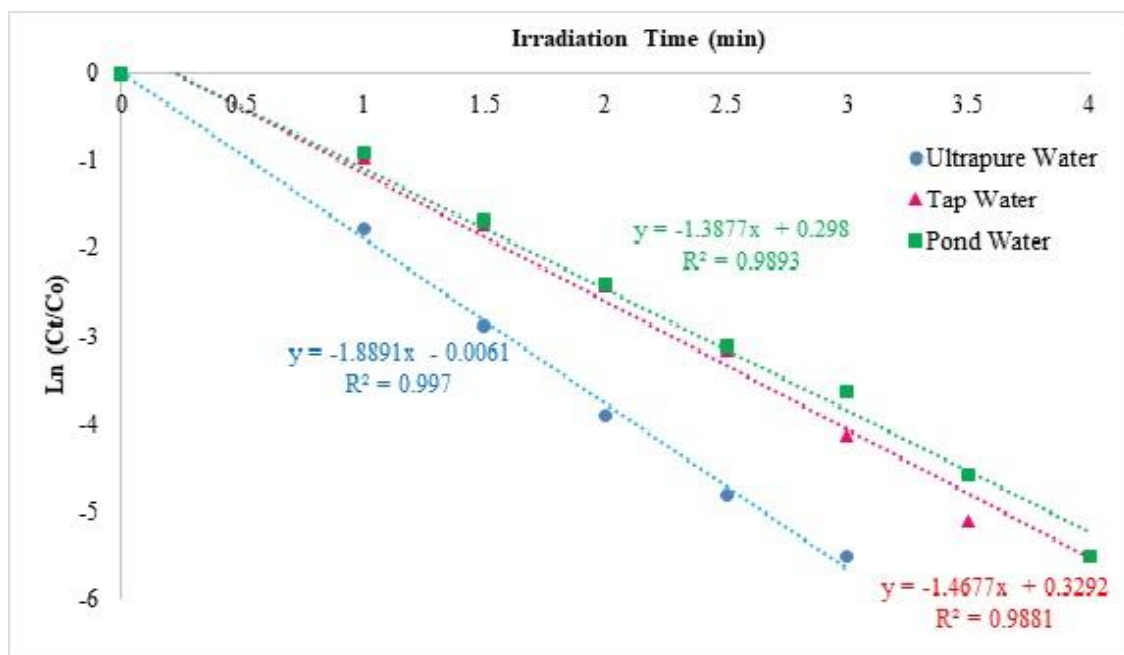


Figure 5.33 Pseudo first-order degradation of Imidacloprid ($C_0 = 5$ mg/L) in various water matrices. The results are average of three replicates.

Table 5.6 VUV induced pseudo first order degradation rate constants of Imidacloprid ($C_0 = 5$ mg/L) in various water matrices (ultrapure water, tap water, and pond water).

Water Matrix	Pseudo First Order Degradation Equation
Ultrapure water	$y = -1.8891x - 0.0061$ $R^2 = 0.997$
Tap water	$y = -1.4677x + 0.3292$ $R^2 = 0.9881$
Pond water	$y = -1.3877x + 0.298$ $R^2 = 0.9893$

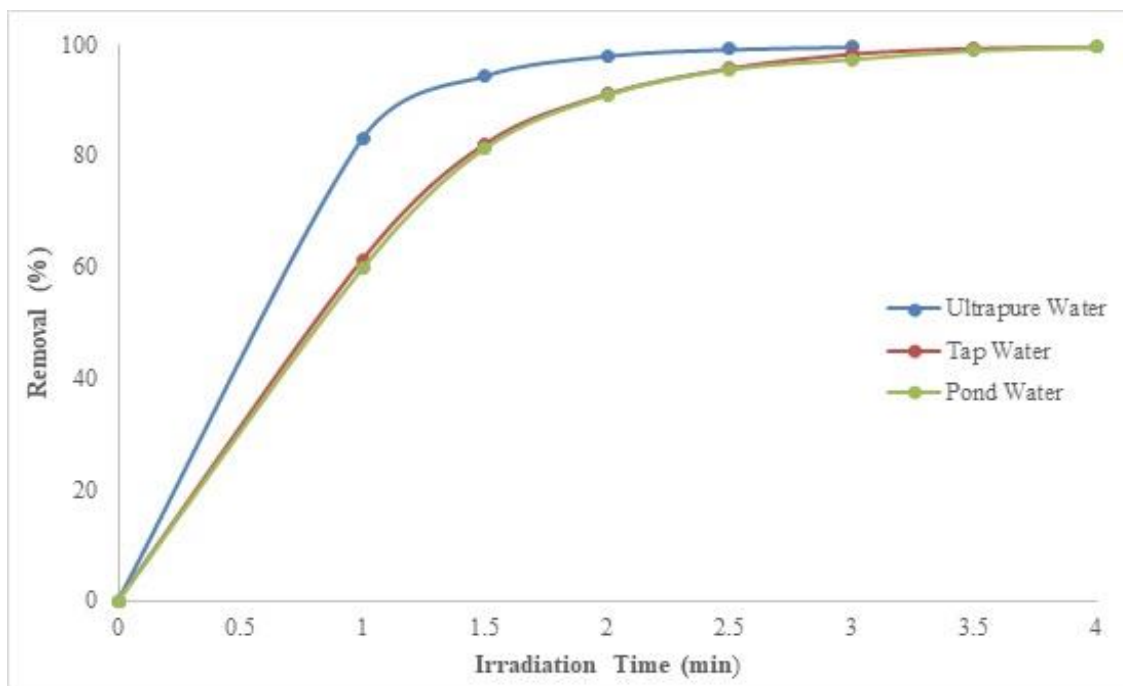


Figure 5.34 Imidacloprid ($C_0 = 5 \text{ mg/L}$) removal efficiency by VUV induced photodegradation in various water matrices. The results are average of three replicates.

5.4.6. Effects of Oxygenated and Deoxygenated conditions on the degradation of Imidacloprid

Effects of dissolved oxygen on the degradation as well as mineralization of organic pollutants has been widely studied in AOPs. The reason behind this is that oxygen can react both with generated radicals including intermediate radicals in AOPs and target pollutants and accordingly may alter the degradation performance of applied process positively or negatively depending on the structure and concentration of the target pollutants. Primary radicals of VUV photolysis of water are established to be $\bullet\text{OH}$, $\text{H}\bullet$, and e^-_{aq} . In the presence of dissolved oxygen, target compound and oxygen compete with each other to react with these radicals. In order to observe, therefore, effects of dissolved oxygen on the VUV initiated degradation of imidacloprid, oxygen saturated and oxygen free experiments were carried out within the scope of this research and compared with the degradation experiments of imidacloprid executed with no gas sparging.

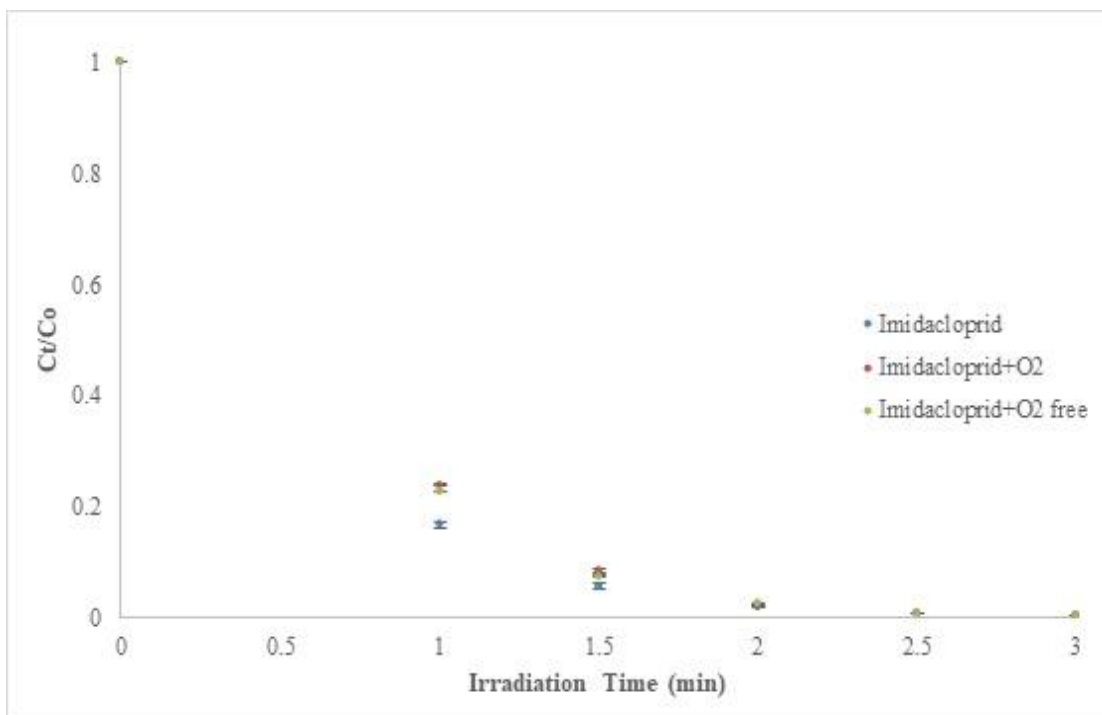


Figure 5.35 VUV induced photodegradation of Imidacloprid ($C_0 = 5$ mg/L) in oxygenated and deoxygenated solutions. Error bars represent the standard deviations of three replicates.

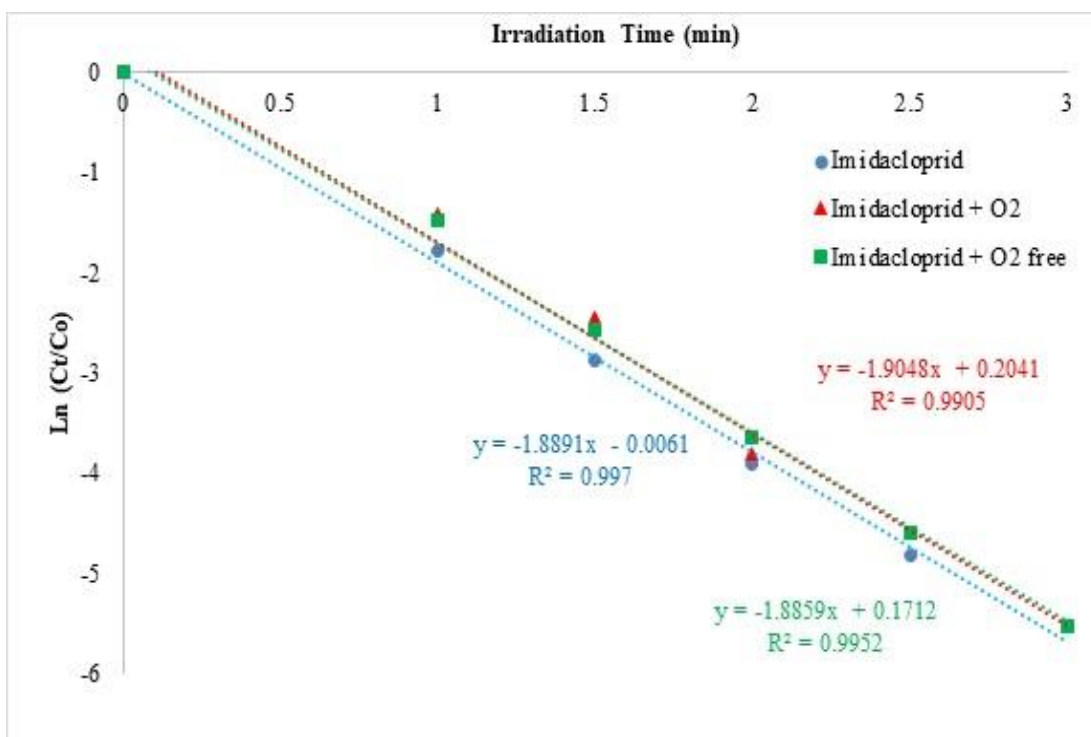
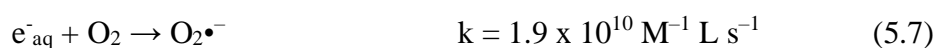
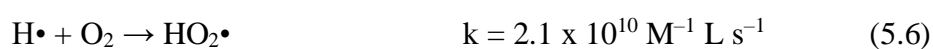
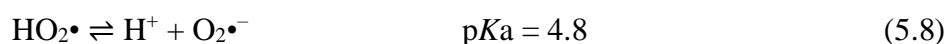


Figure 5.36 Pseudo first-order degradation of Imidacloprid ($C_0 = 5$ mg/L) in oxygenated and deoxygenated solutions. The results are average of three replicates.

Effects of presence and absence of dissolved oxygen on the reduction of imidacloprid by VUV process were presented in Figures 5.35 and 5.36. Pseudo first order degradation kinetics were observed for all the tested conditions as shown in Figure 5.36. Observed rate constants and were very comparable to each other (Table 5.7). Less than 1% increment was observed in the removal rate constant for the oxygenated condition whereas less than 0.17% decrement was for the deoxygenated one. This results showed that dissolved oxygen had negligible impact on the degradation rate of imidacloprid by the VUV process as in agreement with [100]. It is known that reductive $H\bullet$ and e^-_{aq} are rapidly converted to oxidative $HO_2\bullet/O_2\bullet^-$ by reacting with oxygen [74] through Eq. 5.6 and 5.7.



In the pH range of 6 to 9, $HO_2\bullet$ disproportionates to $O_2\bullet^-$ by Eq. 5.8 [104].



In the presence of oxygen, oxidative $HO_2\bullet/O_2\bullet^-$ would coexist with $HO\bullet$. So, contribution of $HO_2\bullet/O_2\bullet^-$ to reduction of imidacloprid was negligible. Furthermore, oxygen absorbs 185 nm photon to produce O_3 in oxygenated solutions. Evidently, O_3 had negligible effect on degradation of imidacloprid by VUV photooxidation as well since only marginal increment was observed in reduction rate. On the other hand, in deoxygenated solution, reductive $H\bullet$ and e^-_{aq} coexisted with $HO\bullet$. $H\bullet$ and e^-_{aq} apparently did not have much contribution on the degradation of imidacloprid either due to their low reactivity compared to $HO\bullet$. This result was in accordance with literature [27][77][99][87]. Results showed that $HO\bullet$ was primary oxidant in degradation of imidacloprid by VUV based AOP.

In conclusion, VUV initiated photodegradation of aqueous imidacloprid was very rapid in both oxygenated and deoxygenated solutions. Complete removal of 5 mg/L initial concentration of imidacloprid was observed by the VUV photooxidation under the tested conditions in less than 3.5 minutes of irradiation (Figure 5.37). The VUV based AOP was very effective for degradation of aqueous imidacloprid irrespective of presence of oxygen.

Table 5.7 VUV induced Imidacloprid ($C_0 = 5 \text{ mg/L}$) degradation rate constants in oxygenated and deoxygenated solutions.

Solution Condition	Pseudo First Order Degradation Equation
Imidacloprid (no gas sparging)	$y = -1.8891x - 0.0061$ $R^2 = 0.997$
Oxygenated	$y = -1.9048x + 0.2041$ $R^2 = 0.9905$
Deoxygenated	$y = -1.8859x + 0.1712$ $R^2 = 0.9952$

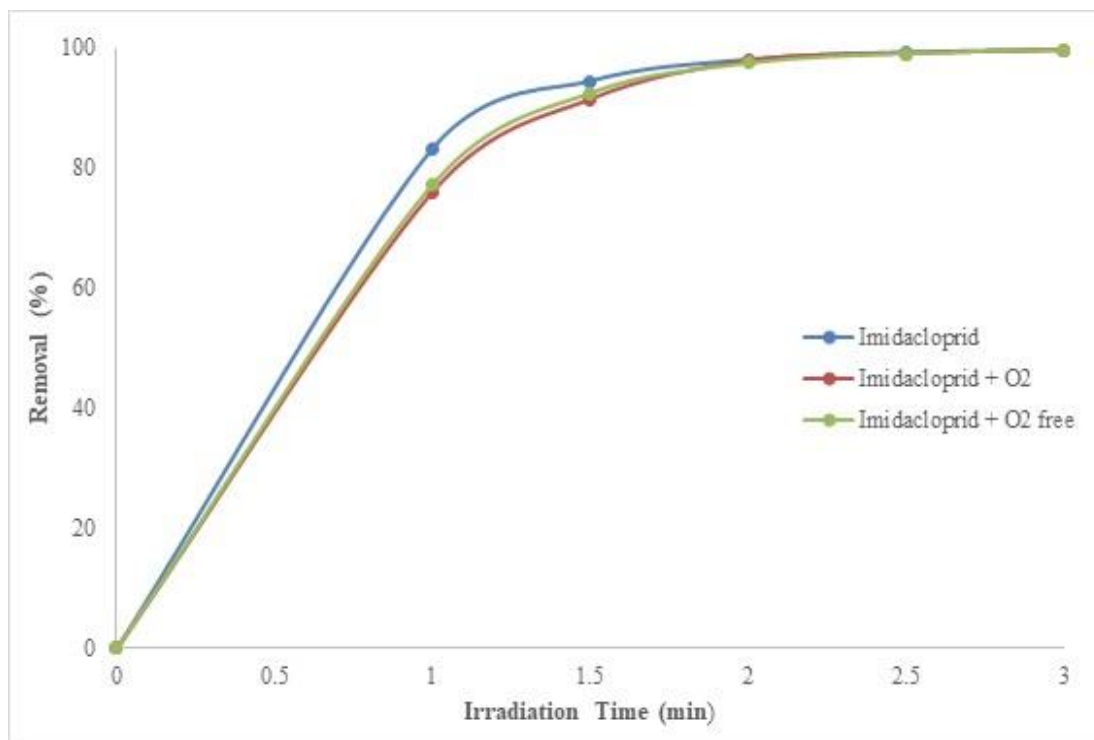


Figure 5.37 Imidacloprid ($C_0 = 5 \text{ mg/L}$) removal efficiency by VUV irradiation in oxygenated and deoxygenated solutions.

5.5. Mineralization of Imidacloprid by VUV photooxidation

Degradation of pollutants (i.e. pesticides) is usually faster than its mineralization. Therefore, several byproducts may exist within the treated water once the complete degradation of target pollutants was achieved. It is therefore important to determine the effectiveness of applied process on the mineralization of the target pollutants. In order to determine the performance of VUV process for the destruction of byproducts of imidacloprid, TOC reduction experiments were exercised within the scope of this research. Additionally, effects of presence and absence of dissolved oxygen on the TOC reduction by the VUV irradiation were also studied since oxygen mostly influence the mineralization of organic pollutants.

5.5.1. Effects of Oxygenated and Deoxygenated conditions on the mineralization of Imidacloprid

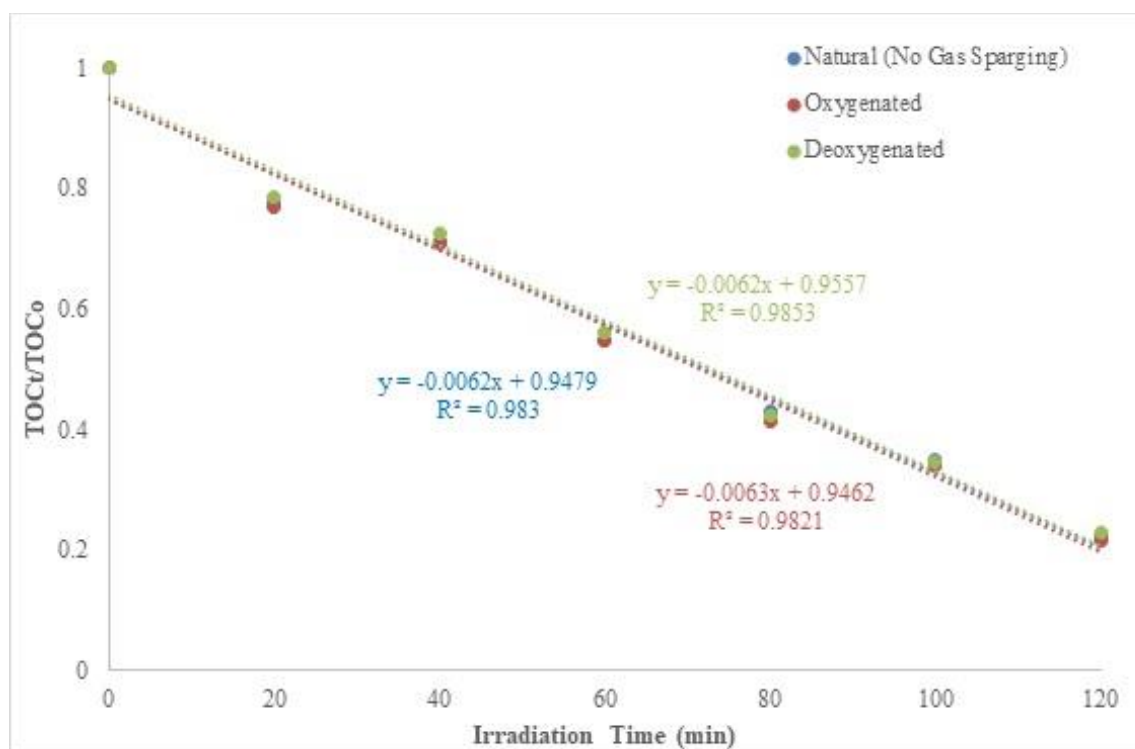


Figure 5.38 Zero-order mineralization (TOC reduction) of Imidacloprid ($C_0 = 10$ mg/L) in oxygenated and deoxygenated solutions.

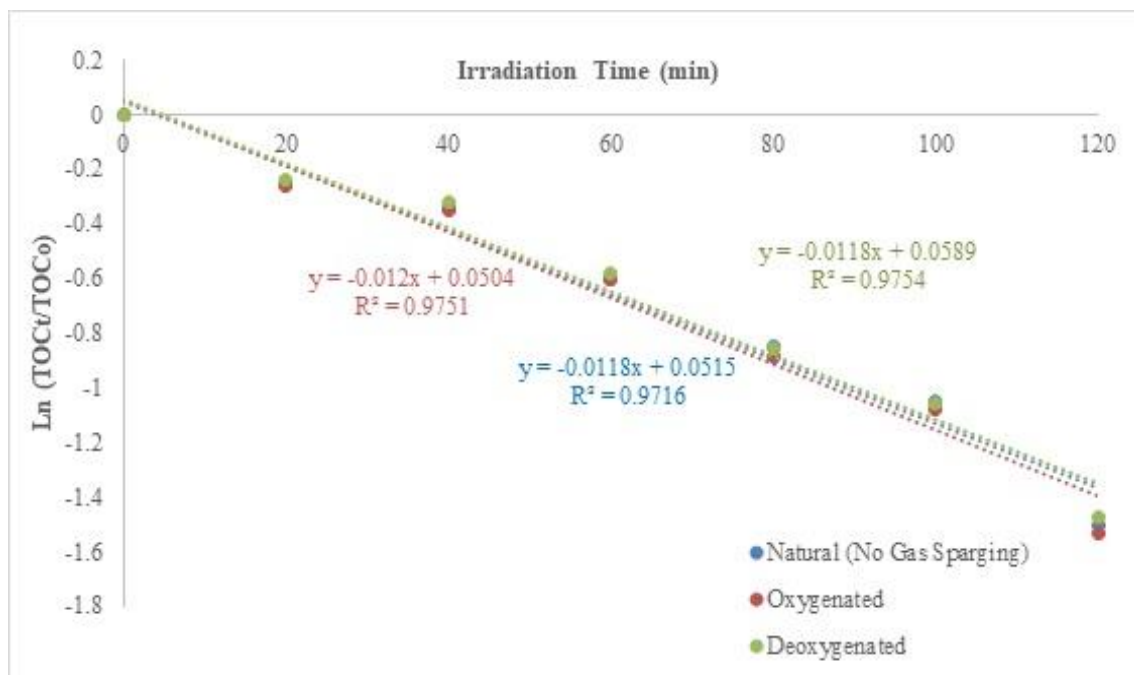


Figure 5.39 First-order mineralization (TOC reduction) of Imidacloprid ($C_0 = 10 \text{ mg/L}$) in oxygenated and deoxygenated solutions.

Effects of VUV process on the mineralization (TOC reduction) of aqueous imidacloprid in the presence and absence of dissolved oxygen were presented in Figures 5.38 and 5.39. Correlation coefficient (R^2) of TOC reduction of imidacloprid as a function of irradiation time (Figure 5.38) was slightly higher and comparable to that of Figure 5.39 constructed from natural logarithm of TOC reduction. Therefore, it was found that mineralization of imidacloprid by applied VUV based AOP followed zero order kinetic pattern (Figure 5.38). This result might be attributed to the complete degradation of imidacloprid within 4 minutes of VUV irradiation as opposed to 120 minutes of reaction time which was required for almost 80% mineralization of imidacloprid and its intermediate products. Imidacloprid was very rapidly degraded by VUV process that around 4% TOC reduction was observed at the time of complete imidacloprid degradation. Therefore, initial concentration of imidacloprid might not have effect on mineralization of imidacloprid and its byproducts with respect to 2 hours of mineralization time. Efficient TOC reduction was achieved in natural (no gas sparging), oxygen saturated, and oxygen free solutions as in agreement with what was reported by Rozsa [100]. Observed TOC reduction rate constants of oxygenated, deoxygenated and natural (no gas sparging) conditions were very comparable to each other (Table 5.8). Same rate constant was determined for both

oxygen free and natural (no gas sparging) solutions while only 1.61% increment was observed in the oxygen saturated condition. This results showed that dissolved oxygen and oxidative $\text{HO}_2^\bullet/\text{O}_2^{\bullet-}$ which were coexisted with HO^\bullet in the presence of oxygen apparently did not have much impact on the VUV induced mineralization of imidacloprid and its byproducts either, which is in agreement with what was attained in degradation experiments. On the other hand, reductive H^\bullet and e^-_{aq} had negligible effect on the mineralization of imidacloprid and formed byproducts as well since there is no difference observed in the oxygen free solution either. It can then be concluded that HO^\bullet was the responsible radical in the mineralization mechanism as in the case of degradation.

Figure 5.40 presents that almost 80% TOC reduction was sought in 2 hours of irradiation under the all tested conditions. The attained TOC reduction efficiency in this doctoral study showed that the VUV process is indeed superior to other previously studied treatment processes in regards of mineralization of imidacloprid and its byproducts [60][62][7][68][64]. Please refer to section 2.2.3 of chapter 2 for detailed information.

Despite complete reduction of aqueous imidacloprid in 4 minutes, 2 hours was required to reach approximately 80% mineralization. These results showed that generated byproducts exhibited higher resistance to primary HO^\bullet , H^\bullet , e^-_{aq} , and secondary radicals $\text{HO}_2^\bullet/\text{O}_2^{\bullet-}$ than imidacloprid in the VUV process. Generation of several byproducts from imidacloprid degradation by the VUV photooxidation was also detected and confirmed in LC/MS Q-TOF analysis.

Table 5.8 VUV induced mineralization (TOC reduction) rate constants of Imidacloprid ($C_0 = 10 \text{ mg/L}$) in oxygenated and deoxygenated solutions.

Solution Condition	Zero Order TOC Reduction Equation
Imidacloprid (no gas sparging)	$y = -0.0062x + 0.9479$ $R^2 = 0.983$
Oxygenated	$y = -0.0063x + 0.9462$ $R^2 = 0.9821$
Deoxygenated	$y = -0.0062x + 0.9557$ $R^2 = 0.9853$

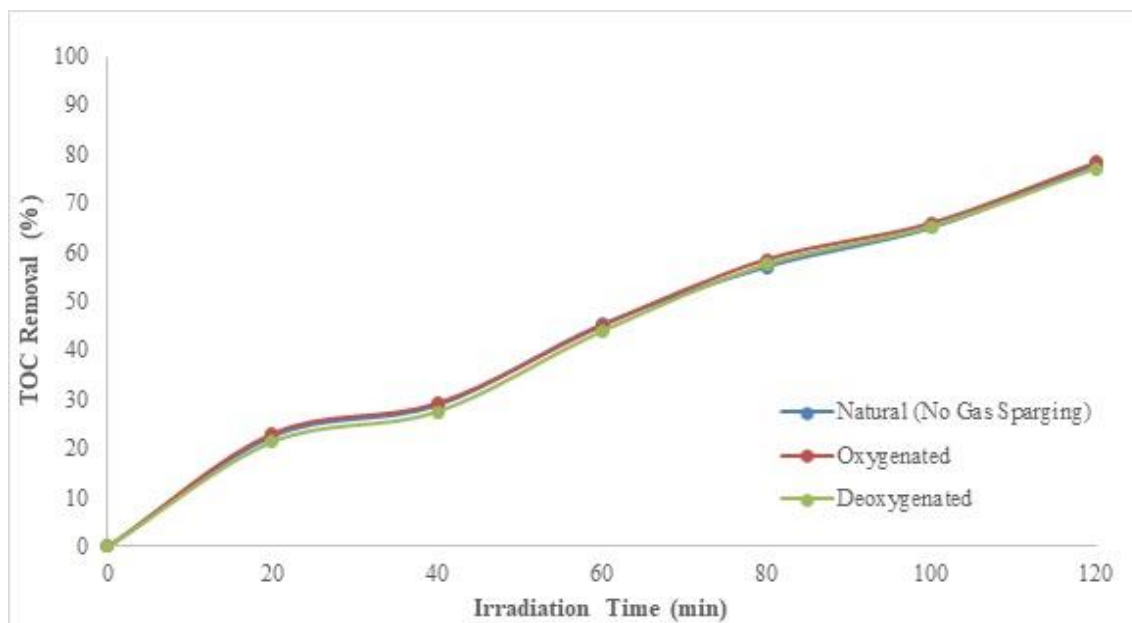


Figure 5.40 Imidacloprid Mineralization (TOC reduction) efficiency of VUV irradiation in oxygenated and deoxygenated solutions.

5.6. VUV photooxidation Byproducts of Imidacloprid

Even though VUV based AOP attained complete removal of aqueous imidacloprid, incomplete reduction of intermediate products might be experienced during the reaction time of complete imidacloprid removal. Therefore, generation of possible byproducts and effectiveness of VUV process onto the formed intermediate products were investigated in the course of this doctoral study and presented herein. Separation and identification of degradation byproducts were executed with LC/MS Q-TOF in positive ionization mode which is defined in detail at section 4.7.2. Detected compounds were considered as intermediate products by observing increase and decrease in their peak area counts as a function of irradiation time. Several possible byproducts some of which were identified, were detected during the reaction time of complete imidacloprid reduction. Some of the detected byproducts increased in their response of LC/MS as imidacloprid was degraded while others decreased slightly. Other than imidacloprid, detected byproducts were present at the time of complete imidacloprid destruction since 4 minutes of VUV irradiation was inadequate for complete destruction of them. LC/MS Q-TOF chromatograms and mass spectrums of imidacloprid along with byproducts were reported in Appendix 1.3 and 2.8 respectively.

Upon collisional excitation of imidacloprid m/z 256 [M + H], fragment ions of m/z 209 and m/z 175 were formed. Loss of HNO_2 from imidacloprid m/z 256 resulted the formation of m/z 209 ion. On the other hand, observed ion m/z 175 was due to loss of NO_2 and subsequently Cl from the parent compound m/z 256. Byproducts with m/z 212, m/z 227, m/z 211, m/z 126, m/z 191 which were attributed to a loss of 44, 29, 45, 130, 65 mass units from imidacloprid and m/z 272 were generated during VUV induced imidacloprid degradation. Imidacloprid urea (m/z 212), imidacloprid hydroxy (m/z 272), imidacloprid desnitro (m/z 211), m/z 227, m/z 223, m/z 191, m/z 205, m/z 183, and m/z 126 ions were previously reported by several researchers [60][54][105][106][107][65] [57][63][7][108]. However, According to our best knowledge this is the first time of m/z 163 to be reported in imidacloprid degradation (Table 5.9).

6-chloronicotinic acid which was reported as main degradation product of imidacloprid in various studies [54][56] was not observed during the VUV irradiation of imidacloprid as in accordance with observation of Lavine [57]. This might be attributed to rapid generation and destruction of 6-chloronicotinic acid under the applied VUV process which also decomposed target compound, imidacloprid, very fast. Another explanation of this observation is that 6-chloronicotinic acid was previously reported by some researchers in literature to be the final product of imidacloprid degradation. In other words, it appeared following the decomposition of generated intermediate products which was not the case observed in this research due to very short reduction time of imidacloprid.

Table 5.9 Detected byproducts/fragment ions of imidacloprid in the VUV process by LC/MS Q-TOF analysis.

Compound Name	Observed m/z	Literature
Imidacloprid urea	212	[63] [65] [105] [107] [57]
Imidacloprid desnitro	211	[7] [54] [57][60] [107] [108]
Imidacloprid hydroxy	272	[7] [63] [65] [107]
Imidacloprid olefin desnitro	209	[54] [65] [57][108]

Compound Name	Observed <i>m/z</i>	Literature
Unknown A	175	[65] [105]
Unknown B	227	[57]
Unknown C	126	[65]
Unknown D	191	[65]
Unknown E	205	[63]
Unknown F	183	[54]
Unknown G	163	Not reported

5.7. Degradation of Reactive Textile Dyes by VUV photooxidation

In order to study versatility and effectiveness of the VUV based AOP to oxidize various pollutants from water, experiments of discoloration of two commercially available reactive textile dyes (Synozol Red KH-L and Synozol Yellow KH-L) by the same VUV photooxidation system were also carried out in this doctoral research. Effects of solution flowrate, initial dye concentration and sleeve materials (clear fused quartz and high purity synthetic quartz) on the discoloration kinetic, disappearance rate constant and percentage were reported and discussed in the subsequent subsections. Supplementary data of the all following subsections and related experiments were reported in Appendix 3.

5.7.1. Effects of Flowrate of the experimental solution

As mentioned before, mass transfer limitation plays an important role on the VUV (185 nm photon) initiated photooxidation of the target pollutant. This limitation can be overcome to some extent by manipulating hydrodynamic conditions of the system (for detailed information please refer to section 5.4.1). Therefore, effects of hydrodynamic conditions on the disappearance of a target textile dye were investigated at different solution flowrates, 350, 500, 750 mL/min in presence of clear fused quartz sleeve. Red dye was selected and used in flow rates experiments.

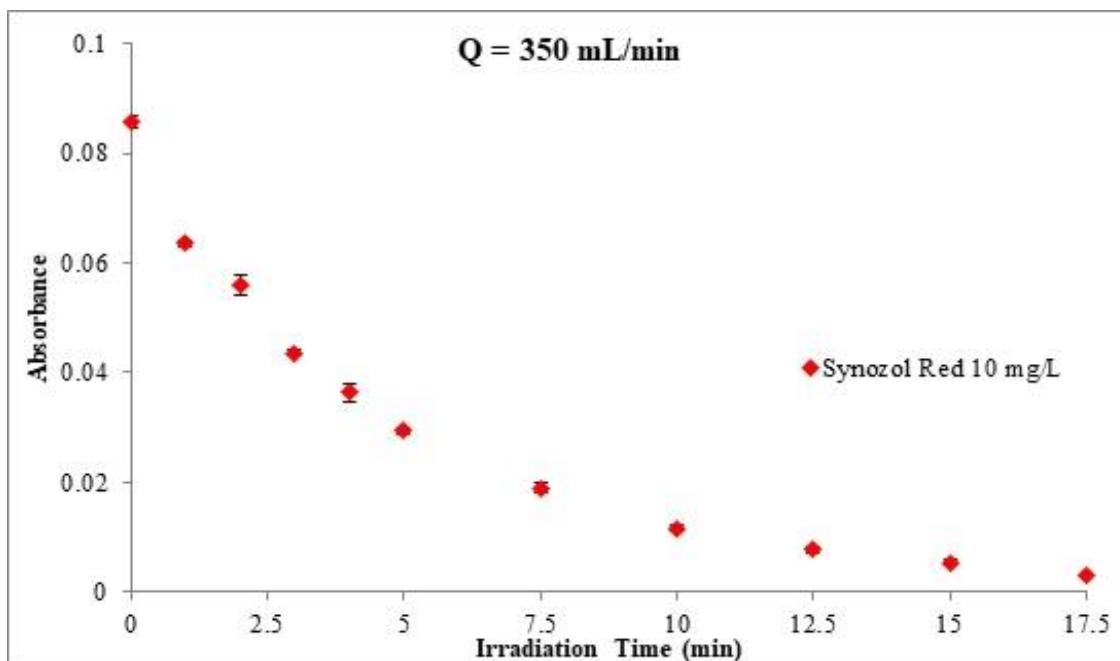


Figure 5.41 VUV induced discoloration of Red dye ($C_o = 10$ mg/L) under $Q = 350$ mL/min flow rate condition. Error bars represent the standard deviations of three replicates.

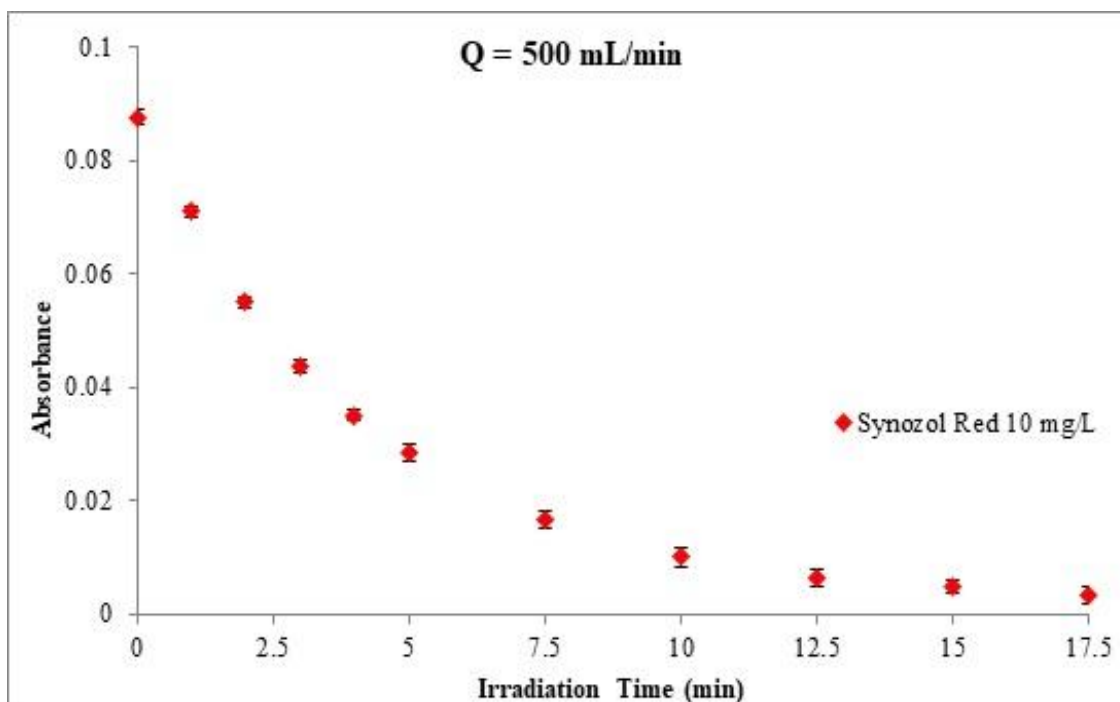


Figure 5.42 VUV induced discoloration of Red dye ($C_o = 10$ mg/L) under $Q = 500$ mL/min flow rate condition. Error bars represent the standard deviations of three replicates.

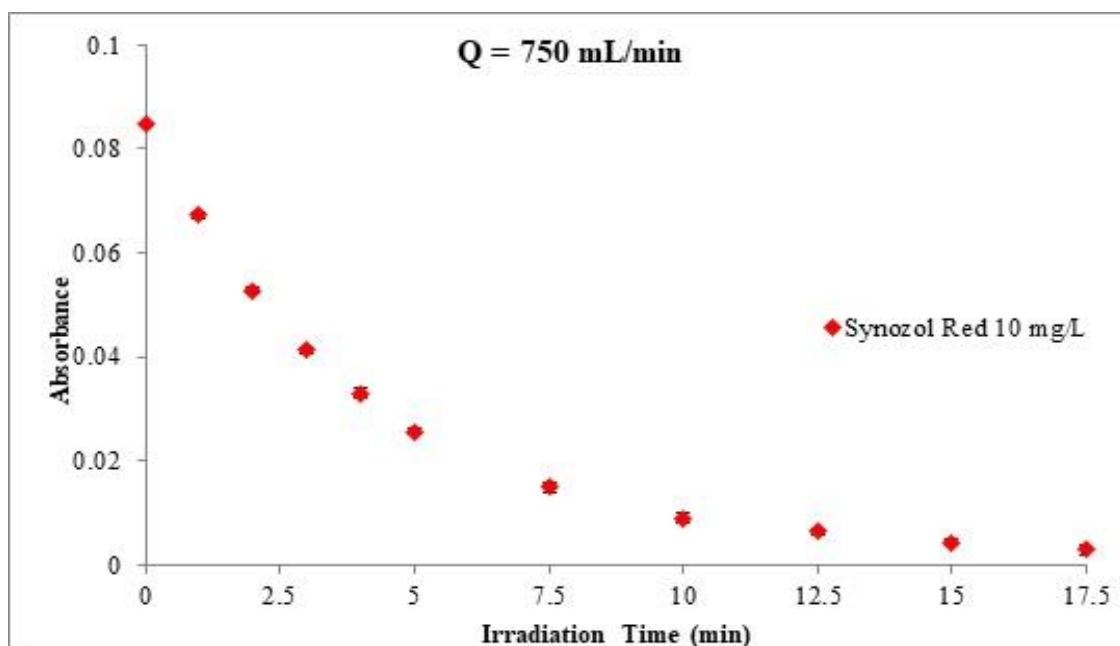


Figure 5.43 VUV induced discoloration of Red ($C_o = 10$ mg/L) under $Q = 750$ mL/min flow rate condition. Error bars represent the standard deviations of three replicates.

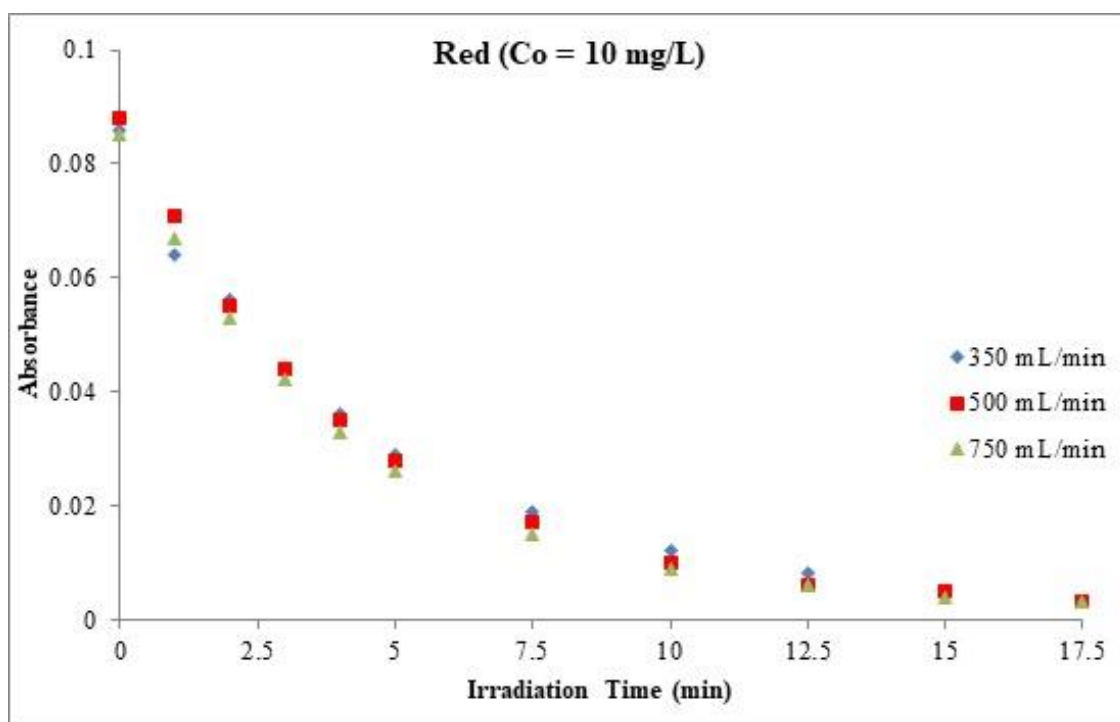


Figure 5.44 VUV induced discoloration of Red dye ($C_o = 10$ mg/L) under various flow rate condition. Error bars represent the standard deviations of three replicates.

Effects of solution flow rate on the VUV induced discoloration of red dye were presented herein. Figures 5.41, 5.42, and 5.43 present VUV initiated discoloration of aqueous red dye under 350, 500, 750 mL/min flow rates respectively. Figures 5.44 and 5.45 display that pseudo first order disappearance kinetic ($R^2 \geq 99\%$) was observed for the all tested flowrates. Even though $\bullet\text{OH}$, which is the responsible reactive in reduction of pollutants in AOPs based treatment, reacts with organic compounds in second order rate, pseudo first order disappearance kinetic was observed with red dye since generation rate of $\bullet\text{OH}$ was equal to consumption rate and reached very quickly to steady state condition, so $\bullet\text{OH}$ concentration was considered as constant. Therefore, discoloration of red dye by VUV based AOP took place as a function of only its own concentration, rather than concentration of both red dye and $\bullet\text{OH}$, which explains the observed reduction kinetic well. Detailed information about observed pseudo first order kinetic was provided in section 5.4.1.

Rate of disappearance of red dye increased with an increment in flow rate as in agreement with what was observed for degradation of imidacloprid in this research (Figure 5.45; Table 5.10). This was probably due to better mixing of solution within the reactor at higher flow rate and hence increasing contact of red dye with $\bullet\text{OH}$ that is primarily responsible for oxidation of imidacloprid. Even though there was no substantial difference on observed disappearance rate constants of red dye with tested flow rates, slightly higher rate constant was observed at 750 mL/min flow rate value due to slightly higher turbulent hydrodynamic condition and accordingly better mixing that 750 mL/min flow rate generated in the photoreactor. Increments in the observed rate constants were 4% and 5.4% for 500 and 750 mL/min flow rates respectively.

The results showed that VUV initiated discoloration of red dye was rapid even in the presence of clear fused quartz sleeve which evidently transmits less 185 nm photon. 100 % removal efficiency of 10 mg/L initial concentration of red dye was observed by the VUV photooxidation under the all tested flow rates within 20 minutes of irradiation (Figure 5.46). It can be concluded that VUV based AOP was effective for discoloration of aqueous red dye irrespective of flow rates.

Since there is no much difference of observed rate constants between the tested flow rates, 500 mL/min flow rate value was chosen and used for the all following experiments.

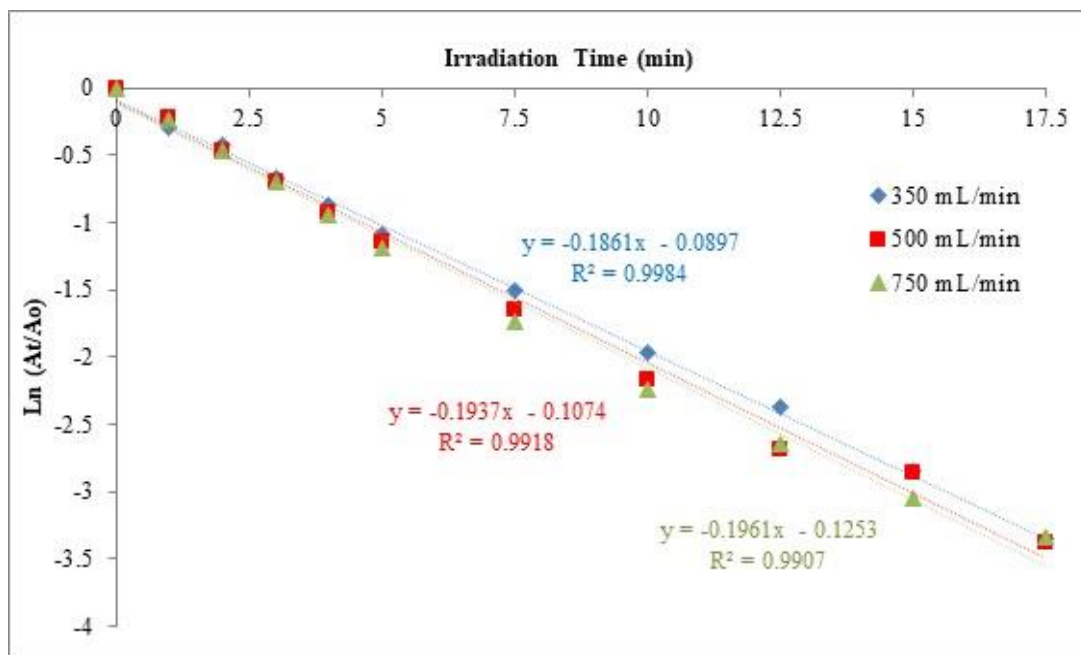


Figure 5.45 Pseudo first-order discoloration of Red dye under various flow rate conditions. The results are average of three replicates.

Table 5.10 VUV induced discoloration rate constants of Red dye ($C_o = 10$ mg/L) under various flow rate conditions.

Flow Rate	Pseudo First Order Discoloration Equation
350 mL/min	$y = -0.1861x - 0.0897$ $R^2 = 0.9984$
500 mL/min	$y = -0.1937x - 0.1074$ $R^2 = 0.9918$
750 mL/min	$y = -0.1961x - 0.1253$ $R^2 = 0.9907$

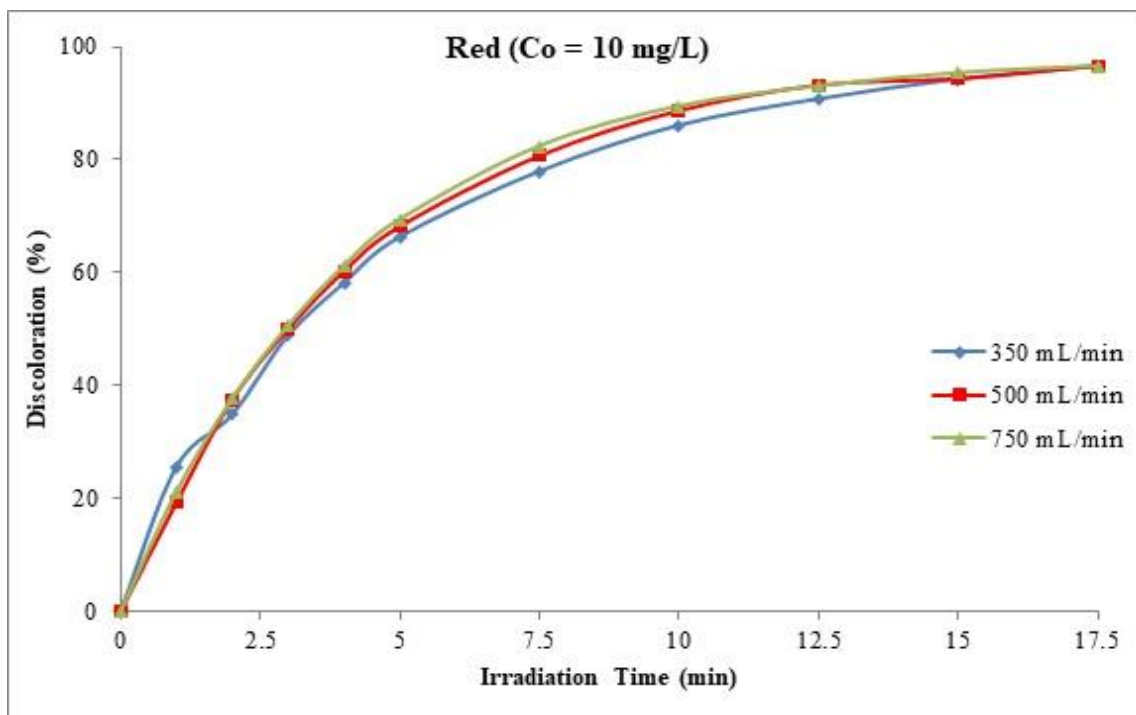


Figure 5.46 Red dye disappearance efficiency of VUV irradiation under various flow rates. The results are average of three replicates.

5.7.2. Effects of initial concentration of the reactive textile dyes

Concentration of pollutants in the influent of water and wastewater treatment plants may show variations. Therefore, it is important to determine effectiveness of applied process to treat various concentrations of the target pollutants before its application. Besides, pollutants may show different pattern in degradation kinetic at various concentration level under the same treatment process. For these reasons, various initial concentrations of red and yellow dyes, 10, 25 and 50 mg/L were investigated to observe removal efficiency of VUV induced AOP and discoloration kinetics of textile dyes at tested initial concentrations in the presence of clear fused quartz. The results were presented in following subsections.

5.7.2.1. Effects of initial concentration on the discoloration of red dye

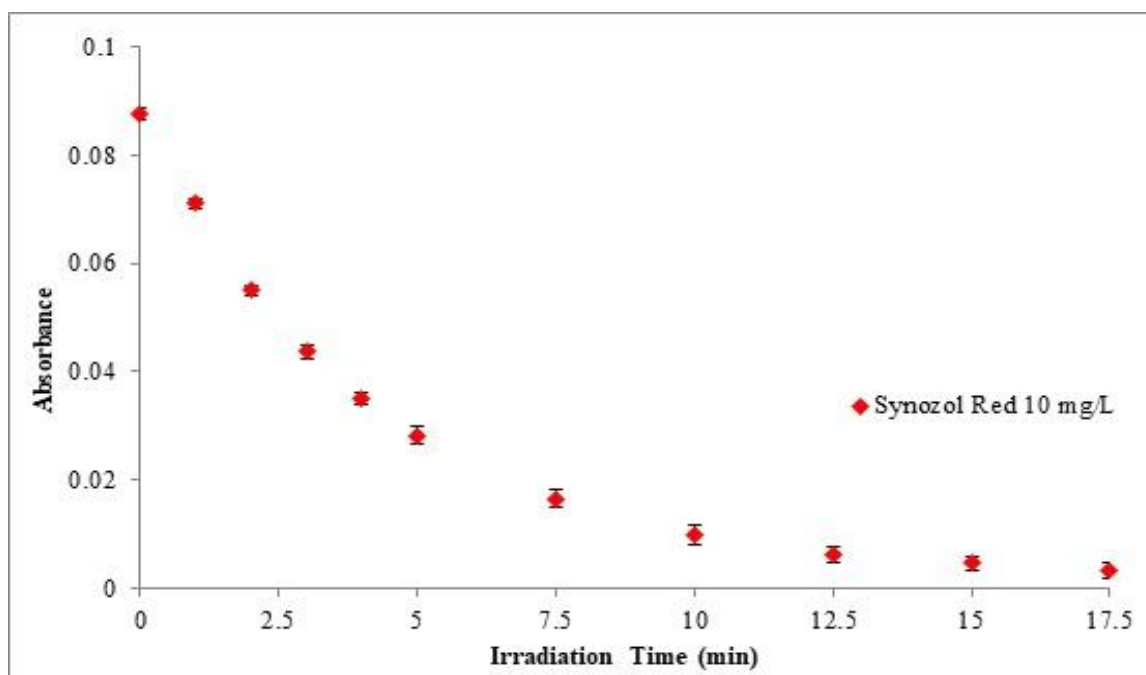


Figure 5.47 VUV induced discoloration of Red dye (C₀ = 10 mg/L). Error bars represent the standard deviations of three replicates.

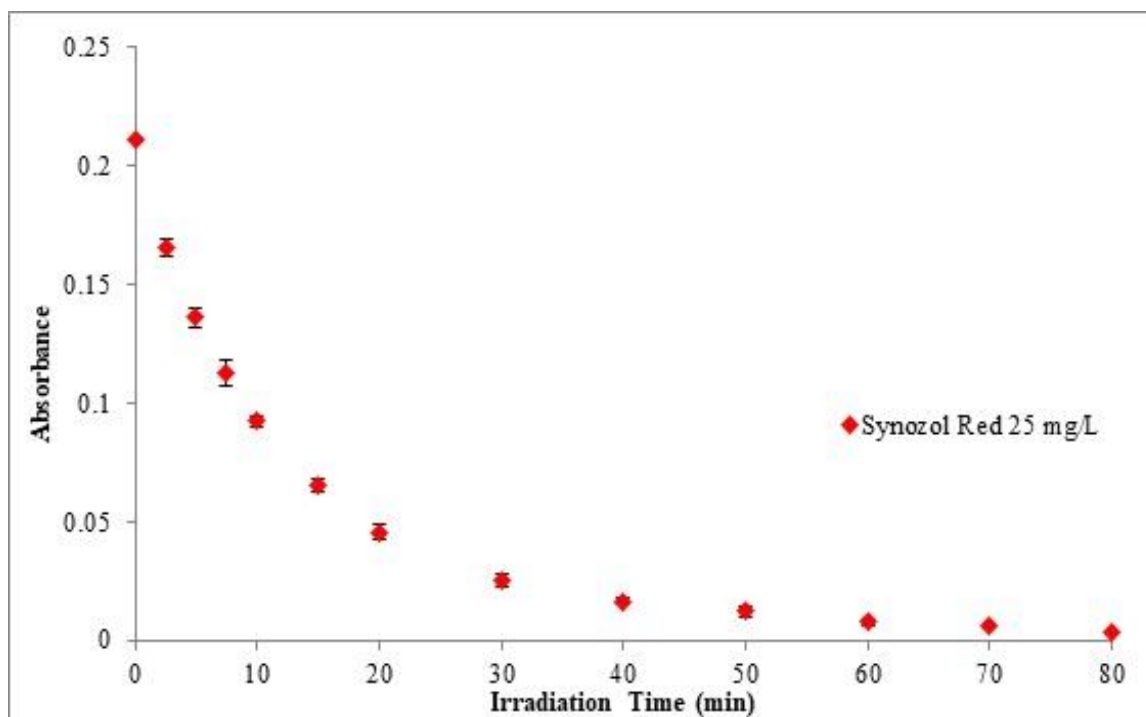


Figure 5.48 VUV induced discoloration of Red dye (C₀ = 25 mg/L). Error bars represent the standard deviations of three replicates.

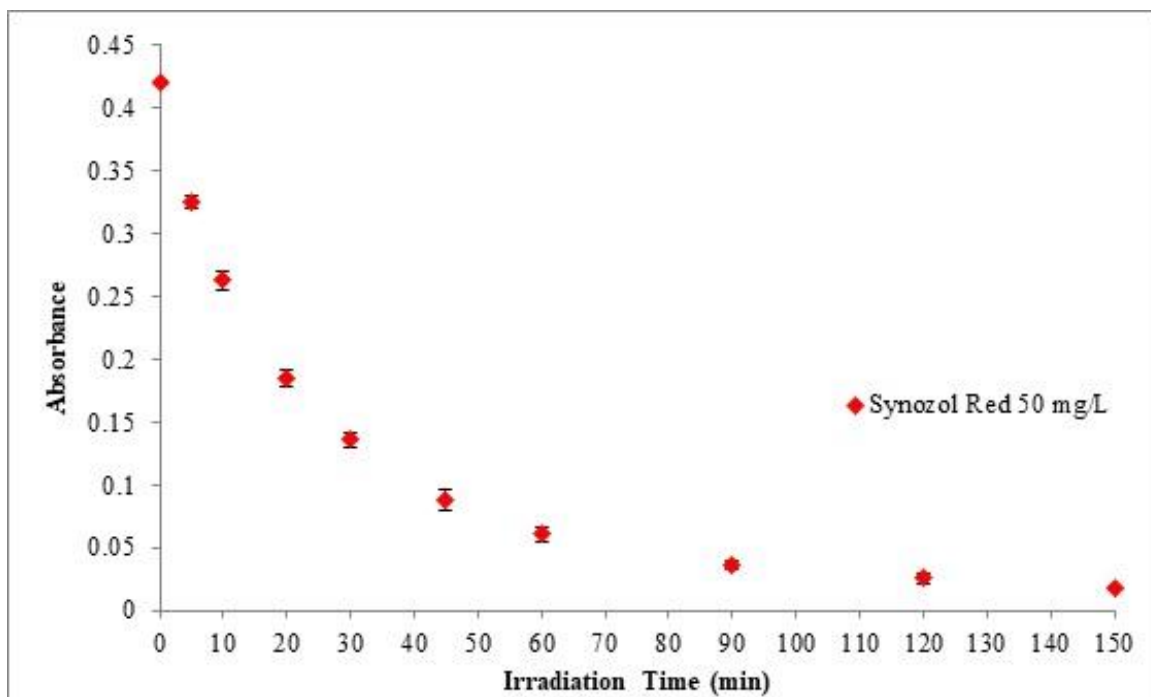


Figure 5.49 VUV induced discoloration of Red dye ($C_0 = 50 \text{ mg/L}$). Error bars represent the standard deviations of three replicates.

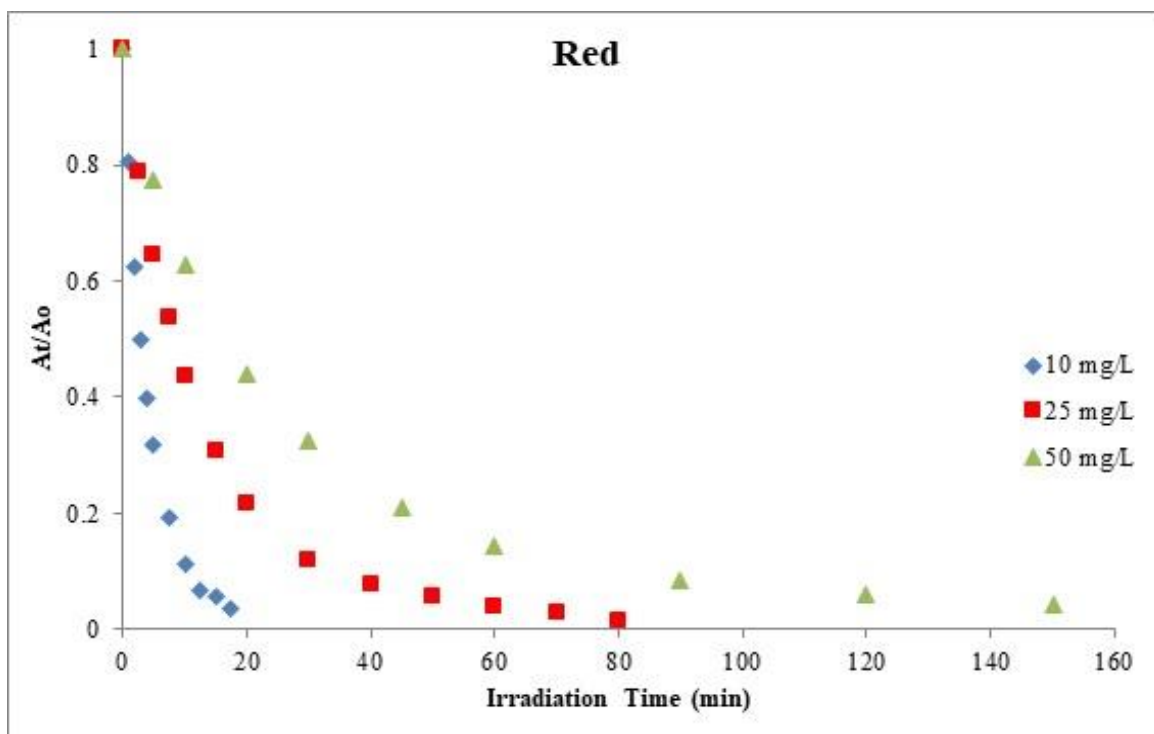


Figure 5.50 VUV initiated discoloration of Red dye under various initial concentrations. The results are average of three replicates.

Effects of initial concentration of red dye on the discoloration of itself by the VUV process were presented herein. Figures 5.47, 5.48, and 5.49 present VUV induced disappearance of aqueous red dye with initial concentrations of 10 mg/L, 25 mg/L, and 50 mg/L respectively. Figures 5.50 and 5.51 show that pseudo first order discoloration kinetic was observed for all the tested initial red dye concentrations as in the case of flow rates. Figure 5.51 shows that even though first order kinetic was observed at the tested highest initial concentration (50 mg/L), discoloration kinetic seemed to be shifting towards to second order kinetic. This finding shows that red dye with initial concentration of higher than 50 mg/L may follow second order disappearance kinetic which is sometimes observed at high concentration of organic pollutants treated with AOPs. The reason might be that at elevated concentration of target compound, higher amount of degradation byproducts may be generated, which are sometimes not further degraded or require longer treatment time than applied one. Therefore, such byproducts coexist with the target compound long enough to affect degradation kinetic.

Observed disappearance rate and efficiency were decreased with the increment of initial concentration (Figures 5.51 and 5.52; Table 5.11). The reason behind this finding might be reduction of ratio of hydroxyl radical ($\bullet\text{OH}$) to red dye since the amount of produced $\bullet\text{OH}$ by the VUV process was constant even though concentration of red dye was increased. This result might also be attributed to the fact that higher amount of $\bullet\text{OH}$ reacted with red dye at higher concentration and hence available steady state concentration of $[\bullet\text{OH}]$ became less. As a result, since pseudo first order degradation rate constant, $k' = k_{\text{OH,C}} \times [\bullet\text{OH}]$, is proportional to the steady state concentration of $[\bullet\text{OH}]$, decrement in $[\bullet\text{OH}]$ might have caused the decrease in the observed rate constant.

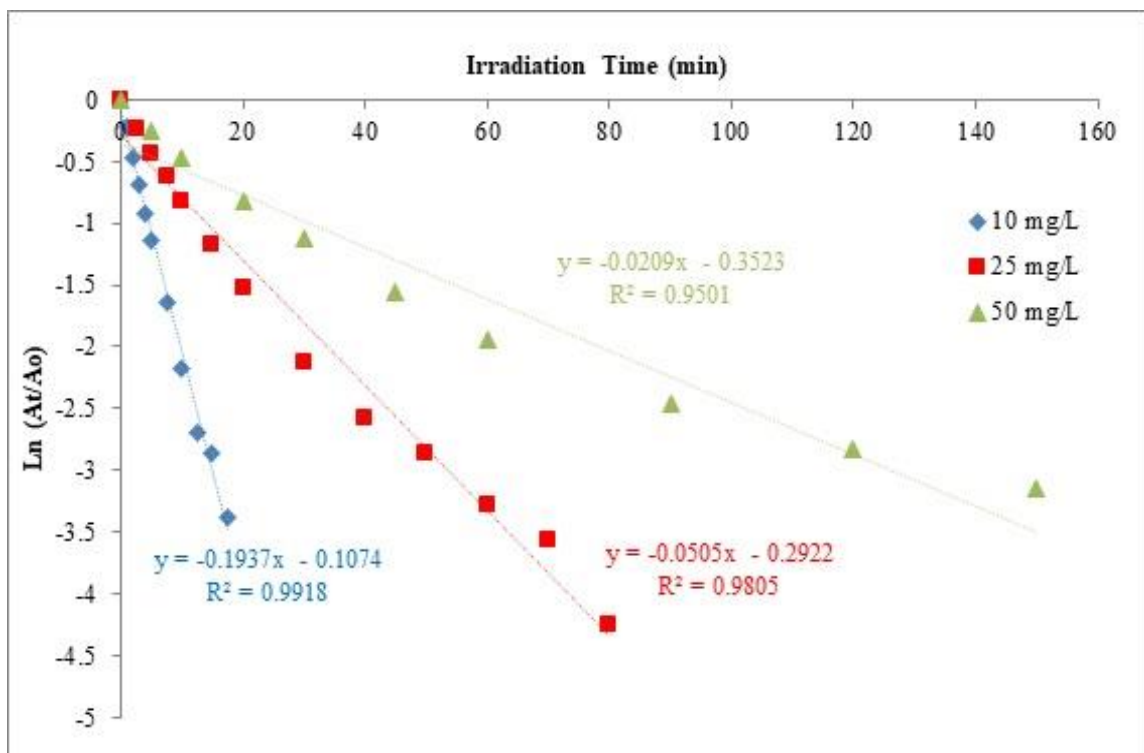


Figure 5.51 Pseudo first-order discoloration of Red dye under various initial concentrations. The results are average of three replicates.

Table 5.11 VUV induced discoloration rate constants of Red dye at various concentrations.

Initial Concentration	Pseudo First Order Discoloration Equation
10 mg/L	$y = -0.1937x - 0.1074$ $R^2 = 0.9918$
25 mg/L	$y = -0.0505x - 0.2922$ $R^2 = 0.9805$
50 mg/L	$y = -0.0209x - 0.3523$ $R^2 = 0.9501$

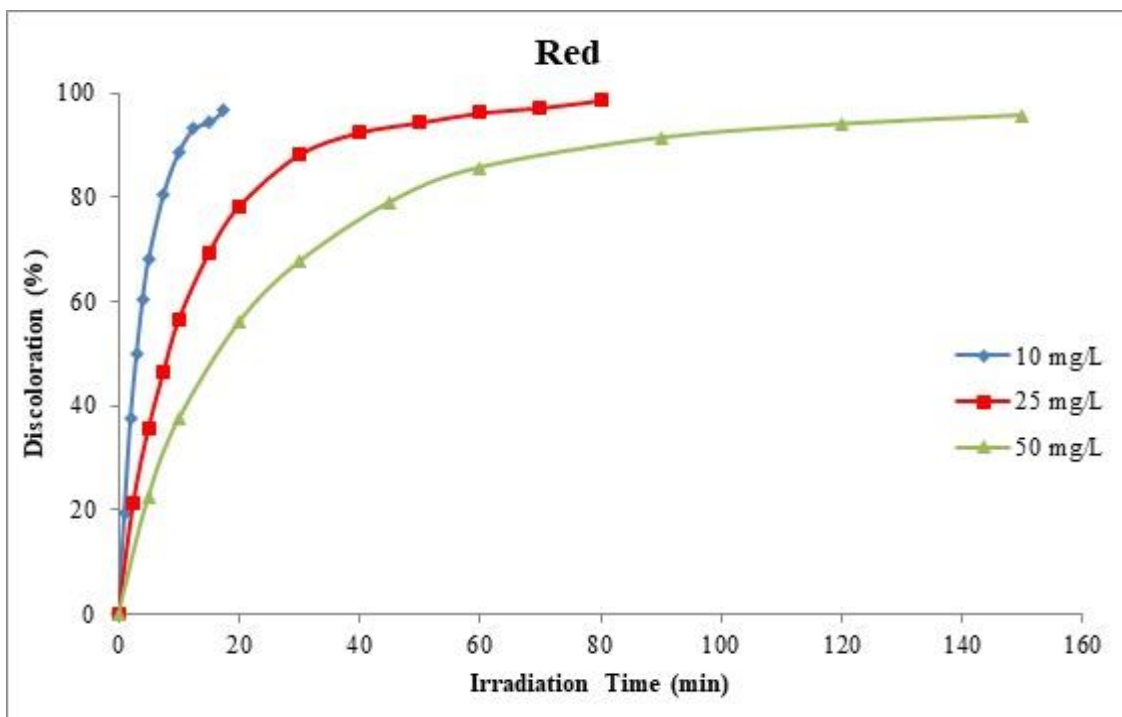


Figure 5.52 Red dye disappearance efficiency of VUV irradiation under various initial concentrations. The results are average of three replicates.

5.7.2.2. Effects of initial concentration on the discoloration of yellow dye

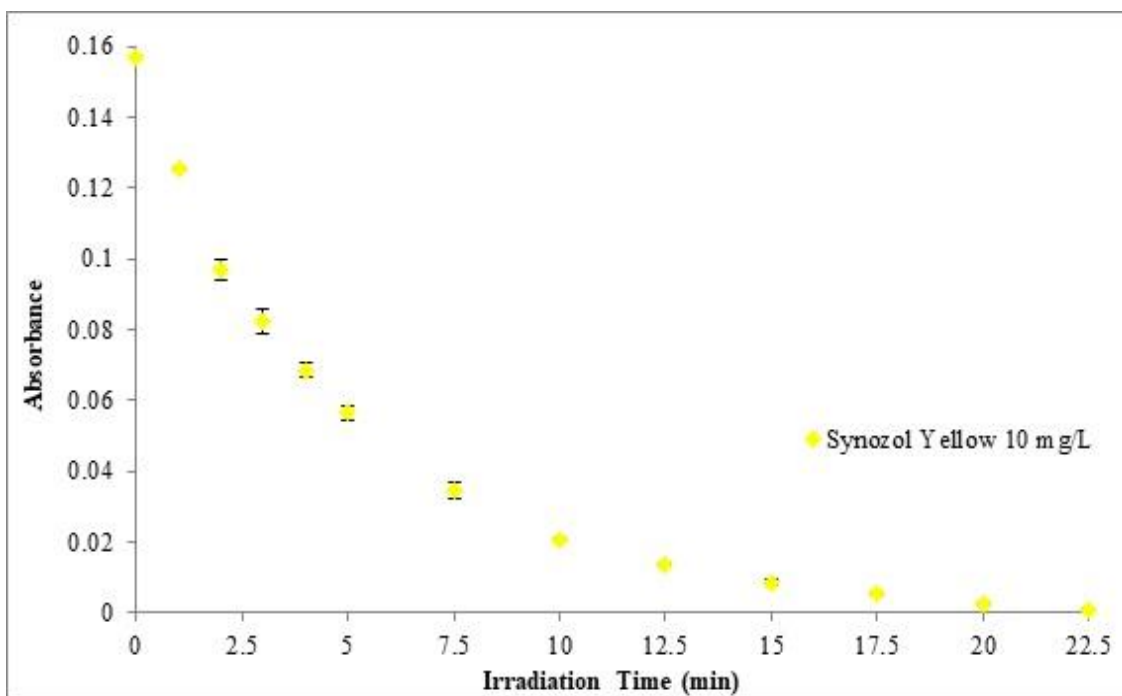


Figure 5.53 VUV induced discoloration of Yellow dye ($C_0 = 10$ mg/L). Error bars represent the standard deviations of three replicates.

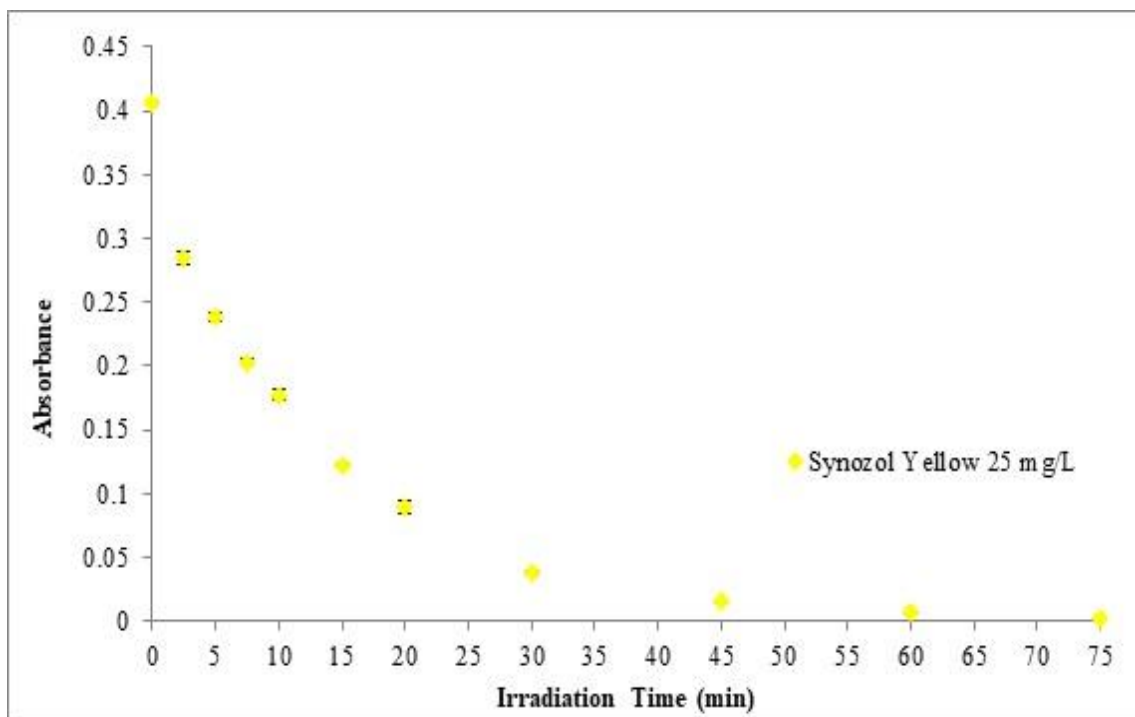


Figure 5.54 VUV induced discoloration of Yellow dye ($C_0 = 25 \text{ mg/L}$). Error bars represent the standard deviations of three replicates.

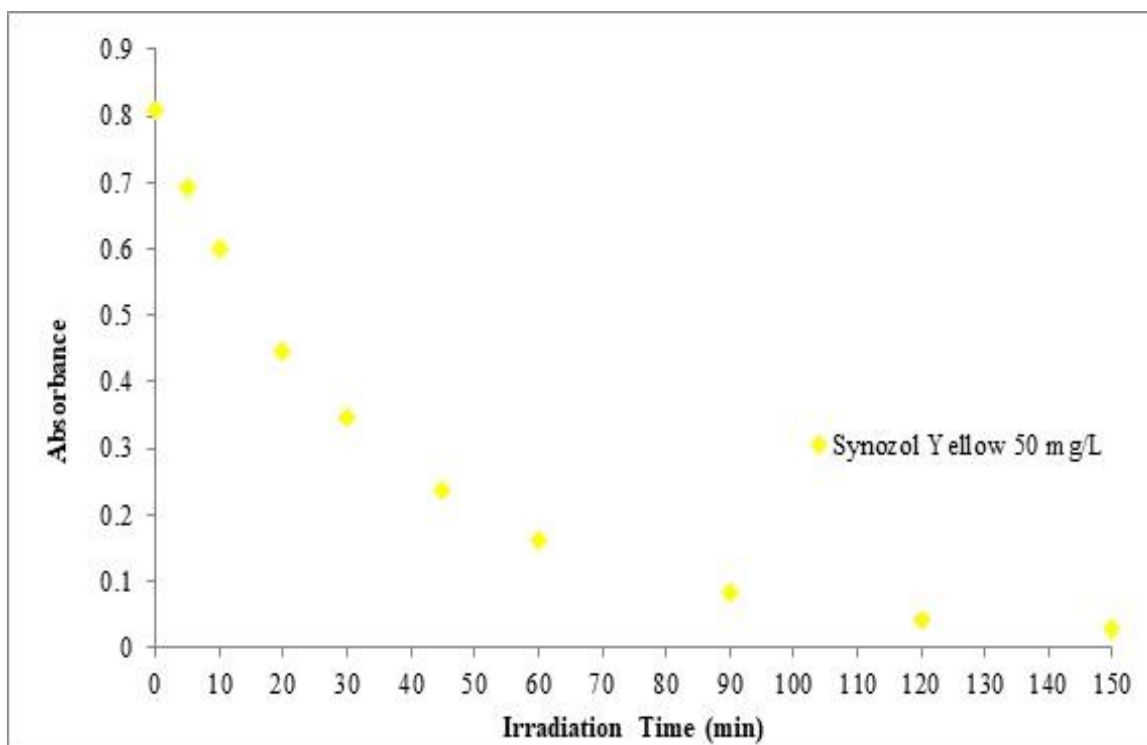


Figure 5.55 VUV induced discoloration of Red dye ($C_0 = 50 \text{ mg/L}$). Error bars represent the standard deviations of three replicates.

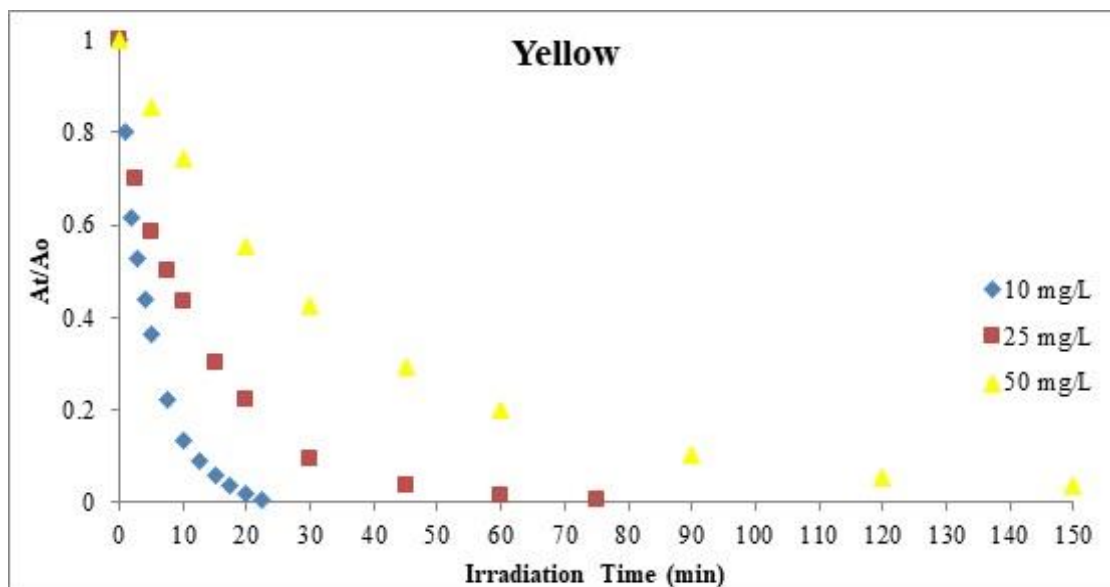


Figure 5.56 VUV initiated discoloration of Yellow dye under various concentrations. The results are average of three replicates.

Figures 5.53, 5.54, and 5.55 present VUV induced disappearance of aqueous yellow dye with initial concentrations of 10, 25 and 50 mg/L respectively. Figures 5.56 and 5.57 show that pseudo first order discoloration kinetic was observed for all the tested initial yellow dye concentrations as in the case of red dye. Figures 5.57 and 5.58; Table 5.12 show that rate and efficiency of yellow dye disappearance were decreased with the increase of initial concentration. The reason behind this finding was explained in the case of red dye (please refer to section 5.7.2.1.).

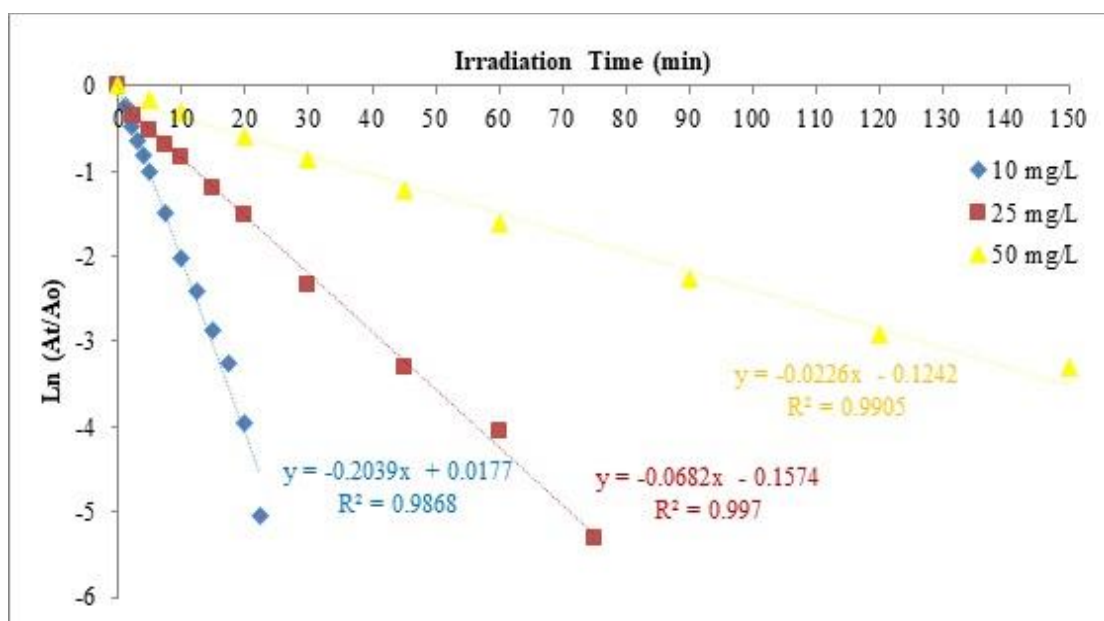


Figure 5.57 Pseudo first-order discoloration of Yellow dye under various initial concentrations. The results are average of three replicates.

Table 5.12 VUV induced discoloration rate constants of Yellow dye at various concentrations.

Initial Concentration	Pseudo First Order Discoloration Equation
10 mg/L	$y = -0.2039x + 0.0177$ $R^2 = 0.9868$
25 mg/L	$y = -0.0682x - 0.1574$ $R^2 = 0.997$
50 mg/L	$y = -0.0226x - 0.1242$ $R^2 = 0.9905$

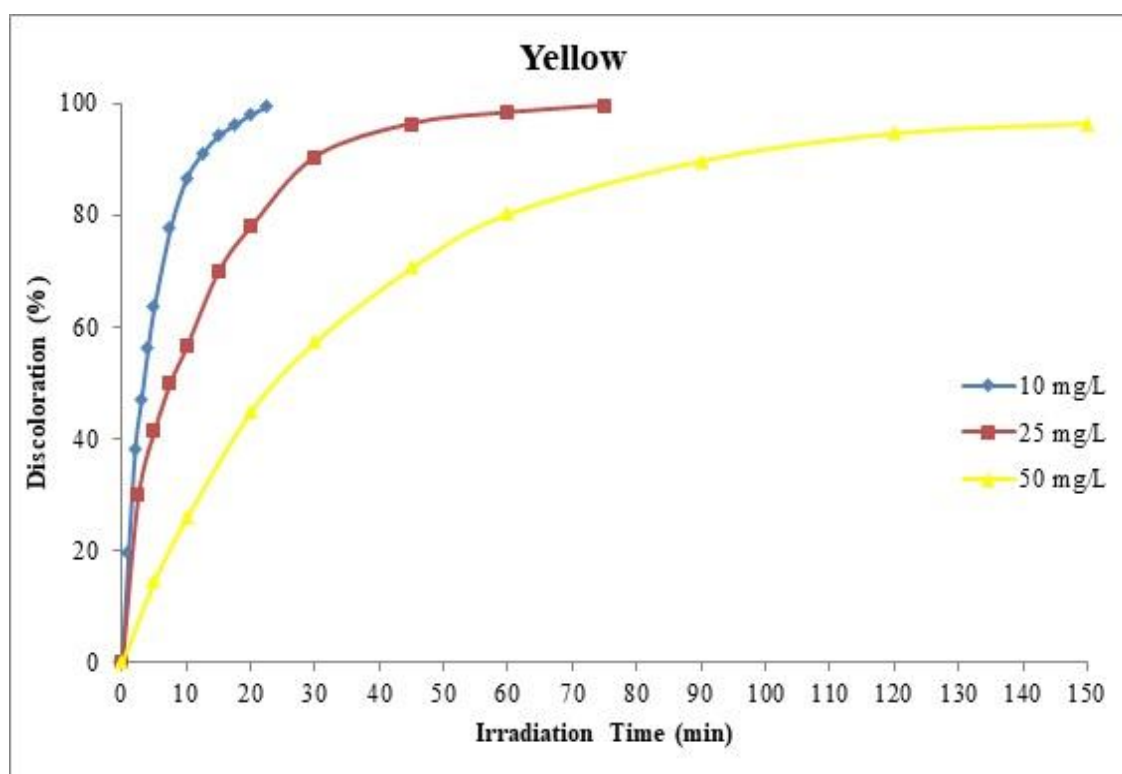


Figure 5.58 Yellow dye disappearance efficiency of VUV irradiation under various initial concentrations. The results are average of three replicates.

5.7.2.3. Comparison of discoloration of red and yellow dyes

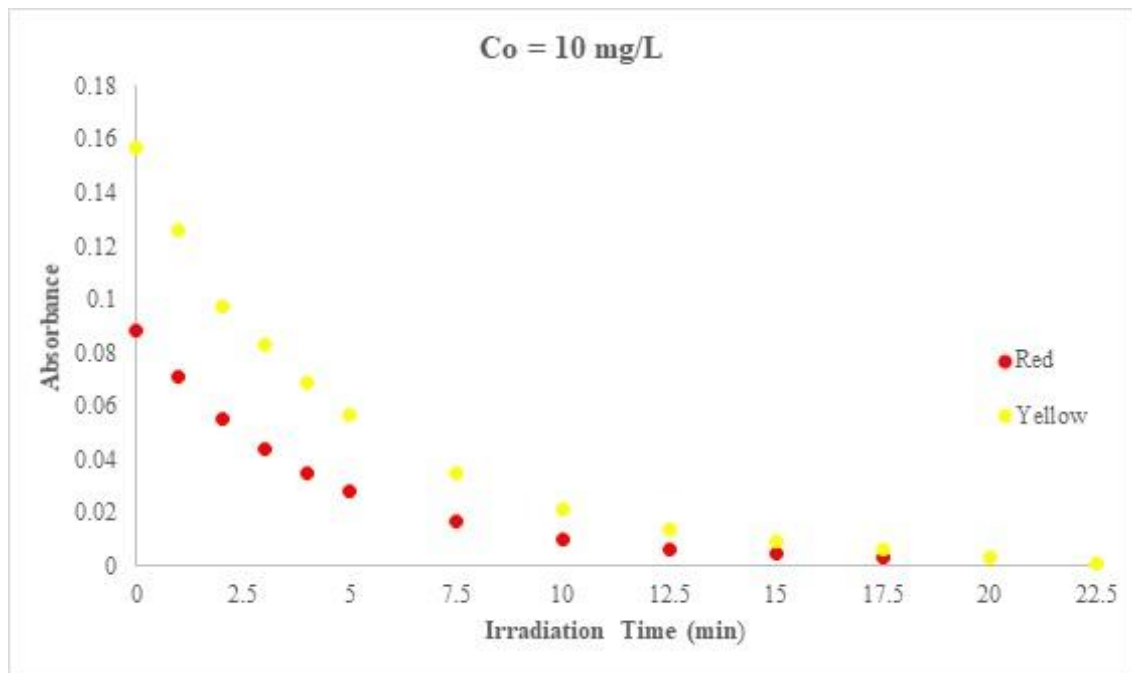


Figure 5.59 VUV induced discoloration of Red and Yellow dyes at $C_o = 10$ mg/L. The results are average of three replicates.

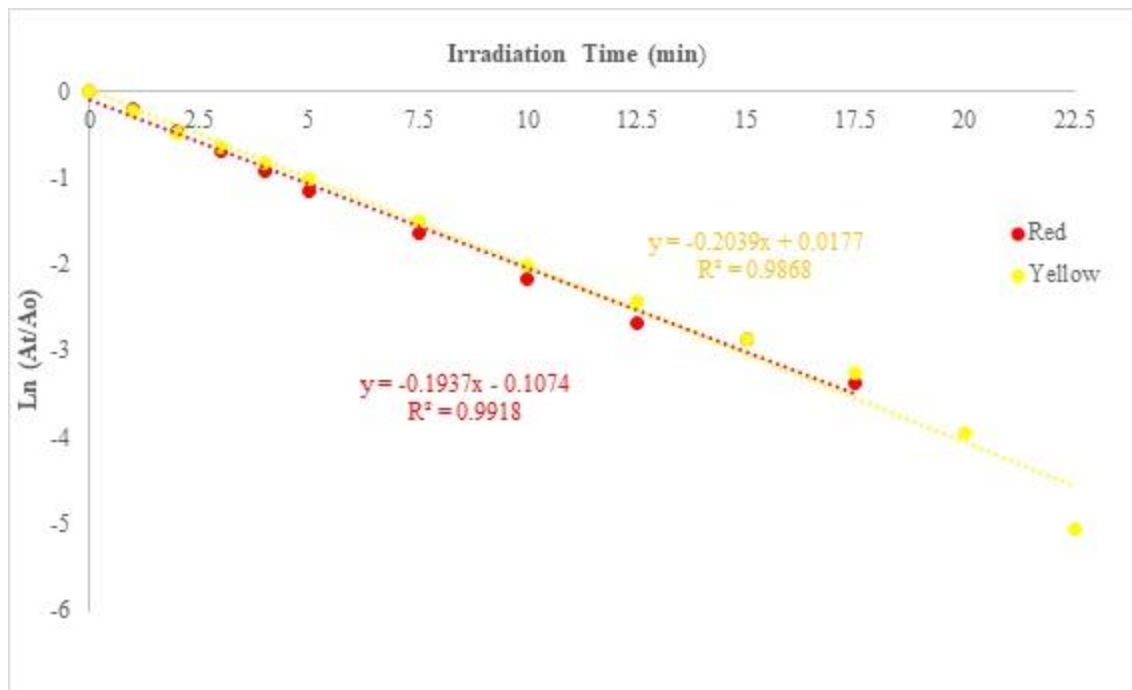


Figure 5.60 VUV initiated discoloration kinetic of Red and Yellow dyes at $C_o = 10$ mg/L. The results are average of three replicates.

It was found that VUV initiated disappearance of red and yellow dyes showed same discoloration kinetic and comparable rate constants at 10 mg/L initial concentration (Figures 5.59 and 5.60). Observed discoloration rate of yellow dye was slightly higher than that of red dye as presented in Table 5.13.

Table 5.13 VUV induced discoloration rate constants of Red and Yellow dyes at $C_0 = 10$ mg/L initial concentration.

Reactive Textile Dye	Pseudo First Order Discoloration Equation
Red	$y = -0.1937x - 0.1074$ $R^2 = 0.9918$
Yellow	$y = -0.2039x + 0.0177$ $R^2 = 0.9868$

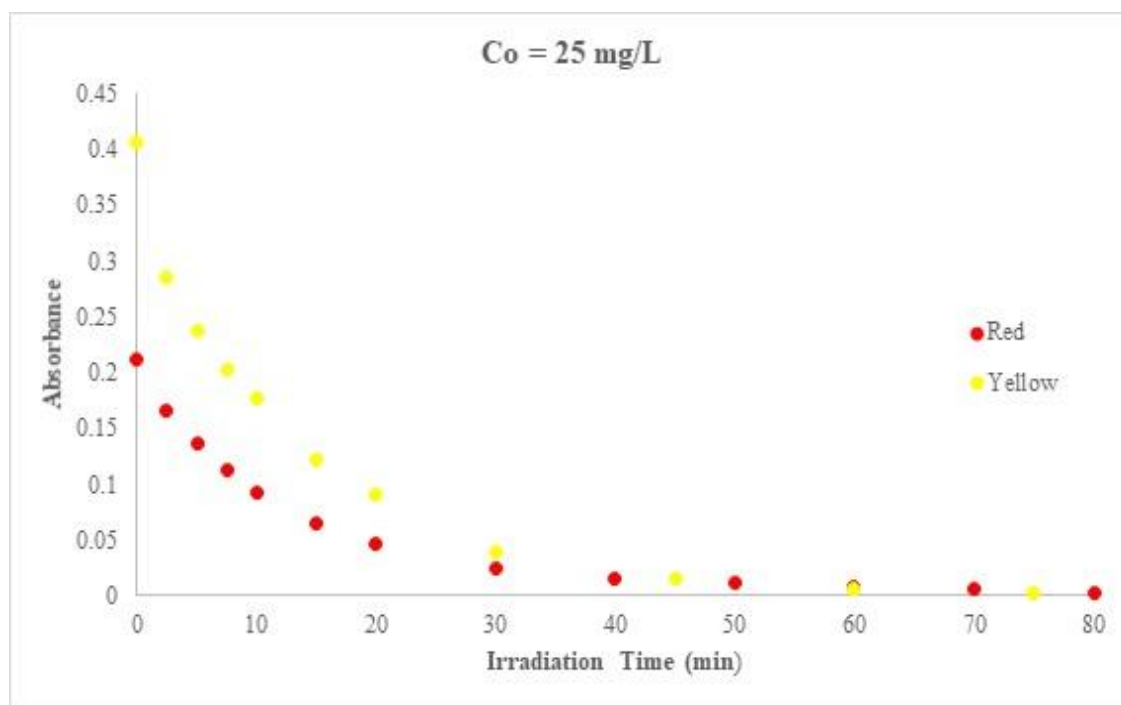


Figure 5.61 VUV induced discoloration of Red and Yellow dyes at $C_0 = 25$ mg/L. The results are average of three replicates.

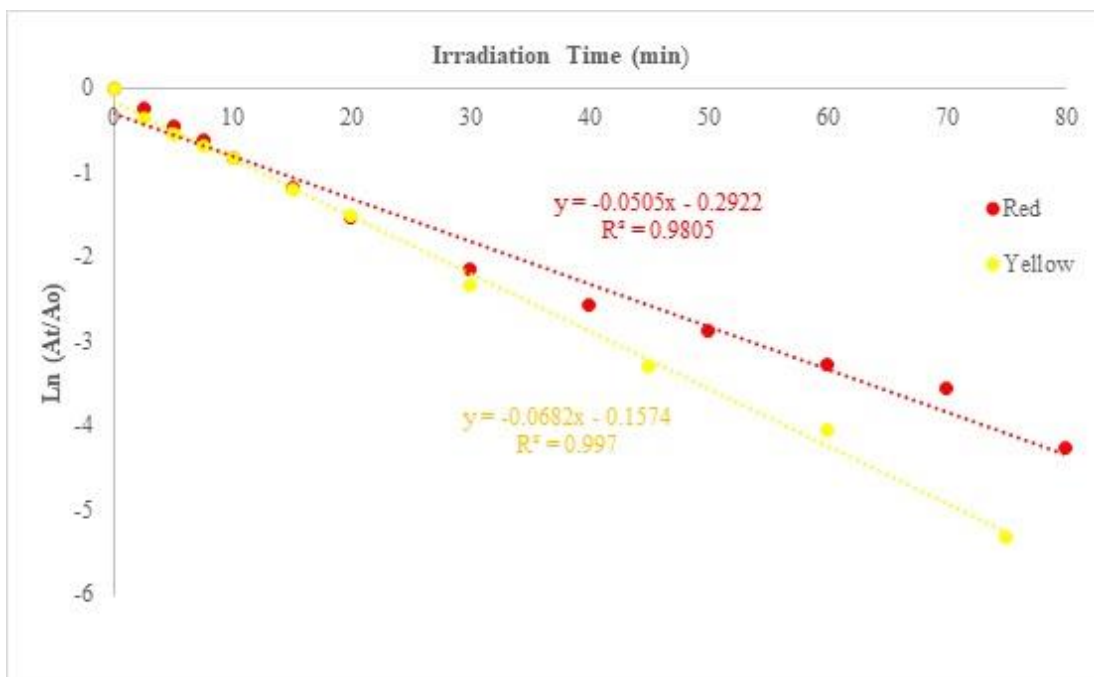


Figure 5.62 VUV initiated discoloration kinetics of Red and Yellow dyes at $C_0 = 25$ mg/L. The results are average of three replicates.

Figures 5.61 and 5.62 show that VUV initiated reduction of red and yellow dyes at 25 mg/L initial concentration followed the same discoloration kinetic as in the case of 10 mg/L initial concentration. However, observed discoloration rate of yellow dye was noticeably higher than that of red dye at this concentration level (Table 5.14). This might be attributed generation of byproducts in the case of red dye at this tested initial concentration, which showed greater resistance to applied treatment process compared to those of yellow dye.

Table 5.14 VUV induced discoloration rate constants of Red and Yellow dyes at $C_0 = 25$ mg/L initial concentration.

Reactive Textile Dye	Pseudo First Order Discoloration Equation
Red	$y = -0.0505x - 0.2922$ $R^2 = 0.9805$
Yellow	$y = -0.0682x - 0.1574$ $R^2 = 0.997$

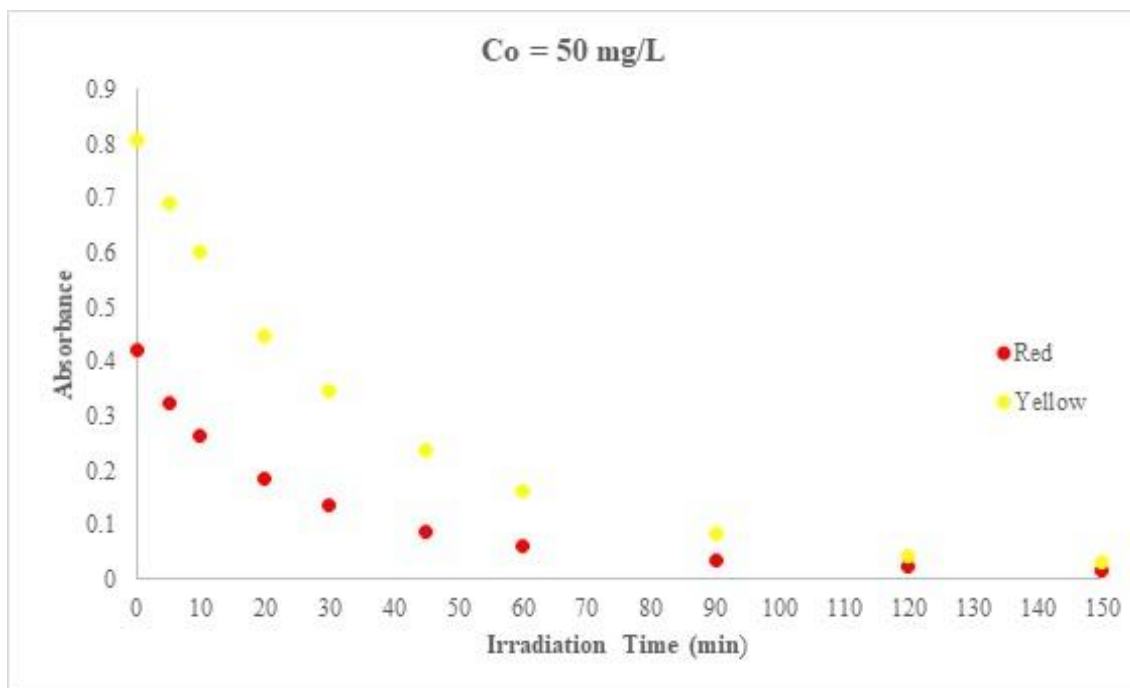


Figure 5.63 VUV induced discoloration of Red and Yellow dyes at $C_o = 50 \text{ mg/L}$. The results are average of three replicates.

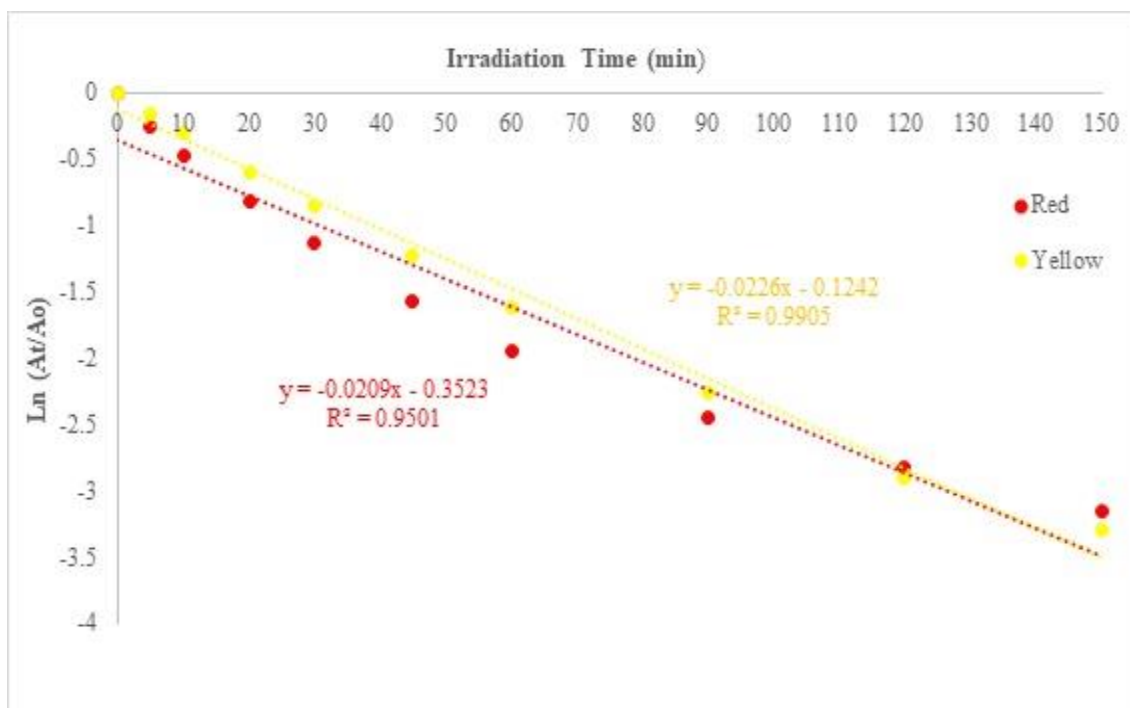


Figure 5.64 VUV initiated discoloration kinetics of Red and Yellow dyes at $C_o = 50 \text{ mg/L}$. The results are average of three replicates.

VUV initiated disappearance of red and yellow dyes showed same discoloration kinetic and comparable rate constants at 50 mg/L initial concentration (Figures 5.63 and 5.64). Observed discoloration rate of yellow dye was slightly higher than that of red dye as shown in Table 5.15.

Table 5.15 VUV induced discoloration rate constants of Red and Yellow dyes at $C_0 = 50$ mg/L initial concentration.

Reactive Textile Dye	Pseudo First Order Discoloration Equation
Red	$y = -0.0209x - 0.3523$ $R^2 = 0.9501$
Yellow	$y = -0.0226x + 0.1242$ $R^2 = 0.9905$

5.7.3. Effects of material of quartz sleeve on the discoloration of the reactive textile dye

Purity of quartz material used in the VUV lamp and sleeve may play an important role in VUV based AOP. Therefore, effects of sleeve materials (clear fused quartz and high purity synthetic quartz) were investigated with various initial concentrations of red dye during the discoloration studies. Comparison of observed rates and disappearance percentages were reported herein.

5.7.3.1. Effects of quartz sleeve on the reduction of red dye with 10 mg/L initial concentration

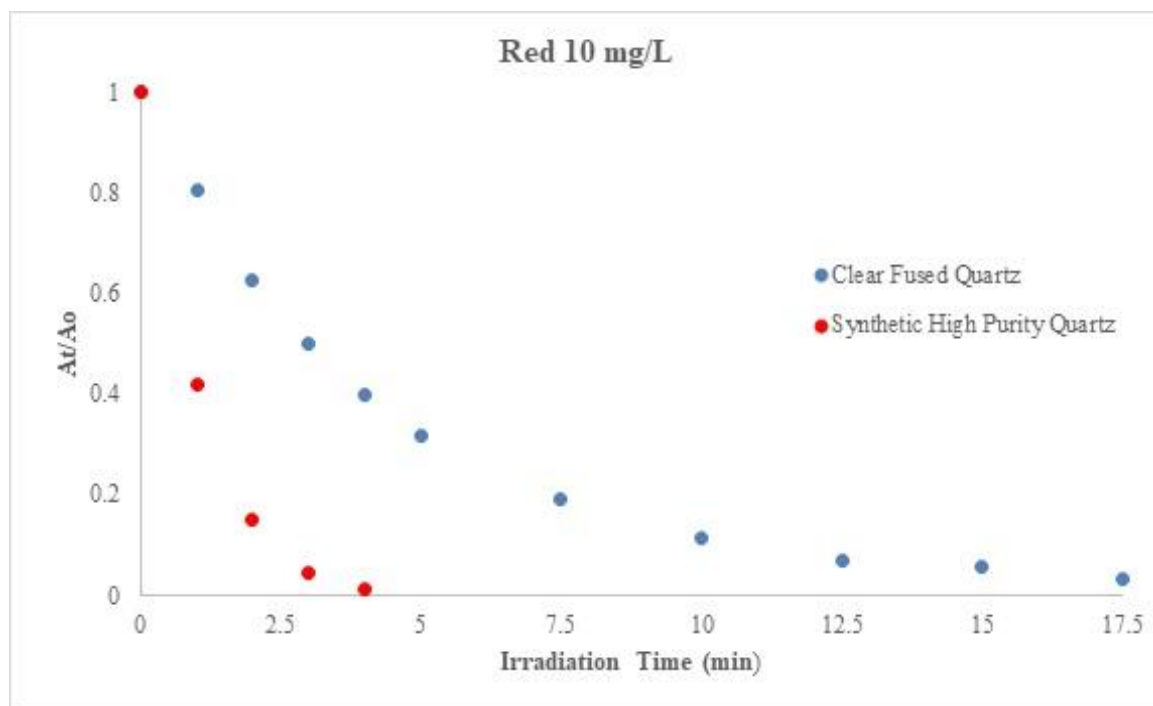


Figure 5.65 Effects of materials of quartz sleeve on discoloration of Red dye ($C_0 = 10$ mg/L). The results are average of three replicates.

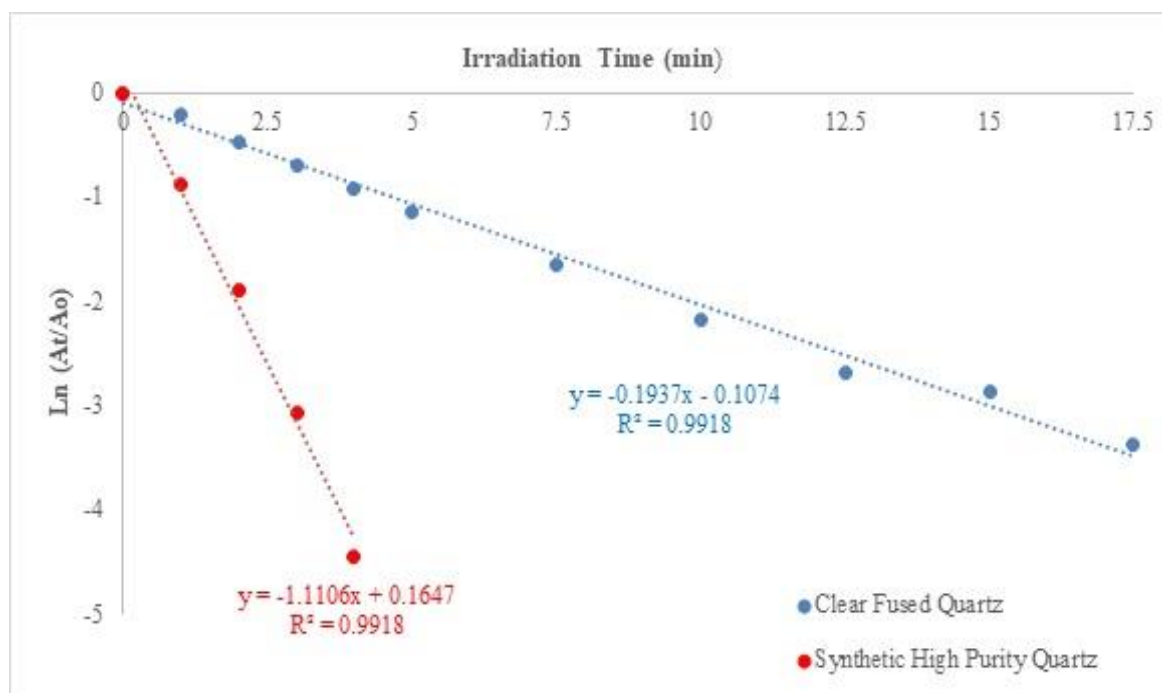


Figure 5.66 Effects of materials of quartz sleeve on discoloration kinetics of Red dye ($C_0 = 10$ mg/L). The results are average of three replicates.

Figures 5.65 and 5.66 shows comparison of disappearance of aqueous red dye with initial concentrations of 10 mg/L by the VUV process in the presence of clear fused quartz and high purity synthetic quartz. Pseudo first order discoloration kinetic was observed in presence of both quartz sleeves. So, materials of the sleeve used in the applied process did not affect the kinetic pattern. However, the results show that the observed discoloration rate constant was significantly increased by using the synthetic high purity quartz sleeve. It was found that rate constant observed in the presence of synthetic high purity quartz sleeve was almost 5.74 times faster than that of clear fused quartz sleeve (Table 5.16). Complete reduction of 10 mg/L red dye was sought in less than 5 minutes of VUV irradiation by using synthetic quartz as shown in Figure 5.67. This finding can be attributed to higher transmission of 185 nm photons into experimental solution by synthetic quartz, which resulted generation of higher amount of •OH that was responsible oxidant for discoloration of the target compound. It can be concluded that purity of quartz material used to enclose VUV lamp can alter efficiency of the VUV based AOP in the removal of pollutants from water.

Table 5.16 VUV induced discoloration rate constants of Red dye ($C_0 = 10$ mg/L) obtained using different materials of quartz sleeve.

Material of Sleeve	Pseudo First Order Discoloration Equation
Clear Fused Quartz	$y = -0.1937x - 0.1074$ $R^2 = 0.9918$
Synthetic High Purity Quartz	$y = -1.1106x + 0.1647$ $R^2 = 0.9918$

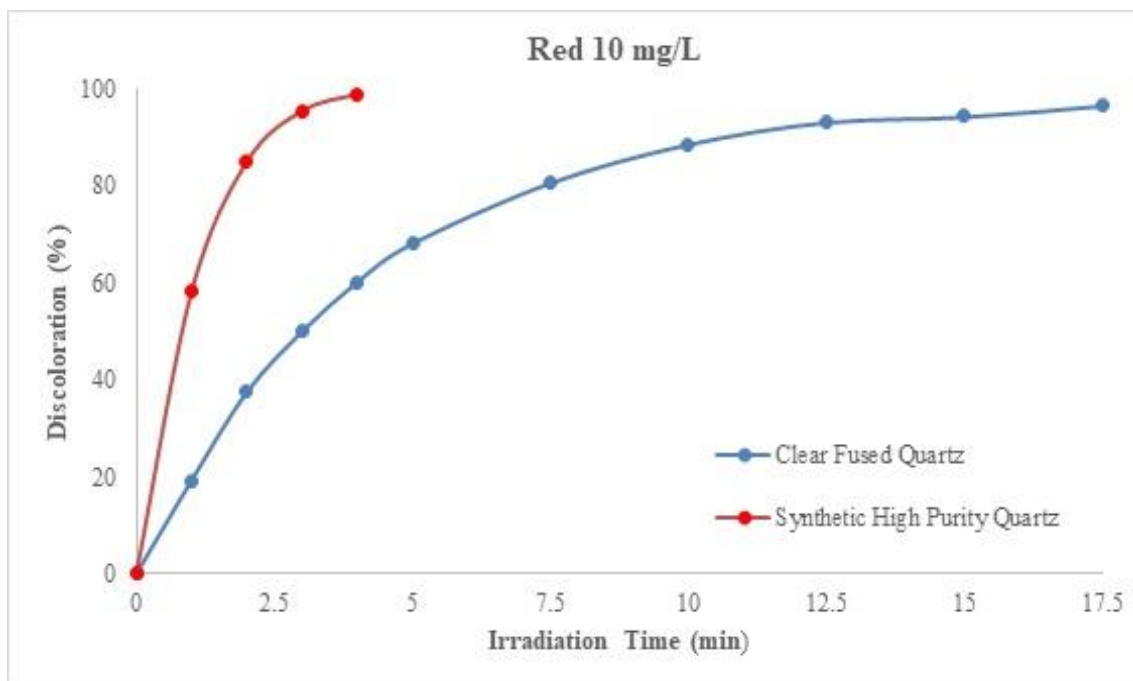


Figure 5.67 Effects of materials of quartz sleeve on discoloration efficiency of Red dye ($C_0 = 10 \text{ mg/L}$). The results are average of three replicates.

5.7.3.2. Effects of quartz sleeve on the reduction of red dye with 25 mg/L initial concentration

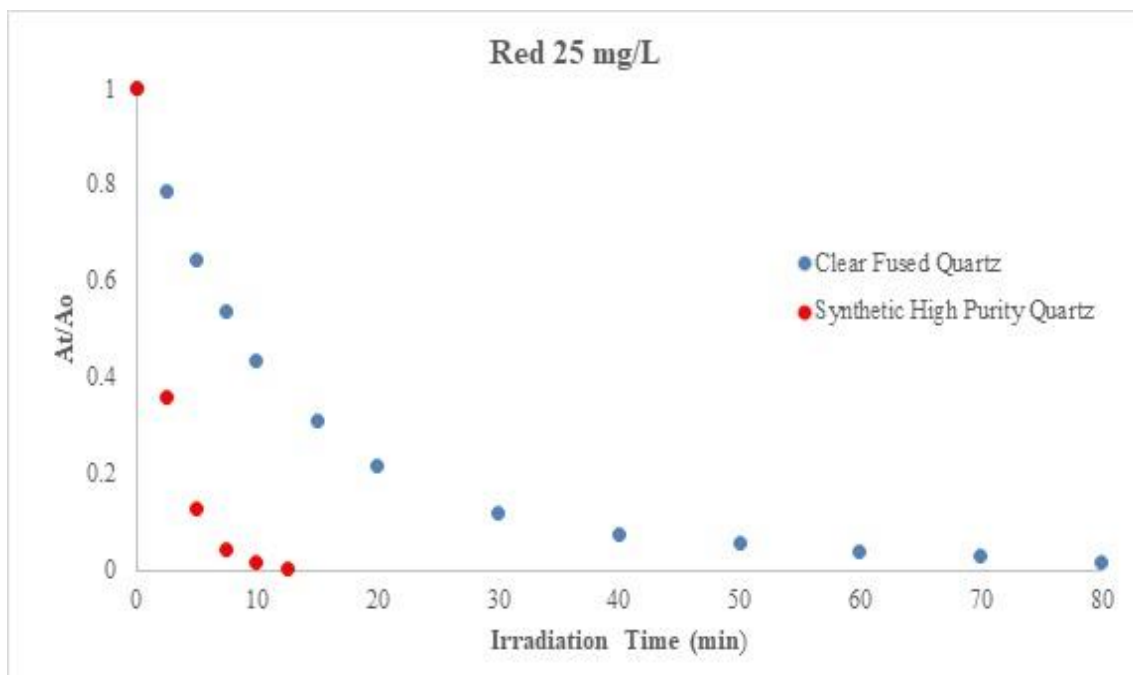


Figure 5.68 Effects of materials of quartz sleeve on discoloration of Red dye ($C_0 = 25 \text{ mg/L}$). The results are average of three replicates.

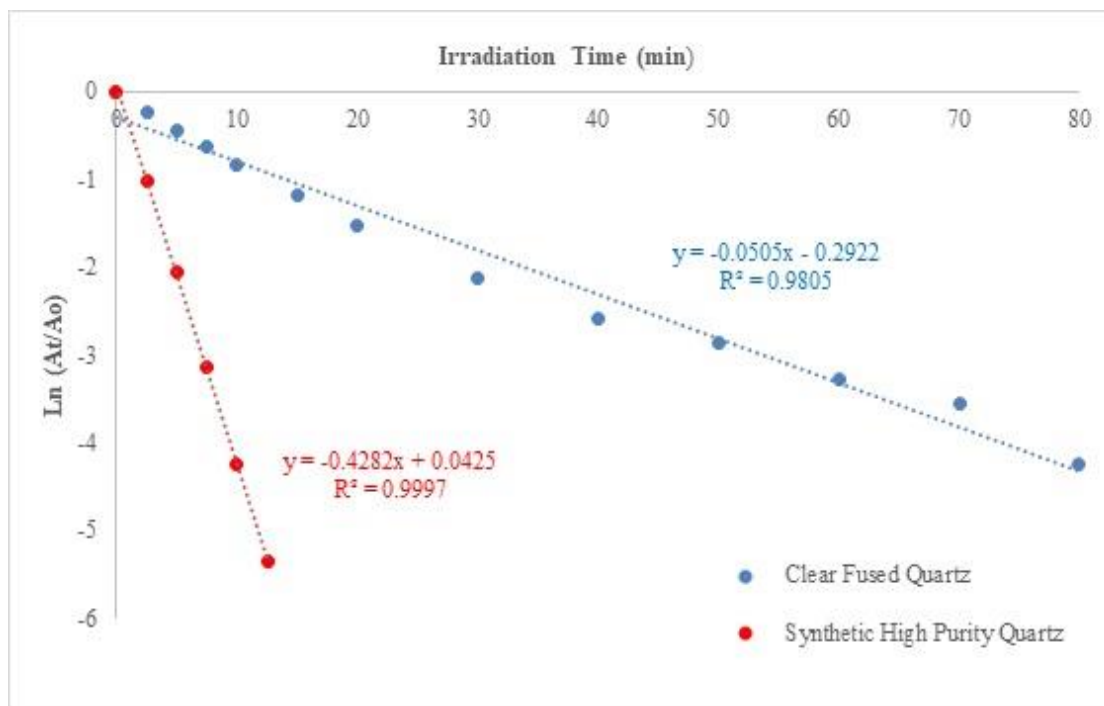


Figure 5.69 Effects of materials of quartz sleeve on discoloration kinetics of Red dye ($C_0 = 25$ mg/L). The results are average of three replicates.

Effects of the sleeve material on the discoloration of aqueous red dye with initial concentrations of 25 mg/L were presented Figures 5.68 and 5.69. As in the case of 10 mg/L, observed pseudo first order discoloration rate constant was significantly increased by using the synthetic high purity quartz sleeve (Figure 5.69; Table 5.17). It was found that increment in rate constant experienced with 25 mg/L initial concentration was even higher than what was observed in 10 mg/L initial concentration. Rate constant attained by using the synthetic high purity quartz sleeve was 8.48 times faster than that of clear fused quartz sleeve in this applied concentration (Table 5.17).

It took only 12.5 minutes for complete reduction of 25 mg/L red dye by using synthetic quartz whereas it required more than 80 minutes to reach same removal efficiency by using clear fused quartz (Figure 5.70). This finding can again be attributed to the generation of higher amount of $\bullet\text{OH}$ due to passage of more 185 nm photons into experimental solution by synthetic quartz. It can be concluded that effect of synthetic quartz on the discoloration of red dye was significant irrespective of initial concentration.

Table 5.17 VUV induced discoloration rate constants of Red dye ($C_0 = 25 \text{ mg/L}$) obtained using different materials of quartz sleeve.

Material of Sleeve	Pseudo First Order Discoloration Equation
Clear Fused Quartz	$y = -0.0505x - 0.2922$ $R^2 = 0.9805$
Synthetic High Purity Quartz	$y = -0.4282x + 0.0425$ $R^2 = 0.9997$

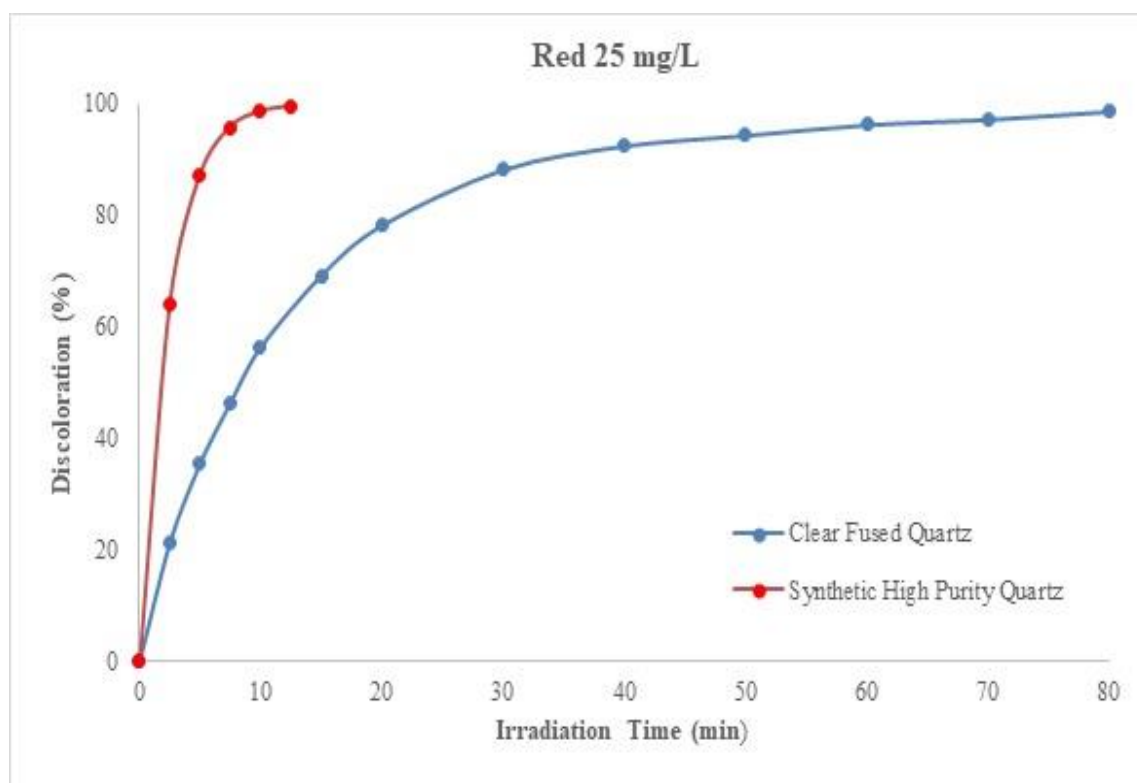


Figure 5.70 Effects of materials of quartz sleeve on discoloration efficiency of Red dye ($C_0 = 25 \text{ mg/L}$). The results are average of three replicates.

5.7.3.3. Effects of quartz sleeve on the reduction of red dye with 50 mg/L initial concentration

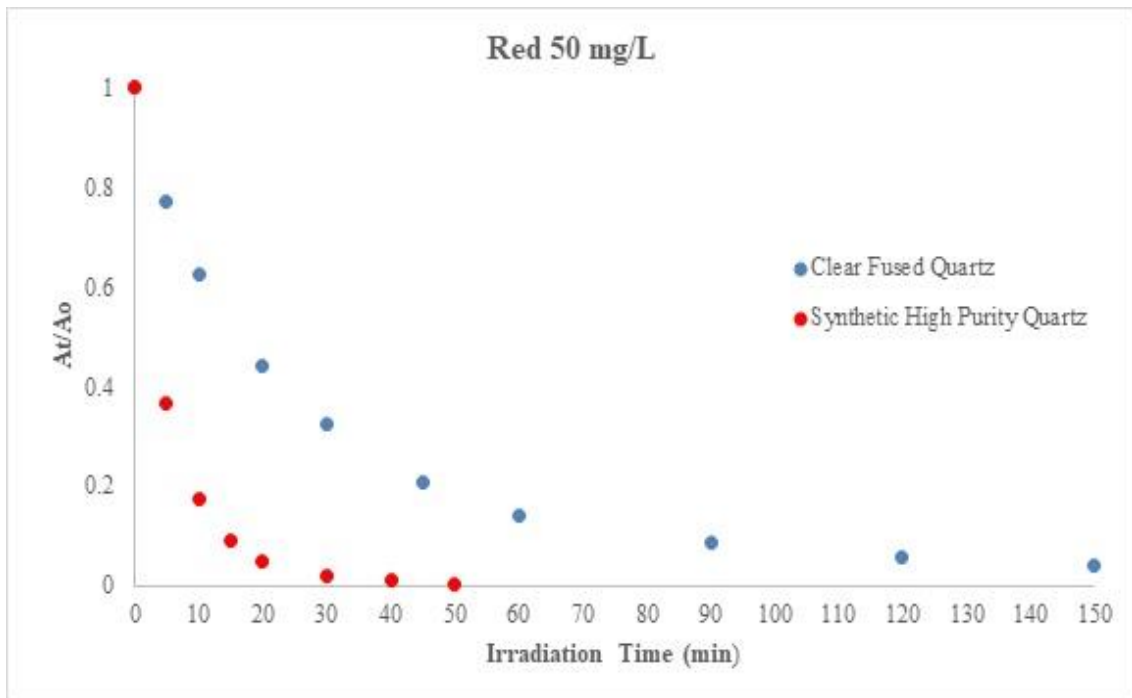


Figure 5.71 Effects of materials of quartz sleeve on discoloration of Red dye (C_o = 50 mg/L). The results are average of three replicates.

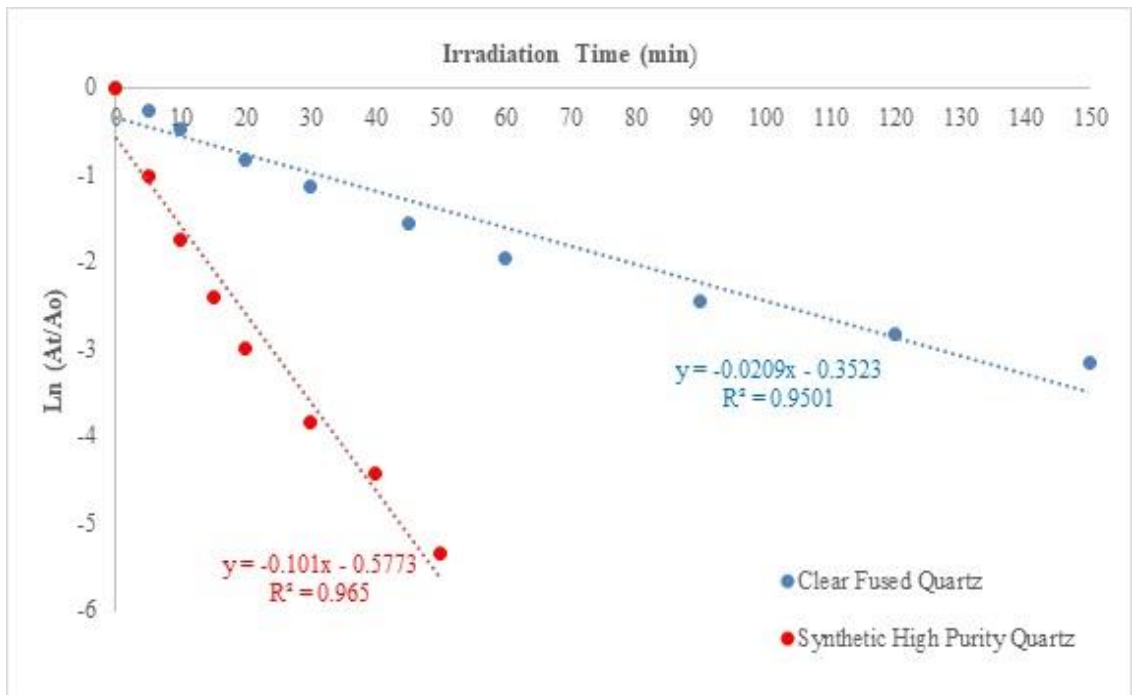


Figure 5.72 Effects of materials of quartz sleeve on discoloration kinetics of Red dye (C_o = 50 mg/L). The results are average of three replicates.

Comparison of discoloration of red dye with 50 mg/L initial concentration by using clear fused quartz and high purity synthetic quartz was presented in Figures 5.71 and 5.72. Once again significant influence of the synthetic quartz on the discoloration of red dye was observed even at the highest concentration of target dye tested in this doctoral study. Almost 5 times faster disappearance rate constant was recorded at this concentration (Table 5.18). It can be seen from Figure 5.73 that time required for complete reduction of red dye was considerably less to 50 minutes in the presence of synthetic quartz.

Table 5.18 VUV induced discoloration rate constants of Red dye ($C_0 = 50$ mg/L) obtained using different materials of quartz sleeve.

Material of Sleeve	Pseudo First Order Discoloration Equation
Clear Fused Quartz	$y = -0.0209x - 0.3523$ $R^2 = 0.9501$
Synthetic High Purity Quartz	$y = -0.101x - 0.5773$ $R^2 = 0.965$

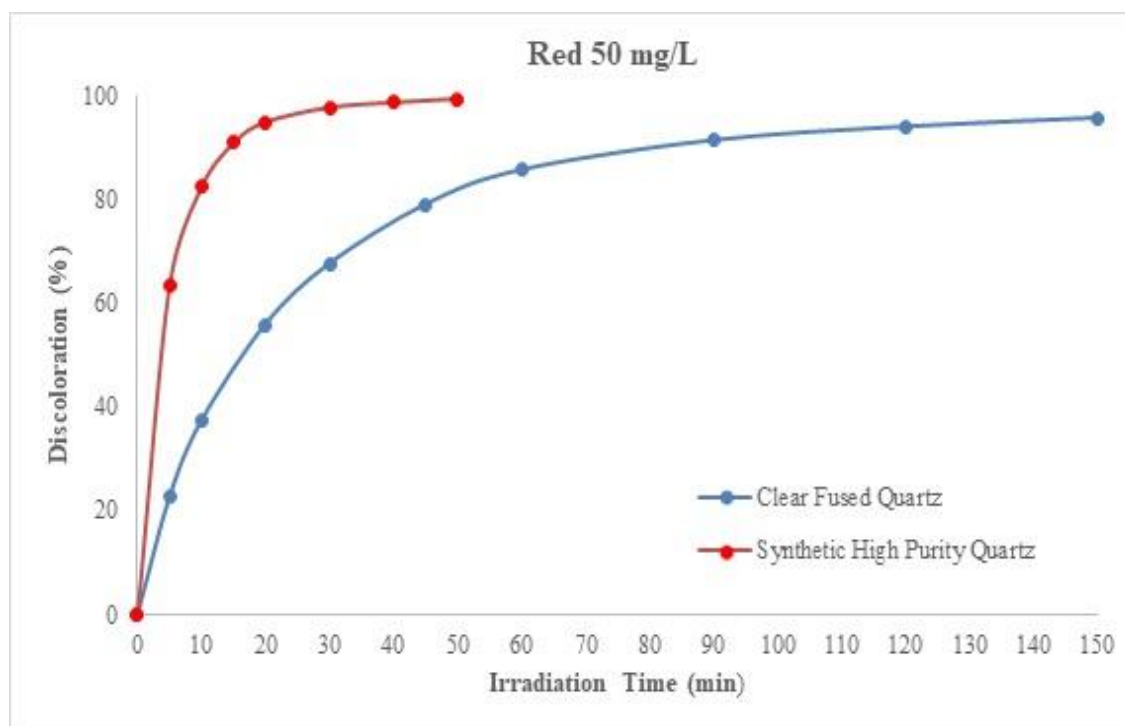


Figure 5.73 Effects of materials of quartz sleeve on discoloration efficiency of Red dye ($C_0 = 50$ mg/L). The results are average of three replicates.

6. CONCLUSION

VUV photooxidation of aqueous imidacloprid with a flow through photoreactor was performed during this doctoral study. Effects of various experimental parameters, flow rate, initial pH of solution, initial concentration, presence of inorganic ions (HCO_3^- , CO_3^{2-} , NO_3^-), water matrix, presence and absence of dissolved oxygen on the VUV induced degradation of imidacloprid were investigated within the scope of this doctoral thesis. Hydrolytic degradation of imidacloprid under various solution pH was also independently studied. Furthermore, effectiveness of the VUV process was assessed by discoloration experiments of commercially available reactive textile dyes (Synozol Red KH-L and Synozol Yellow KH-L) in water. Finally, Effects of sleeve materials (clear fused quartz and high purity synthetic quartz) were studied during the course of discoloration experiments.

The overall conclusions of this research are summarized below:

- Separate hydrolysis experiments revealed that imidacloprid was very stable under acidic (pH=3) and natural (original, pH=6.469) conditions during 104 days of hydrolysis time. Hydrolytic degradation of imidacloprid significantly increased under tested basic (pH=11) condition. First order kinetic pattern with the hydrolytic rate constant of 0.0083 day^{-1} and half-life of 83.51 days was observed at the tested alkaline solution.
- Photon flux (P_{VUV}) of the VUV lamp at 185 nm was calculated as $4.18 \times 10^{-7} \text{ mol}_{\text{photon}} \text{ s}^{-1}$ by using methanol actinometry method at the beginning of irradiation experiments.
- Imidacloprid was rapidly removed from water (ultrapure water, tap water, and pond water) by the VUV process under the all investigated experimental conditions. The results showed that $\bullet\text{OH}$ was the responsible primary radical as opposed to $\text{H}\bullet$, e_{aq}^- for the decomposition of imidacloprid by the VUV based APO. VUV induced degradation of imidacloprid followed pseudo first order kinetic pattern with no exception of experimental conditions. Observed reduction rate constants of imidacloprid ($C_0 = 5 \text{ mg/L}$) depending on these conditions varied between 1.3877 min^{-1} and 1.9213 min^{-1} . Complete removal of imidacloprid was attained between 3.5 and 5 minutes of VUV irradiation time for ultrapure water and pond water respectively.

- Rate of degradation of aqueous imidacloprid increased with an increment in flow rate due to better mixing of solution within the reactor at higher flow rate and hence increased contact of imidacloprid with $\bullet\text{OH}$. Nonetheless, increments in observed rate constant were marginal, only 1.29% and 1.57% for 750 mL/min and 1000 mL/min flow rates respectively, because of mass transfer limitation of imidacloprid to the radical active narrow zone within the photoreactor at studied flow rates. Observed pseudo first order degradation rate constants were 1.8891 min^{-1} , 1.9134 min^{-1} , and 1.9188 min^{-1} for the case of 500 mL/min, 750 mL/min, and 1000 mL/min flow rates respectively. Complete removal of imidacloprid ($C_0 = 5 \text{ mg/L}$) was sought within 3.5 minutes of irradiation time for the all flow rates.
- pH of the experimental solution played an important role in the degradation of imidacloprid by the VUV process. Higher degradation rate constant was observed in the following order of acidic > natural (original) > basic conditions. Significant decrease (15.33%) in the rate of degradation of imidacloprid was observed at basic pH=11 condition due to reduction of oxidation potential of $\bullet\text{OH}$ and conversion of $\bullet\text{OH}$ to less reactive $\bullet\text{O}^-$ radical in strong alkaline solution. Nevertheless, the VUV process performed very high efficiency under the all tested solution pH conditions. It was found that it took only 3.5 minutes of VUV irradiation to obtain complete destruction of imidacloprid ($C_0 = 5 \text{ mg/L}$) under acidic (pH= 3) and natural (original, pH \approx 6.5) conditions while 4 minutes was required for basic (pH=11) condition. Degradation rate constants of 1.8891 min^{-1} , 1.9213 min^{-1} , and 1.5994 min^{-1} were obtained in natural (original), acidic, and basic solutions respectively.
- Imidacloprid removal and accordingly degradation rate by the VUV photooxidation were decreased with the increment of initial imidacloprid concentration since higher amount of $\bullet\text{OH}$ reacted with imidacloprid at elevated initial concentration, which resulted lower steady state concentration of $[\bullet\text{OH}]$ and degradation rate constant because pseudo first order degradation rate constant, $k' = k_{\bullet\text{OH},\text{C}} \times [\bullet\text{OH}]$, is proportional to the steady state concentration of $[\bullet\text{OH}]$. Complete removal of 2.5 mg/L, 5 mg/L, 10 mg/L initial concentration of imidacloprid were obtained with 2.5 min, 3.5 min, and 4.5 min of VUV irradiation respectively. VUV induced degradation rate constants of 2.1814 min^{-1} , 1.8891 min^{-1} , 1.6307 min^{-1} were determined in the same order of concentration.

- Presence of inorganic ions (HCO_3^- , CO_3^{2-} , and NO_3^-) noticeably impacted the decomposition of imidacloprid via VUV photons. Reduction of 10.68%, 9.88%, and 8.87% in the pseudo first order degradation rate constant of imidacloprid were recorded in the presence of CO_3^{2-} , HCO_3^- , and NO_3^- respectively due to higher $\bullet\text{OH}$ scavenging capacity of CO_3^{2-} and HCO_3^- ions compared to NO_3^- which acted as inner filter by absorbing some of VUV (185 nm) photons. Nonetheless, complete removal of imidacloprid in the presence of these ions was observed within 4 minutes of VUV irradiation time accompanied with the rate constants of 1.6873 min^{-1} , 1.7024 min^{-1} , 1.7215 min^{-1} in the presence of CO_3^{2-} , HCO_3^- , and NO_3^- respectively.
- Among the experimental parameters water matrix affected the VUV photooxidation of imidacloprid the most. Inhibition of degradation was higher in the pond water due to presence of natural organic matters (NOM) which usually reported to have high scavenging effects on $\bullet\text{OH}$, than tap water that typically contains mixture of inorganic ions like CO_3^{2-} , HCO_3^- , NO_3^- , and Cl^- . Decrements in the observed rate constant of imidacloprid degradation were 22% and 26.54% in the solutions of tap and pond water respectively. Reduction of imidacloprid in tap water was more pronounced than individual presence of inorganic ions due to synergistic effects of inorganic ions. Pseudo first order degradation rate constants for tap and pond water were determined to be 1.4677 min^{-1} and 1.3877 min^{-1} respectively.
- Presence and absence of dissolved oxygen had negligible impact on the degradation rate of imidacloprid by the VUV process. Less than 1% increment was observed in the removal rate constant for the oxygen saturated condition whereas less than 0.17% decrement was for the oxygen free one. Therefore, contribution of $\text{HO}_2\bullet/\text{O}_2\bullet^-$ as well as $\text{H}\bullet$ and e_{aq}^- to reduction of imidacloprid, respectively, in oxygenated and deoxygenated solutions were insignificant due to their low reactivity with imidacloprid compared to $\text{HO}\bullet$. Removal rate constants of 1.9048 min^{-1} and 1.8859 min^{-1} were calculated in oxygen saturated and oxygen free solutions respectively.
- Presence and absence of dissolved oxygen did not have much impact on mineralization (TOC reduction) of aqueous imidacloprid by the VUV process either. Almost 80% TOC reduction of imidacloprid ($C_o = 10 \text{ mg/L}$) and its

intermediate products was achieved in 120 minutes of reaction time under the all tested conditions. Zero order mineralization kinetic was observed in oxygenated, deoxygenated and natural (no gas sparging) conditions. Same rate constant was determined for both oxygen free and natural (no gas sparging) solutions while only 1.61% increment was observed in the oxygen saturated condition. This results showed that dissolved oxygen and oxidative $\text{HO}_2\bullet/\text{O}_2\bullet^-$ which were coexisted with $\text{HO}\bullet$ in the presence of oxygen apparently did not have much impact on the VUV induced mineralization of imidacloprid and its byproducts either, which is in agreement with what was attained in degradation experiments. On the other hand, reductive $\text{H}\bullet$ and e_{aq}^- had negligible effect on the mineralization of imidacloprid and formed byproducts as well since there is no difference observed in the oxygen free solution either. Therefore, $\text{HO}\bullet$ was the responsible radical in the mineralization mechanism as in the case of degradation. Despite complete reduction of aqueous imidacloprid ($C_0 = 10 \text{ mg/L}$) in 4 minutes, 2 hours was required to reach approximately 80% mineralization which confirmed that generated byproducts exhibited higher resistance to primary $\text{HO}\bullet$. $\text{H}\bullet$, e_{aq}^- , and secondary radicals $\text{HO}_2\bullet/\text{O}_2\bullet^-$ than imidacloprid in the VUV process. Zero order mineralization rate constants of $0.0062 \text{ mg L}^{-1} \text{ min}^{-1}$ was calculated both in natural (no gas sparging) and oxygen free solutions while $0.0063 \text{ mg L}^{-1} \text{ min}^{-1}$ was in oxygen saturated solution.

- Several possible byproducts some of which were identified, were detected during the reaction time of complete imidacloprid reduction by LC/MS Q-TOF in agreement with findings of imidacloprid mineralization experiments. Other than imidacloprid, detected byproducts were present at the time of complete imidacloprid destruction since 4 minutes of VUV irradiation was inadequate for complete destruction of them. According to our best knowledge this is the first time of m/z 163 to be reported in imidacloprid degradation.
- VUV initiated discoloration of Synozol Red K-HL (red dye) and Synozol Yellow K-HL (yellow dye) were rapid even in the presence of clear fused quartz sleeve which evidently transmits less 185 nm photon. Both discoloration of red and yellow dyes followed pseudo first order disappearance kinetic under the all investigated experimental conditions. Observed rate constant of yellow dye was slightly higher than that of red dye. Discoloration of both textile dyes by the VUV photooxidation were decreased with the increment of initial dye concentration due

to reduction of ratio of hydroxyl radical ($\bullet\text{OH}$) to textile dyes at increased initial concentration. Complete discoloration of textile dyes ($C_0 = 10 \text{ mg/L}$) in the presence of clear fused quartz was observed within 20 minutes of VUV irradiation.

- Rate of disappearance of red dye increased with an increment in flow rate due to better mixing of solution within the reactor at higher flow rate and hence increased contact of imidacloprid with $\bullet\text{OH}$ as in agreement with what was observed for degradation of imidacloprid in this research. Pseudo first order disappearance kinetic was observed under the all tested flowrates. Even though there was no substantial difference on observed disappearance rate constants of red dye with tested flow rates, slightly higher rate constant was observed at 750 mL/min flow rate. Increments in the observed rate constants were 4% and 5.4% for the case of 500 mL/min and 750 mL/min flow rates respectively.
- Materials of quartz sleeve, in other words, purity of quartz sleeve largely impacted discoloration of red dye in the VUV based AOP. The observed discoloration rate constant was significantly increased by using the synthetic high purity quartz sleeve due to higher transmission of 185 nm photons into experimental solution by the synthetic quartz. Apparent rate constants were 0.1937 min^{-1} and 1.1106 min^{-1} for clear fused quartz and synthetic high purity quartz respectively. Evidently, rate constant observed in the presence of synthetic high purity quartz sleeve was almost 5.74 times faster than that of clear fused quartz sleeve. Complete reduction of red dye ($C_0 = 10 \text{ mg/L}$) was obtained in less than 5 minutes of VUV irradiation by using synthetic quartz as opposed to 20 minutes of clear fused quartz.

To sum up briefly, this doctoral research showed that VUV based AOP is indeed a very effective treatment method for removal of imidacloprid and reactive textile dyes from water. Reduction of the target pollutants by the VUV process was mainly achieved by highly reactive $\text{HO}\bullet$. Degradation efficiency of the VUV irradiation was significantly boosted by using the synthetic high purity quartz sleeve. Generation of byproducts was observed and should be carefully monitored since complete degradation of imidacloprid was executed within a very short time of VUV irradiation. Lastly, the VUV process was shown to be a promising and environmentally friendly AOP for the treatment of various recalcitrant pollutants from water with no need of addition of chemicals.

7. RECOMMENDATION

- As mentioned in the thesis VUV photons (185 nm) can only penetrate into water with a depth of around 5 to 5.5 mm due to high absorption coefficient of water at 185 nm fluence. Therefore, produced primary radicals especially HO• exist within a very narrow zone at the interface of lamp and water solution and mass transfer limitation becomes an important drawback of the VUV process. The efficacy of VUV process can be improved by the development of better reactor design or better mixing techniques. It is highly recommended to investigate this possibility.
- Annular VUV photoreactor was operated in batch/semibatch mode and the target pollutant was recirculated through the photoreactor during the treatment in this study. Continuous flow reactors are mostly preferred and used in practical water treatments. Investigation of effectiveness of the VUV process with such reactor designs is encouraged.
- Water matrix especially presence of natural organic matter (NOM) among the investigated experimental parameters affected the degradation of imidacloprid the most. Presence of NOM in surface water bodies at varying degrees is unavoidable. Studying impacts of presence of different NOM and associated functional groups on the performance of the VUV photooxidation ought to be the next step before maybe the possible application of VUV process in a pilot plant.

8. REFERENCES

- [1] E. Eljarrat and D. Barceló, "Priority lists for persistent organic pollutants and emerging contaminants based on their relative toxic potency in environmental samples," *TrAC - Trends Anal. Chem.*, vol. 22, no. 10, pp. 655–665, Nov. 2003, doi: 10.1016/S0165-9936(03)01001-X.
- [2] K. Azrague and S. W. Osterhus, "Persistent organic pollutants (POPs) degradation in natural waters using a V-UV/UV/TiO₂ reactor," *Water Sci. Technol. Water Supply*, vol. 9, no. 6, pp. 653–660, 2009, doi: 10.2166/ws.2009.713.
- [3] D. Kibona, G. Kidulile, and F. Rwabukambara, "Environment, climate warming and water management," *Transit. Stud. Rev.*, vol. 16, no. 2, pp. 484–500, 2009, doi: 10.1007/s11300-009-0084-z.
- [4] K. Matsuda, S. D. Buckingham, D. Kleier, J. J. Rauh, M. Grauso, and D. B. Sattelle, "Neonicotinoids: Insecticides acting on insect nicotinic acetylcholine receptors," *Trends in Pharmacological Sciences*, vol. 22, no. 11. Elsevier Current Trends, pp. 573–580, Nov. 01, 2001, doi: 10.1016/S0165-6147(00)01820-4.
- [5] N. S. Millar and I. Denholm, "Nicotinic acetylcholine receptors: Targets for commercially important insecticides," *Invertebr. Neurosci.*, vol. 7, no. 1, pp. 53–66, 2007, doi: 10.1007/s10158-006-0040-0.
- [6] P. Jeschke, R. Nauen, M. Schindler, and A. Elbert, "Overview of the status and global strategy for neonicotinoids," *J. Agric. Food Chem.*, vol. 59, no. 7, pp. 2897–2908, 2011, doi: 10.1021/jf101303g.
- [7] R. Žabar, T. Komel, J. Fabjan, M. B. Kralj, and P. Trebše, "Photocatalytic degradation with immobilised TiO₂ of three selected neonicotinoid insecticides: Imidacloprid, thiamethoxam and clothianidin," *Chemosphere*, vol. 89, no. 3, pp. 293–301, 2012, doi: 10.1016/j.chemosphere.2012.04.039.
- [8] N. Simon-Delso, G. S. Martin, E. Bruneau, L. A. Minsart, C. Mouret, and L. Hautier, "Honeybee colony disorder in crop areas: The role of pesticides and viruses," *PLoS One*, vol. 9, no. 7, pp. 1–16, 2014, doi: 10.1371/journal.pone.0103073.
- [9] S. U. R. Robin and A. Stork, "Uptake, translocation and metabolism of imidacloprid in plants," *Bull. Insectology*, vol. 56, no. 1, pp. 35–40, 2003.
- [10] D. Goulson, "An overview of the environmental risks posed by neonicotinoid insecticides," *J. Appl. Ecol.*, vol. 50, no. 4, pp. 977–987, 2013, doi: 10.1111/1365-2664.12111.
- [11] T. Tišler, A. Jemec, B. Mozetič, and P. Trebše, "Hazard identification of imidacloprid to aquatic environment," *Chemosphere*, vol. 76, no. 7, pp. 907–914, 2009, doi: 10.1016/j.chemosphere.2009.05.002.
- [12] V. Kitsiou, N. Filippidis, D. Mantzavinos, and I. Poullos, "Heterogeneous and homogeneous photocatalytic degradation of the insecticide imidacloprid in aqueous solutions," *Appl. Catal. B Environ.*, vol. 86, no. 1–2, pp. 27–35, 2009, doi: 10.1016/j.apcatb.2008.07.018.
- [13] K. L. Klarich *et al.*, "Occurrence of neonicotinoid insecticides in finished drinking water and fate during drinking water treatment," *Environ. Sci. Technol. Lett.*, vol.

- 4, no. 5, pp. 168–173, 2017, doi: 10.1021/acs.estlett.7b00081.
- [14] V. Christen, F. Mittner, and K. Fent, “Molecular Effects of Neonicotinoids in Honey Bees (*Apis mellifera*),” *Environ. Sci. Technol.*, vol. 50, no. 7, pp. 4071–4081, 2016, doi: 10.1021/acs.est.6b00678.
- [15] J. P. Van der Sluijs, N. Simon-Delso, D. Goulson, L. Maxim, J. M. Bonmatin, and L. P. Belzunces, “Neonicotinoids, bee disorders and the sustainability of pollinator services,” *Curr. Opin. Environ. Sustain.*, vol. 5, no. 3–4, pp. 293–305, 2013, doi: 10.1016/j.cosust.2013.05.007.
- [16] M. Henry *et al.*, “A common pesticide decreases foraging success and survival in honey bees,” *Science (80-.)*, vol. 336, no. 6079, pp. 348–350, 2012, doi: 10.1126/science.1215039.
- [17] O. Malev, R. S. Klobučar, E. Fabbretti, and P. Trebše, “Comparative toxicity of imidacloprid and its transformation product 6-chloronicotinic acid to non-target aquatic organisms: Microalgae *Desmodesmus subspicatus* and amphipod *Gammarus fossarum*,” *Pestic. Biochem. Physiol.*, vol. 104, no. 3, pp. 178–186, 2012, doi: 10.1016/j.pestbp.2012.07.008.
- [18] A. R. Main, J. V. Headley, K. M. Peru, N. L. Michel, A. J. Cessna, and C. A. Morrissey, “Widespread use and frequent detection of neonicotinoid insecticides in wetlands of Canada’s prairie pothole region,” *PLoS One*, vol. 9, no. 3, 2014, doi: 10.1371/journal.pone.0092821.
- [19] A. R. Main, N. L. Michel, J. V. Headley, K. M. Peru, and C. A. Morrissey, “Ecological and Landscape Drivers of Neonicotinoid Insecticide Detections and Concentrations in Canada’s Prairie Wetlands,” *Environ. Sci. Technol.*, vol. 49, no. 14, pp. 8367–8376, 2015, doi: 10.1021/acs.est.5b01287.
- [20] M. L. Hladik, D. W. Kolpin, and K. M. Kuivila, “Widespread occurrence of neonicotinoid insecticides in streams in a high corn and soybean producing region, USA,” *Environ. Pollut.*, vol. 193, pp. 189–196, 2014, doi: 10.1016/j.envpol.2014.06.033.
- [21] M. L. Hladik and D. W. Kolpin, “First national-scale reconnaissance of neonicotinoid insecticides in streams across the USA,” *Environ. Chem.*, vol. 13, no. 1, pp. 12–20, 2016, doi: 10.1071/EN15061.
- [22] A. M. Sadaria, S. D. Supowit, and R. U. Halden, “Mass Balance Assessment for Six Neonicotinoid Insecticides during Conventional Wastewater and Wetland Treatment: Nationwide Reconnaissance in United States Wastewater,” *Environ. Sci. Technol.*, vol. 50, no. 12, pp. 6199–6206, 2016, doi: 10.1021/acs.est.6b01032.
- [23] C. R. Holkar, A. J. Jadhav, D. V. Pinjari, N. M. Mahamuni, and A. B. Pandit, “A critical review on textile wastewater treatments: Possible approaches,” *J. Environ. Manage.*, vol. 182, pp. 351–366, 2016, doi: 10.1016/j.jenvman.2016.07.090.
- [24] M. Muruganandham and M. Swaminathan, “Photochemical oxidation of reactive azo dye with UV-H₂O₂ process,” *Dye. Pigment.*, vol. 62, no. 3, pp. 269–275, 2004, doi: 10.1016/j.dyepig.2003.12.006.
- [25] N. N. De Brito-Pelegrini, P. De Tarso Ferreira Sales, and R. T. Pelegrini, “Photochemical treatment of industrial textile effluent containing reactivities dyes,” *Environ. Technol.*, vol. 28, no. 3, pp. 321–328, 2007, doi: 10.1080/09593332808618794.

- [26] M. R. Hoffmann, S. T. Martin, W. Choi, and D. W. Bahnemann, "Environmental Applications of Semiconductor Photocatalysis," *Chem. Rev.*, vol. 95, no. 1, pp. 69–96, 1995, doi: 10.1021/cr00033a004.
- [27] M. G. Gonzalez, E. Oliveros, M. Wörner, and A. M. Braun, "Vacuum-ultraviolet photolysis of aqueous reaction systems," *J. Photochem. Photobiol. C Photochem. Rev.*, vol. 5, no. 3, pp. 225–246, 2004, doi: 10.1016/j.jphotochemrev.2004.10.002.
- [28] M. Wang, R. Yang, W. Wang, Z. Shen, S. Bian, and Z. Zhu, "Radiation-induced decomposition and decoloration of reactive dyes in the presence of H₂O₂," *Radiat. Phys. Chem.*, vol. 75, no. 2, pp. 286–291, 2006, doi: 10.1016/j.radphyschem.2005.08.012.
- [29] Jeschke, P. and Nauen, R., "Neonicotinoids-from zero to hero in insecticide chemistry," *Pest Manag. Sci.*, vol. 64, pp. 1084–1098, 2008.
- [30] F. Sánchez-Bayo and R. V. Hyne, "Detection and analysis of neonicotinoids in river waters - Development of a passive sampler for three commonly used insecticides," *Chemosphere*, vol. 99, pp. 143–151, 2014, doi: 10.1016/j.chemosphere.2013.10.051.
- [31] M. Tomizawa and J. E. Casida, "Neonicotinoid insecticide toxicology: Mechanisms of selective action," *Annu. Rev. Pharmacol. Toxicol.*, vol. 45, pp. 247–268, 2005, doi: 10.1146/annurev.pharmtox.45.120403.095930.
- [32] M. A. Sarkar, P. K. Biswas, S. Roy, R. K. Kole, and A. Chowdhury, "Effect of pH and type of formulation on the persistence of imidacloprid in water," *Bull. Environ. Contam. Toxicol.*, vol. 63, no. 5, pp. 604–609, 1999, doi: 10.1007/s001289901023.
- [33] P. Physical and O. R. Active, "Federal Biological Research Centre for Agriculture IDENTITY ISO Common name : Chemical name : IUPAC : CA : CAS number : CIPAC number : Synonym : Structural formula : imidacloprid Molecular formula : Molecular mass," no. 206, pp. 687–1007, 2000.
- [34] "Imidacloprid Technical Fact Sheet." <http://npic.orst.edu/factsheets/archive/imidacloprid.html> (accessed Jan. 24, 2021).
- [35] S. Gupta, V. T. Gajbhiye, Kalpana, and N. P. Agnihotri, "Leaching behavior of imidacloprid formulations in soil," *Bull. Environ. Contam. Toxicol.*, vol. 68, no. 4, pp. 502–508, 2002, doi: 10.1007/s001280283.
- [36] D. Q. Thuyet, B. C. Jorgenson, C. Wissel-Tyson, H. Watanabe, and T. M. Young, "Wash off of imidacloprid and fipronil from turf and concrete surfaces using simulated rainfall," *Sci. Total Environ.*, vol. 414, pp. 515–524, 2012, doi: 10.1016/j.scitotenv.2011.10.051.
- [37] R. F. Mizell and M. C. Sconyers, "Florida Entomological Society Toxicity of Imidacloprid to Selected Arthropod Predators in the Laboratory TOXICITY OF IMIDACLOPRID TO SELECTED ARTHROPOD," vol. 75, no. 2, pp. 277–280, 2015.
- [38] S. F. Smith and V. A. Krischik, "Effects of systemic imidacloprid on *Coleomegilla maculata* (Coleoptera: Coccinellidae)," *Environ. Entomol.*, vol. 28, no. 6, pp. 1189–1195, 1999, doi: 10.1093/ee/28.6.1189.
- [39] C. Zaror, C. Segura, H. Mansilla, M. A. Mondaca, and P. González, "Effect of temperature on Imidacloprid oxidation by homogeneous photo-Fenton processes," *Water Sci. Technol.*, vol. 58, no. 1, pp. 259–265, 2008, doi: 10.2166/wst.2008.661.

- [40] W. Liu, W. Zheng, Y. Ma, and K. Liu, "Sorption and degradation of imidacloprid in soil and water," *J. Environ. Sci. Heal. - Part B Pestic. Food Contam. Agric. Wastes*, vol. 41, no. 5, pp. 623–634, 2006, doi: 10.1080/03601230600701775.
- [41] L. Cox, W. C. Koskinen, and P. Y. Yen, "Sorption-Desorption of Imidacloprid and Its Metabolites in Soils," *J. Agric. Food Chem.*, vol. 45, no. 4, pp. 1468–1472, 1997, doi: 10.1021/jf960514a.
- [42] F. Flores-Céspedes, E. González-Pradas, M. Fernández-Pérez, M. Villafranca-Sánchez, M. Socías-Viciana, and M. D. Ureña-Amate, "Effects of Dissolved Organic Carbon on Sorption and Mobility of Imidacloprid in Soil," *J. Environ. Qual.*, vol. 31, no. 3, pp. 880–888, 2002, doi: 10.2134/jeq2002.8800.
- [43] W. Zheng and W. Liu, "Kinetics and mechanism of the hydrolysis of imidacloprid," *Pestic. Sci.*, vol. 55, no. 4, pp. 482–485, 1999, doi: 10.1002/(SICI)1096-9063(199904)55:4<482::AID-PS932>3.0.CO;2-3.
- [44] C. A. Morrissey *et al.*, "Neonicotinoid contamination of global surface waters and associated risk to aquatic invertebrates: A review," *Environ. Int.*, vol. 74, pp. 291–303, 2015, doi: 10.1016/j.envint.2014.10.024.
- [45] D. Goulson, "Ecology: Pesticides linked to bird declines," *Nature*, vol. 511, no. 7509, pp. 295–296, 2014, doi: 10.1038/nature13642.
- [46] C. A. Hallmann, R. P. B. Foppen, C. A. M. Van Turnhout, H. De Kroon, and E. Jongejans, "Declines in insectivorous birds are associated with high neonicotinoid concentrations," *Nature*, vol. 511, no. 7509, pp. 341–343, 2014, doi: 10.1038/nature13531.
- [47] J. M. Bonmatin *et al.*, "Environmental fate and exposure; neonicotinoids and fipronil," *Environ. Sci. Pollut. Res.*, vol. 22, no. 1, pp. 35–67, 2015, doi: 10.1007/s11356-014-3332-7.
- [48] T. C. Van Dijk, M. A. Van Staalduinen, and J. P. Van der Sluijs, "Macro-Invertebrate Decline in Surface Water Polluted with Imidacloprid," *PLoS One*, vol. 8, no. 5, 2013, doi: 10.1371/journal.pone.0062374.
- [49] J. Kreuger, S. Graaf, J. Patring, and S. Adielsson, "Pesticides in surface water in areas with open ground and greenhouse horticultural crops in Sweden 2008," *Swedish Univ. Agric. Sci.*, p. 49, 2010.
- [50] M. Lamers, M. Anyusheva, N. La, V. V. Nguyen, and T. Streck, "Pesticide Pollution in Surface- and Groundwater by Paddy Rice Cultivation: A Case Study from Northern Vietnam," *Clean - Soil, Air, Water*, vol. 39, no. 4, pp. 356–361, 2011, doi: 10.1002/clen.201000268.
- [51] A. Masiá, J. Campo, P. Vázquez-Roig, C. Blasco, and Y. Picó, "Screening of currently used pesticides in water, sediments and biota of the Guadalquivir River Basin (Spain)," *J. Hazard. Mater.*, vol. 263, pp. 95–104, 2013, doi: 10.1016/j.jhazmat.2013.09.035.
- [52] M. B. Forrester, "Neonicotinoid insecticide exposures reported to six poison centers in Texas," *Hum. Exp. Toxicol.*, vol. 33, no. 6, pp. 568–573, 2014, doi: 10.1177/0960327114522500.
- [53] Moza, P.N., Hustert, K., Feicht, E., Kettrup, A., "Photolysis of imidacloprid in aqueous solution" *Chemosphere* vol. 36, no. 3, pp. 497-502, 1998.

- [54] H. Wamhoff and V. Schneider, "Photodegradation of imidacloprid," *J. Agric. Food Chem.*, vol. 47, no. 4, pp. 1730–1734, 1999, doi: 10.1021/jf980820j.
- [55] N. Schippers and W. Schwack, "Photochemistry of imidacloprid in model systems," *J. Agric. Food Chem.*, vol. 56, no. 17, pp. 8023–8029, 2008, doi: 10.1021/jf801251u.
- [56] "Zheng W. et al 2004 Photochemistry of insecticide imidacloprid direct and sensitized photolysis in aqueous medium.pdf" .
- [57] B. K. Lavine, T. Ding, and D. Jacobs, "LC-PDA-MS studies of the photochemical degradation of imidacloprid," *Anal. Lett.*, vol. 43, no. 10–11, pp. 1812–1821, 2010, doi: 10.1080/00032711003654013.
- [58] H. Wamhoff and V. Schneider, "Photodegradation of imidacloprid," *J. Agric. Food Chem.*, vol. 47, no. 4, pp. 1730–1734, 1999, doi: 10.1021/jf980820j.
- [59] E. Oliveros *et al.*, "Reactivity of hydroxyl radicals with neonicotinoid insecticides : mechanism and changes in toxicity," no. Iii, 2009, doi: 10.1039/b900960d.
- [60] A. Agüera, E. Almansa, S. Malato, M. I. Maldonado, and A. R. Fernández-Alba, "Evaluation of photocatalytic degradation of Imidacloprid in industrial water by GC-MS and LC-MS," *Analisis*, vol. 26, no. 7, pp. 245–251, 1998, doi: 10.1051/analisis:1998168.
- [61] S. Malato *et al.*, "Degradation of imidacloprid in water by photo-fenton and TiO₂ photocatalysis at a solar pilot plant: A comparative study," *Environ. Sci. Technol.*, vol. 35, no. 21, pp. 4359–4366, 2001, doi: 10.1021/es000289k.
- [62] N. Philippidis, S. Sotiropoulos, A. Efstathiou, and I. Poulios, "Photoelectrocatalytic degradation of the insecticide imidacloprid using TiO₂/Ti electrodes," *J. Photochem. Photobiol. A Chem.*, vol. 204, no. 2–3, pp. 129–136, 2009, doi: 10.1016/j.jphotochem.2009.03.007.
- [63] J. Fenoll, I. Garrido, P. Hellín, P. Flores, and S. Navarro, "Photodegradation of neonicotinoid insecticides in water by semiconductor oxides," *Environ. Sci. Pollut. Res.*, vol. 22, no. 19, pp. 15055–15066, 2015, doi: 10.1007/s11356-015-4721-2.
- [64] A. Akbari Shorgoli and M. Shokri, "Photocatalytic degradation of imidacloprid pesticide in aqueous solution by TiO₂ nanoparticles immobilized on the glass plate," *Chem. Eng. Commun.*, vol. 204, no. 9, pp. 1061–1069, 2017, doi: 10.1080/00986445.2017.1337005.
- [65] M. Bourgin, F. Violleau, L. Debrauwer, and J. Albet, "Ozonation of imidacloprid in aqueous solutions: Reaction monitoring and identification of degradation products," *J. Hazard. Mater.*, vol. 190, no. 1–3, pp. 60–68, 2011, doi: 10.1016/j.jhazmat.2011.02.065.
- [66] S. Raut-Jadhav, V. K. Saharan, D. V. Pinjari, D. R. Saini, S. H. Sonawane, and A. B. Pandit, "Intensification of degradation of imidacloprid in aqueous solutions by combination of hydrodynamic cavitation with various advanced oxidation processes (AOPs)," *J. Environ. Chem. Eng.*, vol. 1, no. 4, pp. 850–857, 2013, doi: 10.1016/j.jece.2013.07.029.
- [67] O. Iglesias, J. Gómez, M. Pazos, and M. Á. Sanromán, "Electro-Fenton oxidation of imidacloprid by Fe alginate gel beads," *Appl. Catal. B Environ.*, vol. 144, pp. 416–424, 2014, doi: 10.1016/j.apcatb.2013.07.046.

- [68] A. L. Patil, P. N. Patil, and P. R. Gogate, "Degradation of imidacloprid containing wastewaters using ultrasound based treatment strategies," *Ultrason. Sonochem.*, vol. 21, no. 5, pp. 1778–1786, 2014, doi: 10.1016/j.ultsonch.2014.02.029.
- [69] W. Han, P. Zhang, W. Zhu, J. Yin, and L. Li, "Photocatalysis of p-chlorobenzoic acid in aqueous solution under irradiation of 254 nm and 185 nm UV light," *Water Res.*, vol. 38, no. 19, pp. 4197–4203, 2004, doi: 10.1016/j.watres.2004.07.019.
- [70] Oppenländer, T. (Ed.), "Photochemical Purification of Water and Air," Wiley-VCH, 2003.
- [71] Getoff N. and Schenck G.O. "Primary products of liquid water photolysis at 1236, 1470 and 1849 Å," *Photochemistry and Photobiology*, vol. 8, pp. 167–178, 1968.
- [72] O. Legrini, E. Oliveros, and A. M. Braun, "Photochemical Processes for Water Treatment," *Chem. Rev.*, vol. 93, no. 2, pp. 671–698, 1993, doi: 10.1021/cr00018a003.
- [73] N. Getoff, "Purification of drinking water by irradiation. A review," *J. Chem. Sci.*, vol. 105, no. 6, pp. 373–391, 1993, doi: 10.1007/BF03040811.
- [74] G. V. Buxton, C. L. Greenstock, W. P. Helman, and A. B. Ross, "Critical Review of rate constants for reactions of hydrated electrons, hydrogen atoms and hydroxyl radicals ($\cdot\text{OH}/\cdot\text{O}^-$ in Aqueous Solution)," *J. Phys. Chem. Ref. Data*, vol. 17, no. 2, pp. 513–886, 1988, doi: 10.1063/1.555805.
- [75] M. A. Malik, A. Ghaffar, and S. A. Malik, "Water purification by electrical discharges," *Plasma Sources Sci. Technol.*, vol. 10, no. 1, pp. 82–91, 2001, doi: 10.1088/0963-0252/10/1/311.
- [76] F. Al-Momani, E. Touraud, J. R. Degorce-Dumas, J. Roussy, and O. Thomas, "Biodegradability enhancement of textile dyes and textile wastewater by VUV photolysis," *J. Photochem. Photobiol. A Chem.*, vol. 153, no. 1–3, pp. 191–197, 2002, doi: 10.1016/S1010-6030(02)00298-8.
- [77] K. Kutschera, H. Börnick, and E. Worch, "Photoinitiated oxidation of geosmin and 2-methylisoborneol by irradiation with 254 nm and 185 nm UV light," *Water Res.*, vol. 43, no. 8, pp. 2224–2232, 2009, doi: 10.1016/j.watres.2009.02.015.
- [78] L. Furatian and M. Mohseni, "Inuence of major anions on the 185 nm advanced oxidation process - Sulphate, bicarbonate, and chloride," *Chemosphere*, vol. 201, pp. 503–510, 2018, doi: 10.1016/j.chemosphere.2018.02.160.
- [79] F. Visentin, S. Bhartia, M. Mohseni, S. Dorner, and B. Barbeau, "Performance of vacuum UV (VUV) for the degradation of MC-LR, geosmin, and MIB from cyanobacteria-impacted waters," *Environ. Sci. Water Res. Technol.*, vol. 5, no. 11, pp. 2048–2058, 2019, doi: 10.1039/c9ew00538b.
- [80] Weeks, J.L., Meaburn, G.M.A.C., Gordon, S., "Absorption Coefficients of Liquid Water and Aqueous Solutions in the Far Ultraviolet," *Radiation Research*, vol. 19, no. 3, pp. 559–567, 1963.
- [81] A. S. Mora, "UV / Vacuum-UV Advanced Oxidation Process For The Treatment Of Micropollutants From Drinking Water Sources Under Common Operational Temperature," *Ubc*, no. April, 2016.
- [82] C. Duca, "Effect of water matrix on Vacuum UV process for the removal of organic micropollutants in surface water," no. February, p. 64, 2015.

- [83] L. Yang, M. Li, W. Li, Y. Jiang, and Z. Qiang, "Bench- and pilot-scale studies on the removal of pesticides from water by VUV/UV process," *Chem. Eng. J.*, vol. 342, no. February, pp. 155–162, 2018, doi: 10.1016/j.cej.2018.02.075.
- [84] G. Heit, A. Neuner, P. Y. Saugy, and A. M. Braun, "Vacuum-UV (172 nm) actinometry. The quantum yield of the photolysis of water," *J. Phys. Chem. A*, vol. 102, no. 28, pp. 5551–5561, 1998, doi: 10.1021/jp980130i.
- [85] Oppenländer, T. and Schwarzwälder, R., "Vacuum-UV oxidation (H₂O-VUV) with a xenon excimer flow-through lamp at 172 nm: use of methanol as actinometer for VUV intensity measurement and as reference compound for OH radical competition kinetics in aqueous systems", *J. Adv. Oxid. Technol.* vol. 5, no. 2, pp. 155–163, 2002.
- [86] M. Li, Z. Qiang, C. Pulgarin, and J. Kiwi, "Accelerated methylene blue (MB) degradation by Fenton reagent exposed to UV or VUV/UV light in an innovative micro photo-reactor," *Appl. Catal. B Environ.*, vol. 187, pp. 83–89, 2016, doi: 10.1016/j.apcatb.2016.01.014.
- [87] K. Zoschke, H. Börnick, and E. Worch, "Vacuum-UV radiation at 185nm in water treatment - A review," *Water Res.*, vol. 52, pp. 131–145, 2014, doi: 10.1016/j.watres.2013.12.034.
- [88] V. Guzsvány, J. Csanádi, and F. Gaál, "NMR study of the influence of pH on the persistence of some neonicotinoids in water," *Acta Chim. Slov.*, vol. 53, no. 1, pp. 52–57, 2006.
- [89] V. J. Guzsvány, F. F. Gaál, L. J. Bjelica, and S. N. Ökrész, "Voltammetric determination of imidacloprid and thiamethoxam," *J. Serbian Chem. Soc.*, vol. 70, no. 5, pp. 735–743, 2005, doi: 10.2298/JSC0505735G.
- [90] I. Engan, "The Effect of pH, Dissolved Metals and Suspended Minerals on the Hydrolysis of Neonicotinoids," *Int. Ser. Oper. Res. Manag. Sci.*, vol. 184, no. July, pp. 421–445, 2013.
- [91] M. L. Dell'Arciprete *et al.*, "Reactivity of hydroxyl radicals with neonicotinoid insecticides: Mechanism and changes in toxicity," *Photochem. Photobiol. Sci.*, vol. 8, no. 7, pp. 1016–1023, 2009, doi: 10.1039/b900960d.
- [92] W. H. Koppenol and J. F. Liebman, "The oxidizing nature of the hydroxyl radical. A comparison with the ferryl ion (FeO₂⁺)," *J. Phys. Chem.*, vol. 88, no. 1, pp. 99–101, 1984, doi: 10.1021/j150645a024.
- [93] G. Moussavi, M. Rezaei, and M. Pourakbar, "Comparing VUV and VUV/Fe²⁺ processes for decomposition of cloxacillin antibiotic: Degradation rate and pathways, mineralization and by-product analysis," *Chem. Eng. J.*, vol. 332, no. June 2017, pp. 140–149, 2018, doi: 10.1016/j.cej.2017.09.057.
- [94] L. Chen, T. Cai, C. Cheng, Z. Xiong, and D. Ding, "Degradation of acetamiprid in UV/H₂O₂ and UV/persulfate systems: A comparative study," *Chem. Eng. J.*, vol. 351, no. March, pp. 1137–1146, 2018, doi: 10.1016/j.cej.2018.06.107.
- [95] S. M. Kim and A. Vogelpohl, "Degradation of Organic Pollutants by the Photo-Fenton-Process," *Chem. Eng. Technol.*, vol. 21, no. 2, pp. 187–191, 1998, doi: 10.1002/(SICI)1521-4125(199802)21:2<187::AID-CEAT187>3.0.CO;2-H.
- [96] E. Arany *et al.*, "Degradation of naproxen by UV, VUV photolysis and their combination," *J. Hazard. Mater.*, vol. 262, pp. 151–157, 2013, doi:

- 10.1016/j.jhazmat.2013.08.003.
- [97] E. Arany, “PhD Thesis The role of reactive oxygen species in the vacuum ultraviolet photolysis of four nonsteroidal anti-inflammatory drugs Eszter Arany Doctoral School of Environmental Sciences Thesis supervisors : Dr . Tünde Alapi , professor ’ s assistant Dr . K,” 2014.
- [98] G. Moussavi, M. Pourakbar, E. Aghayani, and M. Mahdavianpour, “Investigating the aerated VUV/PS process simultaneously generating hydroxyl and sulfate radicals for the oxidation of cyanide in aqueous solution and industrial wastewater,” *Chem. Eng. J.*, vol. 350, no. February, pp. 673–680, 2018, doi: 10.1016/j.cej.2018.05.178.
- [99] P. Xie *et al.*, “Degradation of organic pollutants by Vacuum-Ultraviolet (VUV): Kinetic model and efficiency,” *Water Res.*, vol. 133, pp. 69–78, 2018, doi: 10.1016/j.watres.2018.01.019.
- [100] G. Rózsa *et al.*, “Photocatalytic, photolytic and radiolytic elimination of imidacloprid from aqueous solution: Reaction mechanism, efficiency and economic considerations,” *Appl. Catal. B Environ.*, vol. 250, no. September 2018, pp. 429–439, 2019, doi: 10.1016/j.apcatb.2019.01.065.
- [101] J. L. Weeks and J. Rabani, “The pulse radiolysis of deaerated aqueous carbonate solutions. I. Transient optical spectrum and mechanism. II. pK for OH radicals,” *J. Phys. Chem.*, vol. 70, no. 7, pp. 2100–2106, 1966, doi: 10.1021/j100879a005.
- [102] W. H. Glaze, Y. Lay, and J. W. Kang, “Advanced Oxidation Processes. A Kinetic Model for the Oxidation of 1,2-Dibromo-3-chloropropane in Water by the Combination of Hydrogen Peroxide and UV Radiation,” *Ind. Eng. Chem. Res.*, vol. 34, no. 7, pp. 2314–2323, 1995, doi: 10.1021/ie00046a013.
- [103] G. McKay, M. M. Dong, J. L. Kleinman, S. P. Mezyk, and F. L. Rosario-Ortiz, “Temperature dependence of the reaction between the hydroxyl radical and organic matter,” *Environ. Sci. Technol.*, vol. 45, no. 16, pp. 6932–6937, 2011, doi: 10.1021/es201363j.
- [104] B. H. J. Bielski, D. E. Cabelli, R. L. Arudi, and A. B. Ross, “Reactivity of HO₂/O₂ Radicals in Aqueous Solution,” *J. Phys. Chem. Ref. Data*, vol. 14, no. 4, pp. 1041–1100, 1985, doi: 10.1063/1.555739.
- [105] C. Blasco, M. Fernández, Y. Picó, G. Font, and J. Mañes, “Simultaneous determination of imidacloprid, carbendazim, methiocarb and hexythiazox in peaches and nectarines by liquid chromatography-mass spectrometry,” *Anal. Chim. Acta*, vol. 461, no. 1, pp. 109–116, 2002, doi: 10.1016/S0003-2670(02)00255-6.
- [106] N. Schippers and W. Schwack, “Photochemistry of imidacloprid in model systems,” *J. Agric. Food Chem.*, vol. 56, no. 17, pp. 8023–8029, 2008, doi: 10.1021/jf801251u.
- [107] N. Schippers and W. Schwack, “Phototransformation of imidacloprid on isolated tomato fruit cuticles and on tomato fruits,” *J. Photochem. Photobiol. B Biol.*, vol. 98, no. 1, pp. 57–60, 2010, doi: 10.1016/j.jphotobiol.2009.11.004.
- [108] D. Redlich, N. Shahin, P. Ekici, A. Friess, and H. Parlar, “Kinetic study of the photoinduced degradation of imidacloprid in aquatic media,” *Clean - Soil, Air, Water*, vol. 35, no. 5, pp. 452–458, 2007, doi: 10.1002/clen.200720014.

APPENDICES

APPENDIX 1

APPENDIX 1.1. Supplementary Data for Screening of pH Adjusters for Acidic and Alkaline Conditions

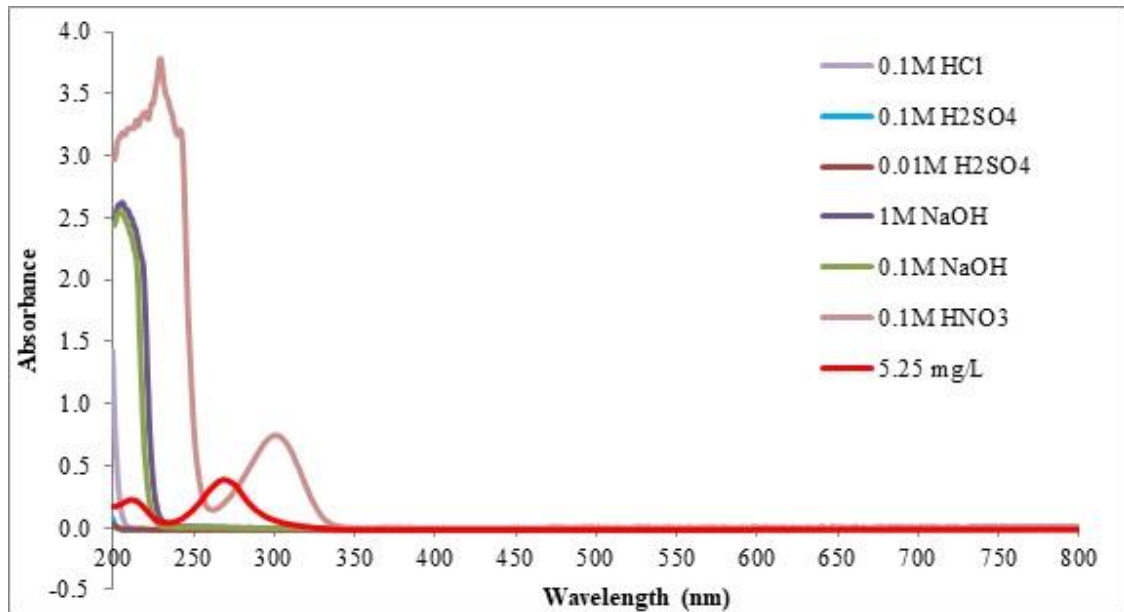


Figure A.1.1 UV-Vis Absorbance Spectrum of H₂SO₄, HCl, HNO₃, NaOH and Confidor Imidacloprid (C₀ = 5.25 mg/L).

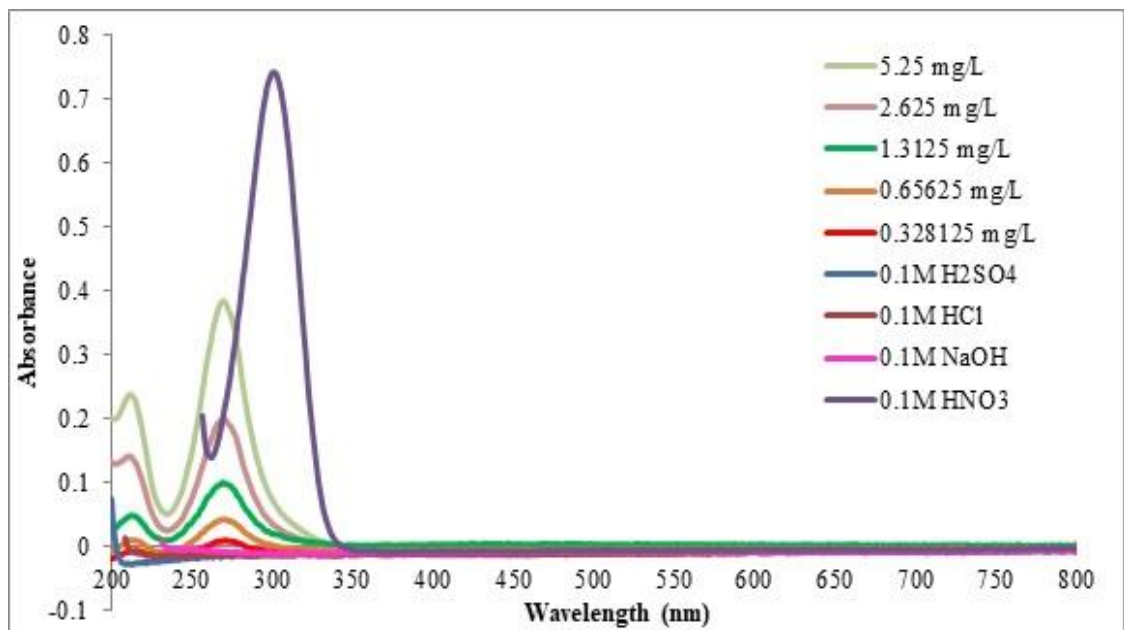


Figure A.1.2 UV-Vis Absorbance Spectrum of various Confidor Imidacloprid concentration along with H₂SO₄, HCl, HNO₃ and NaOH.

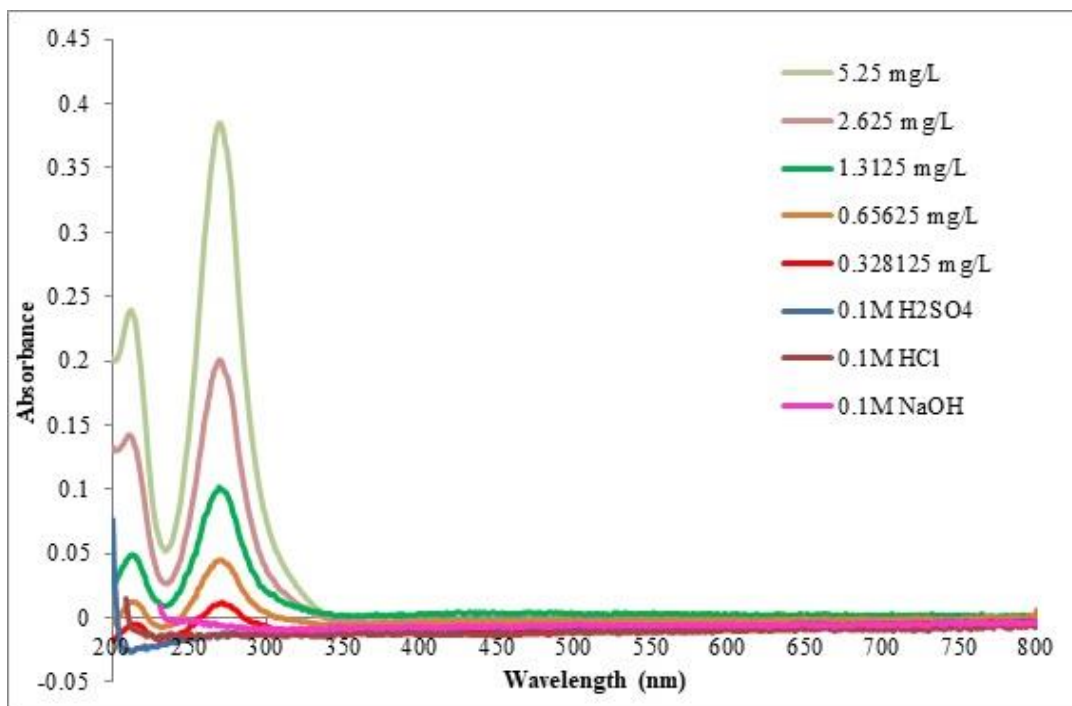


Figure A.1.3 UV-Vis Absorbance Spectrum of various Confidor Imidacloprid concentration along with H₂SO₄, HCl, and NaOH.

APPENDIX 1.2. Supplementary Data for UV-Vis Analysis

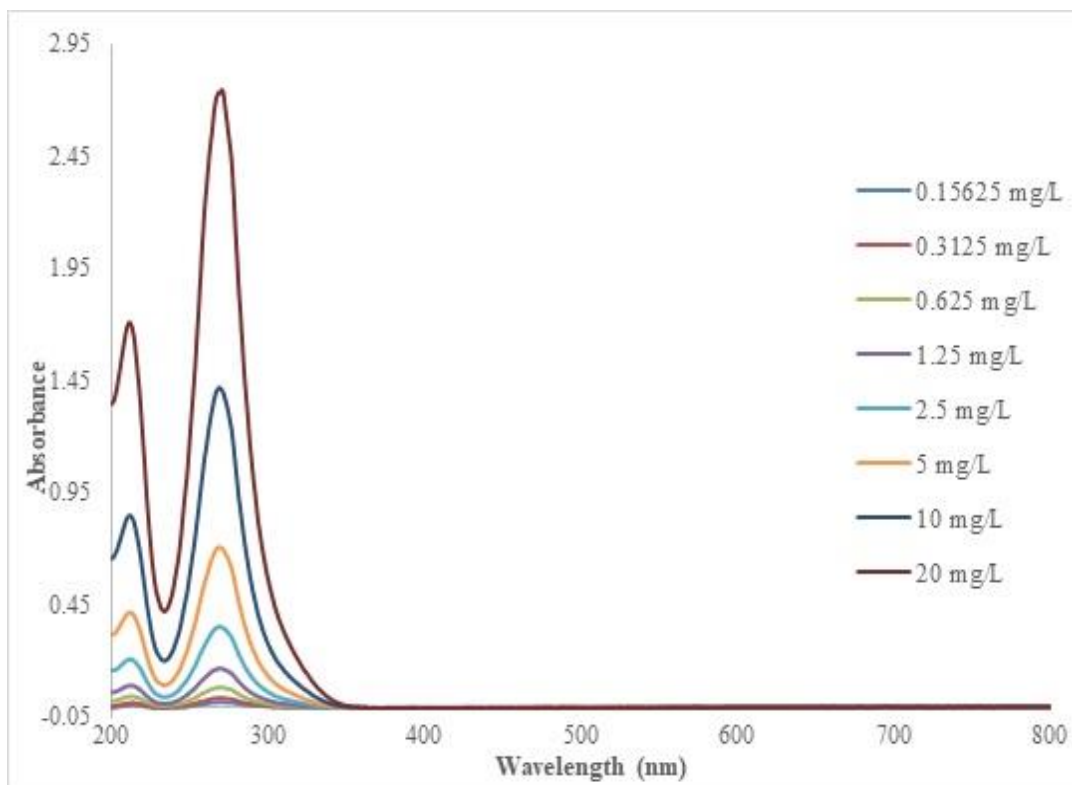


Figure A.1.4 Absorbance Spectrum of Standard Imidacloprid.

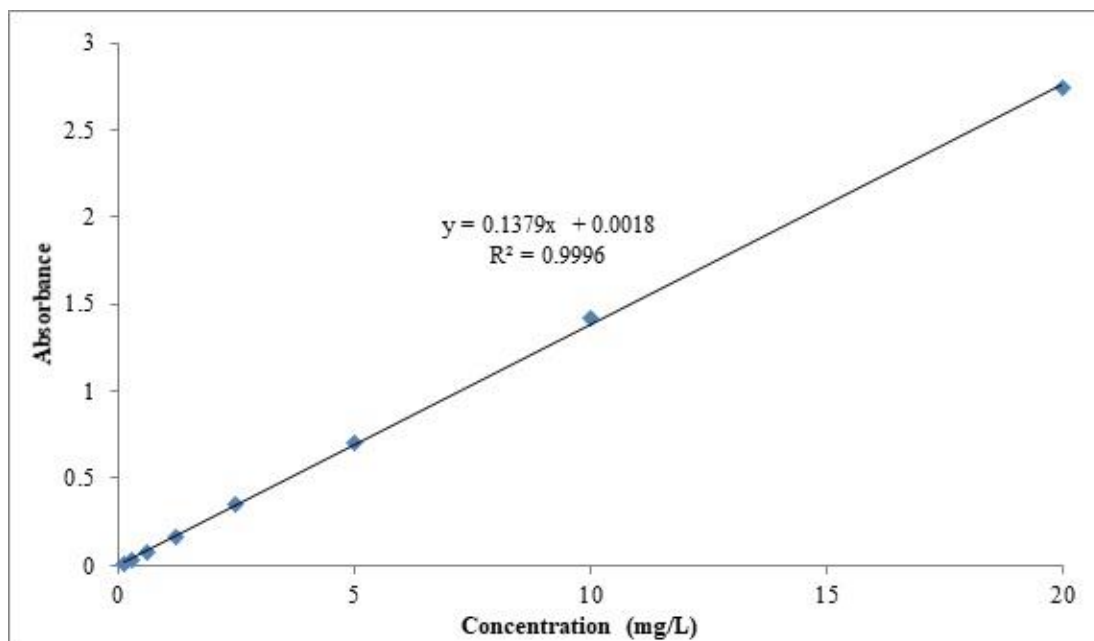


Figure A.1.5 UV-Vis Calibration Curve and Correlation Coefficient (R^2) of Standard Imidacloprid at 270 nm wavelength.

APPENDIX 1.3. Supplementary Data for LC/MS Q-TOF Analysis

Optimized separation and detection conditions of imidacloprid samples with LC/MS Q-TOF was presented below.

Table A.1.1 Separation Condition of Analytical Column.

Parameter	Value
Eluents	30% ACN + 70% H ₂ O with 0.1% FA
Injection Volume	20 μ L
Column Flow rate	0.5 mL/min
Column Temperature	40 $^{\circ}$ C

Table A.1.2 Operational Condition of Q-TOF MS.

Parameter	Value
Gas Temperature	300 °C
Drying Gas Flow	8 L/min
Nebulizer	40 psi
Sheath Gas Temperature	350 °C
Sheath Gas Flow	11 L/min
Capillary Voltage	3500 V

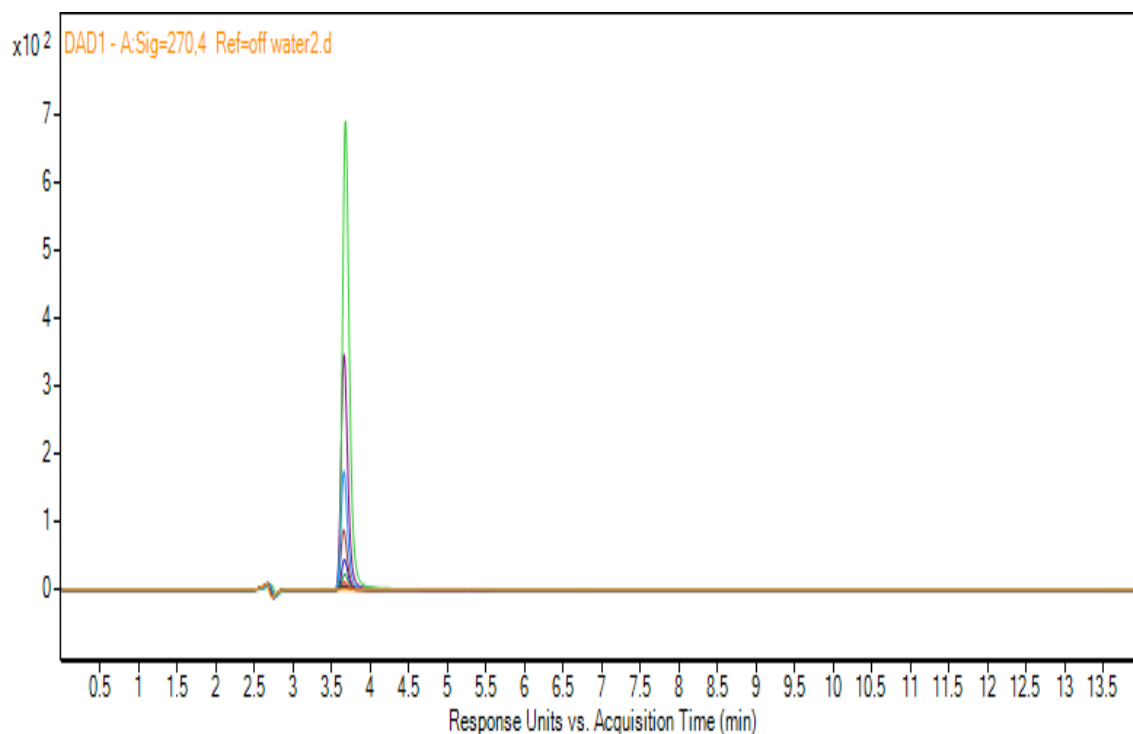


Figure A.1.6 LC/MS Q-TOF Calibration Chromatogram of Standard Imidacloprid using DAD at 270 nm wavelength.

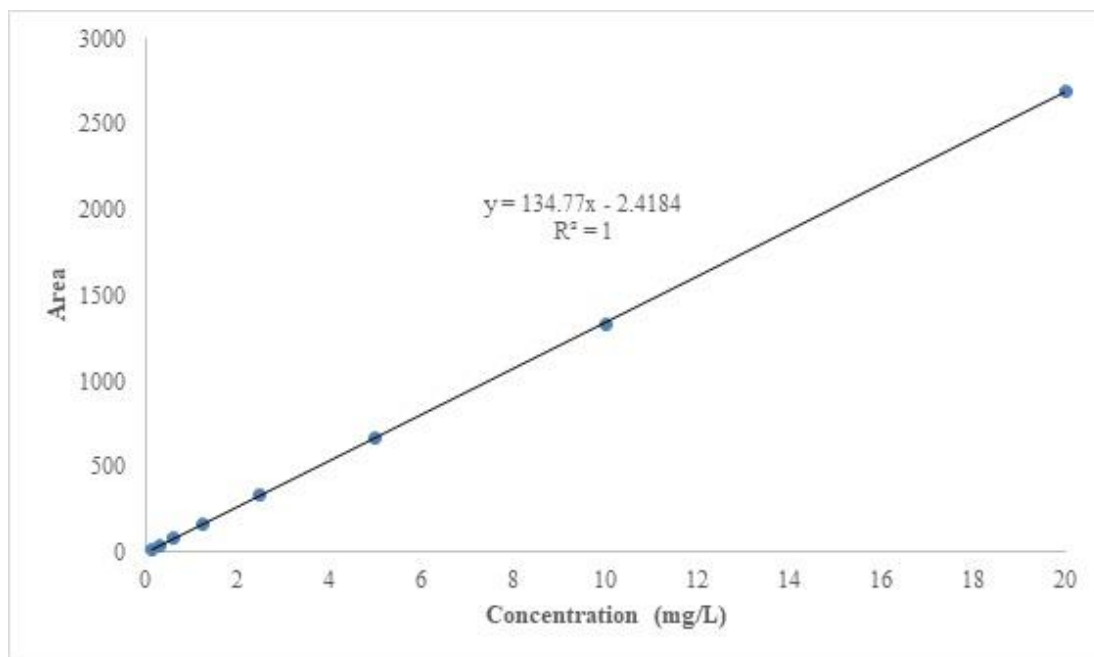


Figure A.1.7 LC/MS Q-TOF Calibration Curve and Correlation Coefficient (R^2) of Standard Imidacloprid.

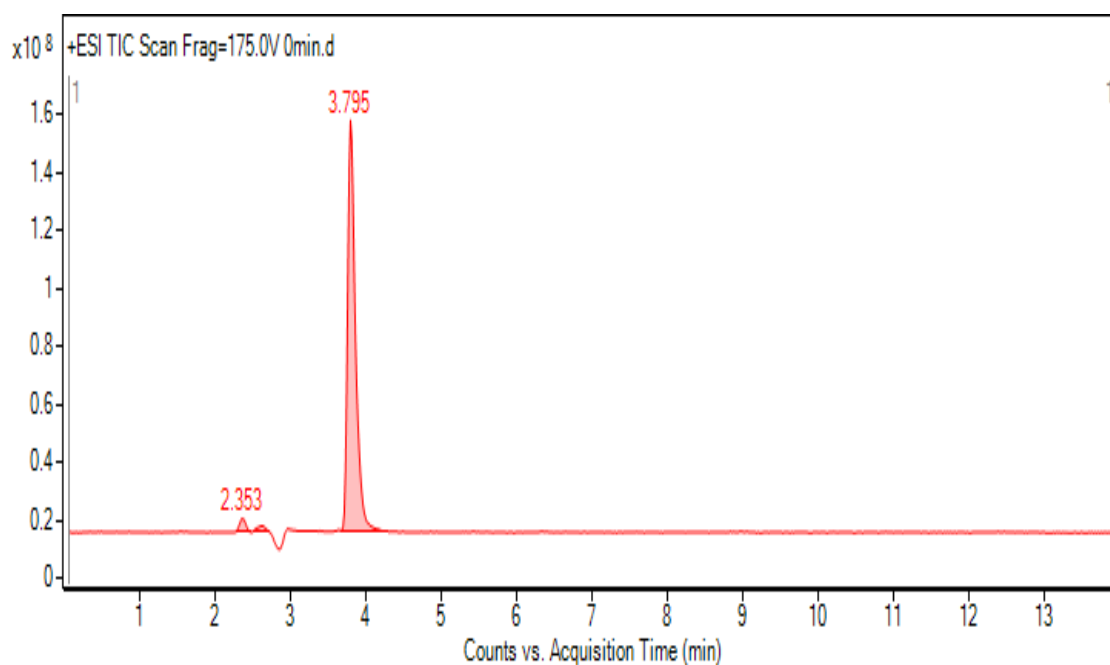


Figure A.1.8 LC/MS Q-TOF Chromatogram of 5 mg/L Imidacloprid Standard at 0 (zero) minute of irradiation time.

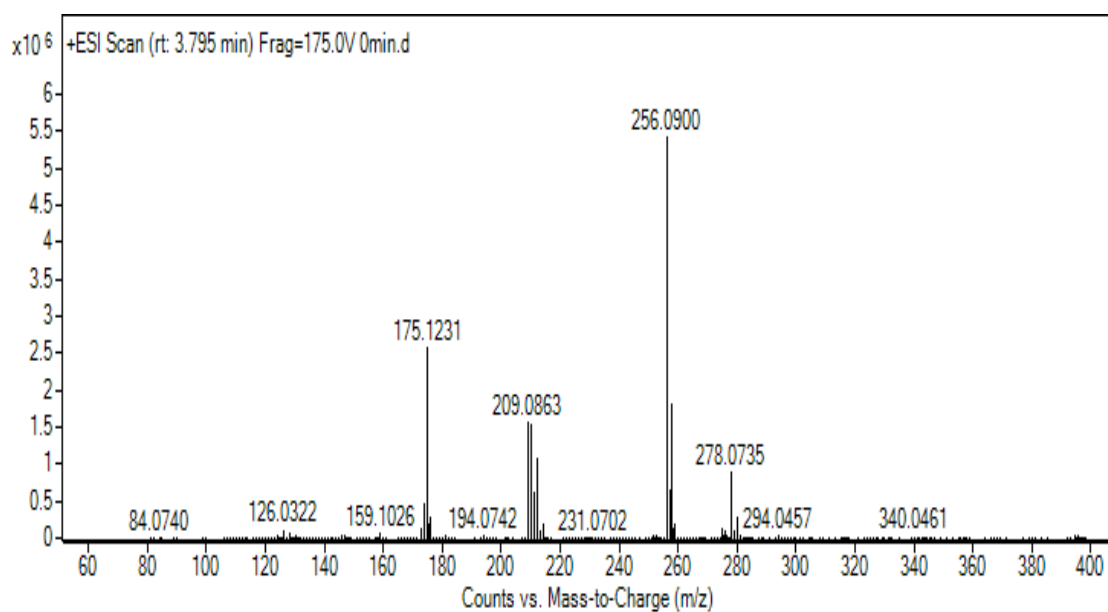


Figure A.1.9 LC/MS Q-TOF mass spectrum of Imidacloprid Standard

APPENDIX 1.4. Supplementary Data for GC/MS Analysis

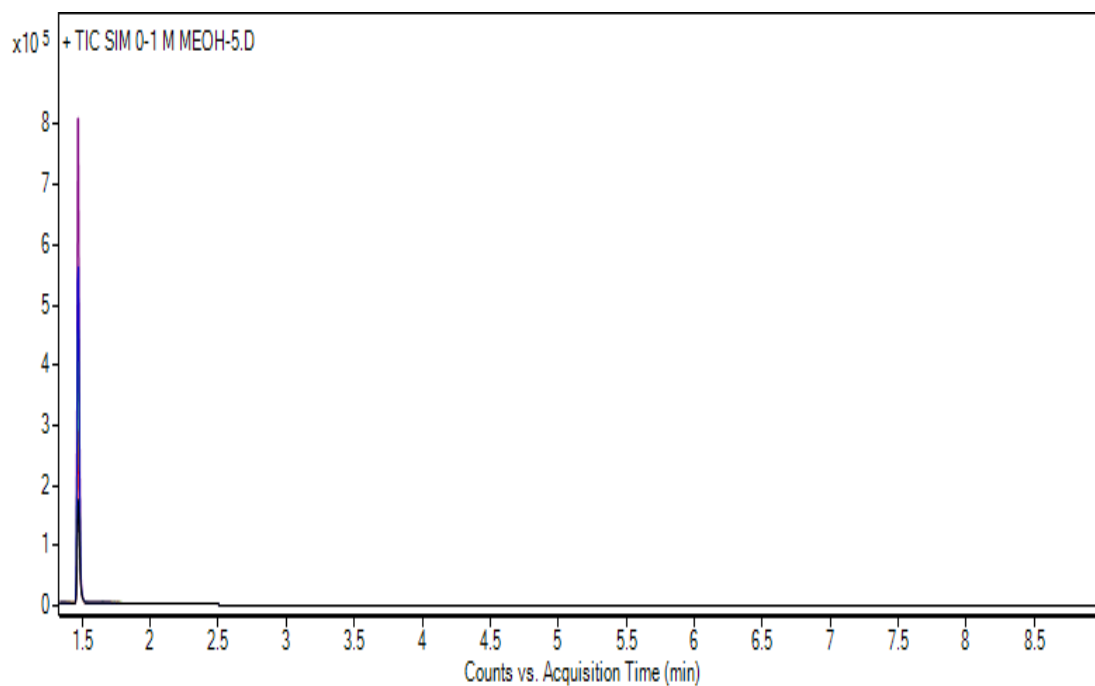


Figure A.1.10 GC/MS Calibration Chromatogram of Methanol.

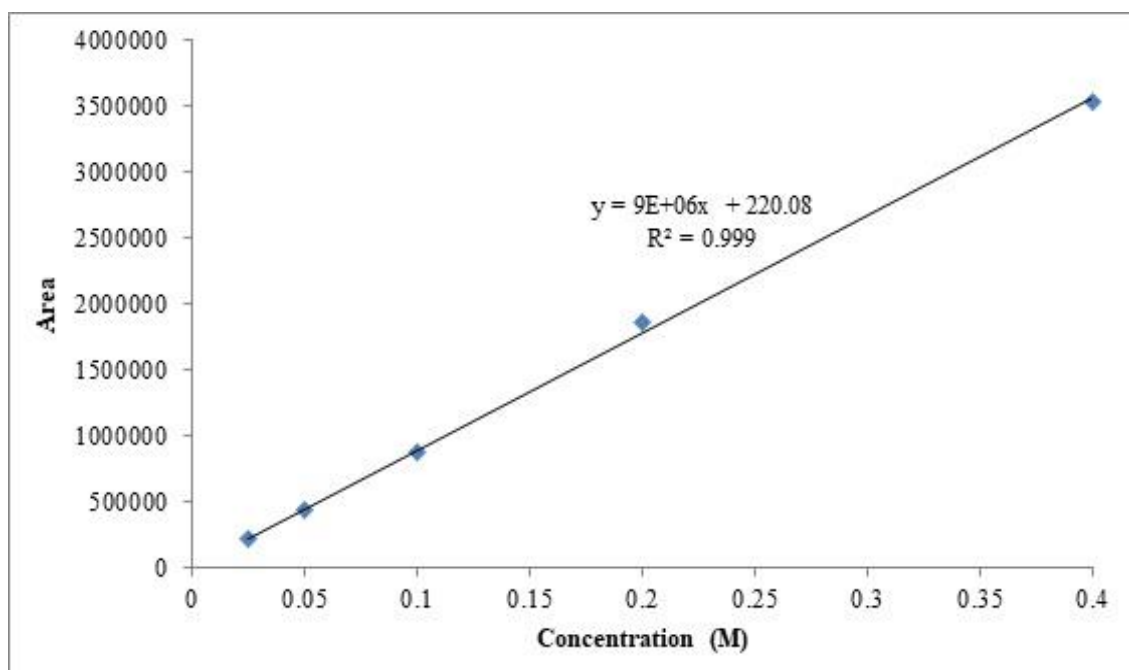


Figure A.1.11 GC/MS Calibration Curve and Correlation Coefficient (R^2) of Methanol.

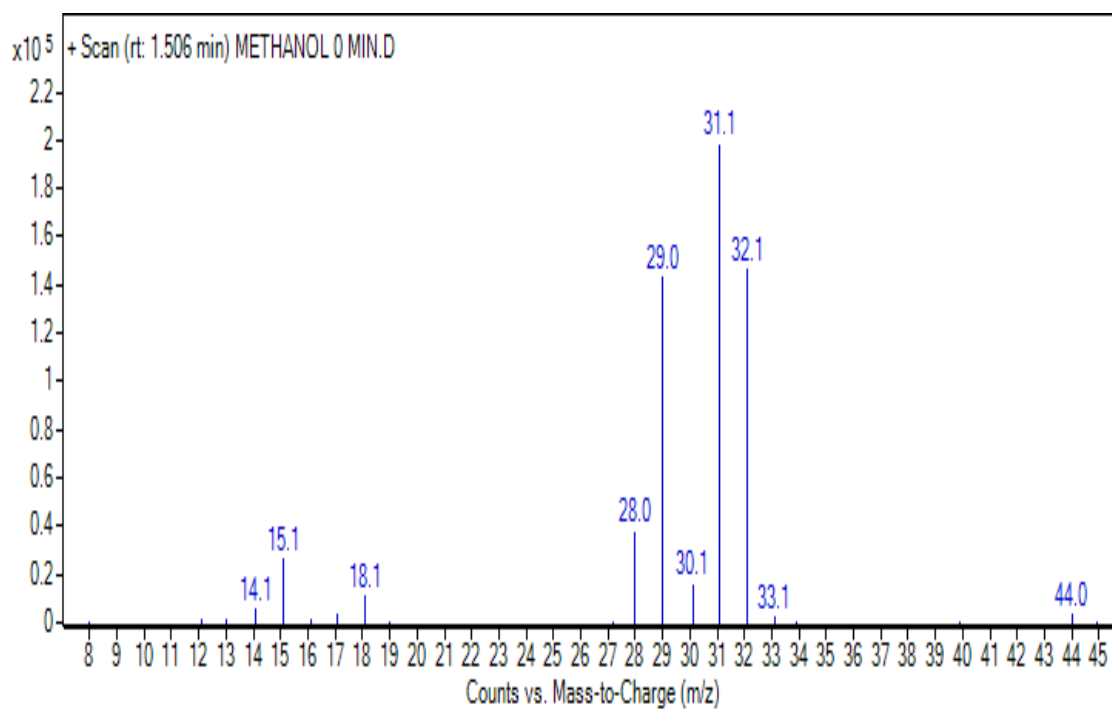


Figure A.1.12 GC/MS mass spectrum of Methanol.

APPENDIX 2

APPENDIX 2.1. Supplementary Data for Effects of Flowrate of the experimental solution on the degradation of Imidacloprid

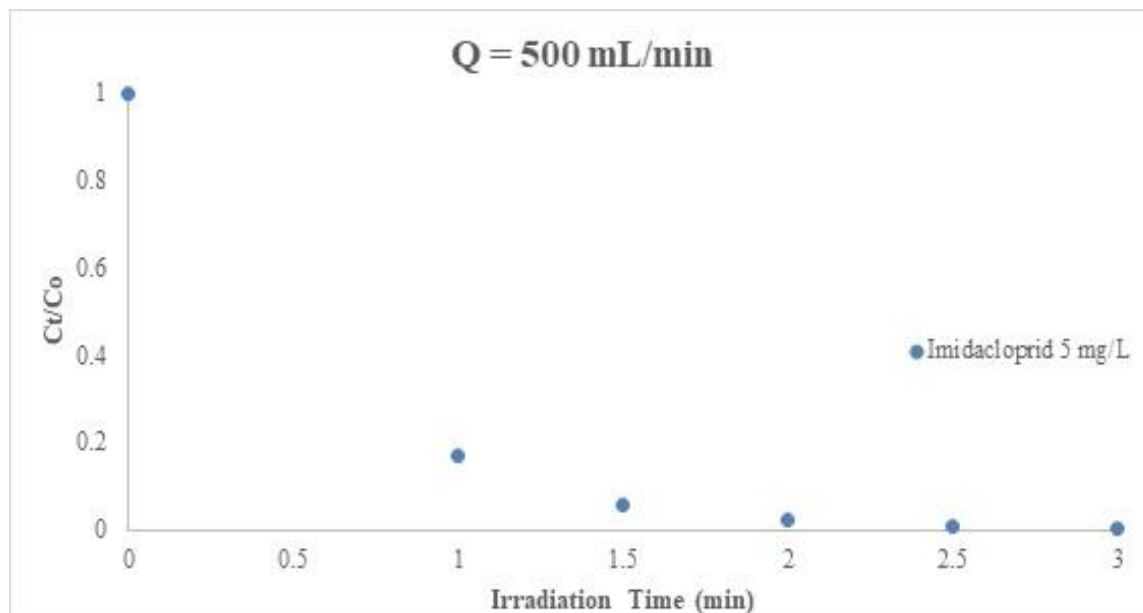


Figure A.2.1 VUV induced photodegradation of Imidacloprid ($C_0 = 5$ mg/L) under $Q = 500$ mL/min flow rate condition. The results are average of three replicates.

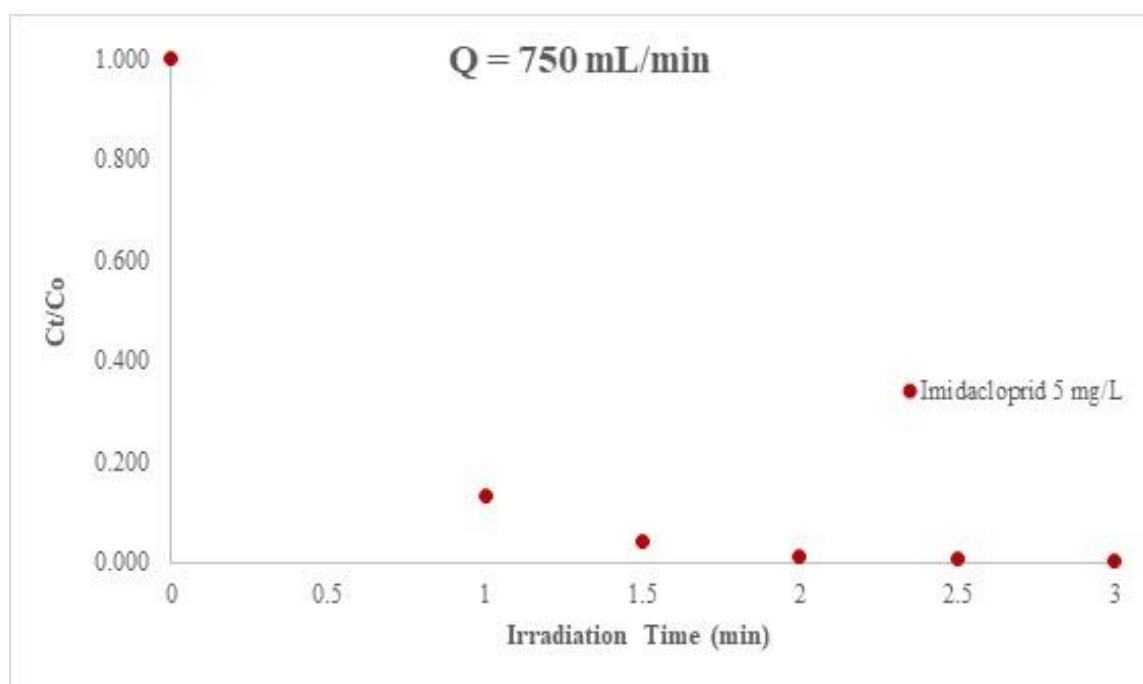


Figure A.2.2 VUV induced photodegradation of Imidacloprid ($C_0 = 5$ mg/L) under $Q = 750$ mL/min flow rate condition. The results are average of three replicates.

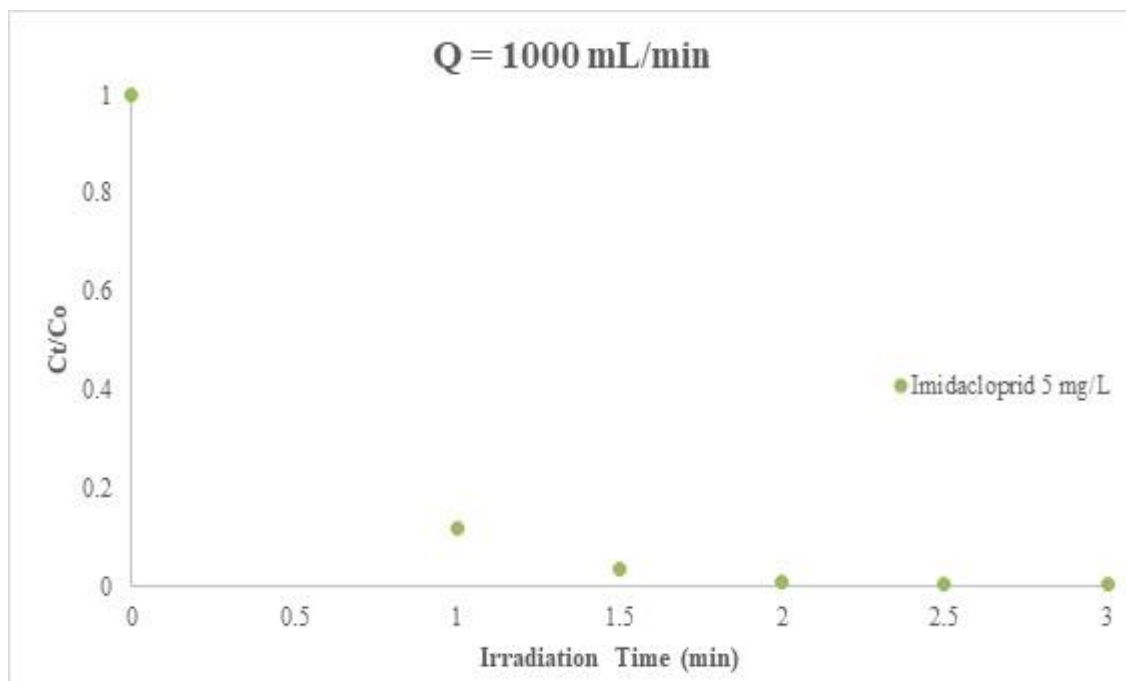


Figure A.2.3 VUV induced photodegradation of Imidacloprid ($C_0 = 5$ mg/L) under $Q = 1000$ mL/min flow rate condition. The results are average of three replicates.

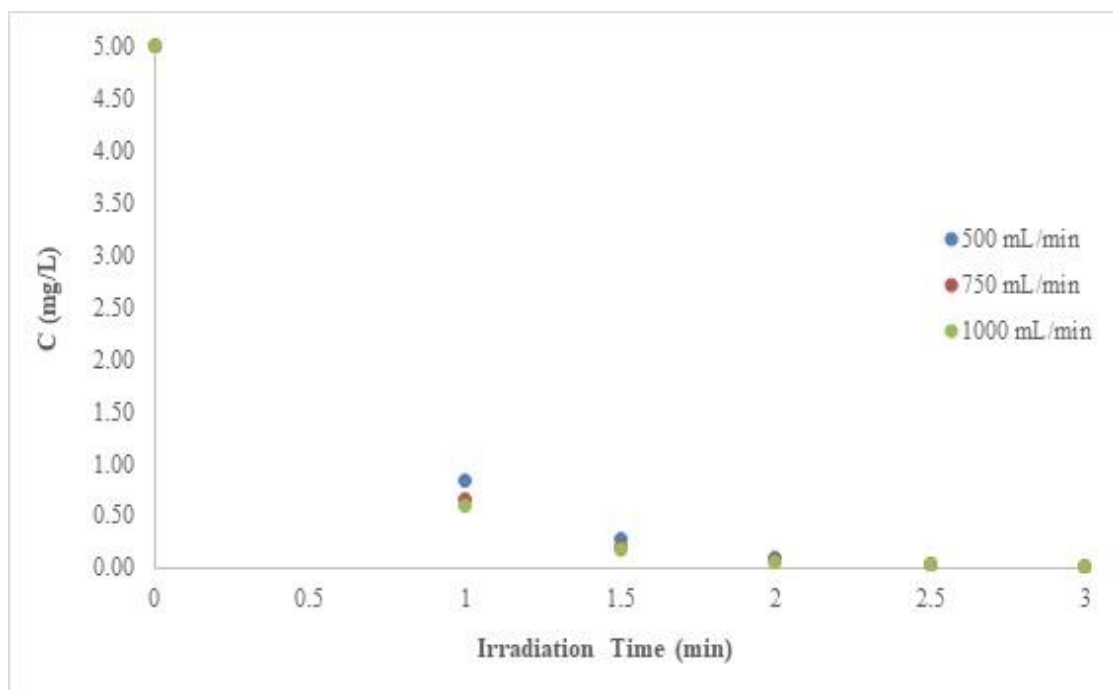


Figure A.2.4 VUV induced photodegradation of Imidacloprid ($C_0 = 5$ mg/L) under various flow rate conditions. The results are average of three replicates.

APPENDIX 2.2. Supplementary Data for Effects of initial pH of the experimental solution on the degradation of Imidacloprid

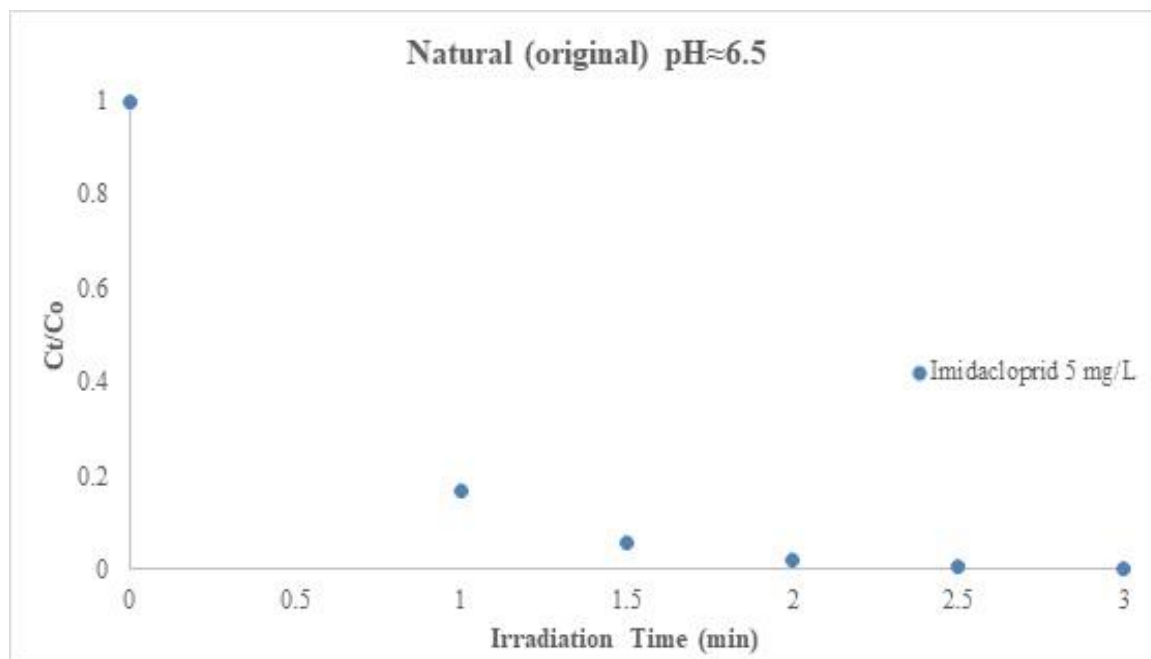


Figure A.2.5 VUV induced photodegradation of Imidacloprid ($C_o = 5$ mg/L) under natural (original, pH≈6.5) condition. The results are average of three replicates.

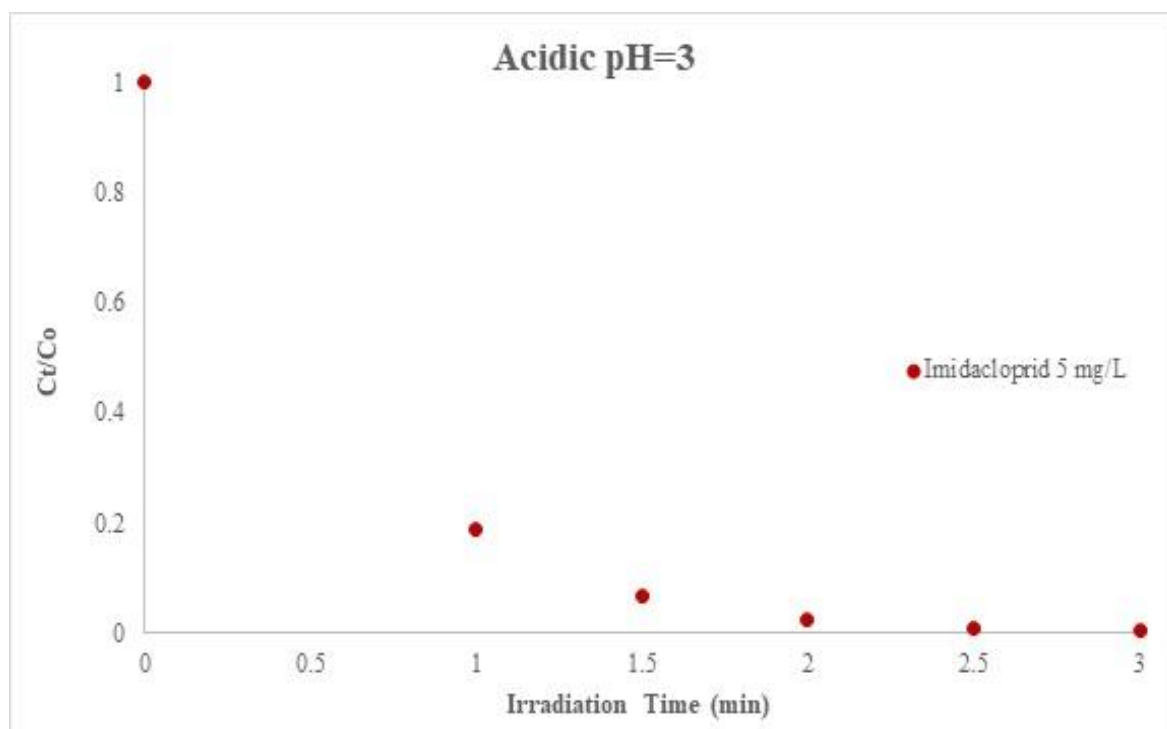


Figure A.2.6 VUV induced photodegradation of Imidacloprid ($C_o = 5$ mg/L) under acidic (pH=3) condition. The results are average of three replicates.

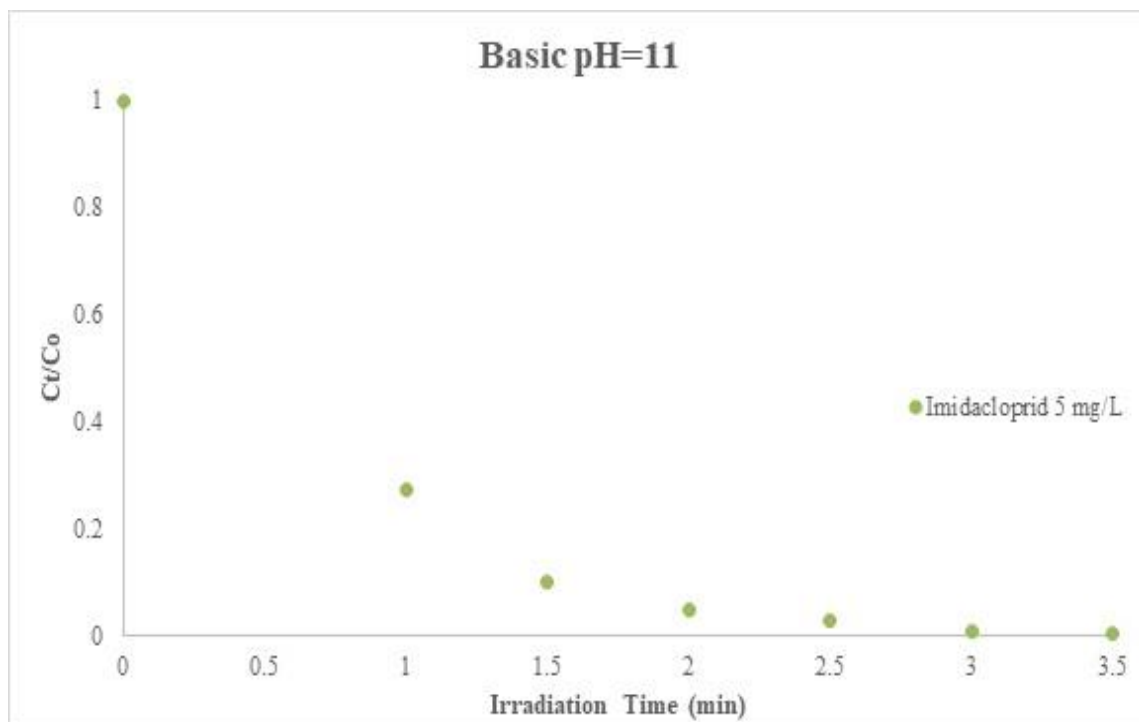


Figure A.2.7 VUV induced photodegradation of Imidacloprid ($C_0 = 5 \text{ mg/L}$) under basic (pH=11) condition. The results are average of three replicates.

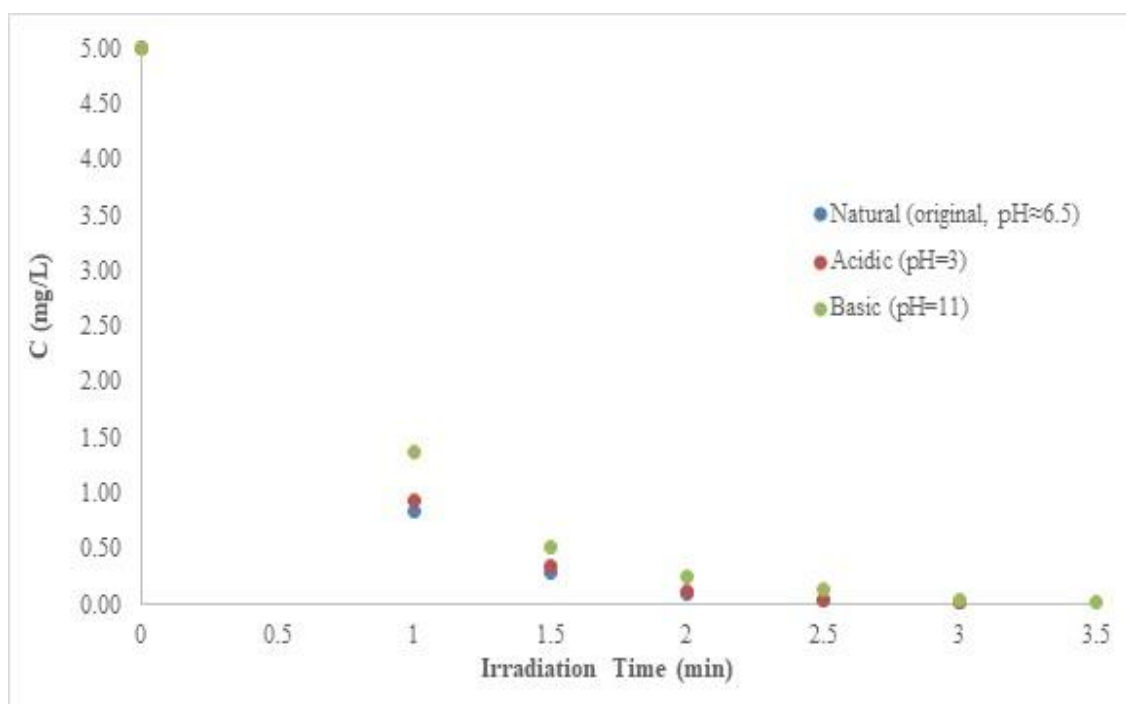


Figure A.2.8 VUV induced photodegradation of Imidacloprid ($C_0 = 5 \text{ mg/L}$) under different pH conditions. The results are average of three replicates.

APPENDIX 2.3. Supplementary Data for Effects of initial concentration of imidacloprid on the degradation of Imidacloprid

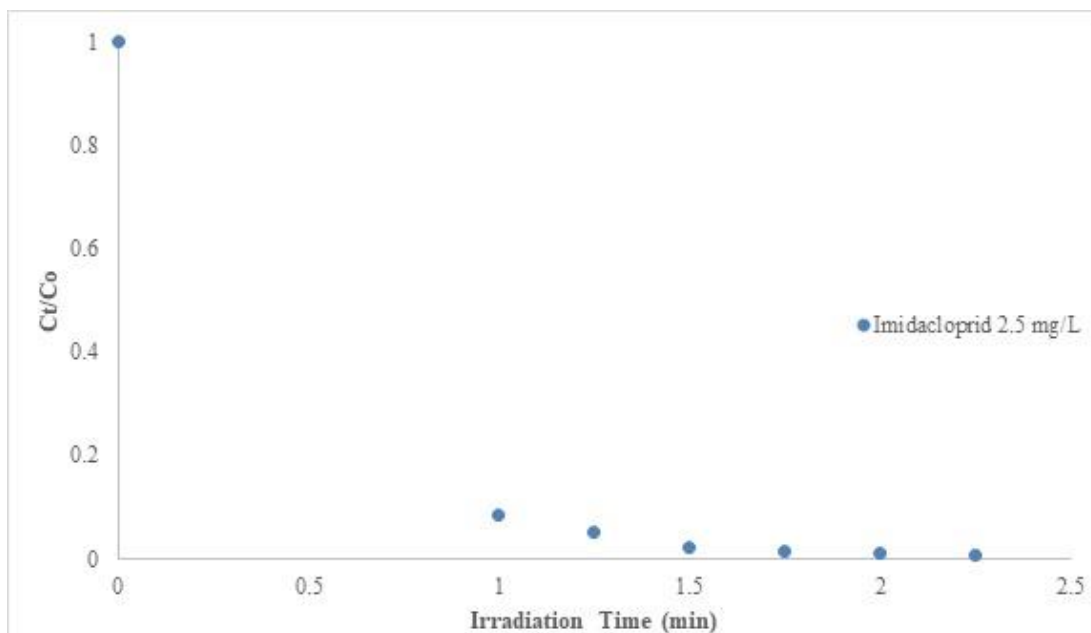


Figure A.2.9 VUV induced photodegradation of Imidacloprid ($C_0 = 2.5$ mg/L). The results are average of three replicates.

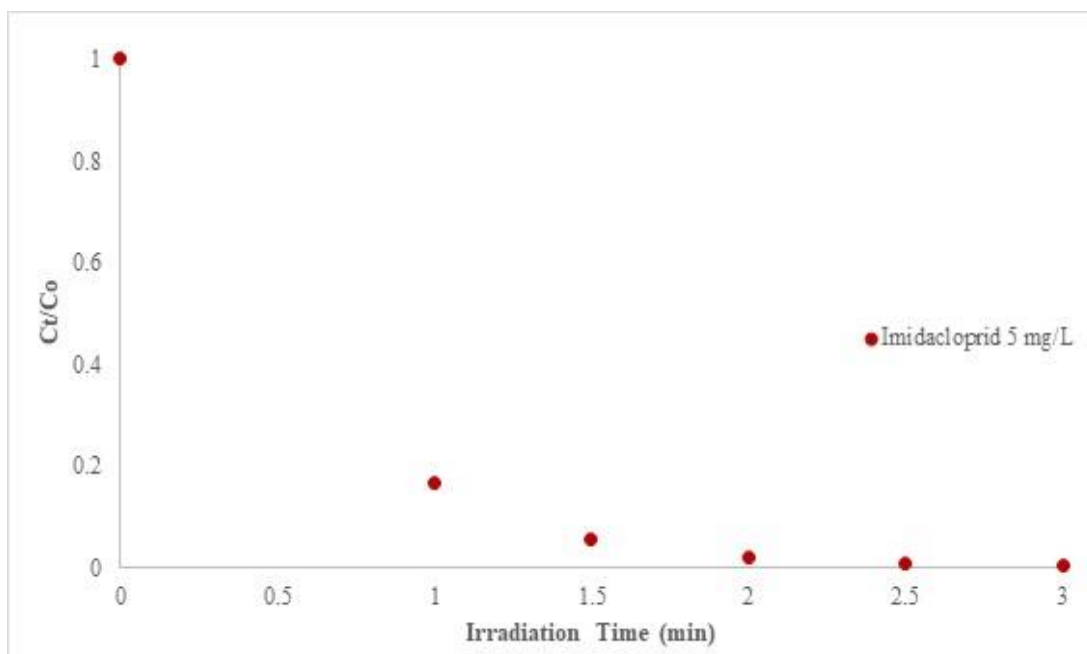


Figure A.2.10 VUV induced photodegradation of Imidacloprid ($C_0 = 5$ mg/L). The results are average of three replicates.

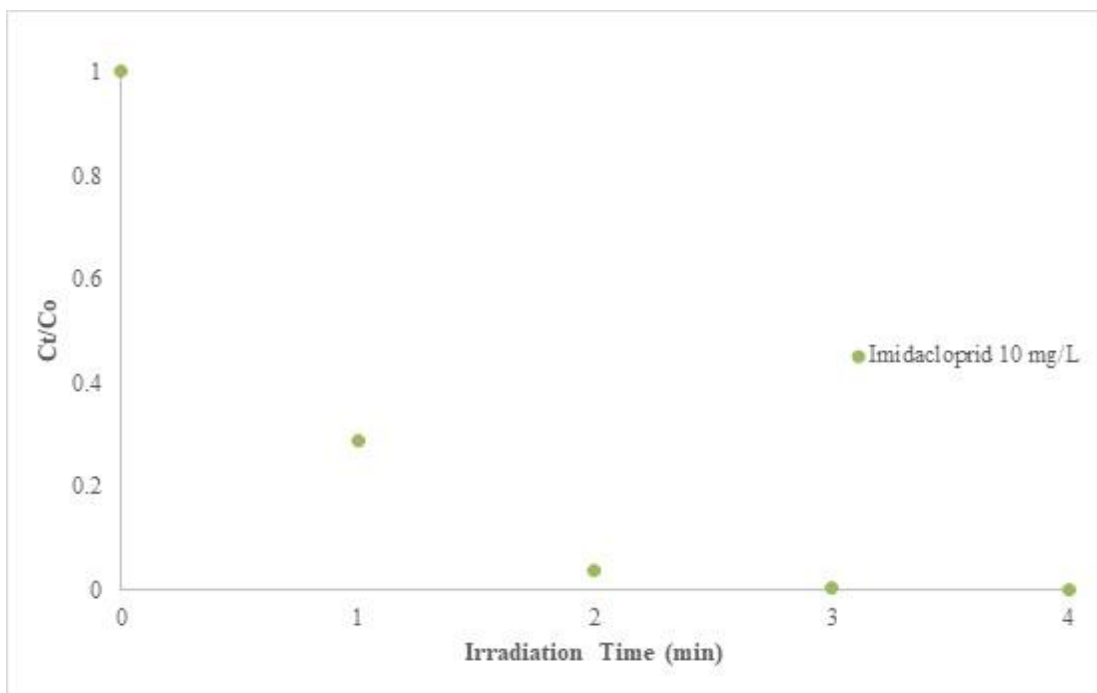


Figure A.2.11 VUV induced photodegradation of Imidacloprid ($C_0 = 10$ mg/L. The results are average of three replicates.

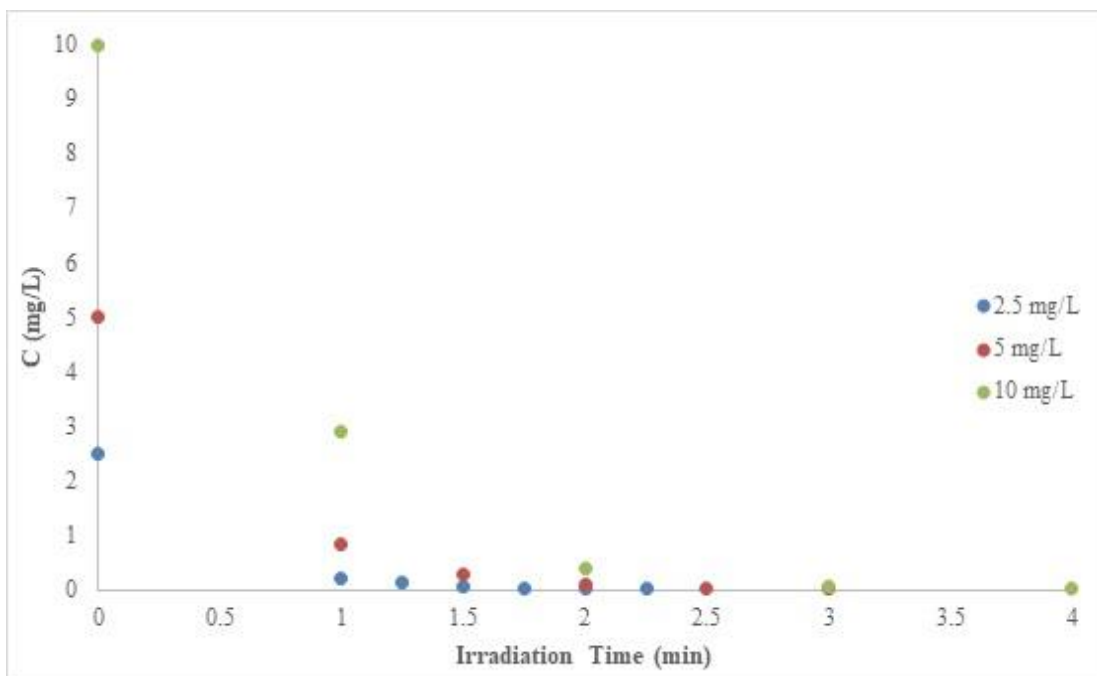


Figure A.2.12 VUV induced photodegradation of Imidacloprid under various initial concentrations. The results are average of three replicates.

APPENDIX 2.4. Supplementary Data for Effects of inorganic ions on the degradation of Imidacloprid

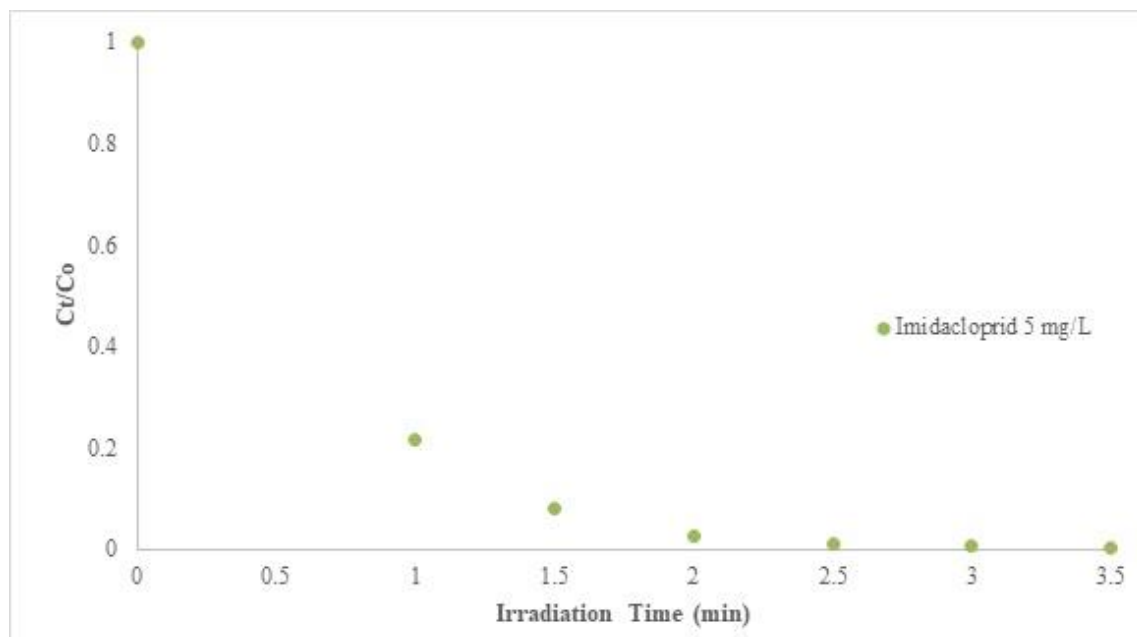


Figure A.2.13 VUV induced photodegradation of Imidacloprid ($C_0 = 5$ mg/L) in presence of carbonate ion ($\text{CO}_3^{2-} = 5$ mg/L). The results are average of three replicates.

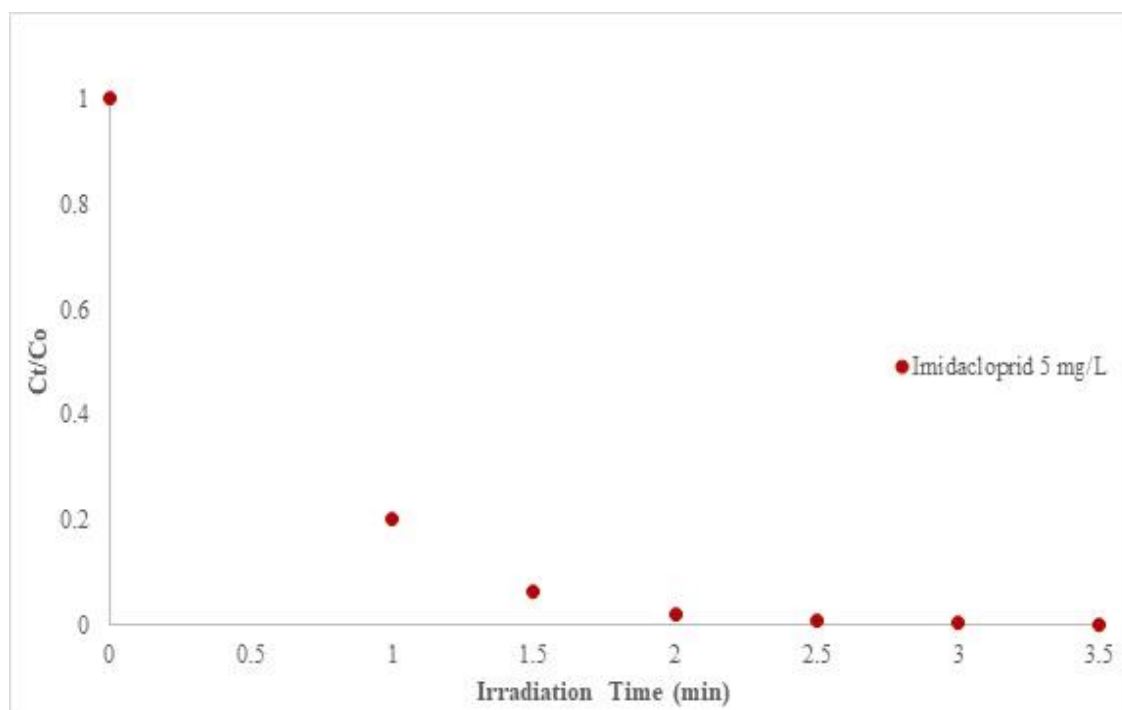


Figure A.2.14 VUV induced photodegradation of Imidacloprid ($C_0 = 5$ mg/L) in presence of bicarbonate ion ($\text{HCO}_3^- = 5$ mg/L). The results are average of three replicates.

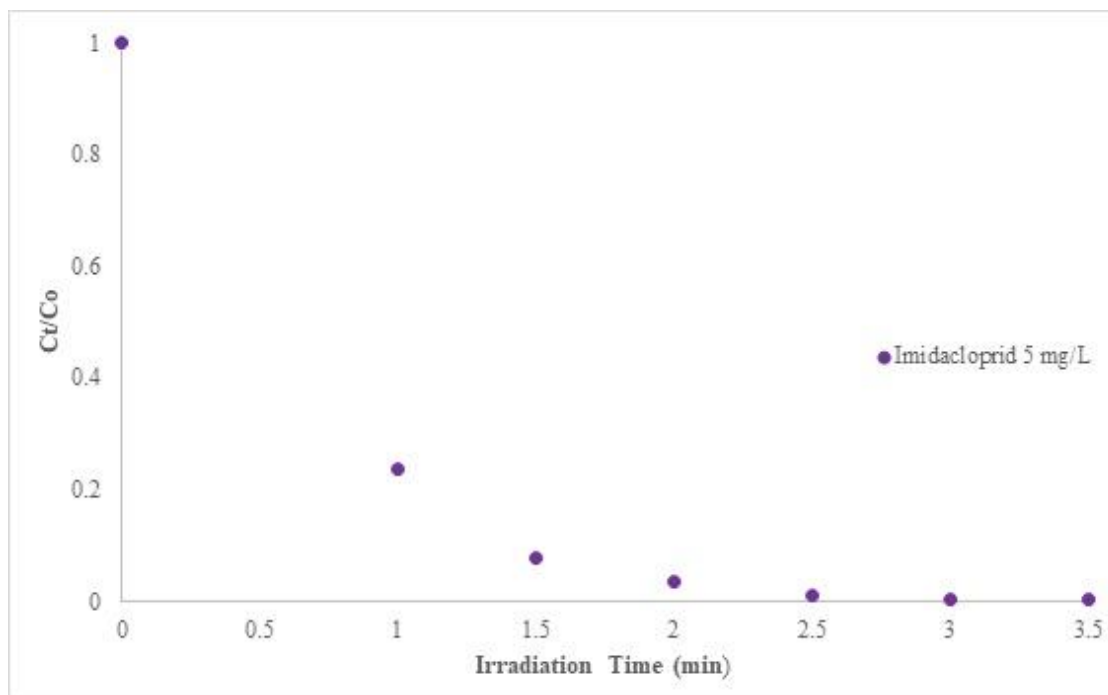


Figure A.2.15 VUV induced photodegradation of Imidacloprid ($C_0 = 5 \text{ mg/L}$) in presence of nitrate ion ($\text{NO}_3^- = 5 \text{ mg/L}$). The results are average of three replicates.

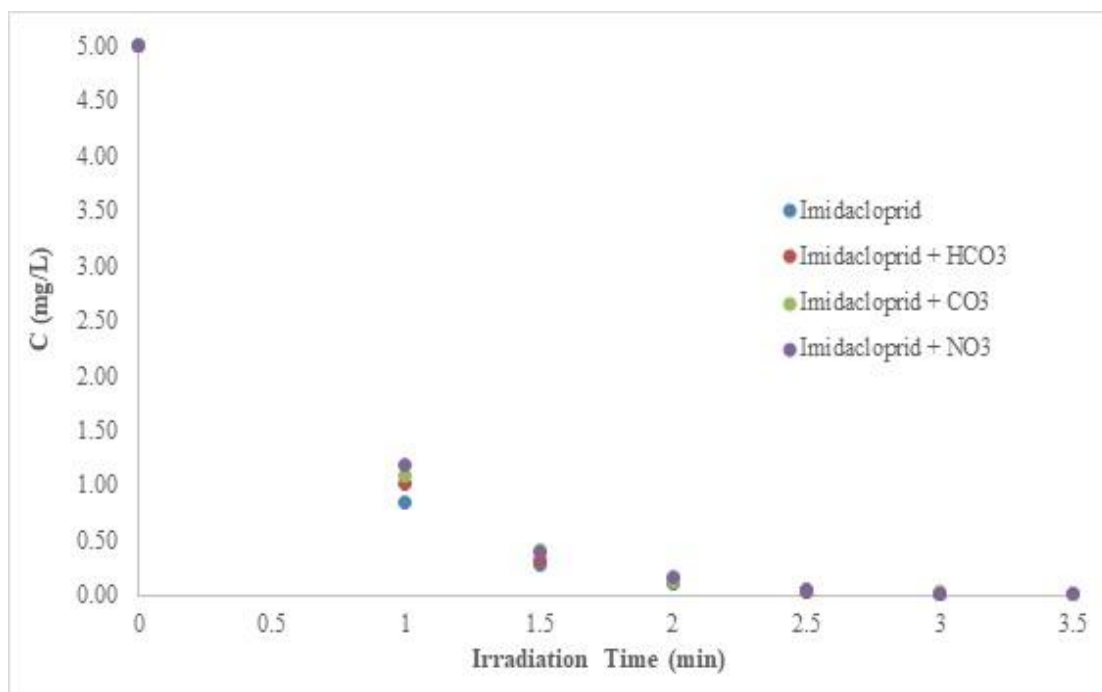


Figure A.2.16 VUV induced photodegradation of Imidacloprid ($C_0 = 5 \text{ mg/L}$) in presence of various inorganic ions. The results are average of three replicates.

APPENDIX 2.5. Supplementary Data for Effects of Water Matrix on the degradation of Imidacloprid

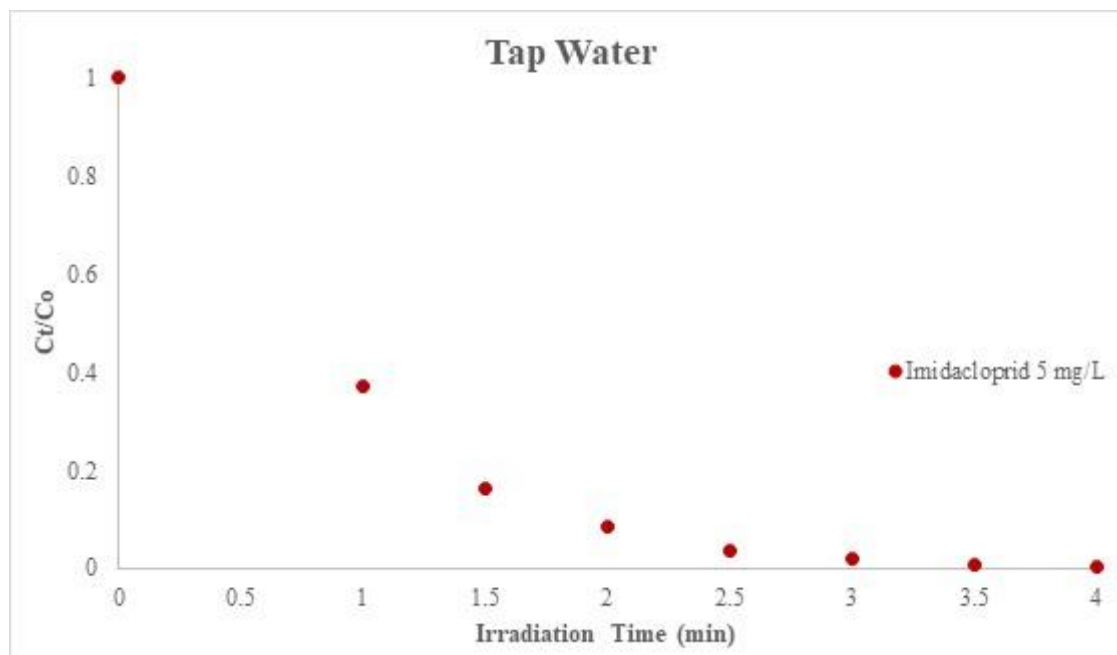


Figure A.2.17 VUV induced photodegradation of Imidacloprid ($C_0 = 5$ mg/L) in tap water. The results are average of three replicates.

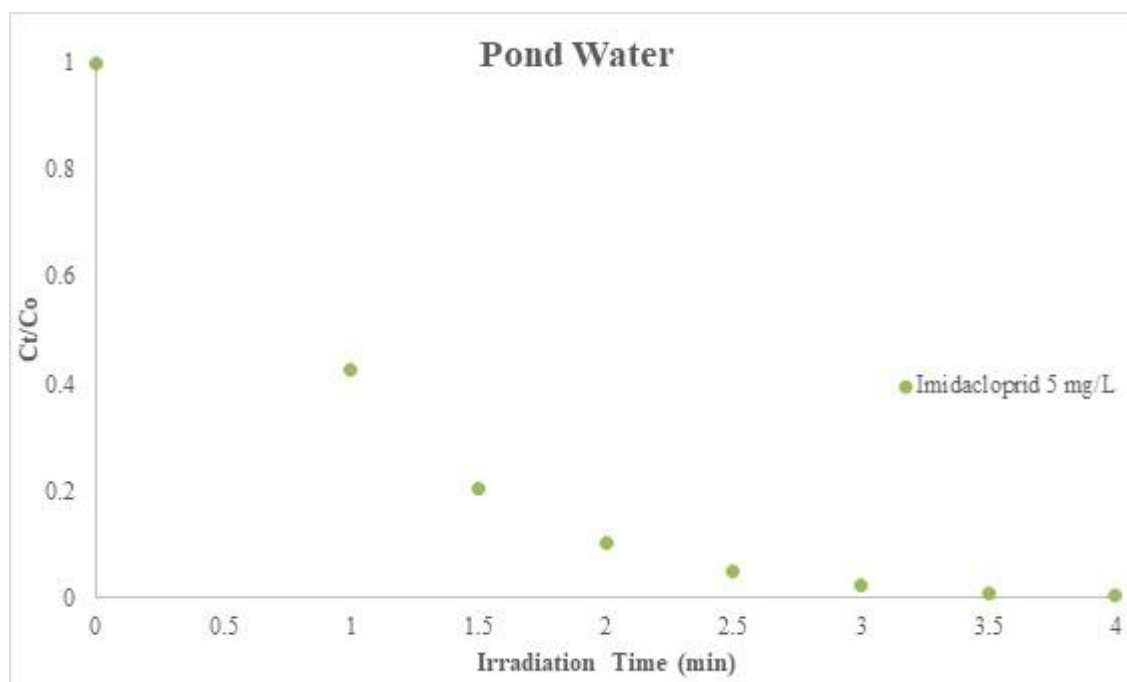


Figure A.2.18 VUV induced photodegradation of Imidacloprid ($C_0 = 5$ mg/L) in pond water. The results are average of three replicates.

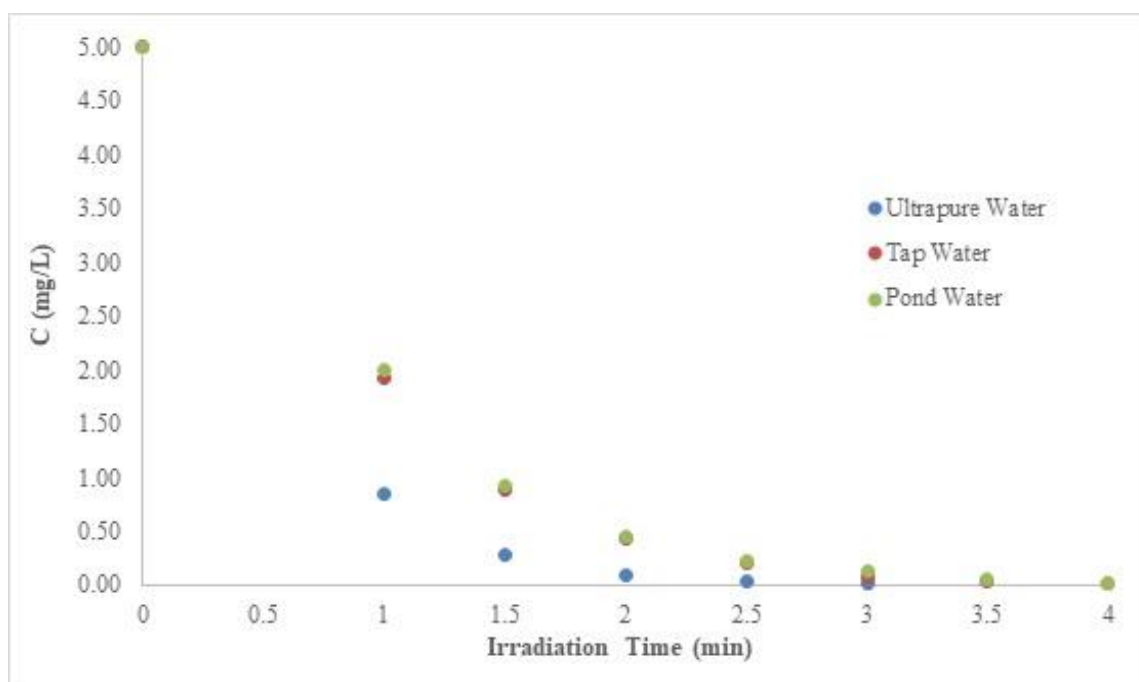


Figure A.2.19 VUV induced photodegradation of Imidacloprid ($C_0 = 5 \text{ mg/L}$) in various water matrix. The results are average of three replicates.

APPENDIX 2.6. Supplementary Data for Effects of Oxygen saturated condition on the degradation of Imidacloprid

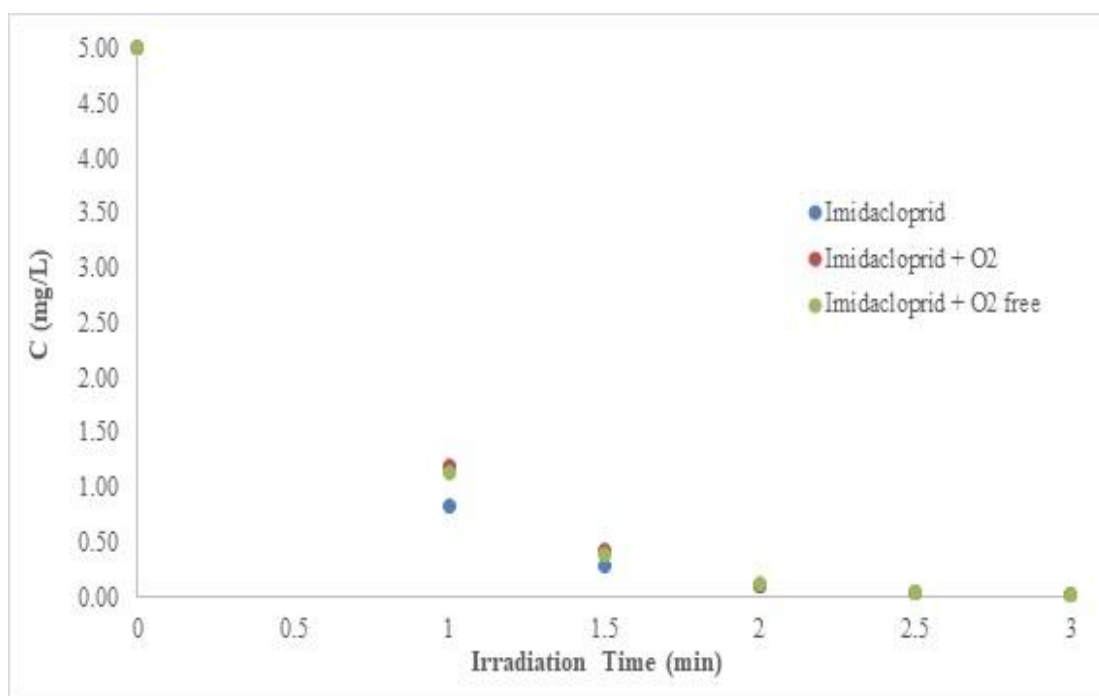


Figure A.2.20 VUV induced photodegradation of Imidacloprid ($C_0 = 5 \text{ mg/L}$) in presence and absence of oxygen.

APPENDIX 2.7. Supplementary Data for Effects of Oxygenated and Deoxygenated conditions on the mineralization of Imidacloprid

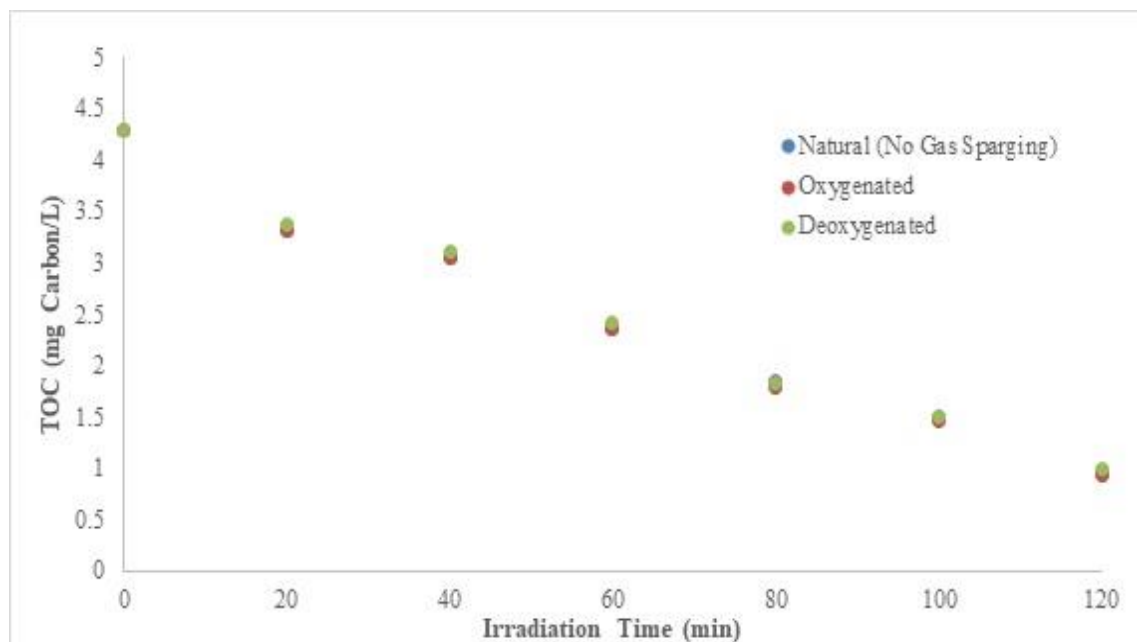


Figure A.2.21 VUV induced mineralization (TOC reduction) of Imidacloprid ($C_0 = 10$ mg/L) in presence and absence of oxygen.

APPENDIX 2.8. Supplementary Data for VUV photooxidation Byproducts of Imidacloprid

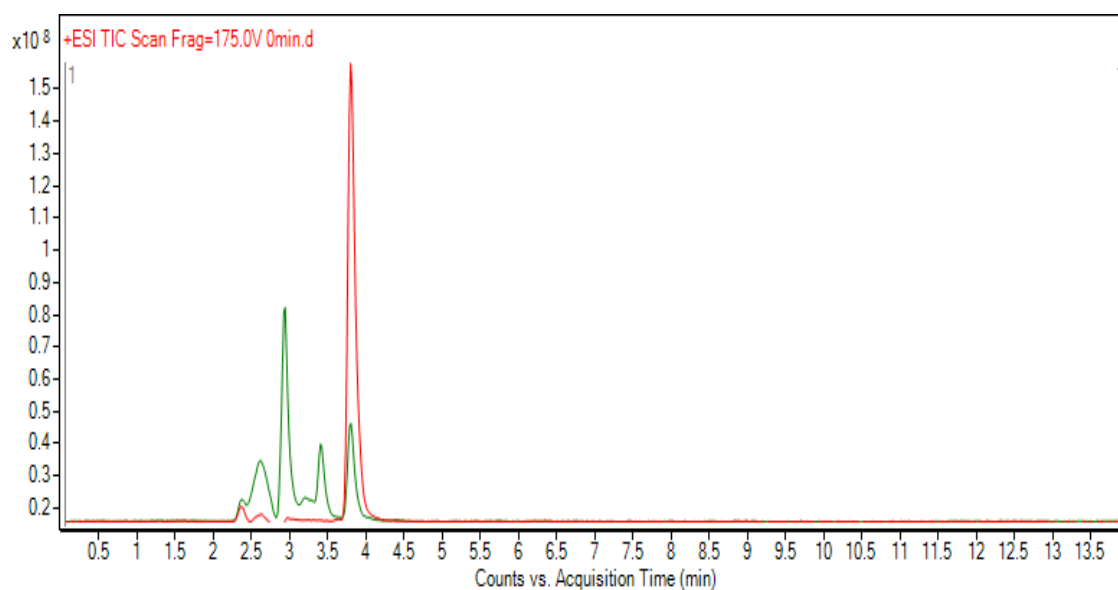


Figure A.2.22 Overlapped LC/MS Q-TOF chromatograms of 5 mg/L imidacloprid at 0 and 1 min of VUV irradiation time

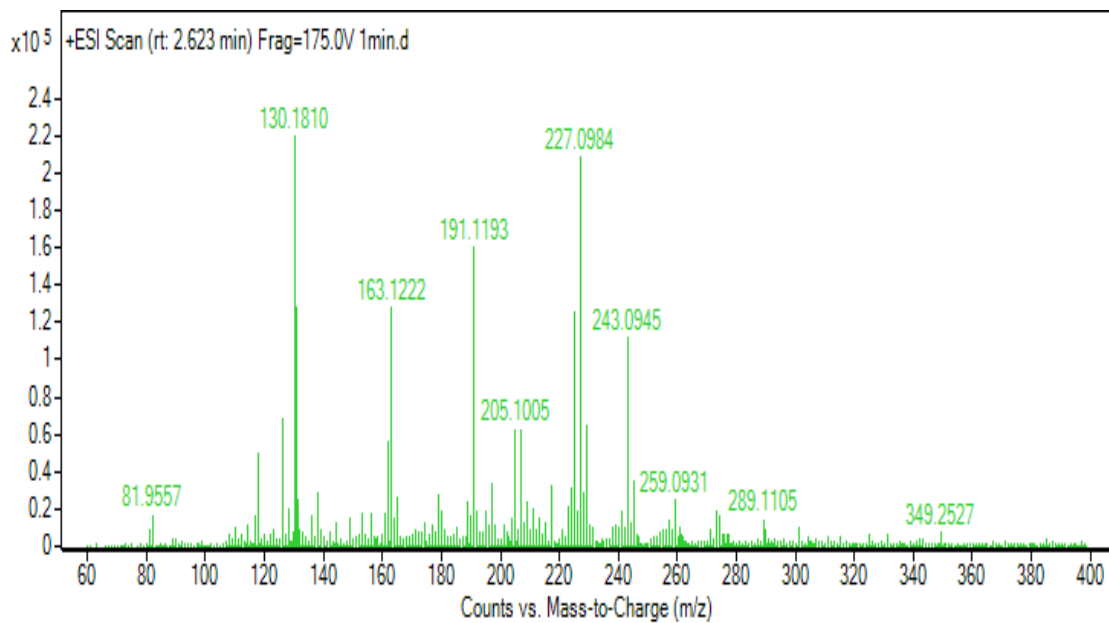


Figure A.2.23 LC/MS Q-TOF mass spectrum of byproduct set 1 at 1 min of irradiation time (at retention time of 2.623 min)

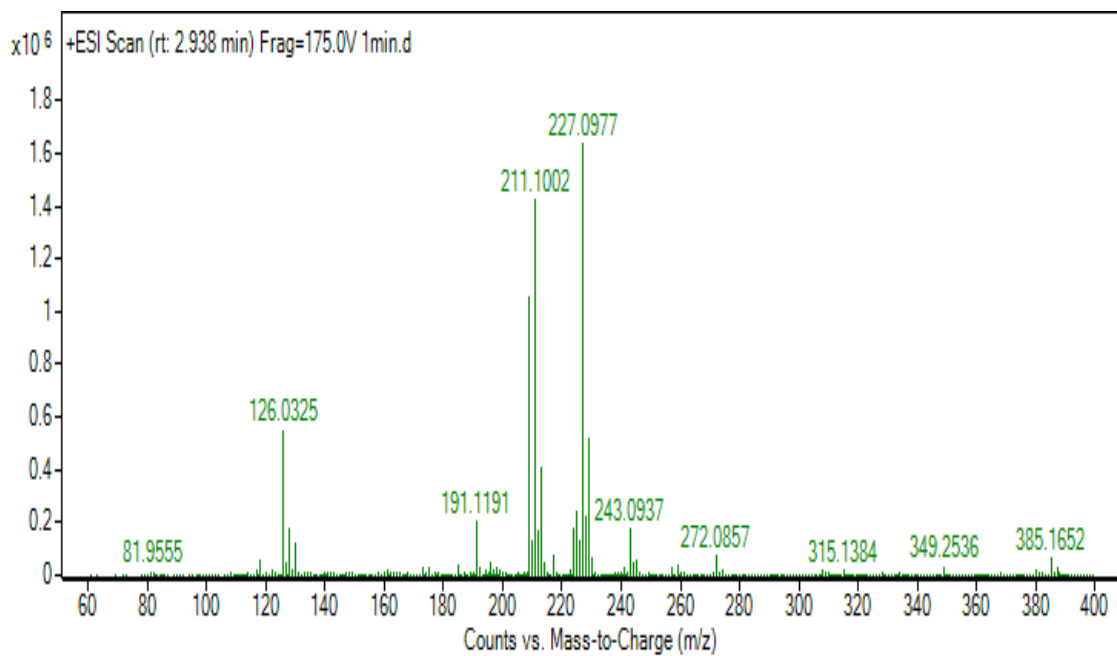


Figure A.2.24 LC/MS Q-TOF mass spectrum of byproduct set 2 at 1 min of irradiation time (at retention time of 2.938 min)

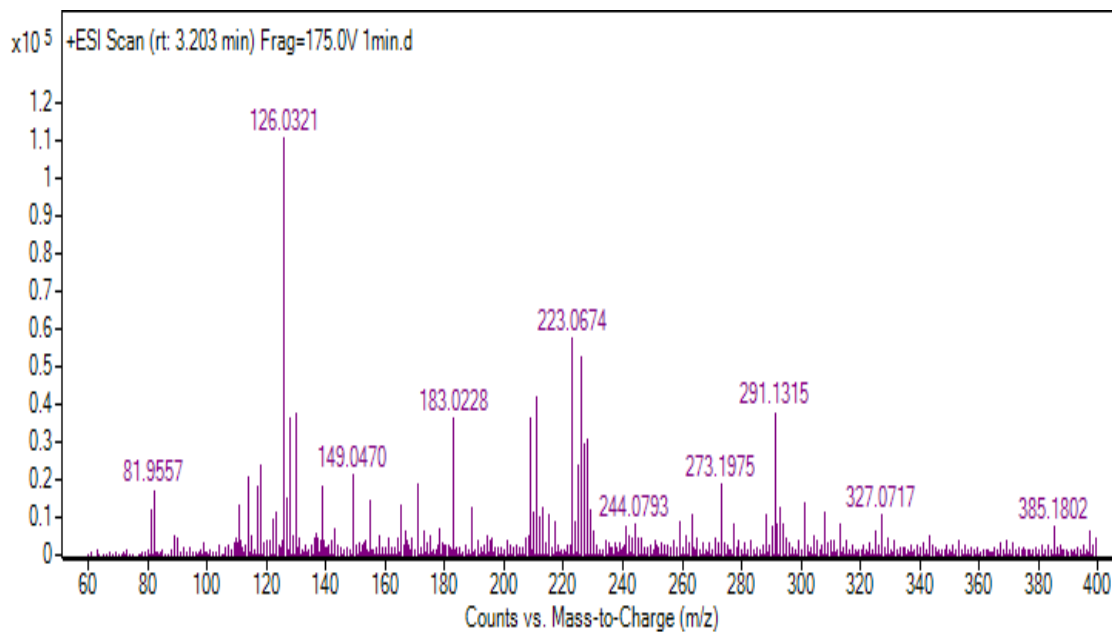


Figure A.2.25 LC/MS Q-TOF mass spectrum of byproduct set 3 at 1 min of irradiation time (at retention time of 3.203 min)

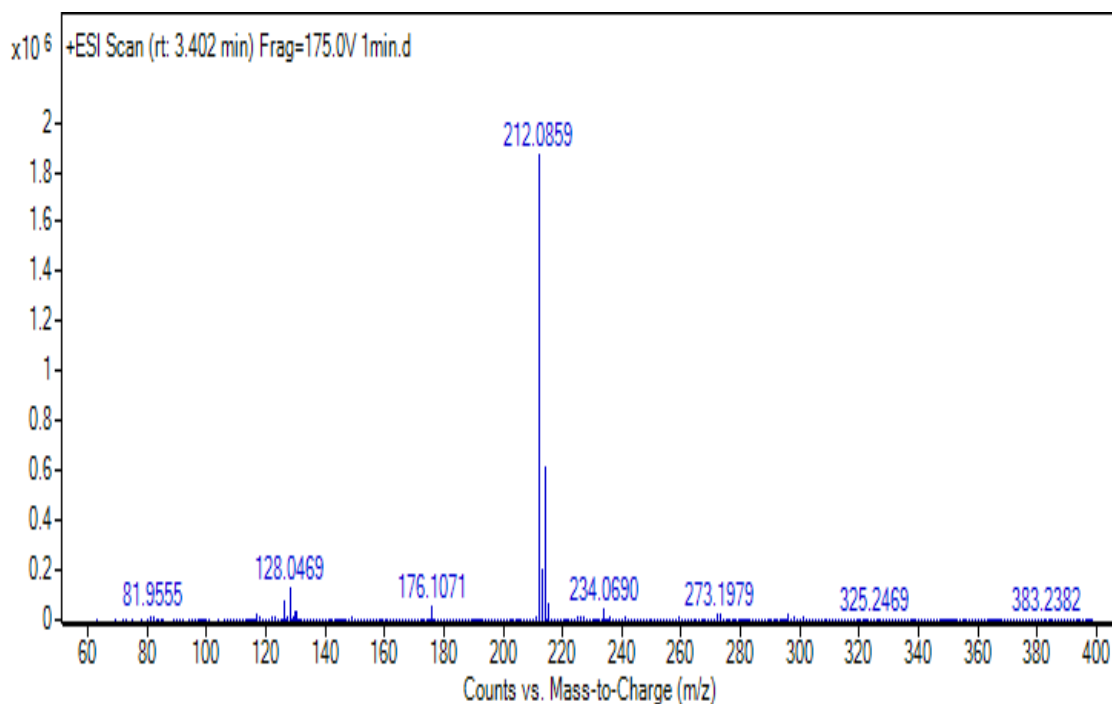


Figure A.2.26 LC/MS Q-TOF mass spectrum of byproduct set 4 at 1 min of irradiation time (at retention time of 3.402 min)

APPENDIX 3

APPENDIX 3.1. Supplementary Data for Effects of Flowrate of the experimental solution on the discoloration of Red Dye

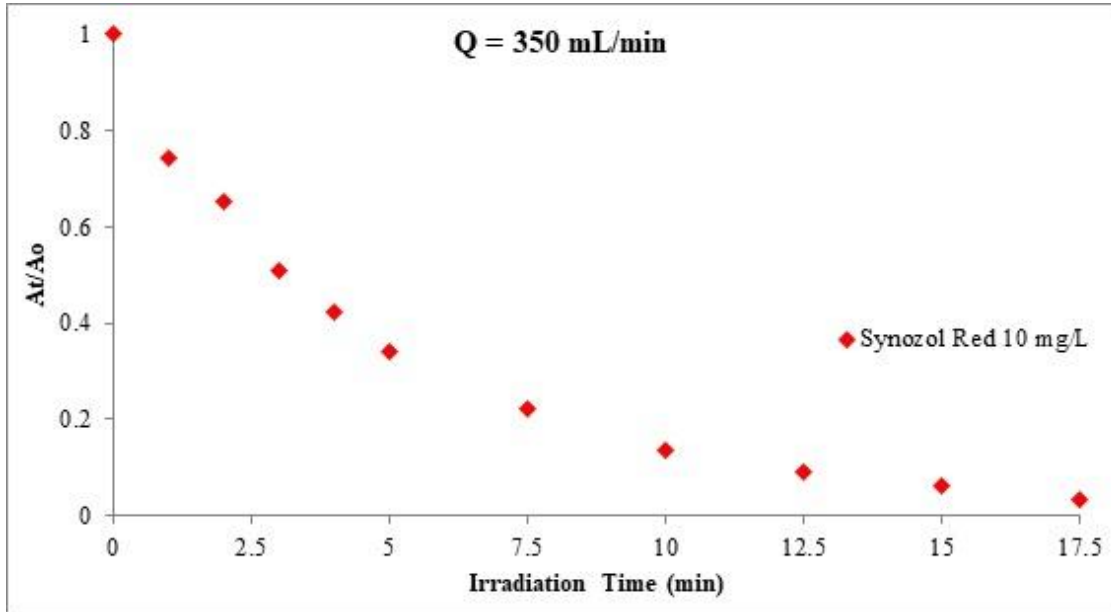


Figure A.3.1 VUV initiated discoloration of Red dye ($C_0 = 10$ mg/L) under $Q = 350$ mL/min flow rate condition.

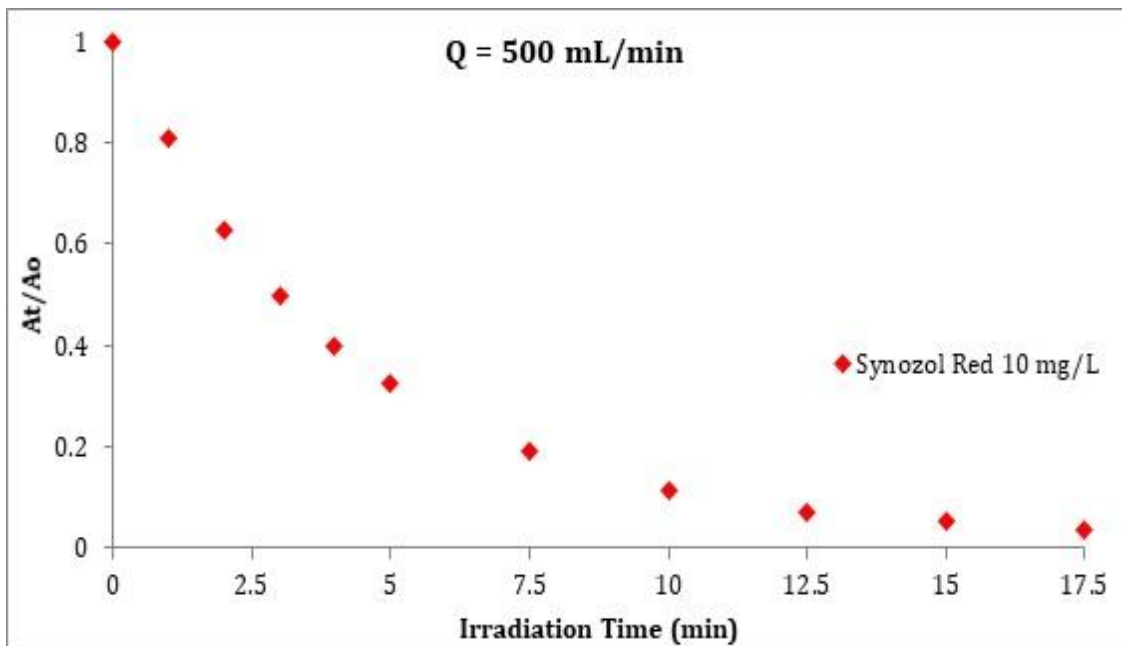


Figure A.3.2 VUV initiated discoloration of Red dye ($C_0 = 10$ mg/L) under $Q = 500$ mL/min flow rate condition.

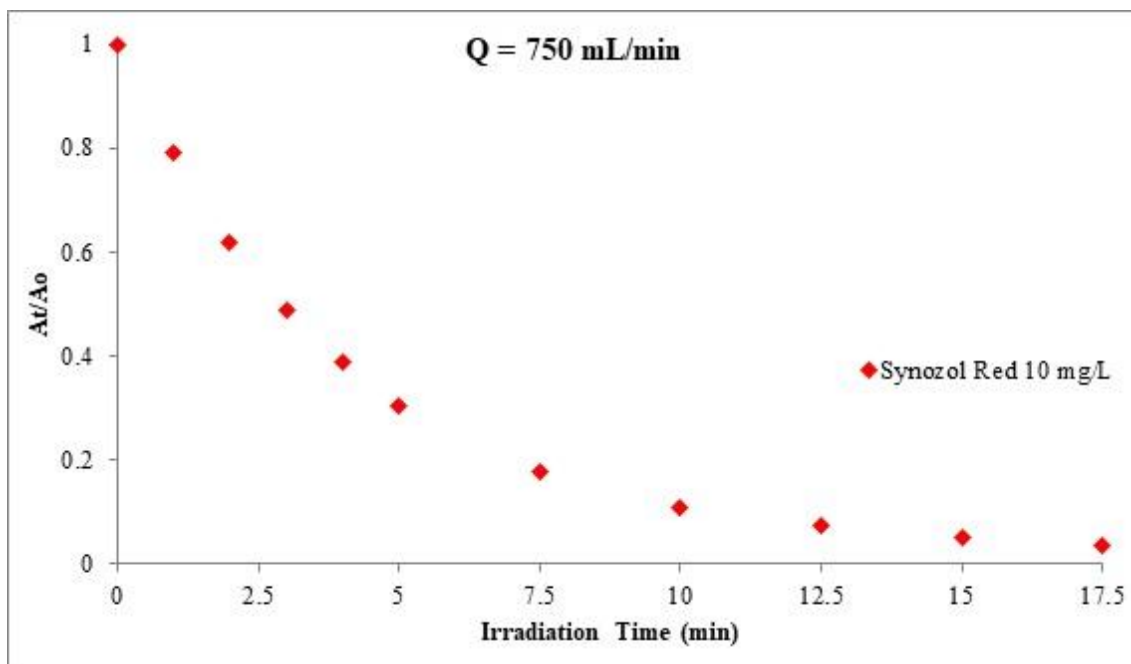


Figure A.3.3 VUV initiated discoloration of Red dye ($C_0 = 10 \text{ mg/L}$) under $Q = 750 \text{ mL/min}$ flow rate condition.

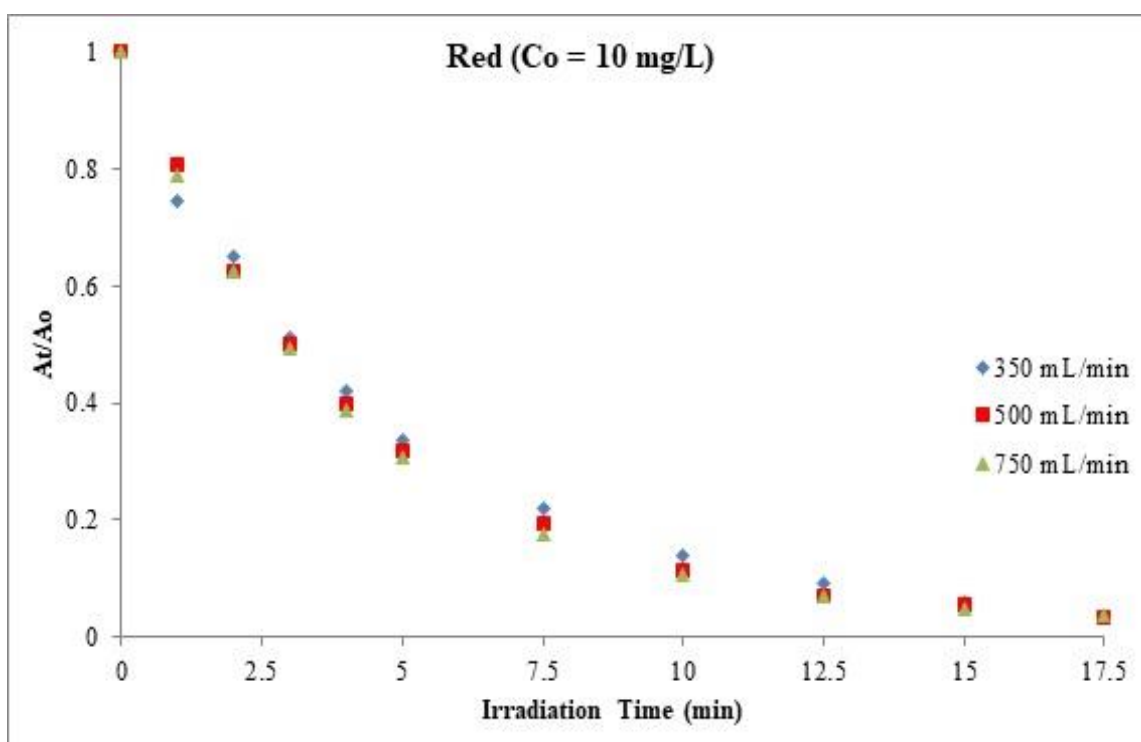


Figure A.3.4 VUV initiated discoloration of Red dye ($C_0 = 10 \text{ mg/L}$) under various flow rate condition.

APPENDIX 3.2. Supplementary Data for Effects of initial concentration of imidacloprid on the discoloration of Reactive Textile Dyes

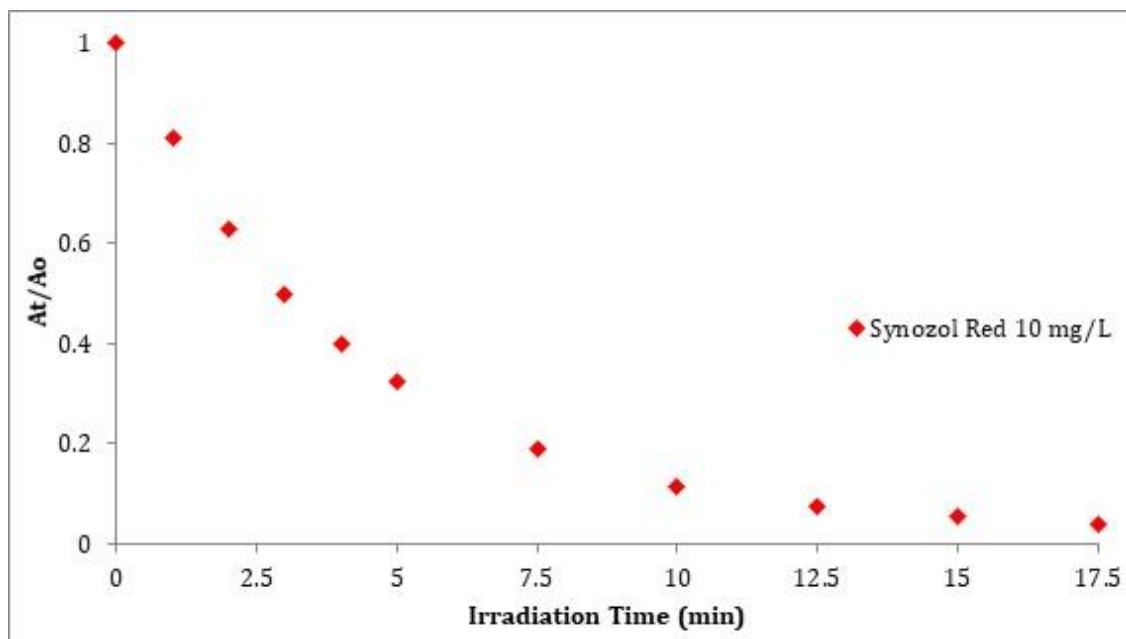


Figure A.3.5 VUV initiated discoloration of Red dye ($C_o = 10$ mg/L). The results are average of three replicates.

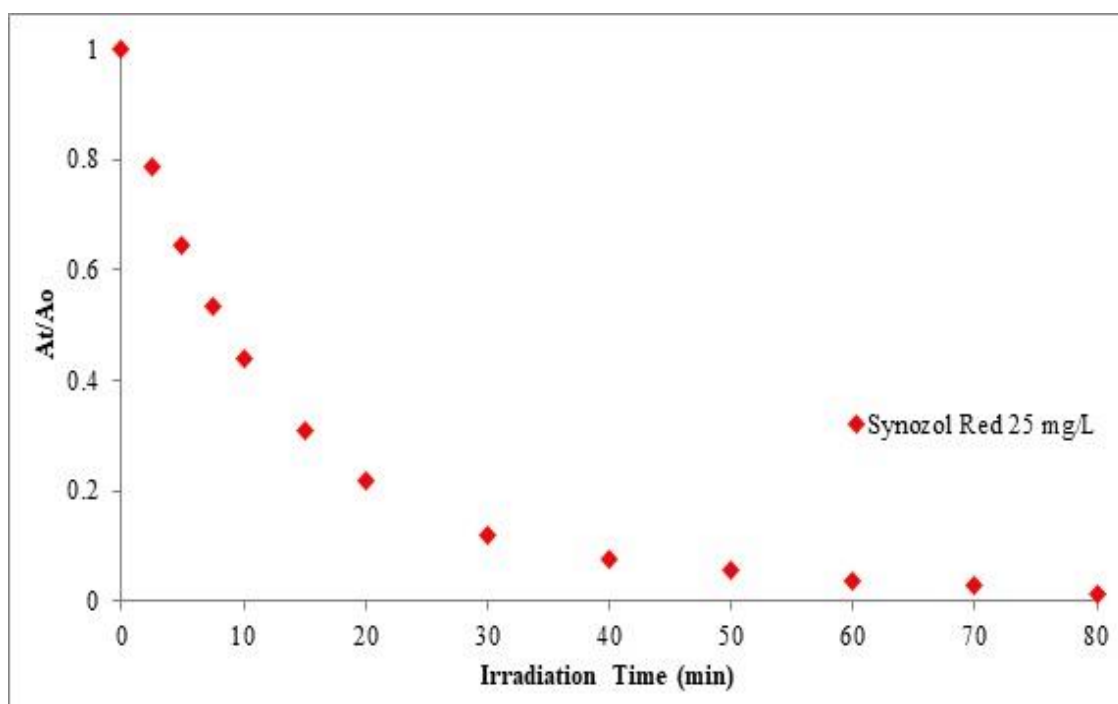


Figure A.3.6 VUV initiated discoloration of Red dye ($C_o = 25$ mg/L). The results are average of three replicates.

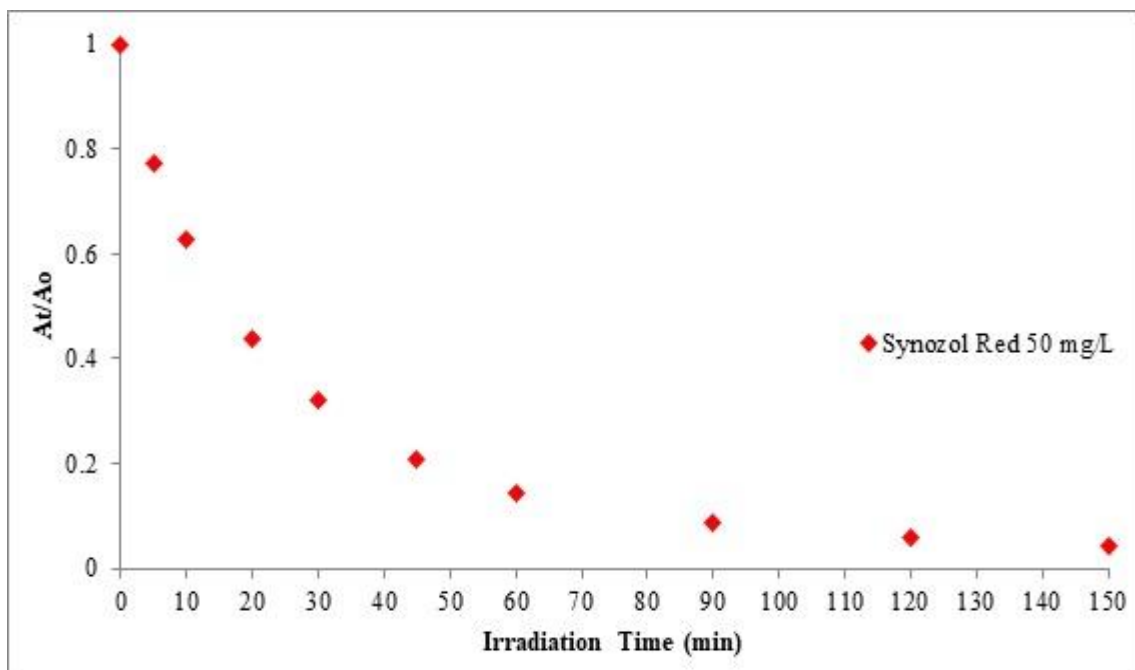


Figure A.3.7 VUV initiated discoloration of Red dye ($C_0 = 50 \text{ mg/L}$). The results are average of three replicates.

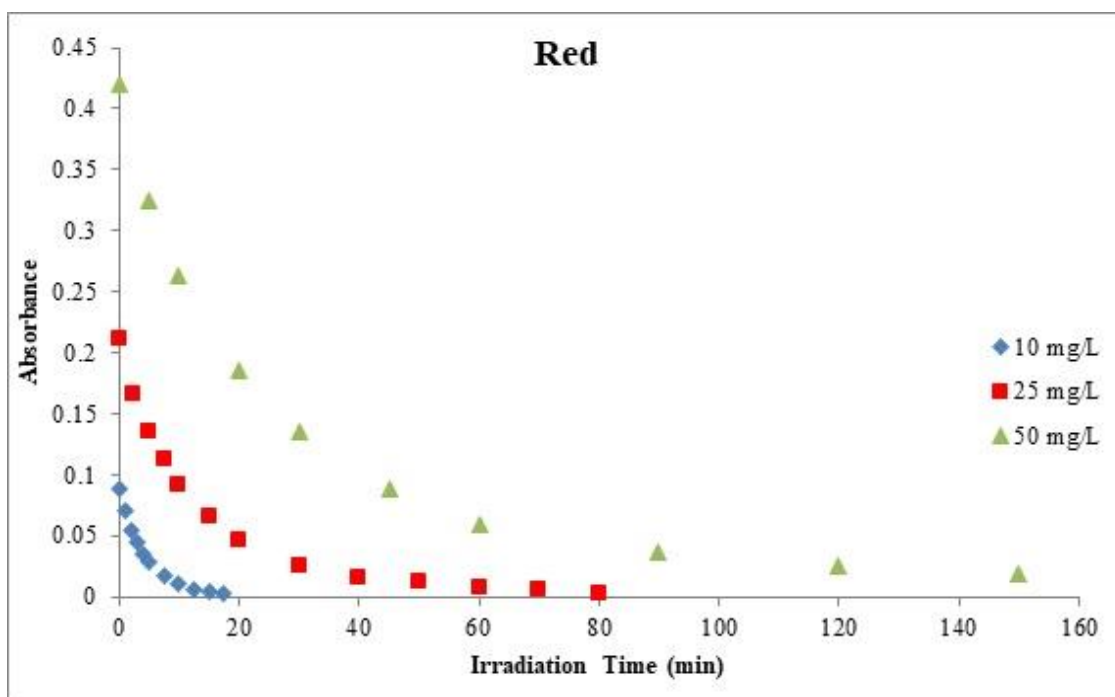


Figure A.3.8 VUV induced discoloration of Red dye under various initial concentrations. The results are average of three replicates.

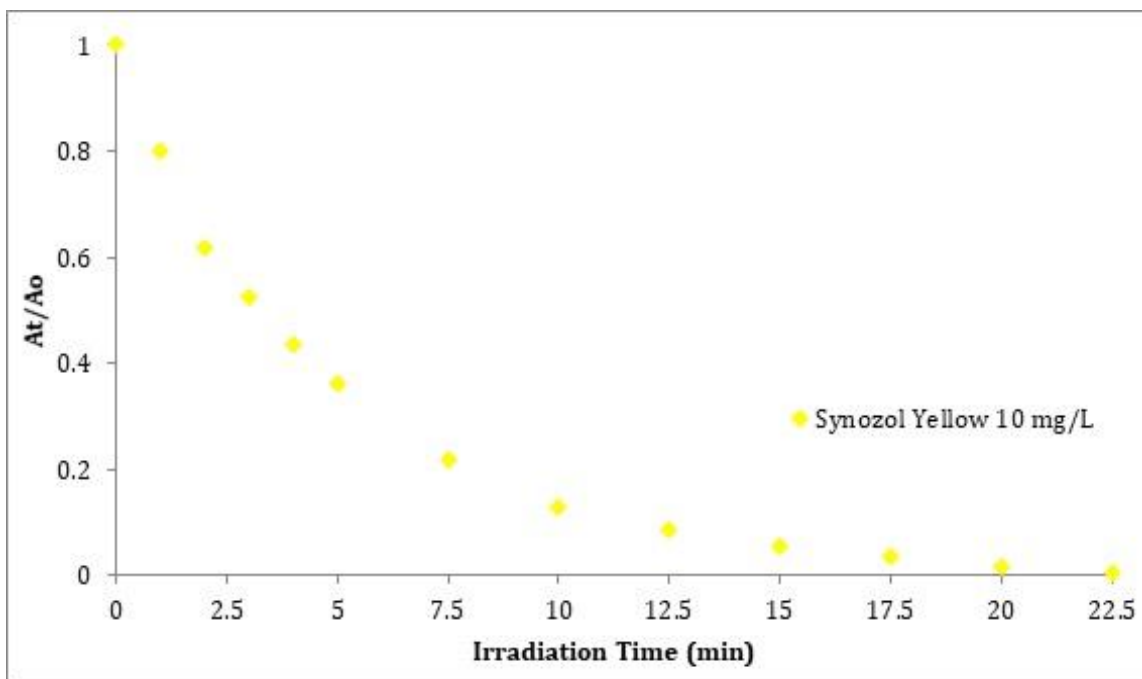


Figure A.3.9 VUV initiated discoloration of Yellow dye ($C_0 = 10 \text{ mg/L}$). The results are average of three replicates.

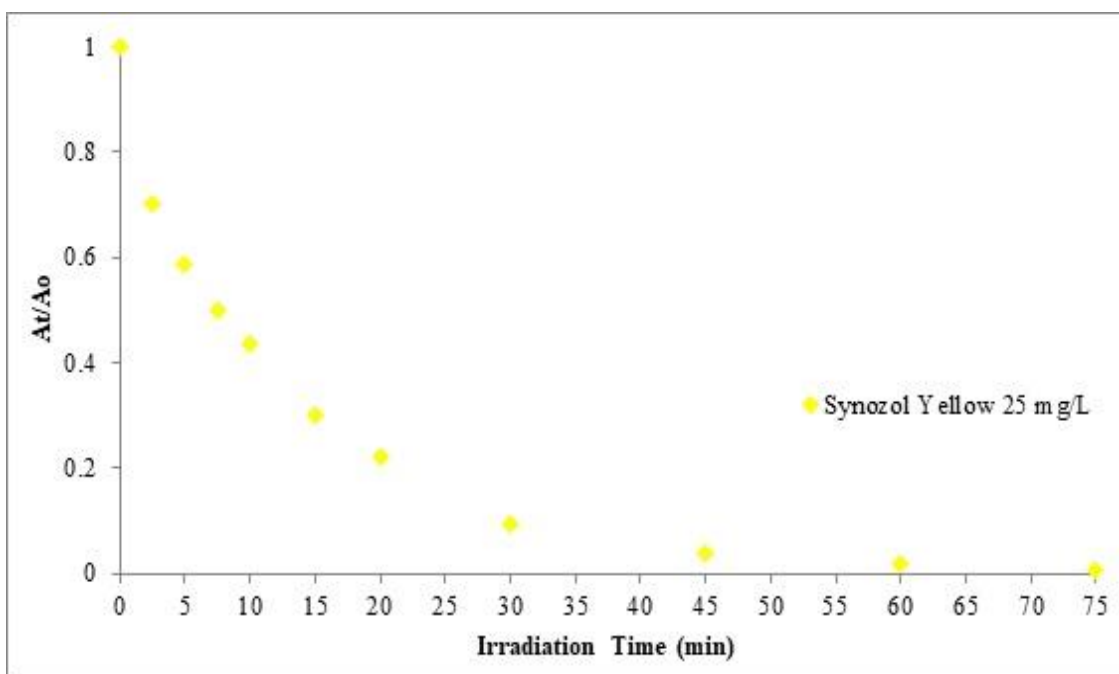


Figure A.3.10 VUV initiated discoloration of Yellow dye ($C_0 = 25 \text{ mg/L}$). The results are average of three replicates.

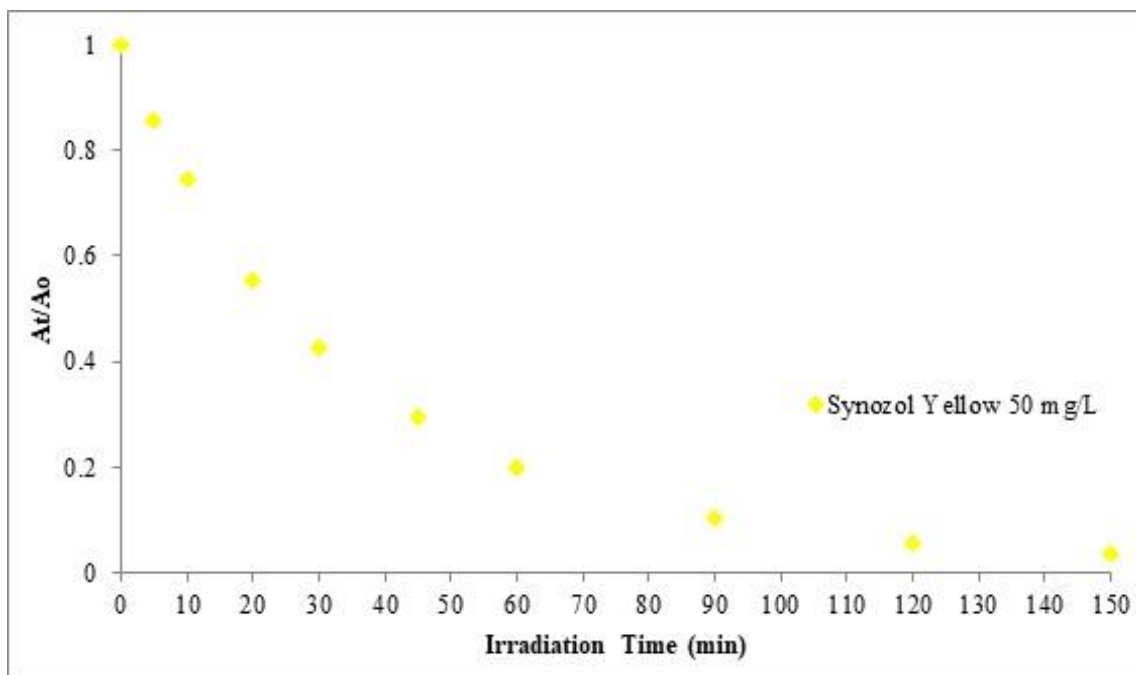


Figure A.3.11 VUV initiated discoloration of Yellow dye ($C_o = 50 \text{ mg/L}$). The results are average of three replicates.

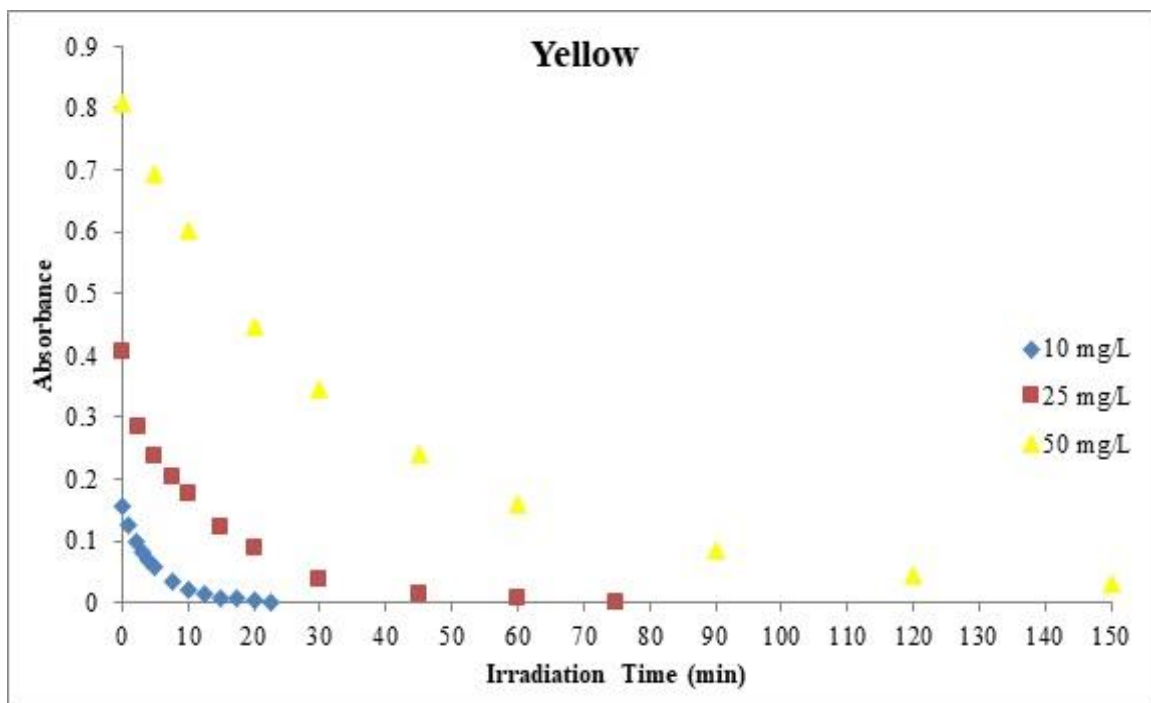


Figure A.3.12 VUV induced discoloration of Yellow dye under various initial concentrations. The results are average of three replicates.

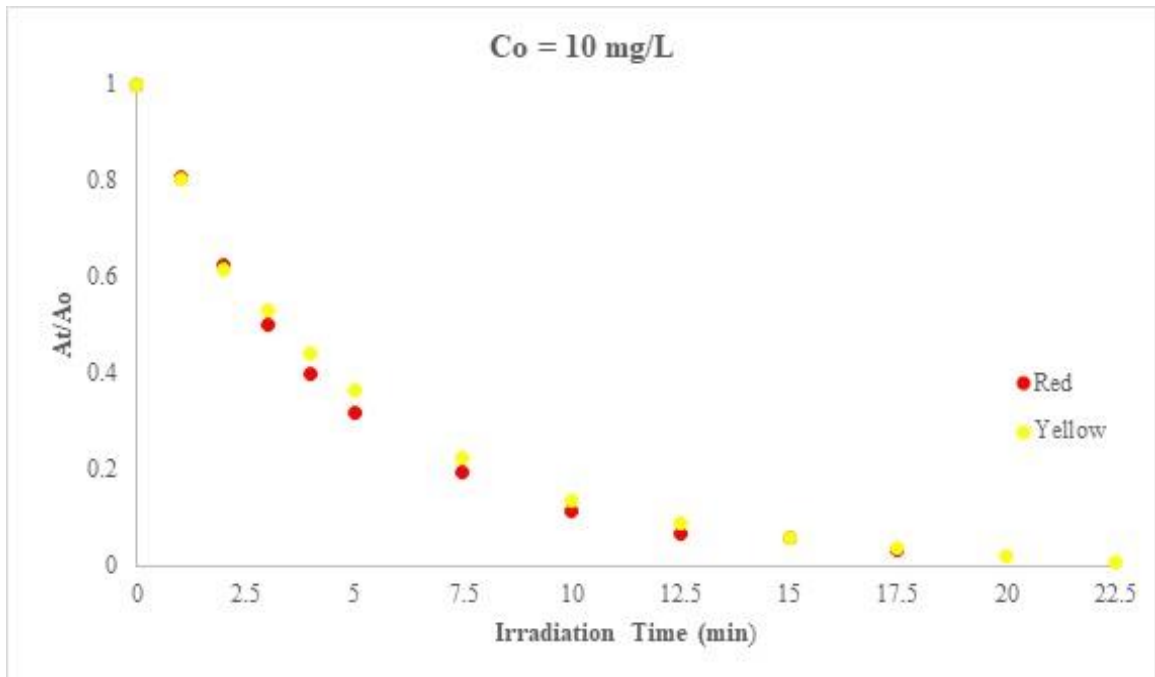


Figure A.3.13 Disappearance of Red and Yellow dyes at $C_o = 10 \text{ mg/L}$. The results are average of three replicates.

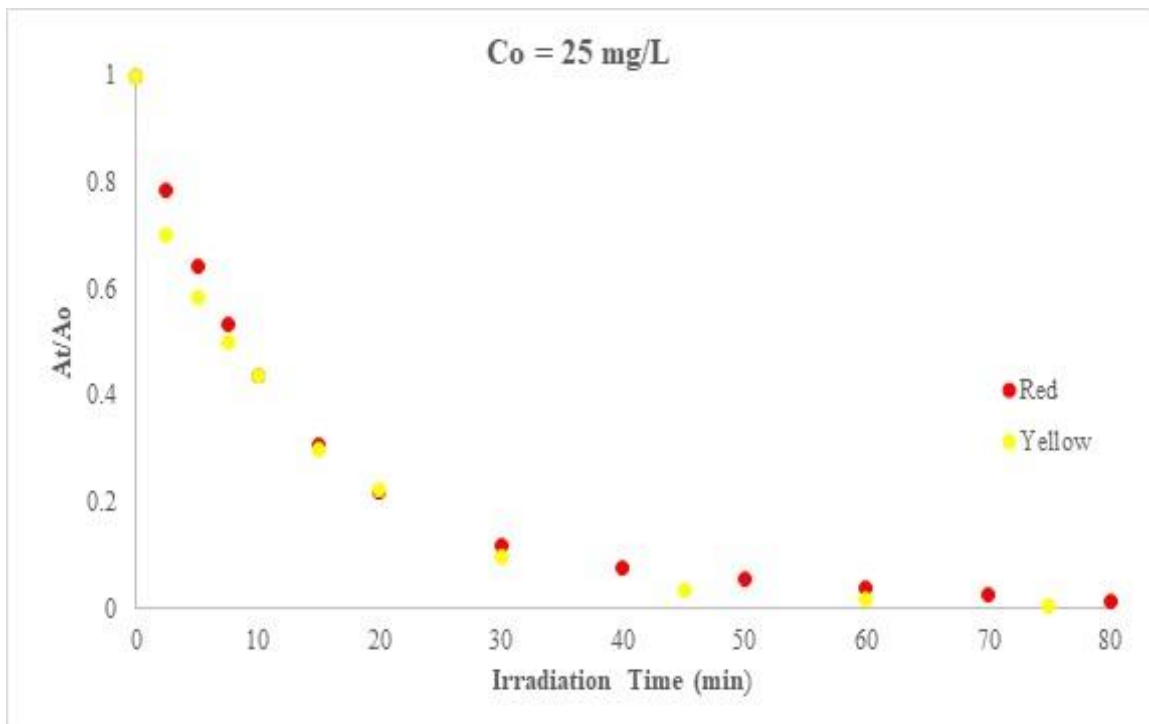


Figure A.3.14 Disappearance of Red and Yellow dyes at $C_o = 25 \text{ mg/L}$. The results are average of three replicates.

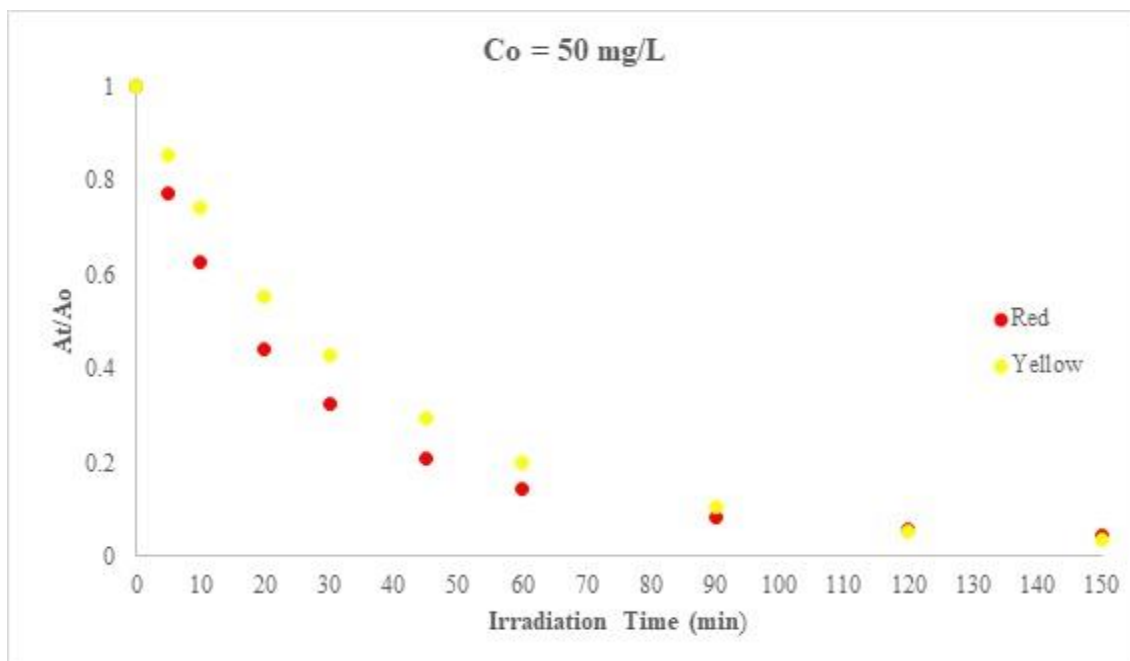


Figure A.3.15 Disappearance of Red and Yellow dyes at $C_o = 50 \text{ mg/L}$. The results are average of three replicates.

APPENDIX 3.3. Supplementary Data for Effects of material of quartz sleeve on the discoloration of the reactive textile dyes

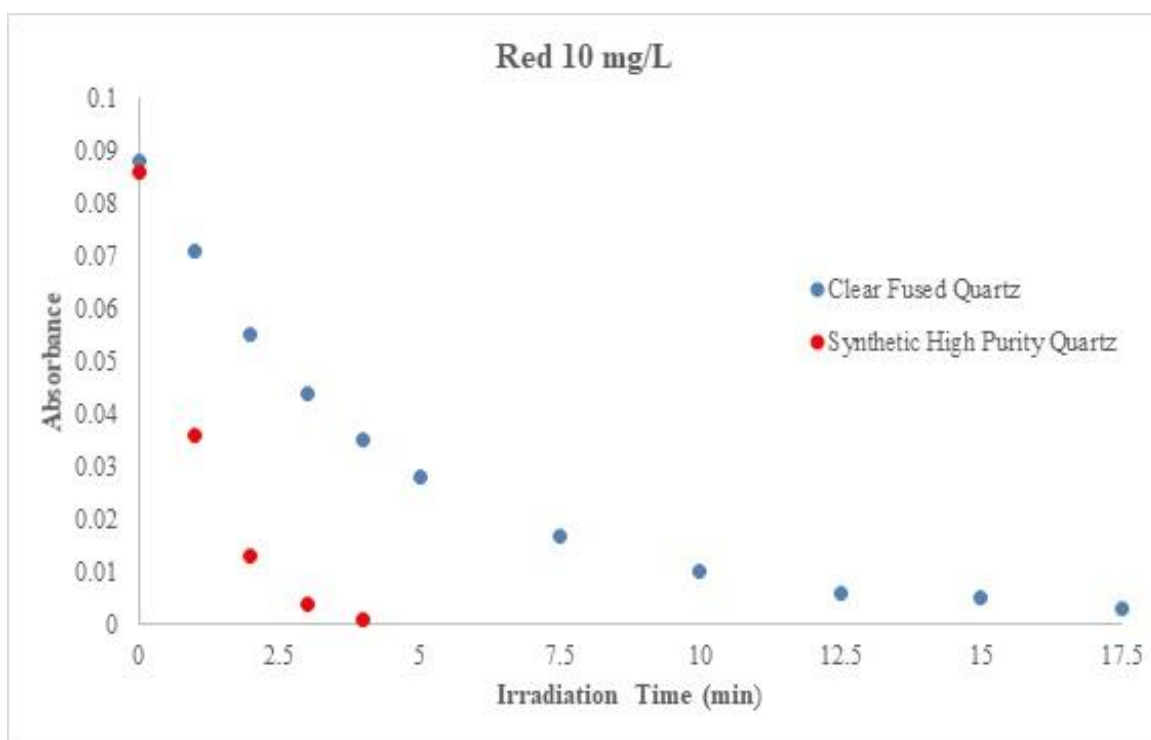


Figure A.3.16 Effects of quartz sleeve on discoloration of Red dye ($C_o = 10 \text{ mg/L}$). The results are average of three replicates.

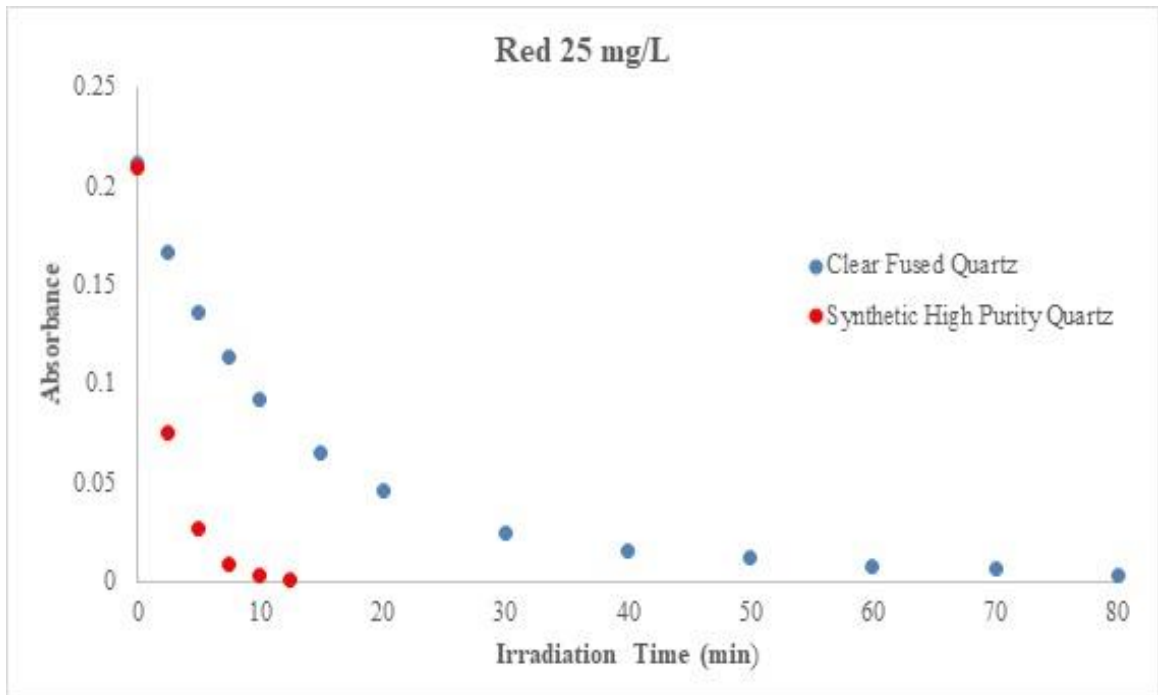


Figure A.3.17 Effects of quartz sleeve on discoloration of Red dye ($C_0 = 25$ mg/L). The results are average of three replicates.

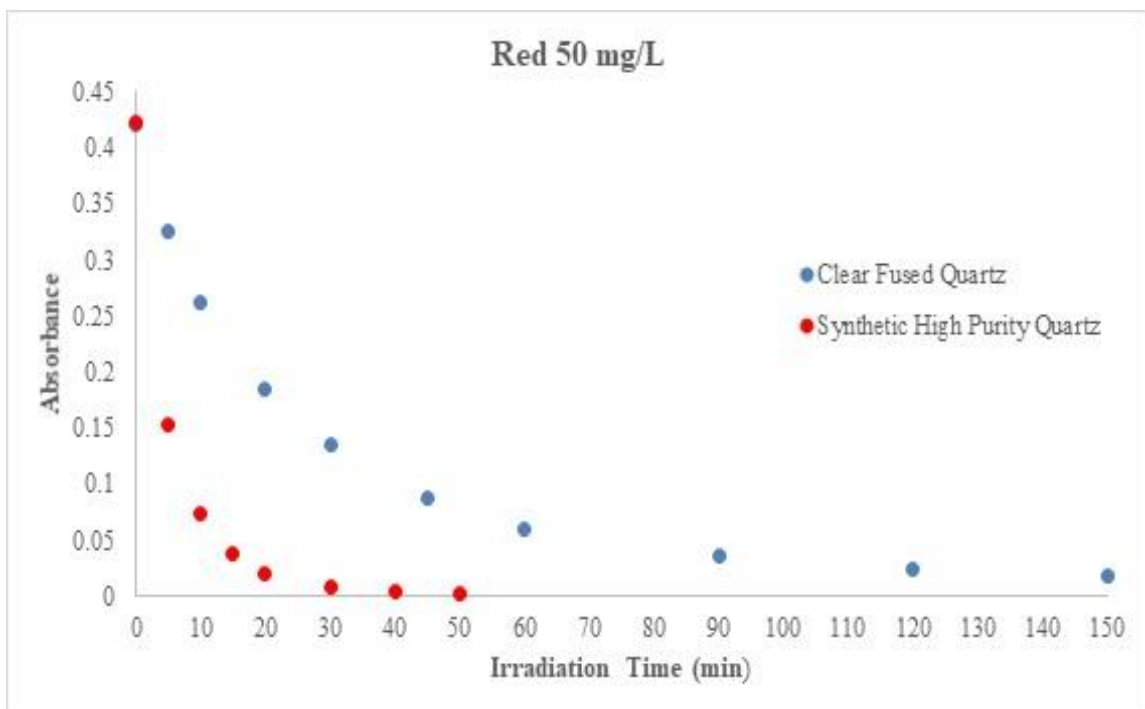


Figure A.3.18 Effects of quartz sleeve on discoloration of Red dye ($C_0 = 50$ mg/L). The results are average of three replicates.

